BioMed Research International

Biomaterials: Chitosan and Collagen for Regenerative Medicine

Guest Editors: Yoshihiko Hayashi, Mitsuo Yamauchi, Se-Kwon Kim, and Hideo Kusaoke

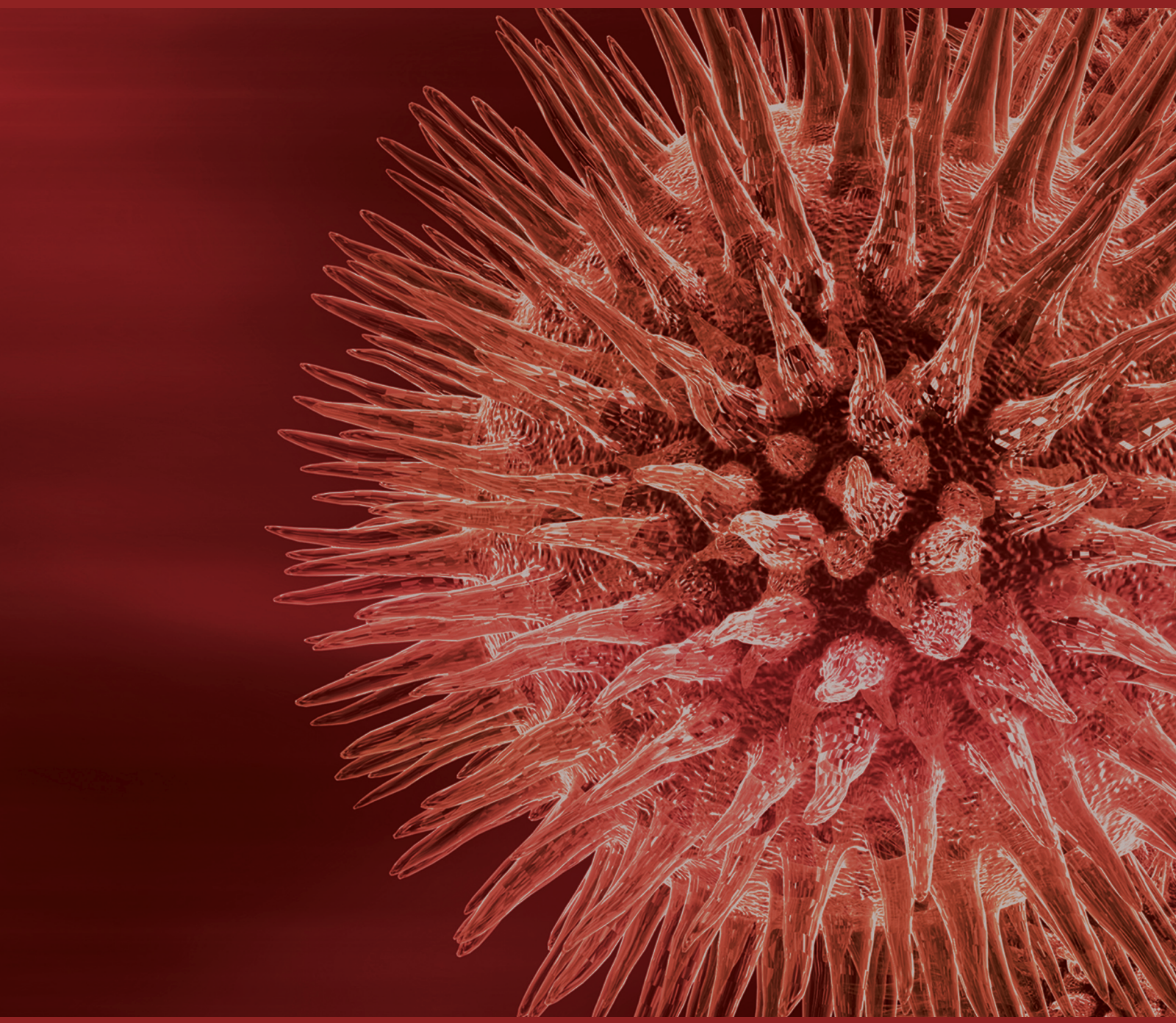

Biomaterials: Chitosan and Collagen for Regenerative Medicine

BioMed Research International

Biomaterials: Chitosan and Collagen for Regenerative Medicine

Guest Editors: Yoshihiko Hayashi, Mitsuo Yamauchi, Se-Kwon Kim, and Hideo Kusaoke

Contents

Hindawi Publishing Corporation
BioMed Research International
Volume 2014, Article ID 690485, 1 page
http://dx.doi.org/10.1155/2014/690485

Editorial

Biomaterials: Chitosan and Collagen for Regenerative Medicine

Yoshihiko Hayashi,[1] Mitsuo Yamauchi,[2] Se-Kwon Kim,[3] and Hideo Kusaoke[4]

[1] *Department of Cariology, Nagasaki University Graduate School of Biomedical Sciences, Nagasaki 852-8588, Japan*
[2] *Department of Oral Biology, NC Oral Health Institute, University of North Carolina, Chapel Hill, NC 27599-7455, USA*
[3] *Department of Chemistry, Marine Bioprocess Research Center, Pukyong National University, Busan 608-737, Republic of Korea*
[4] *Department of Environmental and Biological Chemistry, Faculty of Engineering, Fukui University of Technology, Fukui 910-8505, Japan*

Correspondence should be addressed to Yoshihiko Hayashi; hayashi@nagasaki-u.ac.jp

Received 11 June 2014; Accepted 11 June 2014; Published 1 July 2014

With contributions from USA, Taiwan, Japan, and Korea, this special issue holds great insight. This special issue offers comprehensive knowledge on chitosan and collagen as biomaterials, especially with respect to their basic biological and chemical properties, as well as clinical applications. Two review articles described the preparation and biological application of chitooligosaccharide and its derivatives and the relevance to clinical dentistry of distinct characteristics of mandibular bone collagen. Original articles reported seven experiments: 3 chitosan topics and 4 collagen topics. The former demonstrated the contributions for a proteomic view of chitosan nanoparticle to hepatic cells, the promotion of D-glucosamine to transfection efficiency, and chitin application as skin substitutes. The latter showed the contributions for hydroxyapatite-gelatin nanocomposite, genipin modification of dentin collagen, dentin phosphophoryn/collagen composite for dental biomaterial, and biological safety of fish collagen.

Yoshihiko Hayashi
Mitsuo Yamauchi
Se-Kwon Kim
Hideo Kusaoke

Acknowledgments

We owe heartily gratitude to the reviewers who helped and kindly supported us in the peer reviewing processes. We would also like to thank all the contributors who have selected the best themes and edited the meaningful concepts to this issue.

Hindawi Publishing Corporation
BioMed Research International
Volume 2014, Article ID 837524, 12 pages
http://dx.doi.org/10.1155/2014/837524

Research Article

Biological Assessment of a Calcium Silicate Incorporated Hydroxyapatite-Gelatin Nanocomposite: A Comparison to Decellularized Bone Matrix

Dong Joon Lee,[1] Ricardo Padilla,[2] He Zhang,[1] Wei-Shou Hu,[3] and Ching-Chang Ko[1,4]

[1] *NC Oral Health Institute, School of Dentistry, University of North Carolina, CB 7454, Chapel Hill, NC 27599, USA*
[2] *Department of Diagnostic Sciences, School of Dentistry, University of North Carolina, CB 7454, Chapel Hill, NC 27599, USA*
[3] *Department of Chemical Engineering and Materials Science, University of Minnesota, Minneapolis, MN 55455, USA*
[4] *Department of Orthodontics, School of Dentistry, University of North Carolina, 275 Brauer Hall, CB 7454, Chapel Hill, NC 27599, USA*

Correspondence should be addressed to Ching-Chang Ko; koc@dentistry.unc.edu

Received 31 December 2013; Revised 9 March 2014; Accepted 22 May 2014; Published 26 June 2014

Academic Editor: Mitsuo Yamauchi

Our laboratory utilized biomimicry to develop a synthetic bone scaffold based on hydroxyapatite-gelatin-calcium silicate (HGCS). Here, we evaluated the potential of HGCS scaffold in bone formation *in vivo* using the rat calvarial critical-sized defect (CSD). Twelve Sprague-Dawley rats were randomized to four groups: control (defect only), decellularized bone matrix (DECBM), and HGCS with and without multipotent adult progenitor cells (MAPCs). DECBM was prepared by removing all the cells using SDS and NH_4OH. After 12 weeks, the CSD specimens were harvested to evaluate radiographical, histological, and histomorphometrical outcomes. The *in vitro* osteogenic effects of the materials were studied by focal adhesion, MTS, and alizarin red. Micro-CT analysis indicated that the DECBM and the HGCS scaffold groups developed greater radiopaque areas than the other groups. Bone regeneration, assessed using histological analysis and fluorochrome labeling, was the highest in the HGCS scaffold seeded with MAPCs. The DECBM group showed limited osteoinductivity, causing a gap between the implant and host tissue. The group grafted with HGCS+MAPCs resulting in twice as much new bone formation seems to indicate a role for effective bone regeneration. In conclusion, the novel HGCS scaffold could improve bone regeneration and is a promising carrier for stem cell-mediated bone regeneration.

1. Introduction

A critical-sized defect (CSD) is known as the smallest size tissue defect that will not completely heal by itself over the duration of the experiment or the life of the subject [1, 2]. A CSD caused by neoplastic, inflammatory, congenital, or traumatic etiologies requires a mechanically stiff biomaterial (scaffold) and a cell source (osteoblasts) for the effective regeneration [3–5]. Current available options to repair CSD are autografts allografts and alloplastic grafts (synthetic bone substitutes). The autograft is the gold standard, but there are only a few bones that can be used as donor tissue and frequently result in donor site morbidity. Allografts have a high risk of tissue rejection and potential viral or bacterial transmission; moreover, poor tissue integration with host tissue causes the grafting failure rate of 15 to 25% [6–8]. Since both options are highly limited by the age of the donors/recipients and their availability, the demand for synthetic bone substitutes has been increasing as an alternative source for bone regeneration.

Although hydroxyapatite (HA) is the most widely studied stiff scaffold material, the frequency of its clinical use is less than 10% of all bone grafting procedures due to its unstable fixation and insufficient interaction with host tissues [7]. Instead, hydroxyapatite composites (e.g., hydroxyapatite plus collagen derivatives) have been developed to mimic

biochemical and biomechanical properties of natural bone in order to enhance osteointegration and graft healing for potential biomedical applications [9, 10]. The rapidly evolving technology enables the development of biomimetic nanocomposite biomaterials that fulfill the current requirements of an improved bone scaffold.

Recently, a new biomimetic nanocomposite, hydroxyapatite gelatin-calcium silicate (HGCS), has been developed to address the processability of the hydroxyapatite nanocomposite [11–13]. HGCS amalgamates the hydroxyapatite-gelatin (HG: degraded collagen) composite particles by *in situ* pozzolanic formation of calcium silicate (CS), which interacts among gelatin, silica, and calcium hydroxide ($Ca(OH)_2$). We find that HGCS improves cytocompatibility, increases *in vitro* osteogenesis, and has a greater mechanical strength when compared to previous hydroxyapatite-collagen and hydroxyapatite-gelatin nanocomposites. Above all, the compressive strength of HGCS is significantly higher than that of HG. Notably, the CS formed by the chemical reaction between silica and calcium hydroxide affects the mechanical properties of HGCS scaffolds, which increased from 43.7 to 93.6 MPa (unpublished in-house data). Therefore, the addition of CS could enhance the mechanical strength. The performance of HGCS for *in vitro* and *in vivo* ostegenesis is, however, unknown, which fuels an additional investigation.

Another unique scaffold material is decellularized natural bone matrix (DECBM), which has received attention due to its natural origin and because it is expected to serve as a rigid scaffolding material similar to HGCS. Hashimoto et al. were the first to report a decellularization method for rat femurs using high pressure and measured the potential of cells to repopulate the bone [14]. Their evaluation was restricted to subcutaneous implantation, which requires further investigation with the *in vivo* bony defect model. The present study will develop a simplified laboratory protocol for bone decellularization and compare the applicability of decellularized calvarial bone matrix to HGCS using the rat calvaria CSD model.

Both HGCS and DECBM may be stiff enough to be utilized as scaffolds to restore bone defects. For a CSD, however, regeneration would require production of extracellular matrices by living cells. Stem cells have been known as an ideal cell source because they are readily available, nonimmunodeficient, and disease free when transplanted into patients. Bone regeneration with a cell-seeded scaffold was proven to have better regeneration potential than without cells. Bone marrow-derived mesenchymal stem cells (BMMSCs) have been widely used and proved to have high osteogenic potential both *in vitro* and *in vivo* [15, 16]. Multipotent adult progenitor cells (MAPCs) are adult stem cells originated from bone marrow as well. MAPCs can form all three germ layers, in which mesoderm can give rise to bone tissue when dexamethasone is present [17].

Since MAPCs express higher levels of stem cell makers such as OCT-3/4, show a high proliferative rate, and can exert immunosuppressive effects on T-cell alloreactivity and proliferation, they are expected to become an alternative cell source for bone tissue engineering [18–21]. MAPCs were initially isolated from mice and rats, and specifically applied in bone tissue engineering by Ferreira et al. MAPCs have yielded positively *in vitro* osteogenic differentiation and *in vivo* bone formation [22, 23].

In the present study, we developed the HGCS scaffold and investigated its osteogenic efficiency in healing of CSDs by comparing it with DECBM (natural matrix) and CSDs with no graft as control. We also evaluated whether the bone formation process using the HGCS is related to the presence of MAPCs. Given the known positive effects of CS added to the HG scaffold for bone regeneration, the cooperative interaction between MAPCs and HGCS scaffold showed facilitated bone regeneration.

2. Materials and Methods

2.1. Preparation of HGCS Scaffold and DECBM. The HGCS scaffolds were prepared by *in situ* hybridization of CS with HG powders which were biomimetically synthesized by the coprecipitation method. The method to synthesize HAp-Gel slurry was well described in previous studies [11]. Briefly, the calcium hydroxide powder was mixed with HG powder and cross-linked with enTMOS (bis [3-(trimethoxysilyl)-propyl] ethylenediamine) for 30 seconds. To initiate the sol-gel reaction, calcium chloride solution (48 μL) was added to the mixture. When the mixture began thickening, it was quickly transferred into 1cc syringes with 1 mm inner diameter needles. The HGCS paste was extruded from the syringe as intertwined threads to generate the macroporosity. The samples were dried in air for one week and then sterilized with ethylene oxide gas. To prepare the DECBM, the rat calvaria were harvested (natural bone matrix: NBM) using a trephine burr (8 mm in diameter) and washed with distilled water for 1 hour to remove blood elements. They were placed into a decellularizing solution containing 0.5% sodium dodecyl sulfate (SDS; Sigma-Aldrich, St. Louis, MO, USA) and 0.1% ammonium hydroxide (NH_4OH: Sigma-Aldrich, St. Louis, MO, USA) and placed on a mechanical shaker at room temperature. The detergent solution was replaced every 36 hours for 3 weeks. The completion of the decellularization process was confirmed by histology (hematoxylin and eosin (H&E) staining) and DNA assay. Then, the DECBM samples were repeatedly washed with distilled water until detergents were completely removed from the matrix. The DECBM samples were sterilized using the same dose of gamma irradiation (10,000 Gy) as vascular decellularized grafts before implantation [24].

2.2. Mechanical Property of GEMOSIL-CS and DECBM. The compressive strength of HGCS ($n = 10$) was determined with the use of an Instron (model 4204, Canton, MA, USA) and compared to HG specimens ($n = 10$). All samples were prepared in a cylindrical shape with a 1 : 2 ratio of diameter (3.5 mm) to length (7.0 mm). The uniaxial force (0.5 mm/min) was applied to the samples for compressive strength, and five samples were evaluated per group. The result was determined from the maximum strength value on the stress-strain curve. Due to the inherent shape of the calvaria, decellularized calvaria samples were tested using the

three-point bending method. The strip sample, 6.3 mm in length (L) × 6 mm in width (d) × 0.8 mm in thickness (t), was prepared and tested at the cross-head speed of 0.1 mm/min. The force was recorded in real time and peak force (F) at failure was measured. The bending flexure strength of decellularized calvaria ($n = 10$) was calculated by the formula $3FL/2dt^2$. The fresh calvaria samples (NBM, $n = 10$) were tested for comparison.

2.3. Thermogravimetric Analysis (TGA) of DECBM. The decellularized and nondecellularized (natural) calvarial bone samples were air-dried and ground to powders. Natural calvarial bone powders were used as controls. From each group, 10 mg of powder was placed on a platinum sample holder, which was then loaded inside the Q-500 thermogravimetric analyzer (TA Instrument, New Castle, DE, USA). The test was performed in the temperature range from 30°C to 800°C with a heating rate of 5°C/min. Weight changes were recorded in terms of temperature.

2.4. In Vitro Osteogenic Study of HGCS and DECBM. MC3T3-E1 preosteoblasts were isolated from mouse calvaria and subcultured to test *in vitro* cytocompatibility and osteogenic potential for the materials coated on the 35 mm culture dishes using P-6,000 Spin Coater (Specialty Coating Systems, Inc., Indianapolis, IN, USA). Briefly, finely grounded DECBM was mixed into 1 mL of methanol and 44.4 μL of enTMOS by voltexing for 15 seconds. For HGCS, HG slurry in 1 mL methanol was mixed with 29.6 mg of $Ca(OH)_2$ powder and 44.4 μL of enTMOS by voltexing for 15 seconds. Then 50 μL from each mixture was sprayed in the center of a spinning 35 mm dish on the spin coater and spinned for 20 seconds at 6,000 rpm. The coated dishes were sterilized under UV for 24 hours and washed with PBS before being used.

2.4.1. Focal Adhesion Assay. MC3T3-E1 cell cytoskeletal structures were assessed to reveal cell morphology after 3 days of cell culture on the coated dishes. Following fixation in 4% formaldehyde, the cells were permeabilized in a 0.5% Triton X-100 (Sigma-Aldrich, St. Louis, MO, USA) in PBS for 5 min. After blocking with 5% of BSA solution, the cells were incubated with rhodamine phalloidin (1 : 100 ratio in 5% BSA/PBS, monoclonal, Molecular Probes, OR, USA) and anti-β-tubulin primary antibody (1 : 100 ratio in 5% BSA/PBS, monoclonal anti-human, Sigma, UK) overnight at 4°C. Then, the cells were thoroughly washed in 0.05% Tween 20 in PBS and incubated with FITC conjugated secondary antibody (1 : 50 ratio in 5% BSA/PBS, Vector Laboratories, UK) for 1 h at 4°C. The nuclei of cells were stained with VECTASHIELD® mounting medium with DAPI (Vector laboratories, Inc., Burlingame, CA USA) and images were acquired using a fluorescence microscope (Nikon Eclipse Ti-U, Nikon Instruments, Melville, NY).

2.4.2. MTS Assay. The proliferation of the MC3T3-E1 cells on the coated dishes was conducted using MTS assay as instructed in company manual. The MTS (3-(4,5-dimethylthiazol-2-yl)-5-(3 carboxymethoxyphenyl)-2-(4-Sulfophenyl)-2H-tetrazolium) (Promega Co., Madison, WI, USA) reacted with cells for an hour. Then absorbance of each group was measured on days 1, 3, 5, 7, and 9, respectively, at 490 nm using a Plate reader (Biorad, Hercules, CA, USA).

2.4.3. Mineralization Assay. For differentiation, MC3T3-E1 cells were cultured directly on the HGCS- and DECBM-coated 35 mm dishes with osteogenic media for 4, 7, and 21 days. After washing with PBS, the cells were fixed for 10 minutes in formalin, washed, stained with 40 mM Alizarin Red (Acros Organics, Geel, Belgium) at pH 4.2 for 10 minutes, rinsed with deionized water 6 times, and air-dried. Mineralized nodule images were obtained with a Nikon Eclipse Ti-U microscope (Nikon Instruments Inc., Melville, NY, USA).

2.5. In Vivo Implantation of Scaffolds. Rat MAPCs were isolated, expanded, and seeded onto the HGCS scaffolds ($n = 3$). The isolation, culture, and seeding on the scaffold of rat MAPCs were described in our previous study [23]. Twelve male Sprague-Dawley rats (Charles River, Wilmington, MA, about 250 g, 7 weeks) were initially anesthetized by intramuscular injection of 10 mg/kg Ketamine-HCl (Puteney Inc., Portland, ME, USA) and additional Ketamine was administered during experiment as needed. After shaving and sterilizing the surgical site, an approximately 2 cm mid-sagittal skin incision was made from occipital to frontal scalp, and the subcutaneous tissue was dissected and reflected to each side with the periosteum to expose the osseous surface of the skull. An 8 mm CSD was created without damaging the underlying dura and mid-sagittal blood vessels using a low-speed dental trephine burr. Four treatment groups with three rats each underwent surgery for a total of 12 CSDs. The small sample size ($n = 3$) was chosen because this was a screening/pilot test for a series of developing biomaterials as indicated in our previous reports [23]. Three experimental groups used different types of scaffolds (DECBM, HGCS seeded with MAPCs, and HGCS). The control group consisted of CSDs with no grafting at all. After implantation of the scaffold materials, the periosteum was closed with 4–0 chromic gut suture, and then skin was closed with 3–0 silk suture. To prevent postsurgical infection, 20 mg/kg of cefazolin (Hospira Inc., Lake Forest, IL, USA) was injected intramuscularly once per day for 7 days after surgery. For the mineral apposition rate (MAR) measurement, fluorochrome labels such as Alizarin Red-S (30 mg/kg, Sigma Aldrich, St. Louis, MO, USA) and Calcein (20 mg/kg, Sigma Aldrich, St. Louis, MO, USA) were injected perivascularly to each animal twice during the study. Alizarin Red was administered 10 days after the surgery and calcein was given 15 days before sacrifice. The interlabeling periods were 10 and 70 days for rats sacrificed at 12 weeks.

2.6. Micro-CT Analysis. Rats were sacrificed 12 weeks after scaffold implantation. The calvaria were excised carefully by preserving the implanted sites and then fixed in 10% formaldehyde for 7 days at 4°C. Subsequently, they were

transferred into 70% isopropyl alcohol. The calvaria explants were scanned by using a micro-CT system (mCT 40; Scanco Medical, Brüttisellen, Switzerland) at 70 kV and 114 mA with a 200 ms integration time. Detailed setting parameters for acquisition and analysis of the acquired images were described in a previous study [15]. After 3D reconstruction, the percentage of radiopaque areas in the defects was measured using the Nikon NIS Elements software and tabulated by treatment group. The radiopacity (%) was obtained by dividing the new radiopaque areas in the CSD by the total defect area. The data were presented as average ± standard deviation. One-way ANOVA was used to compare the means among four groups.

2.7. Mineral Apposition Rate (MAR) by Fluorescence Microscopy. Harvested calvaria specimens were dehydrated and subsequently infiltrated with resin (Technovit, Heraeus Kulzer GmbH, Germany) for 23 days. The method for the slide preparation was described previously [20]. The polished sections were viewed using a Nikon fluorescence microscope apparatus with bright field, TRITC and FITC filters, and a Nikon Eclipse Ti-U digital camera (Nikon Instruments Inc., Melville, NY, USA). Each fluorescent image was merged to measure the distance between fluorescent labeled layers at the interface between native bone and the implanted scaffold (INBS) and at the central pore area with the Nikon NIS Elements software (Nikon Instruments Inc., Melville, NY, USA) tools. A total of five measurements were made along the span of each double label. The MAR was calculated using the following equation: MAR (μm/day) = $\sum_{\chi} / nt$, where $\sum_{\chi}$ is the sum of all the measurements between double labels, n is the total number of measurements, and t is the time (days) interval expressed [25–27]. The mean distance of the five regions was subject to statistical analysis and the overall mean distance was calculated for each group. Two-way ANOVA was used to compare the means among four groups.

2.8. Histological Determination for New Bone Tissue Formation. After analysis for MAR study, calvaria specimen slides were further stained with Steven's Blue by counterstaining with Van Gieson to visualize the formation of newly formed bone (NFB) tissue for the quantitation as previously described [23]. Briefly, entire images of the medial (central) sagittal histologic section were acquired with a DP70 color digital camera equipped with color image software (DP11, Olympus USA, Center Valley, PA, USA) under 20x magnification and then merged using Adobe Photoshop CS6 (Adobe Systems Inc., San Jose, CA USA) to recreate as one figure. The new bone surface area (B.Ar.) and the total area of each defect (T.Ar.) were measured in pixels by using an automated image analysis system (Image J software version 1.46R, NIH, Bethesda, MD, USA) to calculate the NFB (in %: B.Ar./T.Ar/0.01) based on the standardized protocols of the American Society for Bone and Mineral Research [28]. The one tail Student t-test was used to compare the means between the groups.

3. Results and Discussion

The two main components of tissue engineering constructs for *in vivo* implantation are the cells and the scaffold material. Since the bone regenerating potential of MAPCs was well reported in previous studies [18, 23], our efforts were focused mainly on the materials aspect to compare natural and synthetic components in bone regeneration. Previously, HG was developed by mimicking natural bone matrix (hydroxyapatite and collagen derivative) with promising properties for bone regeneration [29]. However, the weak bonding force between HG particles and siloxane was prone to brittle fracture and resulted in a relatively low compressive strength when compared to natural bone. Applying CS to HG created a new scaffold material, HGCS, which not only reinforced its mechanical strength but also improved osteoblast adhesion, proliferation, and differentiation by the stimulation of released calcium ions. Another value of this study was to apply a naturally derived biomaterial via removing cellular components from the matrix for the bone regeneration. DECBM was expected to be an ideal candidate for a scaffold due to its function as supporting structure and regulator of cellular functions such as cell viability, proliferation, and differentiation [30–33]. Indeed, the natural ECM is known to have a modulatory effect of signal transduction triggered by bioactive molecules (growth factors and cytokines) [34, 35]. It could be preserved even after decellularization, as described in previous applications on various tissues [36, 37]. Here, we developed an allogenic natural bone scaffold using a decellularization technique to compare it with a synthetic scaffold (HGCS) for the potential of *in vivo* bone regeneration.

3.1. Characterization of DECBM and HGCS. The duration of the decellularization process for rat calvaria was optimized by 0.5% SDS and 0.1% NH_4OH dissolved in distilled water [38, 39]. This process effectively disrupted cell membranes and cleaved DNA to minimize immunological rejection. The completion of decellularization was confirmed by histology and DNA assay. After 2 weeks, H&E staining of the decellularized tissue revealed absence of both nuclei and cytoplasmic compartments (Figures 1(a) and 1(b)) and no DNA was detected from agarose gel electrophoresis (Figure 1(e)). Removing the cells from the matrix is an important step because it may prevent humoral immune reactions against membrane proteins. It is also important to completely remove DNA from the matrix because it can stimulate the immune system by activating cytokine production and B-cell immunoglobulin secretion after allogenic or xenogenic implantation [40]. Scanning electron microscope (SEM) evaluation revealed that both matrices exhibited similar morphology in the distribution of collagen and mineralized fibers residing in the matrix (Figures 1(c) and 1(d)). In NBM cells are attached and embedded into the matrix; in DECBM cells are absent, confirming the effective decellularization from the calvarial bone tissue.

The TGA data reveals the typical pattern of mineral tissues with a higher inorganic to organic ratio in DECBM than in NBM (Figure 2(b)). Absorbed water inside the DECBM

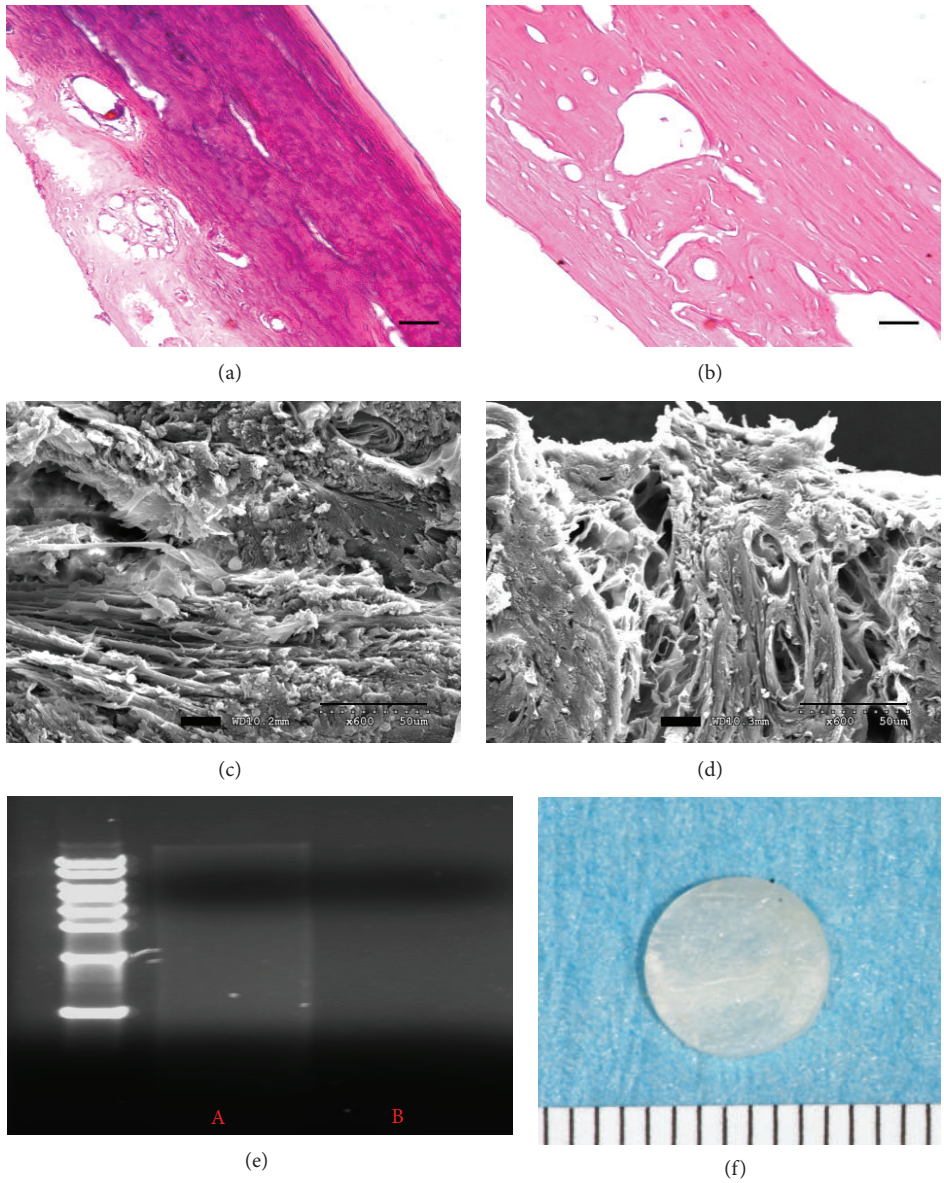

Figure 1: Decellularized rat calvaria. Hematoxylin and eosin-stained cross-section of calvaria before (a) and after (b) decellularization (scale bar: 50 μm). SEM analyses visualize the presence of cells in NBM (c) and the maintained ECM structure after decellularization (d); scale bar: 50 μm. DNA assay was used to detect any residual DNA before (lane A) and after the decellularization of calvaria (lane B). Gross image of rat calvaria after the decellularization process (f); scale: 1 mm.

and NBM could be removed completely by heating to 200°C. The weight loss of the samples was attributed to the thermal degradation of proteins including collagen, noncollagenous proteins, and cell membranes (300–560°C) [41]. The NBM samples indicated a continuous weight drop from 300 to 550°C. The DECBM samples showed an abrupt weight drop from 300°C to 400°C, ceased at 450°C, and then followed with a gradual weight drop until 600°C. The final weight remainder represents the percentage of inorganic content in the matrix. In fact, the final weight % of DECBM (65%) was greater than that of NBM (58%), indirectly verifying that approximately 7% of the organic contents were removed through the decellularizing process.

The integrity of the bone matrix directly associated with mechanical strength was measured by the three-point bending test and the compression test in DECBM and HGCS, respectively. The mean values of the three-point bending test were 72.00 ± 14.14 MPa and 89.36 ± 17.34 MPa for decellularized and nondecellularized bones, respectively (Figure 2(a)). The decellularization process decreased the mechanical strength by 19.42% ($n = 10$, $P < 0.05$) in DECBM compared to NBM. The difference was possibly caused by an enzymatic effect on the structural proteins and more likely due to a loss of soluble protein by SDS during the decellularizing process. SDS was considered to be a better choice than nonionic agents to thoroughly

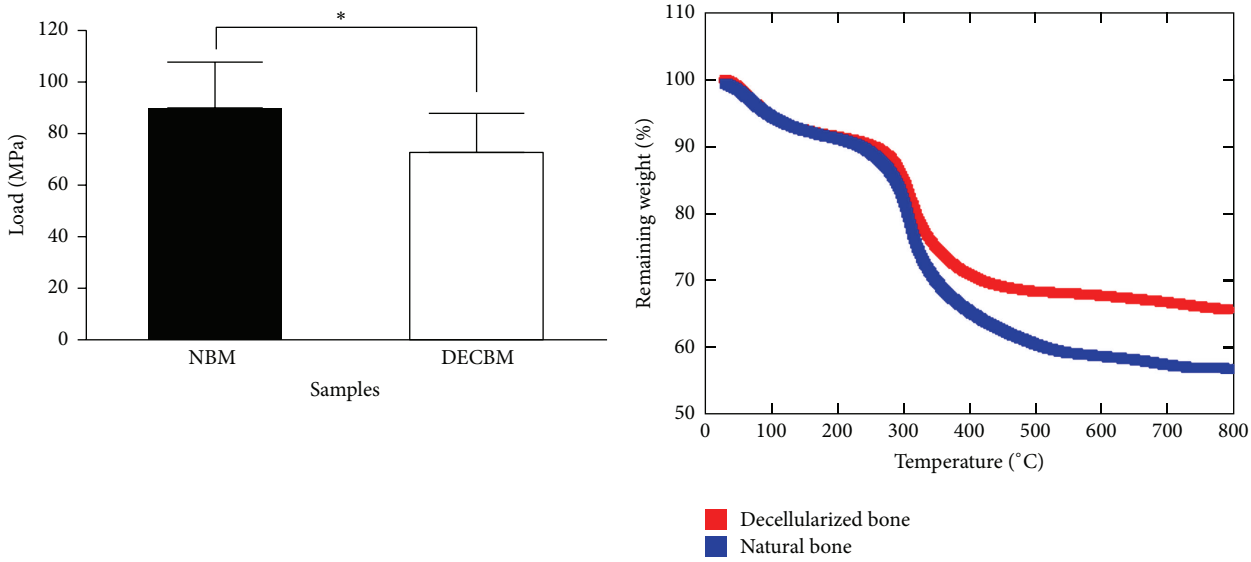

Figure 2: Three-point bending test of natural bone matrix (NBM) versus decellularized bone matrix (DECBM) of calvaria with a sample size $n = 5$ (a). Samples were maintained hydrated with PBS during experiment. The strength was decreased by 19.42 MPa after decellularization ($P < 0.05$). A typical TGA result showed the weight loss versus temperature. Distinct weight drop patterns are attributed to the degradation of water (initial drop in the curve prior to 100°C) and organic materials (second drop at 300) (b).

remove soluble proteins from the matrix in such a hard and compact tissue like bone (in-house nonpublished data). The compressive strength of HGCS was significantly higher than that of HG. Certainly, CS played a role in increasing this mechanical property of the HGCS scaffold from 43.7 to 93.6 MPa (in-house nonpublished data). This reinforcement is attributed to the *in situ* formation of CS due to the chemical reaction between silica and calcium hydroxide. Therefore, both DECBM and HGCS implants can provide strength approaching that of natural bone though the values were still inferior to natural bone.

3.2. In Vitro Osteoblasts Attachment, Growth, and Osteogenic Differentiation on DECBM- and HGCS-Coated Dishes. To understand osteoblast-scaffold interactions, their *in vivo* bioactivity, and cell integration within the scaffold material during bone regeneration, the materials were assessed *in vitro* by culturing osteoblasts directly on HGCS and grounded DECBM-coated dishes. Prior to use, the quality of the coating was confirmed by observing them under a microscope for even distribution of the materials and consistency of coating. In the control group (no-coating), the focal adhesion assay with MC3T3-E1 preosteoblasts generally indicated a round cell morphology in which their actin filaments were spread out in multiple directions by attaching with well-distributed vinculins in the dish (Figure 3(a)). Cells grown on the DECBM- and HGCS-coated dishes demonstrated less spreading but still had similar morphology as the control group cells. Most of the vinculins were observed near or on the material particles, which supports DECBM and HGCS as being good substrates for cell attachment (Figures 3(b) and 3(c)). MTS assay and mineralization studies were performed for *in vitro* osteogenic potential with MC3T3-E1 cells on material-coated dishes. Since a higher number of cells represent a higher formazan activity, we analyzed the MTS assay for the cell proliferative potential by measuring the formazan activity over time. Figure 3(d) shows the MTS activity of the MC3T3-E1 cells measured on days 1, 3, 5, and 7. The number of cells on both DECBM- and HGCS-coated dishes increased up to 7 days. Cells on HGCS-coated dishes showed a higher proliferative potential than those on DECBM, but less potential than those of the control group between days 1 and 7. The lower growth potential on DECBM compared to the control group was partially due to the growth behavior of the cells on the coated matrix. The topography of DECBM coatings would delay the cell growth in early time points due to an increased surface area, but the cells grew similarly to the control group after 7 days. The cells on DECBM grew by aggregating around DECBM particles and formed thread-like collagen structures (data not shown), which resulted in a multilayered cell culture, unlike HGCS and control groups.

Mineralization was evaluated by nodule formation on days 7, 14, and 21 after differentiation with the osteogenic media (α-MEM with 10 mM β-glycerophosphate (Sigma-Aldrich, St. Louis, MO, USA) and 0.2 mM ascorbic acid (Sigma-Aldrich, St. Louis, MO, USA)). In the controls, calcium nodules were visible 14 days after differentiation and became darker and larger at 21 days, consistent with the typical mineralization pattern of MC3T3-E1 cells under our differentiation conditions (Figure 3(e)). DECBM-coated dishes showed earlier nodule formation and overall were more intense and larger than in the control dish at days 14 and 21 (Figure 3(g)). However, the microscopic pattern of calcium

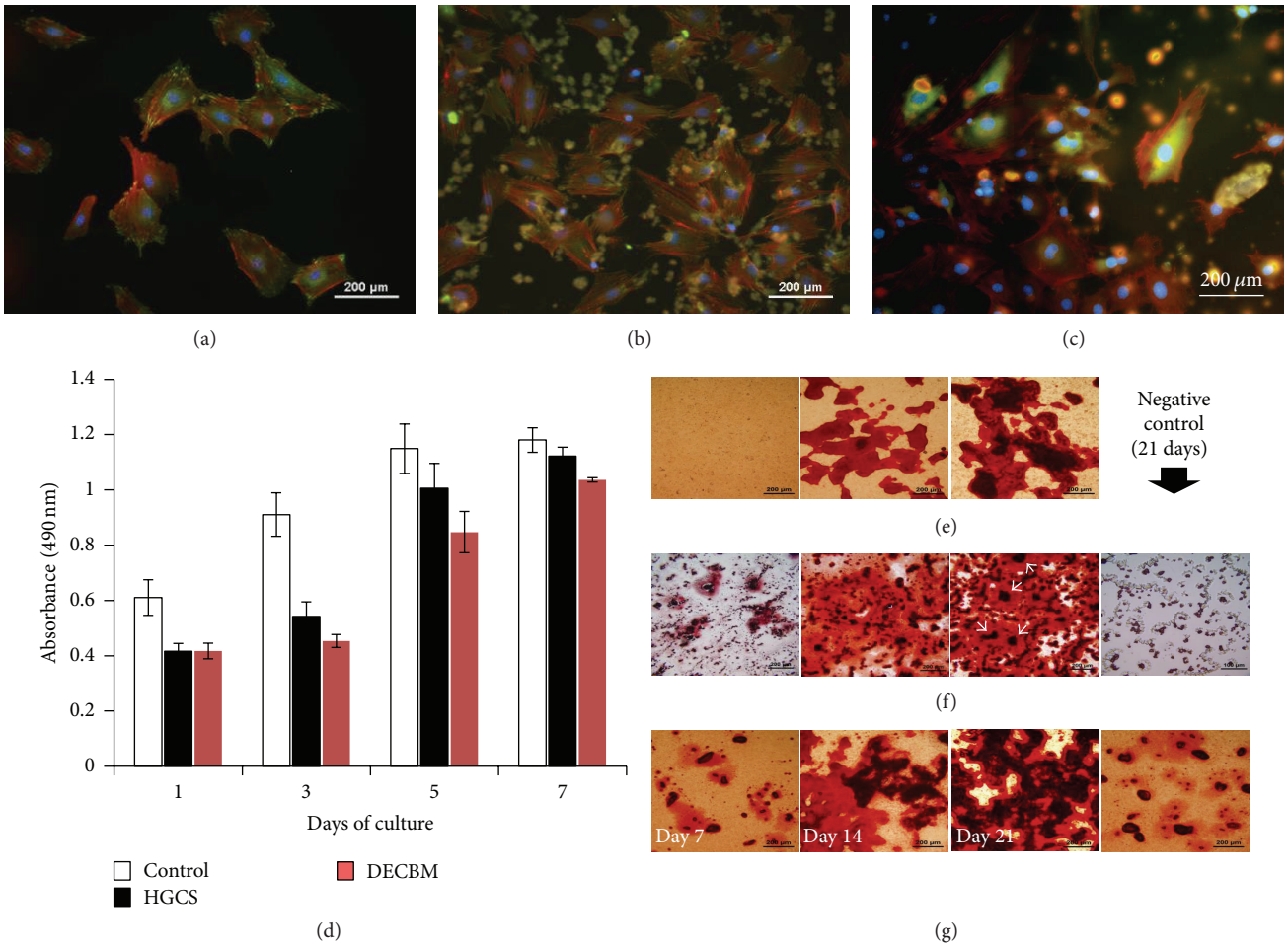

Figure 3: *In vitro* assessment of osteoblast activity on the material-coated dishes. (1) Focal adhesion assay of MC3T3 cells on the coated culture plate with no coating as control (a), HGCS (b), and DECBM (c) after 3 days of culture. MTS assay for MC3T3-E1 cell proliferation on the coated culture plate with DECBM, GEMOSIL-CS, and no coating as control on 1, 3, 5, and 7 days of culture (d). Mineralized nodules were detected by Alizarin Red staining after culturing MC3T3 cells with osteogenic media on the coated culture plate with no coating as control (e), HGCS (f), and DECBM (g) after 7, 14, and 21 days. Negative control was also tested as coated culture plate without cells for 21 days with osteogenic media.

deposition on the HGCS-coated dish was very different than on the DECBM and the control dishes (Figure 3(f)). Cells on the HG started to form small nodule particles, which then enlarged and surrounded the $Ca(OH)_2$ particles (white arrows). Alizarin Red staining revealed that $Ca(OH)_2$ particles were located in the middle of most nodules and likely promoted osteogenic differentiation by providing calcium ions. $Ca(OH)_2$-coated dishes without cells were also stained to serve as negative control.

3.3. In Vivo Bone Regeneration (Mineral Apposition Rate). Four groups were tested for bone regeneration in the rat calvaria critical-sized defect model: empty defects (control group), DECBM, HGCS scaffolds seeded with MAPCs (HGCS+MAPCs), and HGCS scaffolds only. After 12 weeks of postimplantation, the entire calvarial was harvested for MAR, gross, radiographic, and histomorphometric analyses. To evaluate the bone formation rate, MAR was assessed by measuring a total of six randomly selected points along the span of each scaffold. These were double-labeled at both the interface between the host tissue and the scaffold (IBHS) and in the middle of the defect where healing bone infiltrated into the porous scaffold (SID). The results of fluorochrome labeled histology (a to d) and the MAR measurements (e) are presented in Figure 4. At the IBHS, both HGCS+MAPCs and HGCS groups demonstrated higher MAR values ($2.72 \pm 0.34\ \mu$m/day and $2.67 \pm 0.2\ \mu$m/day, resp.) than the empty defect control group, which had MAR of $1.6 \pm 0.53\ \mu$m/day. In addition, the MAR value in the DECBM group was $0.87 \pm 0.07\ \mu$m/day, which was the lowest rate of mineral apposition. At the IBHS of the DECBM group, only a few areas expressed the fluorochromes, signifying that osteoblasts were scantly present and that there was low osteoblastic activity. According to the previous study by Parfitt et al., the total rate of bone formation was affected by the number of osteoblasts and the average volume of matrix secreted by the osteoblasts [42, 43].

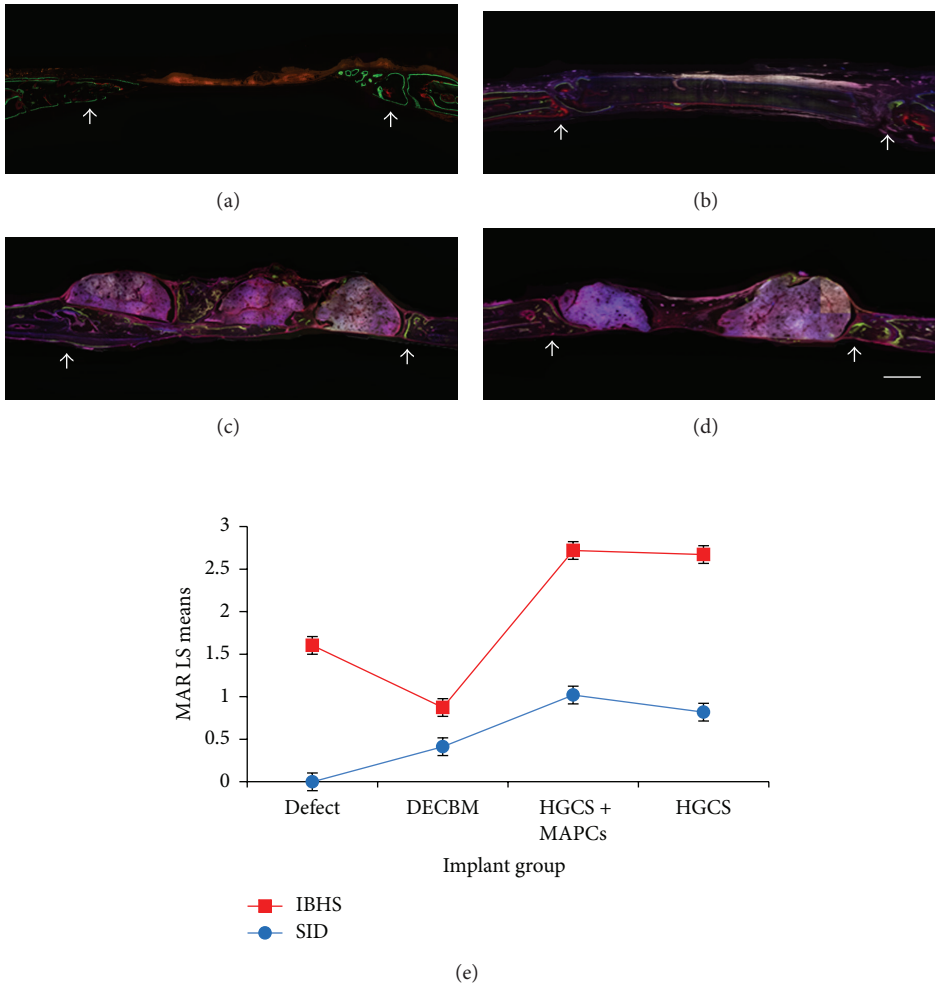

Figure 4: Fluorescence image of histological cross-section represented fluorochrome-labeled mineral deposition in defect (a), DECBM (b), HGCS with MAPCs (c), and HGCS (d). Calcein (green) and Alizarin Red (red) were administered in series. Mineral apposition rate (MAR) at the interface between host bone-scaffold (IBHS) and inside scaffold in the defect (SID) was determined at 12 weeks after implantation of scaffolds (e). Data are shown as mean ± SD of three independent experiments, $P < 0.05$ (scale bars: 1 mm). White arrows represent the margin of the defect.

The highest MAR in the SID was in the HGCS+MAPCs group (1.02 ± 0.23 μm/day). The MAR in the HGCS-only group (0.82 ± 0.1 μm/day) was greater than in the DECBM group (0.41 ± 0.1 μm/day). The difference in MAR between the HGCS group and the HGCS+MAPCs group may be due to the MAPCs differentiating into osteoblasts *in vivo*, therefore increasing their activity and the rate of bone mineral apposition in the SID. The MAR of the DECBM group in the SID can only be measured on the surface of the DECBM and not inside of the scaffold. In the control group, the MAR in the SID could not be calculated because the empty defects did not heal after 12 weeks (Figure 4(e)).

Overall, the HGCS+MAPCs and HGCS groups showed increased MAR over the DECBM and the empty defect (control) groups. In addition, the MAR in the DECBM group was only detectable on the surface of the DECBM. Fluorochromes were observed to be deposited only on the surface of the DECBM scaffold because DECBM has inadequate pores; there was no cell migration into the matrix to regenerate bone. In the HGCS with and without MAPCs groups, fluorochrome labels could be seen extensively with measureable distances, whereas the empty defect group had them only at the periphery of the defect. Although MAR was a significant indicator for mineral apposition rate at a specified timeframe, further assessment by histomorphometry and radiographic analysis can provide more information regarding the total new bone formation (NBF).

3.4. In Vivo Bone Regeneration (Histomorphometry and 3D Micro-CT Evidence). After fluorochrome imaging, the undecalcified resin sections were stained with Steven Blue and Van Gieson histochemistry to identify new bone formation (fresh red) in the defect site. Histological evaluation demonstrated that the defect within the HGCS+MAPCs group was filled with new bone that bridged with the host bone by 12 weeks. In the HGCS scaffold-only group new bone was moderate, primarily at the periphery of the defect (Figure 5(c)). From all

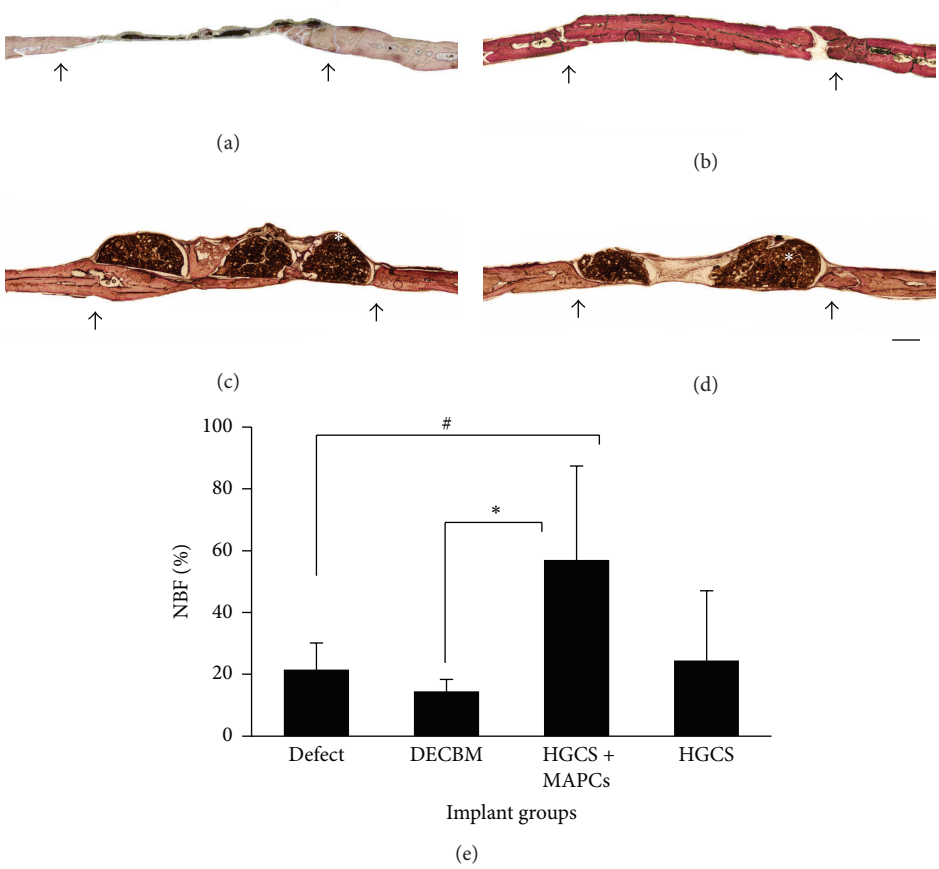

Figure 5: Histological sections were processed for sagittal section of the defect area after 12 weeks of implantation and stained with Steven Blue and Van Gieson. The representative section was shown from each group of defects (a), DECBM (b), HGCS with MAPCs (c), and HGCS (d). The area of new bone formation (NFB) was quantified in % using Image J software (e). White asterisk indicates HGCS material, $P < 0.05$ (scale bars: 1 mm). Black arrows represent the margin of the defect.

perspectives, bone regeneration was prominently better in the HGCS+MAPCs group (Figure 5(d)). At 12 weeks of postimplantation, quantitative measurements of NBF demonstrated 56.99 ± 30.44% bone regeneration for the HGCS+MAPCs group, 24.44 ± 3.94% for the HGCS-only group, 14.45 ± 3.94% for the DECBM group, and 21.51 ± 8.60% for the empty defect group. Notably, the newly formed bone in both the HGCS-only and the HGCS+MAPCs groups was well integrated at the interface between host bone and the scaffold. In the middle section of the HGCS-only group, the NBF in the area of macrospores had little calcified tissue; instead fibrous tissues were seen (Figure 5(c)). Contrastingly, the macroporous spaces in the HGCS+MAPCs were filled with newly formed bone tissue (Figure 5(d)). The importance of cells in repairing bone lesions has been documented [16, 18, 23]. In this study we confirm that NBF with HGCS scaffolds also relies on the ability of cells to increase regional bone regeneration, especially in the central area of the CSDs apart from host tissue (Figure 5(c)). The percentage of NBF in the DECBM group was significantly lower than that of the HGCS scaffold alone at 12 weeks (Figure 5(b)). Notably the empty group also promoted NBF above that of DECBM group (Figure 6(e)). Both the empty and HGCS groups relied on the host bone as a cell source. The host cells may have produced approximately 23% of NBF when there was an available space (either defect or scaffold bridging). There was an absence of NBF between DECBM and host tissue with intervening fibrous tissue. In the middle of section, the NBF was slightly formed along the outer surface of the DECBM with little osteointegration (Figures 5 and 6). This demonstrates that DECBM of calvarial bone does not allow cell infiltration.

In Figure 6, micro-CT analysis shows 3D reconstructed calvaria at 12 weeks after implantation (a to d). The percentage of radiopaque area in the defect was calculated (e). While the DECBM group showed the highest radiopaque area (94.1 ± 0.31%), the HGCS+MAPCs scaffolds revealed greater radiopaque areas (90.58 ± 0.98%) than HGCS scaffolds alone (64.76 ± 5.53%) or empty defects (54.7 ± 0.79%). The micro-CT data, except for the DECBM group, were consistent with the histological measurements providing an indirect validation of NBF. The reason for the DECBM group difference is due to the DECBM having the same inorganic matrix content as natural bone (Figure 6), making it difficult to differentiate newly formed bone from DECBM radiographically.

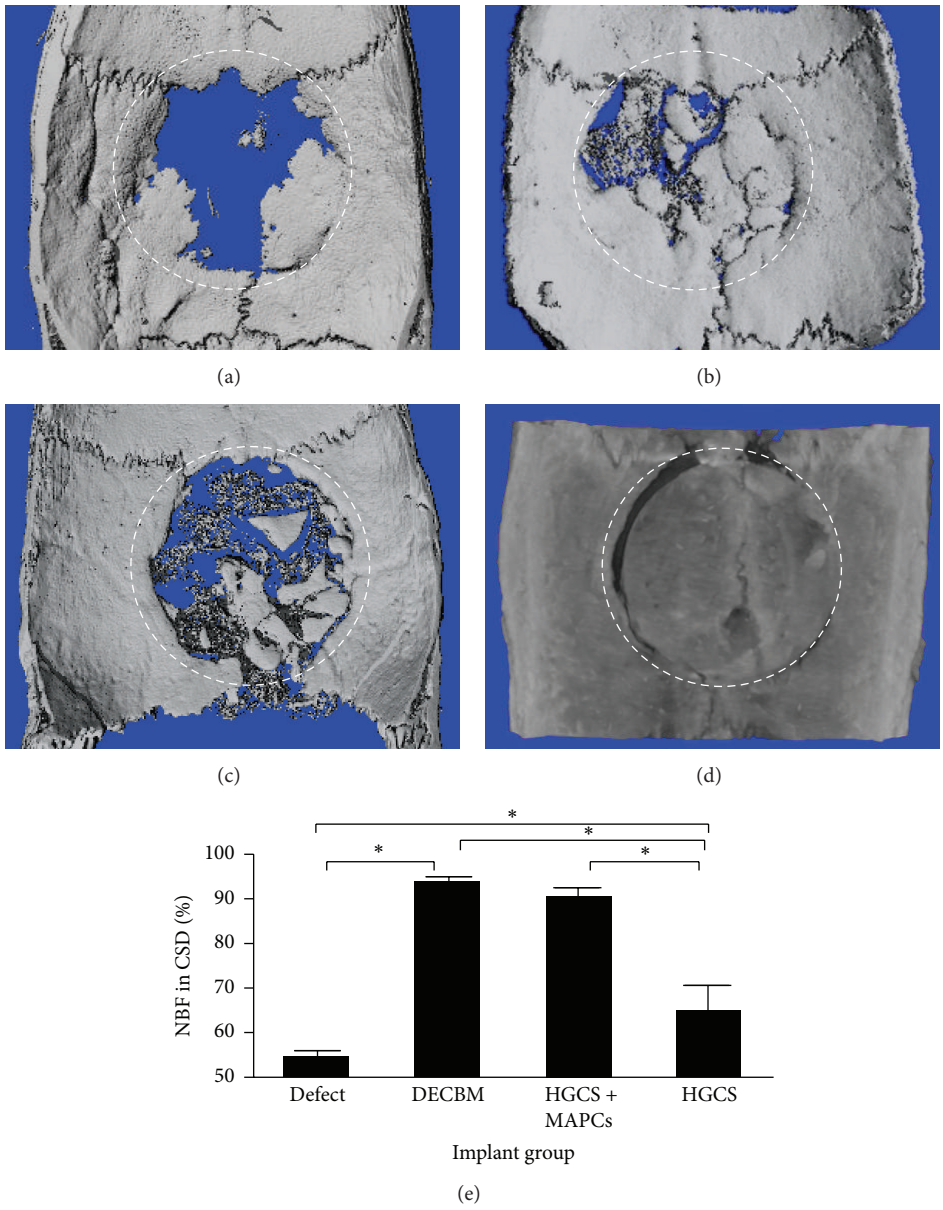

Figure 6: Micro-CT images of critical-sized calvarial defects at 12 weeks. Panels represent empty defect (a), DECBM (b), HGCS with MAPCs (c), and HGCS groups (d). Radiopaque area in the defect was calculated in % (e). Data were represented as mean ± STD ($n = 3$, $P < 0.05$).

Taken together, our *in vivo* analyses confirmed that HGCS is stiff enough to support porous spaces for cell ingrowth and is compatible with MAPCs for osteogenic differentiation. The use of HGCS+MAPCs could facilitate new bone formation and further advance the success of bone regeneration. Although DECBM showed a higher osteogenic differentiation potential than HGCS *in vitro*, its application as 3D structural scaffold is limited due to the inability for cellular migration into the compact structure of bone.

4. Conclusion

Our data support that HGCS possesses osteoinductive properties as a novel synthetic biomaterial for bone regeneration and that seeding it with MAPCs yields a synergic effect to enhance bone regeneration in rat calvarial critical-sized defects. This study also confirms that the natural biomaterial, DECBM, is not suitable as a bone scaffold. Our findings suggest that further studies are needed to adapt optimal microarchitectures of HGCS to promote bone regeneration and to find alternative applications of DECBM as a scaffold in bone regeneration.

Conflict of Interests

The authors declare that there is no conflict of interests regarding the publication of this paper.

Acknowledgments

The authors would like to thank Rene Cutting, Emily Hearne, and Sesha Jackson-Woodard for kindly providing animal tissue. They would also like to thank John Whitley for technical assistance. Research reported in this publication was supported, in part, by NIH/NIDCR K08DE018695 and R01DE022816.

References

[1] J. P. Schmitz and J. O. Hollinger, "The critical size defect as an experimental model for craniomandibulofacial nonunions," *Clinical Orthopaedics and Related Research*, vol. 205, pp. 299–308, 1986.

[2] G. M. Cooper, M. P. Mooney, A. K. Gosain, P. G. Campbell, J. E. Losee, and J. Huard, "Testing the critical size in calvarial bone defects: revisiting the concept of a critical-size defect," *Plastic and Reconstructive Surgery*, vol. 125, no. 6, pp. 1685–1692, 2010.

[3] H. Petite, V. Viateau, W. Bensaïd et al., "Tissue-engineered bone regeneration," *Nature Biotechnology*, vol. 18, no. 9, pp. 959–963, 2000.

[4] T. Albrektsson and C. Johansson, "Osteoinduction, osteoconduction and osseointegration," *European Spine Journal*, vol. 10, no. 2, pp. S96–S101, 2001.

[5] M. Spector, "The tissue engineer's toolbox manifesto," *Biomedical Materials*, vol. 9, no. 1, Article ID 010201, 2014.

[6] M. P. Bostrom and D. A. Seigerman, "The clinical use of allografts, demineralized bone matrices, synthetic bone graft substitutes and osteoinductive growth factors: a survey study," *Hss Journal*, vol. 1, pp. 9–18, 2005.

[7] V. M. Goldberg and S. Stevenson, "Bone graft options: fact and fancy," *Orthopedics*, vol. 17, no. 9, pp. 809–821, 1994.

[8] B. L. Taylor, T. Andric, and J. W. Freeman, "Recent advances in bone graft technologies," *Recent Patents on Biomedical Engineering*, vol. 6, no. 1, pp. 40–46, 2013.

[9] D. A. Wahl and J. T. Czernuszka, "Collagen-hydroxyapatite composites for hard tissue repair," *European Cells and Materials*, vol. 11, pp. 43–56, 2006.

[10] C. Sionkowska and J. Kozłowska, "Characterization of collagen/hydroxyapatite composite sponges as a potential bone substitute," *International Journal of Biological Macromolecules*, vol. 47, no. 4, pp. 483–487, 2010.

[11] M. C. Chang, C. Ko, and W. H. Douglas, "Preparation of hydroxyapatite-gelatin nanocomposite," *Biomaterials*, vol. 24, no. 17, pp. 2853–2862, 2003.

[12] T.-J. M. Luo, C.-C. Ko, C.-K. Chiu, J. Llyod, and U. Huh, "Aminosilane as an effective binder for hydroxyapatite-gelatin nanocomposites," *Journal of Sol-Gel Science and Technology*, vol. 53, no. 2, pp. 459–465, 2010.

[13] J. C. Dyke, K. J. Knight, H. Zhou, C. Chiu, C. Ko, and W. You, "An investigation of siloxane cross-linked hydroxyapatite-gelatin/copolymer composites for potential orthopedic applications," *Journal of Materials Chemistry*, vol. 22, no. 43, pp. 22888–22898, 2012.

[14] Y. Hashimoto, S. Funamoto, T. Kimura, K. Nam, T. Fujisato, and A. Kishida, "The effect of decellularized bone/bone marrow produced by high-hydrostatic pressurization on the osteogenic differentiation of mesenchymal stem cells," *Biomaterials*, vol. 32, no. 29, pp. 7060–7067, 2011.

[15] H. Lin, G. Yang, J. Tan, and R. S. Tuan, "Influence of decellularized matrix derived from human mesenchymal stem cells on their proliferation, migration and multi-lineage differentiation potential," *Biomaterials*, vol. 33, no. 18, pp. 4480–4489, 2012.

[16] M. F. Pittenger, A. M. Mackay, S. C. Beck et al., "Multilineage potential of adult human mesenchymal stem cells," *Science*, vol. 284, no. 5411, pp. 143–147, 1999.

[17] Y. Jiang, B. N. Jahagirdar, R. L. Reinhardt et al., "Pluripotency of mesenchymal stem cells derived from adult marrow," *Nature*, vol. 418, no. 6893, pp. 41–49, 2002.

[18] J. R. Ferreira, M. L. Hirsch, L. Zhang et al., "Three-dimensional multipotent progenitor cell aggregates for expansion, osteogenic differentiation and "in vivo" tracing with AAV vector serotype 6," *Gene Therapy*, vol. 20, no. 2, pp. 158–168, 2013.

[19] A. Luyckx, L. De Somer, O. Rutgeerts et al., "Mouse MAPC-mediated immunomodulation: cell-line dependent variation," *Experimental Hematology*, vol. 38, no. 1, pp. 1–2, 2010.

[20] S. A. Jacobs, J. Pinxteren, V. D. Roobrouck et al., "Human multipotent adult progenitor cells are nonimmunogenic and exert potent immunomodulatory effects on alloreactive T-cell responses," *Cell Transplant*, vol. 22, no. 10, pp. 1915–1928, 2013.

[21] J. L. Reading, J. H. M. Yang, S. Sabbah et al., "Clinical-grade multipotent adult progenitor cells durably control pathogenic T cell responses in human models of transplantation and autoimmunity," *Journal of Immunology*, vol. 190, no. 9, pp. 4542–4552, 2013.

[22] K. Subramanian, Y. Park, C. M. Verfaillie, and W. S. Hu, "Scalable expansion of multipotent adult progenitor cells as three-dimensional cell aggregates," *Biotechnology and Bioengineering*, vol. 108, no. 2, pp. 364–375, 2011.

[23] J. R. Ferreira, R. Padilla, G. Urkasemsin et al., "Titanium-enriched hydroxyapatite-gelatin scaffolds with osteogenically differentiated progenitor cell aggregates for calvaria bone regeneration," *Tissue Engineering A*, vol. 19, no. 15-16, pp. 1803–1816, 2013.

[24] D. J. Lee, J. Steen, J. E. Jordan et al., "Endothelialization of heart valve matrix using a computer-assisted pulsatile bioreactor," *Tissue Engineering A*, vol. 15, no. 4, pp. 807–814, 2009.

[25] H. M. Frost, "Bone histomorphometry: analysis of trabecular bone dynamics," in *Bone Histomorphometry: Techniques and Interpretation*, R. R. Recker, Ed., pp. 109–131, CRC Press, Boca Raton, Fla, USA, 1983.

[26] H. M. Frost, "Bone histomorphometry: choice of marking agent and labeling schedule," in *Bone Histomorphometry: Techniques and Interpretation*, R. R. Recker, Ed., pp. 37–133, CRC Press, Boca Raton, Fla, USA, 1983.

[27] P. P. Spicer, J. D. Kretlow, S. Young, J. A. Jansen, F. K. Kasper, and A. G. Mikos, "Evaluation of bone regeneration using the rat critical size calvarial defect," *Nature Protocols*, vol. 7, no. 10, pp. 1918–1929, 2012.

[28] A. M. Parfitt, M. K. Drezner, F. H. Glorieux et al., "Bone histomorphometry: standardization of nomenclature, symbols, and units. Report of the ASBMR Histomorphometry Nomenclature Committee," *Journal of Bone and Mineral Research*, vol. 2, no. 6, pp. 595–610, 1987.

[29] C. Chiu, J. Ferreira, T. M. Luo, H. Geng, F. Lin, and C. Ko, "Direct scaffolding of biomimetic hydroxyapatite-gelatin nanocomposites using aminosilane cross-linker for bone regeneration," *Journal of Materials Science: Materials in Medicine*, vol. 23, no. 9, pp. 2115–2126, 2012.

[30] E. Adachi, I. Hopkinson, and T. Hayashi, "Basement-membrane stromal relationships: interactions between collagen fibrils and the lamina densa," *International Review of Cytology*, vol. 173, pp. 73–156, 1997.

[31] F. G. Giancotti and E. Ruoslahti, "Integrin signaling," *Science*, vol. 285, no. 5430, pp. 1028–1032, 1999.

[32] Y. Kang, S. Kim, J. Bishop, A. Khademhosseini, and Y. Yang, "The osteogenic differentiation of human bone marrow MSCs on HUVEC-derived ECM and β-TCP scaffold," *Biomaterials*, vol. 33, no. 29, pp. 6998–7007, 2012.

[33] C. Gentili and R. Cancedda, "Cartilage and bone extracellular matrix," *Current Pharmaceutical Design*, vol. 15, no. 12, pp. 1334–1348, 2009.

[34] S. Rahman, Y. Patel, J. Murray et al., "Novel hepatocyte growth factor (HGF) binding domains on fibronectin and vitronectin coordinate a distinct and amplified Met-integrin induced signalling pathway in endothelial cells," *BMC Cell Biology*, vol. 6, article 8, 2005.

[35] P. M. Comoglio, C. Boccaccio, and L. Trusolino, "Interactions between growth factor receptors and adhesion molecules: breaking the rules," *Current Opinion in Cell Biology*, vol. 15, no. 5, pp. 565–571, 2003.

[36] P. M. Crapo, C. J. Medberry, J. E. Reing et al., "Biologic scaffolds composed of central nervous system extracellular matrix," *Biomaterials*, vol. 33, no. 13, pp. 3539–3547, 2012.

[37] C. P. Ng, A. R. Mohamed Sharif, and D. E. Heath, "Enhanced *ex vivo* expansion of adult mesenchymal stem cells by fetal mesenchymal stem cell ECM," *Biomaterials*, vol. 35, no. 13, pp. 4046–4057, 2014.

[38] J. C. Fitzpatrick, P. M. Clark, and F. M. Capaldi, "Effect of decellularization protocol on the mechanical behavior of porcine descending aorta," *International Journal of Biomaterials*, vol. 2010, Article ID 620503, 11 pages, 2010.

[39] T. W. Gilbert, T. L. Sellaro, and S. F. Badylak, "Decellularization of tissues and organs," *Biomaterials*, vol. 27, no. 19, pp. 3675–3683, 2006.

[40] D. S. Pisetsky, "DNA and the immune system," *Annals of Internal Medicine*, vol. 126, no. 2, pp. 169–171, 1997.

[41] A. G. Ward, *The Science and Technology of Gelatin*, Academic Press, London, UK, 1977.

[42] A. M. Parfitt, *Bone-Forming Cells in Clinical Conditions*, Telford Press, Caldwell, NJ, USA, 1990.

[43] A. M. Parfitt, Z. H. Han, S. Palnitkar, D. S. Rao, M. S. Shih, and D. Nelson, "Effects of ethnicity and age or menopause on osteoblast function, bone mineralization, and osteoid accumulation in iliac bone," *Journal of Bone and Mineral Research*, vol. 12, no. 11, pp. 1864–1873, 1997.

Hindawi Publishing Corporation
BioMed Research International
Volume 2014, Article ID 769414, 9 pages
http://dx.doi.org/10.1155/2014/769414

Review Article

Distinct Characteristics of Mandibular Bone Collagen Relative to Long Bone Collagen: Relevance to Clinical Dentistry

Takashi Matsuura, Kentaro Tokutomi, Michiko Sasaki, Michitsuna Katafuchi, Emiri Mizumachi, and Hironobu Sato

Section of Fixed Prosthodontics, Department of Oral Rehabilitation, Fukuoka Dental College, 15-1 Tamura 2-Chome, Sawara-ku, Fukuoka 814-0193, Japan

Correspondence should be addressed to Takashi Matsuura; matsuurt@college.fdcnet.ac.jp

Received 12 February 2014; Accepted 19 March 2014; Published 10 April 2014

Academic Editor: Mitsuo Yamauchi

Bone undergoes constant remodeling throughout life. The cellular and biochemical mechanisms of bone remodeling vary in a region-specific manner. There are a number of notable differences between the mandible and long bones, including developmental origin, osteogenic potential of mesenchymal stem cells, and the rate of bone turnover. Collagen, the most abundant matrix protein in bone, is responsible for determining the relative strength of particular bones. Posttranslational modifications of collagen, such as intermolecular crosslinking and lysine hydroxylation, are the most essential determinants of bone strength, although the amount of collagen is also important. In comparison to long bones, the mandible has greater collagen content, a lower amount of mature crosslinks, and a lower extent of lysine hydroxylation. The great abundance of immature crosslinks in mandibular collagen suggests that there is a lower rate of cross-link maturation. This means that mandibular collagen is relatively immature and thus more readily undergoes degradation and turnover. The greater rate of remodeling in mandibular collagen likely renders more flexibility to the bone and leaves it more suited to constant exercise. As reviewed here, it is important in clinical dentistry to understand the distinctive features of the bones of the jaw.

1. Introduction

Bone is a dynamic tissue that undergoes constant remodeling in order to maintain a healthy skeleton. In clinical dentistry, jawbones frequently require surgical procedures, such as extraction of teeth, periodontal surgery, and implant surgery with or without bone regeneration. Of the many regenerative experiments for bone, few have been tested in the jaw. Because of the unique properties of the jawbone tissue, dentists and dental researchers should be aware that the data regarding other skeletal bones may not be entirely applicable to jawbones.

It is well recognized that the jawbone is remodeled faster than the other skeletal bones [1]. Jaw development is similar to that in other craniofacial bones but distinct from the axial and appendicular skeleton. The jaw arises from neural crest cells of the neuroectoderm germ layer rather than the mesoderm [2] and undergoes intramembranous, instead of endochondral, ossification [3]. Skeletal diseases such as cherubism [4], hyperparathyroid jaw tumor syndrome [5], and bisphosphonate-related osteonecrosis [6] occur only in the jaw. In case of ovariectomy and malnutrition, it is reported that the rat mandible loses trabecular bone and mineral density at a lower rate than the tibiae do [7]. Mesenchymal stem cells or bone marrow stromal cells derived from the jaw show higher osteogenic potential and additional distinctive features compared to other skeletal bones [8–12].

These distinctions owe partly to the unique characteristics of the jawbone matrix. It is important both for regenerative dental surgery and for maintenance of teeth or implants thereafter that dentists and dental researchers are knowledgeable of the unique features of the jawbone

matrix. Though there are many bone matrix components, this review focuses on collagen, the most abundant matrix protein in bone and a determinant of bone strength and quality [13]. Collagen biochemistry is not well characterized in the maxilla; therefore, we focus on research findings for the mandible. We will first describe the role of collagen in bone matrix organization. We will then compare the characteristics of mandibular collagen to long bones to highlight the unique properties of the jawbone matrix that are relevant to clinical dentistry.

2. Role of Collagen on Bone Matrix Organization

Bone matrix consists mainly of a two-phase composite material: mineral and fibrillar collagen. Type I collagen comprises approximately 95% of the entire collagen content of bone. The other types of collagen, such as types III [16] and V [17], are at low levels and appear to modulate the diameter of type I collagen fibrils [17]. Mineral and fibrillar type I collagen are closely associated with each other; the latter functions as a three-dimensional template that organizes the former's deposition and growth [18]. Bone acquires its durability against external forces through this well-organized architectural arrangement between mineral and type I collagen fibrils.

The nature and extent of posttranslational modifications of collagen, many of which are unique to collagen [19], are related to the organization of mineral and collagen fibrils [18]. One such modification, the intermolecular, covalent crosslinking of collagen initiated by the enzymatic oxidative deamination of specific lysine (Lys) and hydroxylysine (Hyl) residues by lysyl oxidase (LOX), contributes to bone strength. In fact, the inhibition of LOX activity by lathyrogens impairs crosslinking, which leads to decreased bone strength caused by increased solubility and abnormal structure of collagen fibrils [20, 21].

Another modification, enzymatic hydroxylation of specific Lys residues by lysyl hydroxylase (LH), also can control bone matrix organization. The Hyl serves as a site of glycosylation [22, 23], and the resultant glycosylated residues affect collagen maturation [23–25], fibrillogenesis, and mineralization [22, 23]. In addition, this modification determines the pattern of intermolecular crosslinking of collagen. Among the 3 isoforms of LH (LH1, 2, and 3), LH2b, a spliced variant of LH2, catalyzes the hydroxylation of Lys residues in the C- or N-terminal, nontriple helical domain (i.e., the telopeptide domain) of collagen, which then directs the subsequent crosslinking towards the hydroxylysine (Hyl^{ald}) pathway in mineralized tissues specifically [26]. Ectopic activation of the Hyl^{ald} pathway by overexpression of LH2b leads to defective collagen fibrillogenesis and matrix mineralization [27]. LH1 catalyzes Lys hydroxylation in the triple helical domain (helical domain), while LH3 has LH activity and, more importantly, galactosylhydroxylysine glucosyltransferase activity [22].

At the beginning of the bone-specific cross-linking pathway, the Hyl residue in the telopeptide domain (formed by LH2b) is converted into an aldehyde (Hyl^{ald}) by LOX (Figure 1). The iminium divalent intermolecular crosslinks are the first to form and they then mature into trivalent crosslinks through condensation reactions (Figure 2). The pairing of Hyl^{ald} with Hyl (formed by LH1) in the helical domain of the neighboring molecule forms the iminium crosslink, dehydrodihydroxylysinonorleucine (deH-DHLNL). By contrast, when the Hyl^{ald} pairs with Lys, dehydrohydroxylysinonorleucine (deH-HLNL) is formed. The major mature crosslink, pyridinoline (Pyr), is a maturational product of deH-DHLNL, formed by any of the following condensation reactions: (1) condensation of their two keto-amines through elimination of a Hyl [28], (2) condensation of a keto-amine and a Hyl^{ald} [29], or (3) condensation of a deH-DHLNL and its keto-amine [30]. A minor, mature cross-link form is deoxypyridinoline (d-Pyr), a lysyl analog of Pyr, made up of two Hyl^{ald} and one Lys in the helical domain [31].

Because these cross-link condensation reactions are usually spontaneous, turnover rate is an important factor in regulating cross-link maturation. For instance, periodontal ligament collagen has low levels of mature cross-links due to its high rate of turnover and, in turn, is more readily degraded due to lack of stable cross-links [25]. As for bone collagen, the levels of the major mature cross-link form, Pyr, versus the major immature cross-link form, deH-DHLNL, indicate the collagen maturation rate [32]. More recently, the research group of Yamauchi has demonstrated that the degree of Hyl glycosylation also influences cross-link maturation [23].

The galactosylhydroxylysine glucosyltransferase activity of LH3 promotes the formation of glucosylgalactosyl (GG)-Hyl from galactosyl (G)-Hyl at the cross-linking site. G- or G free-deH-DHLNL can mature into G-Pyr or G free-Pyr, while GG-deH-DHLNL cannot mature into GG-Pyr. Suppression of galactosylhydroxylysine glucosyltransferase activity of LH3 decreases the speed of cross-link maturation, reduces the amount of both immature and mature crosslinks, increases the diameter of collagen fibrils, and impairs matrix mineralization.

Two articles have demonstrated disordered bone collagen in LOX or LH knock-out mice. Pischon et al. [33] reported that LOX knock-out mice showed a perinatal lethality and that the craniofacial bone of the fetus at embryonic day 18.5 exhibited fragility and thinner collagen fibrils. Their osteoblast cultures revealed retard of osteoblastic differentiation and matrix mineralization. Takaluoma et al. [34] documented that LH1 knock-out mice were viable and fertile but 15% of them were led to sudden death mainly due to aortic ruptures. The femoral bone collagen of the adult LH1 knock-out mice showed a 75% and a 47% smaller amount of Hyl and the major mature crosslink, Pyr, respectively, compared to those of the adult wild-type mice. By contrast, the amount of a minor mature crosslink, d-Pyr, was 1284% greater, and thereby, total amount of Pyr and d-Pyr became 195% greater. Though collagen fibrils and matrix mineralization were not investigated, LH1 deficiency probably affects bone collagen matrix. As described above, the posttranslational

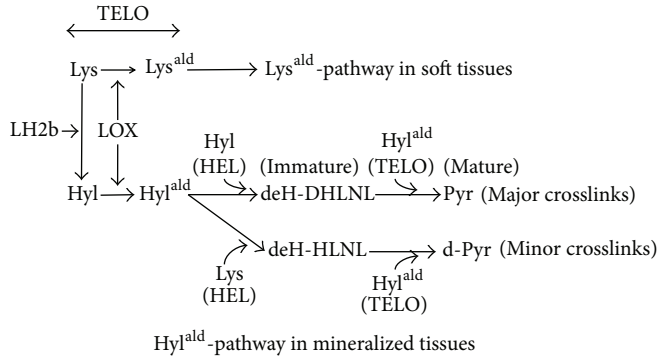

Figure 1: The collagen cross-linking pathway in mineralized tissues. The collagen cross-linking pathway in soft tissues arises from the Lys^{ald} both at the C- and N-telopeptide domains (Lys^{ald}-pathway). In mineralized tissue, it does so from the Hyl^{ald} mostly at the C-telopeptide domain (Hyl^{ald}-pathway). In mineralized tissues, the Lys residue at the C-telopeptide domain is converted into Hyl through the action of LH2b, followed by the conversion of the Hyl into the Hyl^{ald} through the action of LOX. To make the major crosslinks, the immature crosslink, deH-DHLNL, is first formed by pairing of the Hyl^{ald} with the Hyl at the helical domain of the neighboring molecule ($Hyl^{ald} \times Hyl$), and the mature crosslink, Pyr, is then formed by a spontaneous condensation reaction ($Hyl^{ald} \times Hyl^{ald} \times Hyl$). To make the minor crosslinks, the immature crosslink, deH-HLNL, is formed ($Hyl^{ald} \times Lys$), and then the mature crosslink, d-Pyr, is formed ($Hyl^{ald} \times Hyl^{ald} \times Lys$). The value of Pyr/deH-DHLNL presents collagen maturation rate. Lys^{ald} : the aldehyde form of Lys; Hyl^{ald} : the aldehyde form of Hyl; TELO: the telopeptide domain; HEL: the helical domain.

modifications of collagen mediated by LOX and LHs have critical roles on the organization of collagen fibrils and serve as a template for bone mineralization as well as matrix formation.

3. Collagen Content in the Mandible Compared to the Long Bones

The biomechanical roles for collagen in bone are related to both the amount of collagen and its molecular stability and crosslinking. Bailey et al. [35] found that age-related decline in collagen content is nonlinearly correlated to the maximum stress at failure and to the modulus of elasticity in bone from human iliac crest. This does not mean that differences in collagen content are necessarily responsible for these changes but only that they are associated with them. Indeed, in other locations such as the femoral head and neck, no changes in collagen content were detected [36]. Other changes, such as the rate of turnover or degree of mineralization, might affect collagen content and the mechanical properties of bone independently. Despite such complex interactions, collagen content is representative of the status of bone matrix.

We have published the only study comparing the collagen content in the mandibular bone to long bones [37]. We calculated the collagen content in formalin-fixed human cortical bones from 44 cadavers at 3 different sites: the mental region of mandible, the mesial neck of humerus, and the mesial neck of femur. We found that the collagen content was significantly greater in the mandible (165.2 μg/mg of dried bone weight) than in the humerus (146.4 μg/mg) and femur (139.5 μg/mg). Silva et al. [15] compared the bone matrix and mechanical properties of the femur in male SAMP6 mutant mice, a murine model of senile osteoporosis mice, to control SAMR1 mice, a senescence-resistant mutant mouse. They found that both demineralized and intact bones had greater reductions in mechanical strength in SAMP6 mice compared to the SAMR1 mice and that the cortical diaphysis also had a smaller amount of collagen in the SAMP6 mutants (97 μg/mg of dried bone weight at 4 months of age, 106 μg/mg at 12 months of age) versus SAMR1 mutants (113 μg/mg at 4 months of age, 119 μg/mg at 12 months of age). We [14] also investigated the cortical mandibles in males from the same mutant mouse strains at 6 months of age and obtained data similar to that by Silva et al. [15]. The mandible possessed a smaller amount of collagen in SAMP6 (126.4 μg/mg of dried bone weight) than in SAMR1 (149.5 μg/mg). Collagen fibers were also thinner in the SAMP6 mice (35.77 nm) than in the SAMR1 mice (43.71 nm). Despite the difference of age analysis between the two studies, mandibular bone displayed a greater amount of collagen compared to the femoral bone in the two mouse models.

The calvaria, which has the same origin as the jawbones [2], has similar tendency in collagen content. The research group of van den Bos et al. [38] investigated matrix composition of calvaria and long bones (femur, tibia, ulna, and radius) in female mice at 6 months of age and showed that the calvaria (302 μg/mg of dried bone weight) had a greater amount of collagen than the long bones (211 μg/mg).

As the collagen content mentioned above is calculated based on the value of hydroxyproline, it is mostly type I with trace amounts of types III [16] and V [17]. The comparison of type III or type V collagen content between the mandible and long bones has not been performed. Type III collagen is codistributed with type I collagen and is rich in Sharpey's fibers at the periodontal ligament and periosteum, penetrating to the bone [39]. In the mandible, Sharpey's fibers at the periodontal ligament across the entire thickness of alveolar wall and the fibers at the periosteum also penetrate to the cortical bone but become fewer, fragmented, superficial, and shortened with

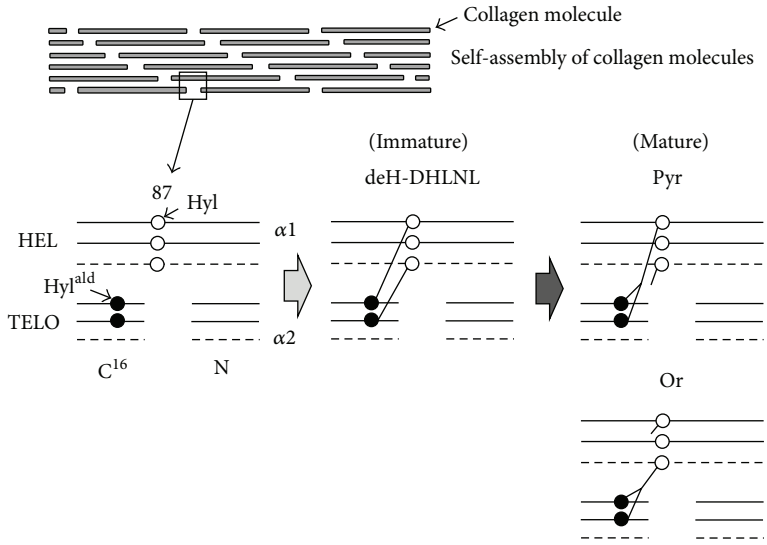

Figure 2: Diagram of the formation and maturation of the major collagen crosslink in mineralized tissues. The procollagen molecule secreted from the cell is processed by cleavages of both the N- and C-terminal propeptide extensions. The processed collagen molecules then self-assemble through clusters of charge and hydrophobicity of the triple helical domain of the molecule to form a fibril. The molecules in the fibril are then stabilized by extensive intermolecular crosslinking. The crosslink involves the Hyl^{ald} at the 16^{C} residue on the C-telopeptide domain of the two α1 chains and the Hyl at the 87 residue on the triple helical domain of the two α1 chains or the single α1 and α2 chains. The immature crosslink, deH-DHLNL, is formed by pairing of the Hyl^{ald} with the Hyl of the neighboring molecule. The mature crosslink, Pyr, is then formed; it owes its origin to the two Hyl^{ald} of α1 chains and the one Hyl of α1 or α2 chain. If the 87th residue on the helical domain is Lys, the minor immature crosslink, deH-HLNL, is formed, and then the minor immature crosslink, d-Pyr, is made up. The solid and dotted lines represent α1 and α2 chains, respectively. Hyl^{ald}: the aldehyde form of Hyl; HEL: the helical domain; TELO: the telopeptide domain; N: N-terminal telopeptide domain; C^{16}: the 16^{C} residue on the C-telopeptide domain; 87: the 87th residue on the helical domain.

age [40]. In the femur, it has been revealed that the periosteal Sharpey fibers are rich at the trochanter and neck regions and penetrate to the cortical bone but decrease the density to the distal portion [41]. Exercise increases the density [42], while ovariectomy decreases it [41]. Type V collagen assembles with type I collagen into heterotypic fibrils [43]. The helical domain of type V collagen is buried within the fibril and type I collagen molecules are present along the fibril surface. The retained N-terminal domains of type V collagen are exposed at the surface and alter accretion of collagen molecules onto fibrils and then lateral growth. In bone, type V collagen does not show so specific distribution that type III collagen does. It shows a weak immunohistochemical staining in bone matrix [44], being preferably at the pericellular area but not in Sharpey's fibers [45].

The collagen content is present at similar levels between cortical and trabecular bones and between male and female [46]. Therefore, it is thought that the mandibular bone matrix including the trabecular bone is rich in collagen. The physiological basis of high collagen content in the mandible is unclear. One possible explanation is a higher rate of collagen turnover in the mandibular bone [1]. It therefore has properties of immature bone, which presumably have a low degree of mineralization resulting in a greater amount of collagen. Collagen fibrils contribute to bone flexibility, while mineral increases bone stiffness [13]. As a result, the mandible is more flexible than the long bones. This mechanical property leaves the bone well adapted to the constant, multidirectional forces associated with chewing and speaking. Another possible explanation for the high abundance of mandibular collagen is the relatively low amount of noncollagenous proteins. Though the mineral and collagen contents usually show a negative correlation, a decrease of collagen is occasionally compensated by an increase of noncollagenous proteins [47]. If the mandible has a smaller amount of noncollagenous proteins, it would then have a greater proportion of collagen. We will now further discuss the characteristics of the posttranslational modifications of collagen in the mandible.

4. Posttranslational Modifications of Collagen in the Mandible Compared to the Long Bones

There is no published data that directly compares collagen crosslinking between the mandible and long bones. In a previous study [14], we compared collagen crosslinking in the mandible of osteoporotic SAMP6 mice and control SAMR1 mice. As shown in Table 1, compared to SAMR1 mice, SAMP6 mice showed a smaller amount of the most abundant immature crosslink, deH-DHLNL (1.16 moles/mole of collagen in SAMP6, 1.30 moles/mole in SAMR1) but the same amount of the major mature crosslink, Pyr (0.34 moles/mole). The two mouse models exhibited the same level of the other measurable crosslinks: the immature crosslink, deH-HLNL

Table 1: Collagen cross-links of the mandible and the femur from SAM mice.

		Mouse	Mandible ($n = 6$)	Femur ($n = 10$)	
			6 months	4 months	12 months
Immature crosslinks	deH-DHLNL	SAMR1	1.30 ± 0.01	—	—
		SAMP6	1.16 ± 0.06	—	—
	deH-HLNL	SAMR1	0.12 ± 0.01	—	—
		SAMP6	0.12 ± 0.02	—	—
Mature crosslinks	Pyr	SAMR1	0.34 ± 0.02	0.62 ± 0.03	0.80 ± 0.02
		SAMP6	0.34 ± 0.02	0.65 ± 0.02	0.84 ± 0.04
	d-Pyr	SAMR1	0.02 ± 0.01	0.028 ± 0.011	0.052 ± 0.007
		SAMP6	0.02 ± 0.00	0.030 ± 0.011	0.048 ± 0.009

Values show mean ± SD (mol/mol collagen). The data of the mandible and the femur was reported by Tokutomi et al. [14] and Silva et al. [15], respectively.

(0.12 moles/mole), and the mature crosslink, d-Pyr (0.02 moles/mole). SAMP6 showed a smaller amount of total crosslinks (1.64 moles/mole in SAMP6, 1.79 moles/mole in SAMR1) due to a decrease in the most abundant crosslink, deH-DHLNL, and a higher rate of collagen maturation (Pyr/deH-DHLNL, 0.29 in SAMP6, 0.25 in SAMR1).

Silva et al. [15] also reported the amount of mature crosslinks, Pyr and d-Pyr, in the femur of the same mouse models at 4 months and 12 months of age. In this study, Pyr showed similar levels between SAMP6 and SAMR1 mice at each age, but the values were greater in the older animals as did d-Pyr crosslinks (Table 1).

Because we [14] used the same mouse models as Silva et al. [15], the data quantifying mature crosslinks can be compared between the mandible and the femur. Although the mandible was tested at an older age than the femur (6 months versus 4 months of age, resp.), the amount of Pyr in the mandible versus the femur of SAMP6 and SAMR1 mice was 52% and 55% smaller, respectively. Similarly, the amount of d-Pyr is 67% smaller in SAMP6 mice and 71% smaller in SAMR1 mice. Given that aging increases the amount of mature crosslinks, it is likely that the mandible has a lower amount of mature crosslinks. Although we cannot compare immature crosslinks between mandible and long bones directly, an abundant quantity of deH-DHLNL, indeed, exists in mandible (Table 1). Thus, we speculate that mandible has a higher rate of immature bone collagen. The high rate of the immature crosslinks allows for easy degradation of the matrix [25] and possibly a lower degree of mineralization [18]. These properties are associated with a high rate of bone turnover.

As for another important posttranslational modification of collagen, Lys hydroxylation, we previously published a comparative study of the mandible, the humerus, and the femur in formalin-fixed cadavers [37]. The extent of Lys hydroxylation (Hyl/Lys + Hyl) was lower in the mandible (11.9%) than in the humerus (14.8%) and the femur (13.7%). However, this data has some caveats. Because formalin crosslinks Lys and Hyl residues and causes formation of their derivatives, the value of Lys and Hyl quantified by amino acid analysis may have diminished during fixation [48]. We also note that Lys hydroxylation varies across different regions of the same bone [49]. The lower Lys hydroxylation in the mandible has a number of potential implications for mandible bone physiology. Bone in senile osteoporotic mice has impaired mechanical function correlated with increased Lys hydroxylation and decreases in collagen amount [14, 15] and in thickness of collagen fibrils [14]. These data are in accordance with findings from other studies showing that overhydroxylation of Lys leads to impairment of collagen fibril formation and bone matrix organization [27, 50]. The lower Lys hydroxylation in the mandible connotes thicker collagen fibrils, which accord with the greater amount of collagen. However, the collagen fibrillogenesis is complex and elaborate by not only its posttranslational modifications but also other factors such as small leucine-rich proteoglycans [51], minor collagens, fibronectin, and integrins [52]. The collagen fibril thickness needs to be investigated.

As shown in Figure 3, the differences in collagen characteristic between the normal and osteoporotic bones are similar to those between the mandibular and long bones. The greater amount of collagen, lower rate of cross-link maturation, and lower extent of Lys hydroxylation in the mandible are suggestive of the higher rate of bone turnover and greater bone flexibility. In fact, high turnover and greater flexibility in mandibular bone are likely necessary to endure the constant and multidirectional forces of routine activities like chewing and speaking. Notably, the force placed on the mandible during mastication is almost twice as intense to the force generated during walking [53, 54]. Further investigation will test these hypotheses.

5. Relevance to Clinical Dentistry

It is important for dentists and dental researchers to understand the specific features of jaw physiology and its impact on the matrix of the jawbones. The jaw has interesting properties related to its function and age-related change in bone volume. Aging is associated with atrophy but not fracture in the jaw. The most plausible explanation is that the jaw undergoes frequent exercise but is not weight bearing.

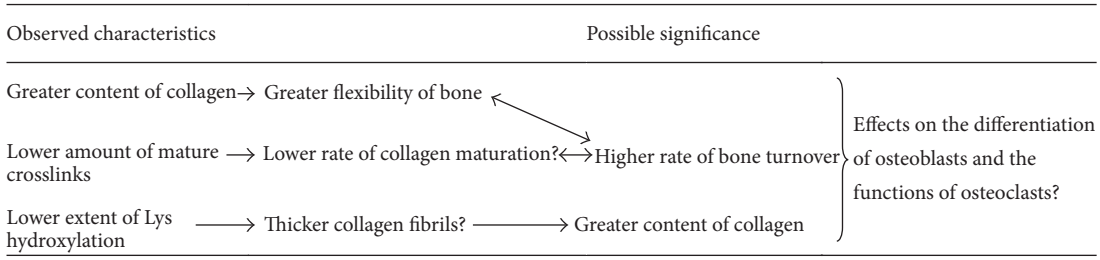

Figure 3: The collagen characteristics of the mandibular bone compared to the long bones and their possible significance.

Unfortunately, collagen in bones of the jaw is given less attention in the literature than other skeletal bones. By focusing on collagen, this review addressed limited but essential aspects of jawbone remodeling and biochemical properties.

Bone is a dynamic tissue that is constantly remodeled by osteoblasts and osteoclasts differentiated from bone marrow mesenchymal or stromal cells. These cells not only produce new bone but are also regulated by the bone matrix. Collagen crosslinking likely influences osteoblastic differentiation. For instance, lathyrogens inhibit the production of deH-DHLNL and Pyr in bone matrix produced by osteoblasts. The disturbed matrix, in turn, influences the osteoblasts by inducing upregulation of type I collagen mRNA and downregulation of osteocalcin mRNA. This suggests that optimal crosslinking accelerates osteoblastic differentiation [55].

Everts et al. hypothesize that the differences in the amount of mature crosslinks and the concomitant degradability of collagen may offer an explanation for the functional heterogeneity of proteases necessary for proper resorption of bone by osteoclasts [38, 56, 57]. Calvarial bone has a greater amount of collagen, a smaller amount of mature crosslinks, and more degradability of collagen with pepsin, cathepsin K, or matrix metalloproteinase (MMP)-2 compared with long bones [38]. The long bone osteoclasts primarily use cysteine proteinases (e.g., cathepsin K) to degrade the mature cross-linked matrix, whereas the calvarial osteoclasts resorb immature cross-linked matrix through MMPs as well [56, 57]. The mandible appears similar to calvaria in total amount of collagen and mature crosslinks. Although the proteinases used for resorption in the mandible are not clear, the osteoclasts do exhibit a number of different properties from those in the long bones [58–60].

Here we have reviewed functionally important and unique characteristics of collagen in the mandible compared to the long bones, including a greater amount of collagen, a smaller amount of mature crosslinks, and a smaller extent of Lys hydroxylation (Figure 3). These properties necessitate a high rate of collagen turnover to meet the mechanical needs of the mandible and the distinct interactions of the mandibular matrix with osteoblasts, osteoclasts, and their precursors.

To the best of our knowledge, there are no reports that characterize maxillary collagen biochemistry. Though they share a common developmental origin, the maxilla exhibits a number of key differences when compared to the mandible, such as absence of the Meckel cartilage during the developmental process [61], more porosity of bone, and a lower rate of bone turnover [1]. Clinical observations demonstrate that the maxilla has lower density and stiffness at the site of dental implant insertion [62]. Indeed, dentists often observe that a smaller force is required for tooth extraction. Though dental implant placed into the maxilla shows a sufficiently high success rate, it is nevertheless lower compared to that for the mandible [63]. In contrast, implant survival rate and changes in the marginal bone level are not associated with bone density or stiffness [62].

These clinical phenomena cannot be explained by differences in the anatomical structure or stiffness of bone alone. Because collagen also regulates cellular activities and bone remodeling, it is likely critical for anchorage and long-term maintenance of teeth and dental implants as well as the preservation of alveolar bones. Further investigation of jawbone collagen's unique biochemical properties, relationship to the matrix, and cellular interactions is needed for dentists to develop better clinical practices and introduce new technologies based on sound scientific evidence.

Conflict of Interests

The authors declare that there is no conflict of interests regarding the publication of this paper.

Acknowledgments

This review was partly supported by Grant-in-Aid 24592945 for Scientific Research (C), Japan. The authors thank Dr. Mitsuo Yamauchi, the Director of the Laboratory of Collagen Biochemistry at Dental Research Center, University of North Carolina, Chapel Hill, NC, USA, for his continuous advice and collaboration.

References

[1] S. S. Huja, S. A. Fernandez, K. J. Hill, and Y. Li, "Remodeling dynamics in the alveolar process in skeletally mature dogs," *Anatomical Record A*, vol. 288, no. 12, pp. 1243–1249, 2006.

[2] Y. Chai and R. E. Maxson Jr., "Recent advances in craniofacial morphogenesis," *Developmental Dynamics*, vol. 235, no. 9, pp. 2353–2375, 2006.

[3] A. Karaplis, "Embryonic development of bone and the molecular regulation of intramembranous and endochondral bone formation," in *Principles of Bone Biology*, J. P. Bilezikian, L. G. Raisz, and G. A. Rodan, Eds., pp. 33–58, Academic Press, San Diego, Calif, USA, 2002.

[4] Y. Ueki, V. Tiziani, C. Santanna et al., "Mutations in the gene encoding c-Abl-binding protein SH3BP2 cause cherubism," *Nature Genetics*, vol. 28, no. 2, pp. 125–126, 2001.

[5] W. F. Simonds, L. A. James-Newton, S. K. Agarwal et al., "Familial isolated hyperparathyroidism: clinical and genetic characteristics of 36 kindreds," *Medicine*, vol. 81, no. 1, pp. 1–26, 2002.

[6] S. L. Ruggiero, B. Mehrotra, T. J. Rosenberg, and S. L. Engroff, "Osteonecrosis of the Jaws Associated with the Use of Bisphosphonates: a review of 63 cases," *Journal of Oral and Maxillofacial Surgery*, vol. 62, no. 5, pp. 527–534, 2004.

[7] A. Mavropoulos, R. Rizzoli, and P. Ammann, "Different responsiveness of alveolar and tibial bone to bone loss stimuli," *Journal of Bone and Mineral Research*, vol. 22, no. 3, pp. 403–410, 2007.

[8] T. Matsubara, K. Suardita, M. Ishii et al., "Alveolar bone marrow as a cell source for regenerative medicine: differences between alveolar and iliac bone marrow stromal cells," *Journal of Bone and Mineral Research*, vol. 20, no. 3, pp. 399–409, 2005.

[9] S. O. Akintoye, T. Lam, S. Shi, J. Brahim, M. T. Collins, and P. G. Robey, "Skeletal site-specific characterization of orofacial and iliac crest human bone marrow stromal cells in same individuals," *Bone*, vol. 38, no. 6, pp. 758–768, 2006.

[10] T. L. Aghaloo, T. Chaichanasakul, O. Bezouglaia et al., "Osteogenic potential of mandibular vs. Long-bone marrow stromal cells," *Journal of Dental Research*, vol. 89, no. 11, pp. 1293–1298, 2010.

[11] M. Damek-Poprawa, D. Stefanik, L. M. Levin, and S. O. Akintoye, "Human bone marrow stromal cells display variable anatomic site-dependent response and recovery from irradiation," *Archives of Oral Biology*, vol. 55, no. 5, pp. 358–364, 2010.

[12] T. Yamaza, G. Ren, K. Akiyama, C. Chen, Y. Shi, and S. Shi, "Mouse mandible contains distinctive mesenchymal stem cells," *Journal of Dental Research*, vol. 90, no. 3, pp. 317–324, 2011.

[13] M. Saito and K. Marumo, "Collagen cross-links as a determinant of bone quality: a possible explanation for bone fragility in aging, osteoporosis, and diabetes mellitus," *Osteoporosis International*, vol. 21, no. 2, pp. 195–214, 2010.

[14] K. Tokutomi, T. Matsuura, P. Atsawasuwan, H. Sato, and M. Yamauchi, "Characterization of mandibular bones in senile osteoporotic mice," *Connective Tissue Research*, vol. 49, no. 5, pp. 361–366, 2008.

[15] M. J. Silva, M. D. Brodt, B. Wopenka et al., "Decreased collagen organization and content are associated with reduced strength of demineralized and intact bone in the SAMP6 mouse," *Journal of Bone and Mineral Research*, vol. 21, no. 1, pp. 78–88, 2006.

[16] A. J. Bailey, S. F. Wotton, T. J. Sims, and P. W. Thompson, "Post-translational modifications in the collagen of human osteoporotic femoral head," *Biochemical and Biophysical Research Communications*, vol. 185, no. 3, pp. 801–805, 1992.

[17] C. Niyibizi and D. R. Eyre, "Bone type V collagen: chain composition and location of a trypsin cleavage site," *Connective Tissue Research*, vol. 20, no. 1–4, pp. 247–250, 1989.

[18] M. Yamauchi, "Collagen: the major matrix molecule in mineralized tissues," in *Calcium and Phosphorus Nutrition in Health and Diseases*, J. J. B. Anderson and S. C. Garner, Eds., pp. 127–145, CRC Press, Boca Raton, Fla, USA, 1996.

[19] K. I. Kivirikko and R. Myllyla, "Post-translational processing of procollagens," *Annals of the New York Academy of Sciences*, vol. 460, pp. 187–201, 1985.

[20] H. Oxlund, M. Barckman, G. Ortoft, and T. T. Andreassen, "Reduced concentrations of collagen cross-links are associated with reduced strength of bone," *Bone*, vol. 17, no. 4, pp. 365S–371S, 1995.

[21] H.-H. Hong, N. Pischon, R. B. Santana et al., "A role for lysyl oxidase regulation in the control of normal collagen deposition in differentiating osteoblast cultures," *Journal of Cellular Physiology*, vol. 200, no. 1, pp. 53–62, 2004.

[22] M. Sricholpech, I. Perdivara, H. Nagaoka, M. Yokoyama, K. B. Tomer, and M. Yamauchi, "Lysyl hydroxylase 3 glucosylates galactosylhydroxylysine residues in type I collagen in osteoblast culture," *Journal of Biological Chemistry*, vol. 286, no. 11, pp. 8846–8856, 2011.

[23] M. Sricholpech, I. Perdivara, H. Nagaoka, M. Yokoyama, K. B. Tomer, and M. Yamauchi, "Lysyl hydroxylase 3 glucosylates galactosylhydroxylysine residues in type I collagen in osteoblast culture," *Journal of Biological Chemistry*, vol. 286, no. 11, pp. 8846–8856, 2011.

[24] M. Yamauchi, C. Noyes, Y. Kuboki, and G. L. Mechanic, "Collagen structural microheterogeneity and a possible role for glycosylated hydroxylysine in type I collagen," *Proceedings of the National Academy of Sciences of the United States of America*, vol. 79, no. 24, pp. 7684–7688, 1982.

[25] M. Yamauchi, E. P. Katz, and G. L. Mechanic, "Intermolecular cross-linking and stereospecific molecular packing in type I collagen fibrils of the periodontal ligament," *Biochemistry*, vol. 25, no. 17, pp. 4907–4913, 1986.

[26] S. Pornprasertsuk, W. R. Duarte, Y. Mochida, and M. Yamauchi, "Lysyl hydroxylase-2b directs collagen cross-linking pathways in MC3T3-E1 cells," *Journal of Bone and Mineral Research*, vol. 19, no. 8, pp. 1349–1355, 2004.

[27] S. Pornprasertsuk, W. R. Duarte, Y. Mochida, and M. Yamauchi, "Overexpression of lysyl hydroxylase-2b leads to defective collagen fibrillogenesis and matrix mineralization," *Journal of Bone and Mineral Research*, vol. 20, no. 1, pp. 81–87, 2005.

[28] D. R. Eyre and H. Oguchi, "The hydroxypyridinium crosslinks of skeletal collagens: their measurement, properties and a proposed pathway of formation," *Biochemical and Biophysical Research Communications*, vol. 92, no. 2, pp. 403–410, 1980.

[29] M. Yamauchi and G. L. Mechanic, "Cross-linking of collagen," in *Collagen*, M. E. Nimni, Ed., pp. 157–172, CRC Press, Boca Raton, Fla, USA, 1988.

[30] S. P. Robins and A. Duncan, "Cross-linking of collagen. Location of pyridinoline in bovine articular cartilage at two sites of the molecule," *Biochemical Journal*, vol. 215, no. 1, pp. 175–182, 1983.

[31] D. R. Eyre, M. A. Paz, and P. M. Gallop, "Cross-linking in collagen and elastin," *Annual Review of Biochemistry*, vol. 53, pp. 717–748, 1984.

[32] M. Saito, S. Soshi, and K. Fujii, "Effect of hyper- and microgravity on collagen post-translational controls of MC3T3-E1 osteoblasts," *Journal of Bone and Mineral Research*, vol. 18, no. 9, pp. 1695–1705, 2003.

[33] N. Pischon, J. M. Mäki, P. Weisshaupt et al., "Lysyl oxidase (Lox) gene deficiency affects osteoblastic phenotype," *Calcified Tissue International*, vol. 85, no. 2, pp. 119–126, 2009.

[34] K. Takaluoma, M. Hyry, J. Lantto et al., "Tissue-specific changes in the hydroxylysine content and cross-links of collagens and alterations in fibril morphology in lysyl hydroxylase 1 knock-out mice," *Journal of Biological Chemistry*, vol. 282, no. 9, pp. 6588–6596, 2007.

[35] A. J. Bailey, T. J. Sims, E. N. Ebbesen, J. P. Mansell, J. S. Thomsen, and L. Mosekilde, "Age-related changes in the biochemical properties of human cancellous bone collagen: relationship to bone strength," *Calcified Tissue International*, vol. 65, no. 3, pp. 203–210, 1999.

[36] A. J. Bailey, S. F. Wotton, T. J. Sims, and P. W. Thompson, "Biochemical changes in the collagen of human osteoporotic bone matrix," *Connective Tissue Research*, vol. 29, no. 2, pp. 119–132, 1993.

[37] M. Sasaki, T. Matsuura, M. Katafuchi, K. Tokutomi, and H. Sato, "Higher contents of mineral and collagen but lower of hydroxylysine of collagen in mandibular bone compared with those of humeral and femoral bones in human," *Journal of Hard Tissue Biology*, vol. 19, no. 3, pp. 175–180, 2010.

[38] T. van den Bos, D. Speijer, R. A. Bank, D. Brömme, and V. Everts, "Differences in matrix composition between calvaria and long bone in mice suggest differences in biomechanical properties and resorption. Special emphasis on collagen," *Bone*, vol. 43, no. 3, pp. 459–468, 2008.

[39] J. E. Aaron, "Periosteal Sharpey's fibers: a novel bone matrix regulatory system?" *Frontiers in Endocrinology*, vol. 3, article 98, pp. 1–10, 2012.

[40] A. Al-Qtaitat, R. C. Shore, and J. E. Aaron, "Structural changes in the ageing periosteum using collagen III immuno-staining and chromium labelling as indicators," *Journal of Musculoskeletal Neuronal Interactions*, vol. 10, no. 1, pp. 112–123, 2010.

[41] F. Luther, H. Saino, D. H. Carter, and J. E. Aaron, "Evidence for an extensive collagen Type III/VI proximal domain in the rat femur: I. Diminution with ovariectomy," *Bone*, vol. 32, no. 6, pp. 652–659, 2003.

[42] H. Saino, F. Luther, D. H. Carter et al., "Evidence for an extensive collagen type III proximal domain in the rat femur: II. Expansion with exercise," *Bone*, vol. 32, no. 6, pp. 660–668, 2003.

[43] D. E. Birk, "Type V collagen: heterotypic type I/V collagen interactions in the regulation of fibril assembly," *Micron*, vol. 32, no. 3, pp. 223–237, 2001.

[44] P. L. Lukinmaa and J. Waltimo, "Immunohistochemical localization of types I, V, and VI collagen in human permanent teeth and periodontal ligament," *Journal of Dental Research*, vol. 71, no. 2, pp. 391–397, 1992.

[45] G. E. Romanos, C. Schröter-Kermani, N. Hinz, H. C. Wachtel, and J. P. Bernimoulin, "Immunohistochemical localization of collagenous components in healthy periodontal tissues of the rat and marmoset (Callithrix jacchus). II. Distribution of collagen types IV, V and VI," *Journal of Periodontal Research*, vol. 26, no. 4, pp. 323–332, 1991.

[46] K. Noris Suarez, M. Romanello, P. Bettica, and L. Moro, "Collagen type I of rat cortical and trabecular bone differs in the extent of posttranslational modifications," *Calcified Tissue International*, vol. 58, no. 1, pp. 65–69, 1996.

[47] J. Aerssens, S. Boonen, G. Lowet, and J. Dequeker, "Interspecies differences in bone composition, density, and quality: potential implications for in vivo bone research," *Endocrinology*, vol. 139, no. 2, pp. 663–670, 1998.

[48] K. W. Fishbein, Y. A. Gluzband, M. Kaku et al., "Effects of formalin fixation and collagen cross-linking on T2 and magnetization transfer in bovine nasal cartilage," *Magnetic Resonance in Medicine*, vol. 57, no. 6, pp. 1000–1011, 2007.

[49] L. Moro, M. Romanello, A. Favia, M. P. Lamanna, and E. Lozupone, "Posttranslational modifications of bone collagen type I are related to the function of rate femoral regions," *Calcified Tissue International*, vol. 66, no. 2, pp. 151–156, 2000.

[50] H. Notbohm, M. Nokelainen, J. Myllyharju, P. P. Fietzek, P. K. Müller, and K. I. Kivirikko, "Recombinant human type II collagens with low and high levels of hydroxylysine and its glycosylated forms show marked differences in fibrillogenesis in vitro," *Journal of Biological Chemistry*, vol. 274, no. 13, pp. 8988–8992, 1999.

[51] S. Kalamajski and A. Oldberg, "The role of small leucine-rich proteoglycans in collagen fibrillogenesis," *Matrix Biology*, vol. 29, no. 4, pp. 248–253, 2010.

[52] K. E. Kadler, A. Hill, and E. G. Canty-Laird, "Collagen fibrillogenesis: fibronectin, integrins, and minor collagens as organizers and nucleators," *Current Opinion in Cell Biology*, vol. 20, no. 5, pp. 495–501, 2008.

[53] A. C. Knoell, "A mathematical model of an in vitro human mandible," *Journal of Biomechanics*, vol. 10, no. 3, pp. 159–166, 1977.

[54] D. J. Daegling and W. L. Hylander, "Occlusal forces and mandibular bone strain: Is the primate jaw "overdesigned"?" *Journal of Human Evolution*, vol. 33, no. 6, pp. 705–717, 1997.

[55] C. Turecek, N. Fratzl-Zelman, M. Rumpler et al., "Collagen cross-linking influences osteoblastic differentiation," *Calcified Tissue International*, vol. 82, no. 5, pp. 392–400, 2008.

[56] V. Everts, W. Korper, D. C. Jansen et al., "Functional heterogeneity of osteoclasts: matrix metalloproteinases participate in osteoclastic resorption of calvarial bone but not in resorption of long bone," *FASEB Journal*, vol. 13, no. 10, pp. 1219–1230, 1999.

[57] V. Everts, W. Korper, K. A. Hoeben et al., "Osteoclastic bone degradation and the role of different cysteine proteinases and matrix metalloproteinases: differences between calvaria and long bone," *Journal of Bone and Mineral Research*, vol. 21, no. 9, pp. 1399–1408, 2006.

[58] A. P. De Souza Faloni, T. Schoenmaker, A. Azari et al., "Jaw and long bone marrows have a different osteoclastogenic potential," *Calcified Tissue International*, vol. 88, no. 1, pp. 63–74, 2011.

[59] A. Azari, T. Schoenmaker, A. P. de Souza Faloni, V. Everts, and T. J. De Vries, "Jaw and long bone marrow derived osteoclasts differ in shape and their response to bone and dentin," *Biochemical and Biophysical Research Communications*, vol. 409, no. 2, pp. 205–210, 2011.

[60] J. A. F. Vermeer, I. D. C. Jansen, M. Marthi et al., "Jaw bone marrow-derived osteoclast precursors internalize more bisphosphonate than long-bone marrow precursors," *Bone*, vol. 57, no. 1, pp. 242–251, 2013.

[61] S. K. Lee, Y. S. Kim, H. S. Oh, K. H. Yang, E. C. Kim, and J. G. Chi, "Prenatal development of the human mandible," *Anatomical Record*, vol. 265, no. 3, pp. 314–325, 2001.

[62] G. Bergkvist, K.-J. Koh, S. Sahlholm, E. Klintström, and C. Lindh, "Bone density at implant sites and its relationship to assessment of bone quality and treatment outcome," *The International Journal of Oral & Maxillofacial Implants*, vol. 25, no. 2, pp. 321–328, 2010.

[63] P. K. Moy, D. Medina, V. Shetty, and T. L. Aghaloo, "Dental implant failure rates and associated risk factors," *International Journal of Oral and Maxillofacial Implants*, vol. 20, no. 4, pp. 569–577, 2005.

Hindawi Publishing Corporation
BioMed Research International
Volume 2014, Article ID 458287, 9 pages
http://dx.doi.org/10.1155/2014/458287

Research Article

Dried Fruit of the *Luffa* Sponge as a Source of Chitin for Applications as Skin Substitutes

Ping-Lun Jiang,[1] Mei-Yin Chien,[2,3] Ming-Thau Sheu,[4,5] Yi-You Huang,[1] Meng-Hsun Chen,[6] Ching-Hua Su,[7] and Der-Zen Liu[6,8]

[1] *Institute of Biomedical Engineering, College of Engineering and College of Medicine, National Taiwan University, Taipei 100, Taiwan*
[2] *School of Dentistry, College of Oral Medicine, Taipei Medical University, Taipei 110, Taiwan*
[3] *Ko Da Pharmaceutical Co., Taoyuan 324, Taiwan*
[4] *School of Pharmacy, College of Pharmacy, Taipei Medical University, Taipei 110, Taiwan*
[5] *Clinical Research Center and Traditional Herbal Medicine Research Center, Taipei Medical University Hospital, Taipei 110, Taiwan*
[6] *Graduate Institute of Biomedical Materials and Tissue Engineering, College of Oral Medicine, Taipei Medical University, Taipei 110, Taiwan*
[7] *Department of Microbiology and Immunology, School of Medicine, College of Medicine, Taipei Medical University, Taipei 110, Taiwan*
[8] *Center for General Education, Hsuan Chuang University, Hsinchu 300, Taiwan*

Correspondence should be addressed to Ching-Hua Su; curator@tmu.edu.tw and Der-Zen Liu; tonyliu@tmu.edu.tw

Received 8 February 2014; Accepted 5 March 2014; Published 9 April 2014

Academic Editor: Yoshihiko Hayashi

LUFFACHITIN obtained from the residue of the sponge-like dried fruit of *Luffa aegyptiaca* was developed as a weavable skin substitute in this study. A chemical analysis revealed that *LUFFACHITIN* was composed of a copolymer containing N-acetyl-glucosamine (~40%) as a major monomer with a filamentary structure as demonstrated by both optical and scanning electron microscopy. The pulp-like white residue of the sponge-like dried fruit of *Luffa aegyptiaca* after treatment was then woven into a thin, porous membrane by filtration and lyophilization as a skin substitute for conducting wound-healing study on rats. The results indicated that the *LUFFACHITIN* membrane showed significant wound-healing enhancement (25 days to complete healing) compared to cotton gauze (>30 days), but not inferior to that of *SACCHACHITIN*. Furthermore, the *LUFFACHITIN* membrane had advantages of having a high yield, better physical properties for fabrication, and a more attractive appearance.

1. Introduction

In an endeavor to develop ideal skin substitutes, the performance of *SACCHACHITIN* membranes, prepared from the residue of the fruiting body of the medicinal fungus, *Ganoderma tsugae*, as an effective skin prosthesis was examined [1]. The effectiveness of the *SACCHACHITIN* membrane in managing excised wounds in guinea pigs was demonstrated to be better than that of gauze and comparable to that of Beschitin, which is mainly composed of chitin from crabs. The *SACCHACHITIN* membrane is able to promote wound healing by inducing cell proliferation. A mildly acute inflammatory reaction attracted a large number of polymorphonuclear leukocytes and some macrophages to clean away debris and blood clots [2]. Also the secretion of cell cytokines and growth factors by these cells provided an excellent environment for wound healing [3, 4]. The migration of fibroblast cells, which was promoted by *SACCHACHITIN*, also plays another important role in accelerating wound healing [1]. Furthermore, the fibrous structure of *SACCHACHITIN* made it convenient to produce a skin substitute with desirable pore characteristics.

Luffa is a genus of tropical and subtropical vines classified in the cucumber (Cucurbitaceae) family. In everyday

nontechnical usage, the name, also spelled loofah, usually refers to the fruit of the two species, *L. aegyptiaca/cylindrical* (Smooth *Luffa*, its fruit somewhat resembles a cucumber) and *L. acutangula* (Angled *Luffa*, its fruit slightly resembles a cucumber or zucchini with ridges). The fruits of these species are cultivated and eaten as a vegetable. When the fruit is fully ripened, it is very fibrous. The fully developed fruit is the source of the loofah scrubbing sponge which is used in bathrooms and kitchens as a sponge tool. *Luffa* has fruits possessing a net-like fibrous vascular system (*Luffa* sponges) consisting of cellulose and lignin (1.4% and 2.9%, respectively, of the sponge dry weight) [5]. The struts of this natural sponge are characterized by a microcellular architecture with continuous hollow microchannels (with diameters of 10~20 μm) which form vascular bundles and yield a multimodal hierarchical pore structure. To the present, *Luffa* sponges have been applied to immobilize biocatalysts such as enzymes, microorganisms, organelles, and plant and animal cells in bioreactors [6–15], scaffolds for tissue engineering [16, 17], and dye absorbents from aqueous solutions [18–20] and for developing biofiber-reinforced bionanocomposites [21–23].

The sponge vegetable from *L. aegyptiaca* is the dried fruit fiber of the sponge cucumber or sponge gourd, which is a commonly eaten vegetable in Taiwan. Similarly, the sponge-like structure of dried fruit fibers makes it suitable for cleaning the body and dishes. These dried fibers are tenacious and can be cooked for a long time with no sign of dissolution, which is similar to the characteristics of *SACCHACHITIN*. It was suspected that the main component in these fibers was chitin just as in *SACCHACHITIN*. The potential of this fibrous material for applications as a skin substitute encouraged us to conduct this study.

2. Materials and Methods

2.1. Materials. Dried fruit fibers of *L. aegyptiaca* were purchased from a local market in Taipei, Taiwan. N-acetylglucosamine, glucosamine, and ketamine were supplied by Sigma (St. Louis, MO, USA). Glucose and galactose were obtained from Nihon Shiyaku Industrial (Taipei, Taiwan). Trifluoroacetic acid and pyridine were provided by Riedel-de Haën (Seelze, Germany). n-Butanol was from Hayashi Pure Chemical (Osaka, Japan). Thin-layer chromatography (TLC) plates (Kieselgel 5554) and the solvents for high-performance liquid chromatography (HPLC) and analytical-grade reagents were obtained from Merck (Hohenbrunn, Germany). Pentobarbital was supplied by Siegfried AG (Zofingen, Switzerland).

2.2. Preparation of Luffa Membranes. The dried fruit fibers were pulverized and autoclaved for 20 min to soften the fibrous structure and then were blended to make a paste. The paste was then digested with 1 N NaOH at 85°C for 4 h. The residue was collected and washed with deionized water to remove any residual NaOH. Hypochlorite at 0.1% was then used to depigment the fibers. After removal of any residual hypochlorite by repeated washing with deionized water, the fibers of lengths ranging 10~50 μm were collected and dispersed in deionized water to form a suspension. The suspension was filtered using filter paper under aseptic conditions. The membrane formed on the filter paper was then freeze-dried (EYELA, model FD-5N, Japan) to obtain the final product for further analysis and animal tests. The membrane so obtained was called "*LUFFACHITIN*."

2.3. Chemical Analysis of Membrane Components

2.3.1. Sugar Components [24]. Two grams of the *LUFFACHITIN* membrane was first pulverized, and then 5 mg of this powder, selected randomly, was digested with 0.25 mL of either 2 N HCl (HC-) or CF_3COOH (HF-) at 100°C for 5 (HC-5; HF-5), 10 (HC-10; HF-10), and 15 h (HC-15; HF-15) in a sealed ampoule. After hydrolysis, each 250 μL of distilled water and pyridine was added to each ampoule and mixed thoroughly. The hydrolyte residue of this mixture was divided into two portions and separately analyzed by TLC for aldose/ketose and amino sugar using glucose (galactose) and N-acetylglucosamine (glucosamine), respectively, as reference standards. The developing agent used in the TLC analysis was pyridine : n-butanol : 0.1 N HCl at 30 : 50 : 20, and the respective visualizing agents were naphthoresorcinol for aldose (purple)/ketose (red or pink) and the Elson-Morgan solution for amino sugar.

HPLC was also used to determine the kind of monosaccharides (glucose, galactose, mannose, glucosamine, and N-acetylglucosamine) in the hydrolyte of the *LUFFACHITIN* membrane. The HPLC system consisted of a pump (Shimadzu LC-10AT, Tokyo, Japan), a manual injector (Rheodyne, Tokyo, Japan), and a column (CHO-620, 250 × 4.6 mm, 5 μm, Merck) operated at 63°C. The mobile phase consisted of only deionized water at a flow rate of 0.5 mL/min. The eluent was detected with an RI detector (Shimadzu, RID-10A, Tokyo, Japan).

2.4. Sugar Skeleton Analysis. The sugar skeleton of *LUFFACHITIN* was determined by a gas chromatography/mass spectroscopic (GC/MS) method (Hewlett Packard 5890 plus series II and Hewlett Packard, mass spectrometer 5989B). After methylation, hydrolysis, reduction, and acetylation, the pattern of fragmentation of the mass spectrum of the final product was compared to reference standards for elucidation of the sugar skeleton. GC was equipped with a capillary column (with a length of 50 m and an inner diameter of 0.25 mm) packed with dimethyl siloxane. The temperature of the injector port was 250°C, and heating was programmed from 150 to 240°C at a rate of 2°C/min. Helium was the carrier gas delivered at 1.8 mL/min with a split ratio giving a flow rate of 1.53 mL/min and maintaining a constant pressure of 1.8 kg/cm^2. Glucose, galactose, mannose, glucosamine, and N-acetylglucosamine were used as reference standards in both the TLC and GC analyses.

2.5. Scanning Electronic Microscopic (SEM) Examinations. Dried samples were loaded onto aluminum studs and coated with gold for 3 min at 8 mA under a pressure of 0.1 torr.

Samples were scanned and examined using a Hitachi model S-2400 SEM.

2.6. Wound-Healing Studies. This animal experiment was approved by the Institutional Animal Care and Use Committee of Taipei Medical University (approval number LAC-100-0101). Prior to the study, rats were anesthetized with separate intraperitoneal (i.p.) injections of ketamine (35 mg/kg) and pentobarbital (12 mg/kg). The dorsal hair of the rats was removed with an electric razor. Equal areas of two parts in a mirror image were marked along the spinal cord, 4.5 cm behind the ear of the rats and 1 cm away from the spinal cord, and two pieces of full-thickness skin, each with a surface area of about 4.0 cm^2, were excised. The lesion on the left-hand side was covered with an equal size of *SACCHACHITIN* or cotton gauze for comparison. The right-hand side was covered with the *LUFFACHITIN* membrane prepared above. Treated rats were placed in individual cages with an air-filtering device at 30°C and 55±% humidity, where they had free access to food and water. After surgery, changes in the area of the wounds were measured on days 4, 7, 11, 14, 18, 21, and 25, after which fresh dressings were applied. A digital camera was used to document the lesion, and Image-Pro Plus was used to calculate the wound area on the image of the lesion so obtained. Five male rats for each group were included in two comparative studies, and results are reported as the mean with the standard deviation (SD). Student's *t*-test was performed using the SPSS statistic software (PASW Statistics 18.0). Difference was considered significant when the *P* value was less than 0.05.

3. Results

Figure 1 shows the appearance of *LUFFACHITIN* (Figure 1(a1), from *L. aegyptiaca*) developed in different stages of treatment compared to that of *SACCHACHITIN* (Figure 1(b1), from the fruiting body of *Ganoderma*). Dried fruit fibers of *L. aegyptiaca* appeared fiber-like with a light-yellow color as shown in Figures 1(a2) and 1(a3), whereas the fruiting body of *Ganoderma* was a reddish-brown color with a less-fibrous form and a more-tendon-like structure demonstrated by Figures 1(b2) and 1(b3). Microscopic examination of the *LUFFACHITIN* membrane (Figure 1(a4)) clearly showed that the light-yellow fibers of *L. aegyptiaca* were transformed into soft, transparent fibers that formed a porous structure, while *SACCHACHITIN* fibers appeared to be opaque that formed a porous structure as well (Figure 1(b4)).

The TLC analysis of the acid-treated hydrolyte of *LUFFACHITIN* membrane is shown in Figure 2. With hydrolysis at the same concentration and time interval, a spot visualized by naphthoresorcinol to be purple appeared in all hydrolytes except that reacting with HCl for only 5 h (HCl-5, Figure 2(a)) as shown in Figure 2(a). Since a purple spot was visualized after treatment with naphthoresorcinol and appeared at similar retention time with glucose/galactose standard in TLC plate, it was concluded that aldose of glucose/galactose is one of the major sugar components of *LUFFACHITIN*. Figure 2(b) reveals the presence of N-acetylglucosamine in all acid-treated hydrolytes of the *LUFFACHITIN* membrane, which was confirmed by referring to the N-acetylglucosamine standard with visualization of a purple-violet color. Another purple spot corresponding to the glucosamine standard only appeared in hydrolytes treated with a stronger acid for the longest time interval (CF-15, lane 8, Figure 2(b)). It was concluded that amino sugar of N-acetylglucosamine is another major sugar component of *LUFFACHITIN*.

Figures 3(a)–3(e) illustrated the results of HPLC analysis for monosaccharide standards of glucose, galactose, mannose, glucosamine, and N-acetylglucosamine, respectively, and Figure 3(f) revealed that for acidic hydrolytes of *LUFFACHITIN* as exemplified by HF-15, which was hydrolyzed in CF_3COOH for 15 h. In comparison with aldose standards, it is obvious that the major broad peak in HPLC graph of HF-15 at a retention time around 5.5 min corresponds with the mixture of aldoses, including glucose (5.697 min), galactose (5.287 min), and mannose (5.653 min). This result conforms to that of TLC as deduced above. Another major peak in HPLC graph of HF-15 appears at a retention time similar to that of N-acetylglucosamine standard (Figure 3(e)) but not glucosamine (Figure 3(d)). This result is also consistent with that revealed by TLC analysis. Since a complete acidic hydrolysis of *LUFFACHITIN* in CF_3COOH for 15 h was expectable, the area under the peak corresponding to N-acetylglucosamine would be the highest amount of N-acetylglucosamine released by acidic treatment of *LUFFACHITIN*. The area under this peak was calculated to be ~ 40% of total peak area in HPLC graph, which means that *LUFFACHITIN* is composed of ~40% N-acetylglucosamine and the rest of 60% is glucose (or a mixture of aldoses).

Figure 4 shows a GC graph (Figure 4(a)) of the final products of *LUFFACHITIN* after methylation, hydrolysis, reduction, and acetylation treatments with corresponding mass spectra for elution peaks at 4.64 (Figure 4(c)), 5.95 (Figure 4(d)), 6.66 (Figure 4(e)), and 6.95 (Figure 4(f)) min. Figure 4(b) reveals that the characteristic fragments for N-acetylglucosamine in the structure of poly[β-1,4-N-acetyl-D-glucosamine] included 45, 71, 73, and 189 m/z. The mass spectrum of the elution peak at 6.66 min demonstrated those characteristic fragments, further confirming poly[β-1,4-N-acetyl-D-glucosamine] to be part of the structural unit of *LUFFACHITIN*. Following the same principle as elucidated by the fragmentation of poly[β-1,4-N-acetyl-D-glucosamine], characteristic fragments for poly-β-1,4-glucose and poly-β-1,3-glucose (β-1,3-glucan) were 45, 117, 161, and 205 m/z and 45, 117, 161, and 233 m/z, respectively. All those characteristic fragments except 205 m/z for poly-β-1,4-glucose and 233 m/z for poly-β-1,3-glucose appeared in the mass spectra for elution peaks at 4.64, 5.95, and 6.95 min. It seems to indicate that besides the most abundant structural units of poly-β-1,4-glucose in nature being a part of structural unit of *LUFFACHITIN*, poly-β-1,3-glucose backbone could not be excluded.

The wound-healing process for the wound covered by the *LUFFACHITIN* membrane was compared to both cotton gauze and *SACCHACHITIN*. Photographic results are shown

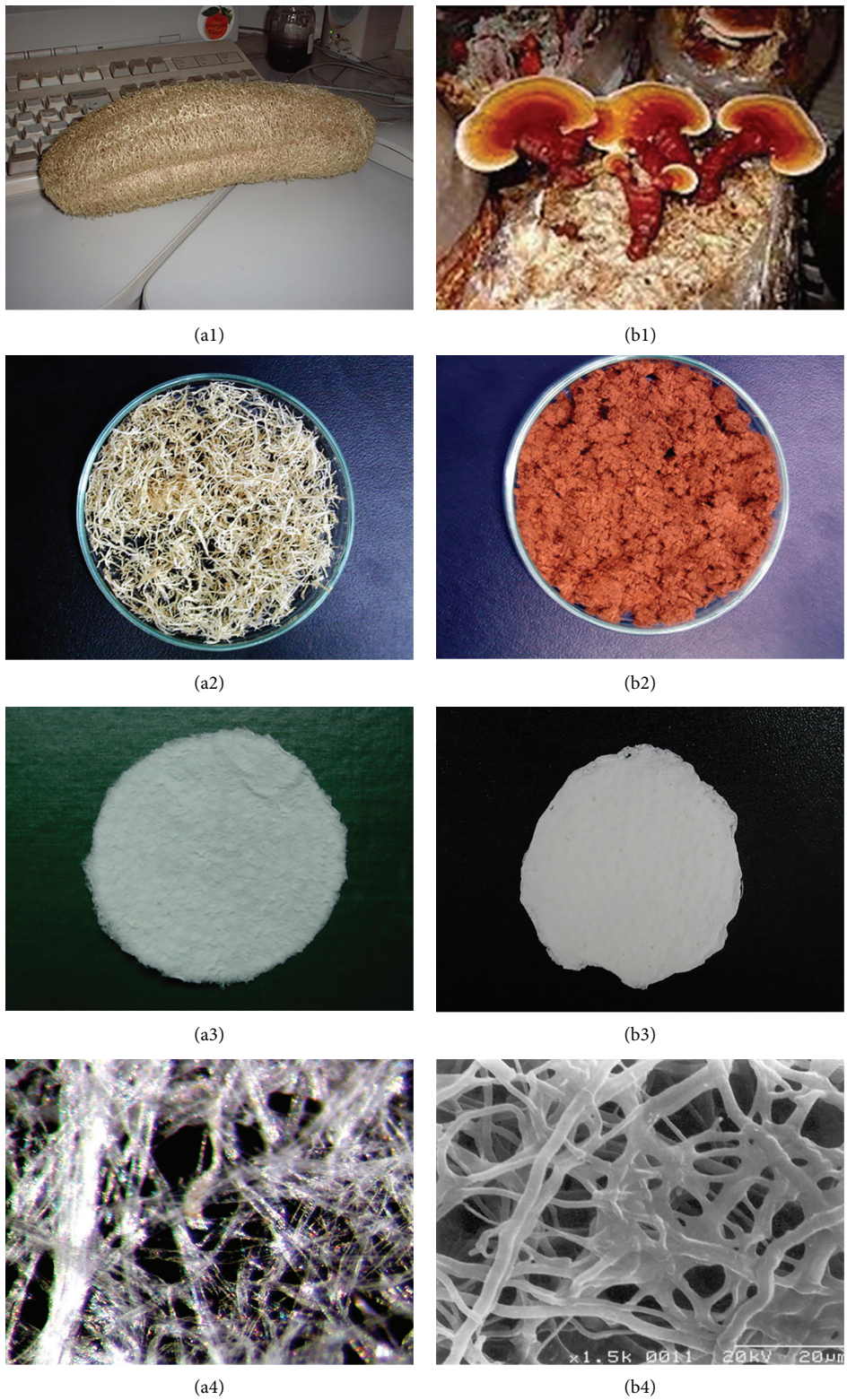

Figure 1: Appearance of the *LUFFACHITIN* membrane collected at different stages of purification. (a) *Luffa aegyptiaca* and (b) *Ganoderma*; (1) original material; (2) residue after alkaline treatment; (3) the final product; (4) microscopic photographs. The scale bar of (a4) is the same with that of (b4).

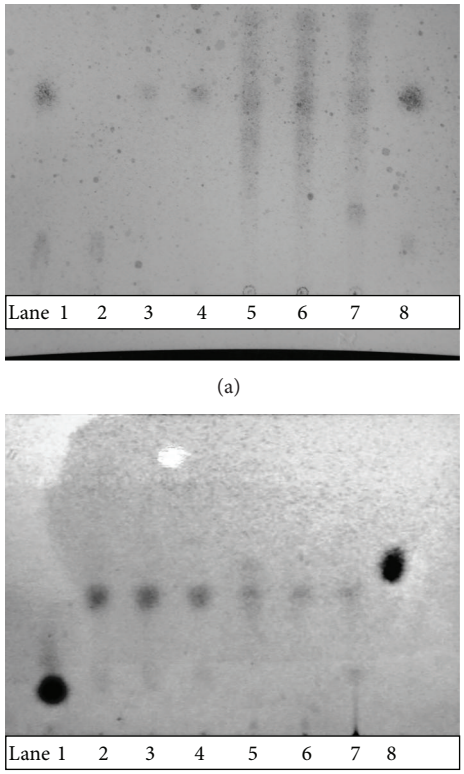

Figure 2: Thin-layer chromatography of the acid-treated hydrolysate (HCl: HC-5, HC-10, and HC-15; CF_3COOH: HF-5, HF-10, and HF-15) of the *LUFFACHITIN* membrane developed by pyridine : n-butanol : 0.1 N HCl at 30 : 50 : 20 and visualized by spraying the naphthoresorcinol reagent (a) or Elson-Morgan reagent (b) and heating to 100°C for 3 min. Lanes 1~8: glucose (N-acetylglucosamine), HC-5, HC-10, HC-15, HF-5, HF-10, HF-15, and galactose (glucosamine).

in the upper panel of Figures 5 and 6. The wound area contraction plotted versus time was shown in the bottom panels of Figures 5 and 6, respectively, to compare the progress of wound healing using these different skin substitutes or wound dressings. In comparison to the control covered with cotton gauze, quite significant improvement in the wound-healing process with the *LUFFACHITIN* membrane was observed by the change in the wound area. The difference between the *LUFFACHITIN* and *SACCHACHITIN* membranes was observed to be minimal. The wound lesion of 4.0-cm^2 had completely healed after covering with either substance for 25 days. Skin tissue with normal function recovered, and dorsal hairs also regrew in the healed wound area.

4. Discussion

During treatment, it was found that a longer time in harsher conditions was taken to soften and depigment the *SACCHACHITIN* preparation than the *LUFFACHITIN* preparation. Because of that, the total recovery for *LUFFACHITIN* was about 70%, whereas it was only about 20% for *SACCHACHITIN*. To be effective as a skin substitute or dressing to treat wounds like with *SACCHACHITIN*, the porous structures that appeared in the *LUFFACHITIN* membrane were recognized as an important characteristic. Microscopic examination clearly showed that the *LUFFACHITIN* membrane is composed of soft and transparent fibers that formed a porous structure. The pore size of these membranes could be optimally controllable by adjusting the fiber concentration of the filtrate during preparation of the membrane. Furthermore, the *LUFFACHITIN* membrane was softer like facial tissues with better water-absorption ability than the *SACCHACHITIN* membrane (personal observation). The softness allowed the membrane to easily attach to the skin contour, and the better ability to absorb water led to the efficient expulsion of exudates. It would be expectable to have a minimal injury to skin surface where it attached to and enhance the skin recovery.

It was confirmed that the main constituents of *LUFFACHITIN* are aldose of glucose/galactose and amino sugar of N-acetylglucosamine by TLC and HPLC. The acetylation products of the hydrolyte determined by GC analysis (data not shown) were also demonstrated to be these two ingredients (glucose and N-acetylglucosamine). In comparison with a calibration standard curve, the ratio of these two components was found to be 60.15 to 39.85. The TLC diagram was also used to validate that the sugar components are released by digestion with various enzymes (data not shown). It demonstrates that only β-glucosidase and chitinase are able to hydrolyze *LUFFACHITIN* and the resulting sugar components were determined to be glucose and N-acetylglucosamine. Measurement of the protein content of *LUFFACHITIN* produced no color reaction implying that *LUFFACHITIN* contains virtually no protein. The total nitrogen content was determined to be 3.46%, which was equivalent to the total nitrogen content of N-acetylglucosamine, further confirming that sponge gourd from *Luffa aegyptiaca* is composed mainly of the β-form of glucan and poly-N-acetylglucosamine.

Regarding the wound-healing improvement, quite significant improvement with the *LUFFACHITIN* membrane was observed in comparison to the control covered with cotton gauze. The difference between the *LUFFACHITIN* and *SACCHACHITIN* membranes was observed to be minimal. Overall, the *LUFFACHITIN* membrane could be utilized as a wound dressing or skin substitute with an efficacy comparable to that of *SACCHACHITIN* but better than gauge. As reposted, the chitin (polymeric N-acetyl-glucosamine) was demonstrated to play an important role for chitin-containing materials in the wound-healing process [25–27]. Previously, the proliferation of human F1000 fibroblasts was also found to correlate with the chitin content of various fungal cultures [28]. As revealed above, N-acetylglucosamine is one of the two main components of the *LUFFACHITIN* membrane. Therefore, the comparable efficacy of the *LUFFACHITIN* membrane with respect to *SACCHACHITIN* in the wound-healing process can partly be attributed to N-acetylglucosamine, a major monomer in the structure of chitin. In addition, the immunological effects and influence

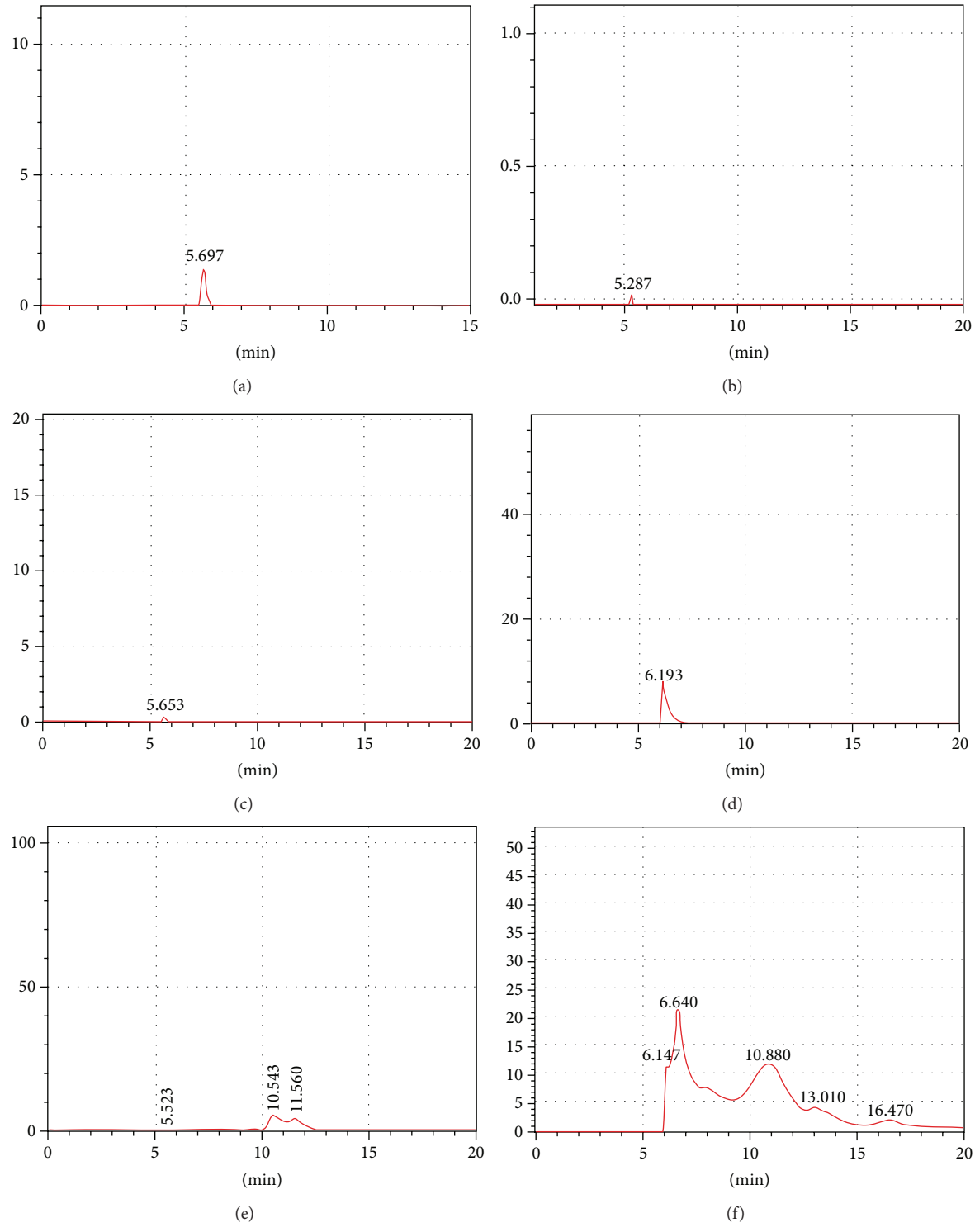

Figure 3: HPLC analytical graphs for various sugar standards and HF-15. (a) Glucose (5 mg/mL, 5.697 min); (b) galactose (1 mg/mL, 5.287 min); (c) mannose (1 mg/mL, 5.653 min); (d) glucosamine (0.5 mg/mL, 6.193 min); (e) N-acetyl-D-glucosamine (0.5 mg/mL, minor/5.523; major/10.543 and 11.560 min); (f) HF-15.

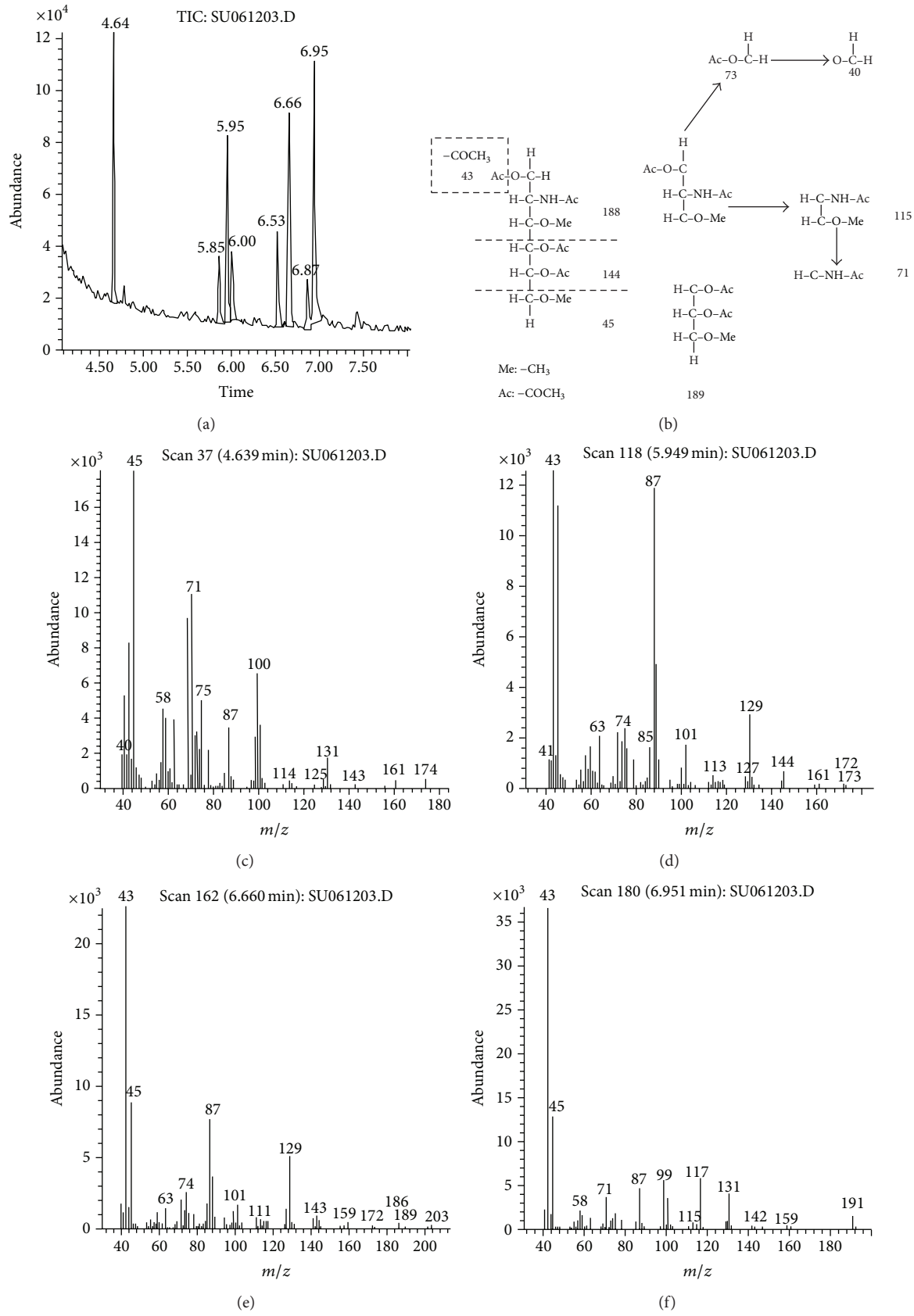

Figure 4: Gas chromatography/mass spectrum (GC/MS) of the final product of *LUFFACHITIN* after methylation, hydrolysis, reduction, and acetylation treatments. (a) GC chromatography; (b) proposed fragmentation of poly-N-acetylglucosamine after treatment; (c)–(f) mass spectra of respective elution peaks at 4.64, 5.95, 6.66, and 6.95 min.

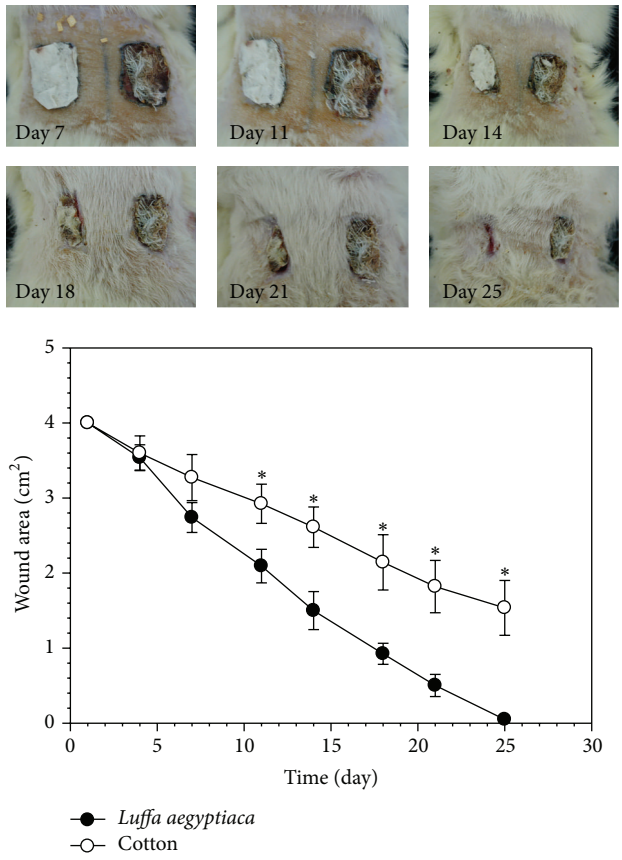

Figure 5: Top panel: example of photographic illustrations of the wound-healing process using covering with either cotton gauze (right-hand side) or *LUFFACHITIN* membrane (left-hand side) on days 7, 11, 14, 18, 21, and 25. Bottom panel: comparison of the contraction curves of the wound areas after treatment with cotton gauze (○) and the *LUFFACHITIN* membrane (●) ($n = 5$). $^*P < 0.05$.

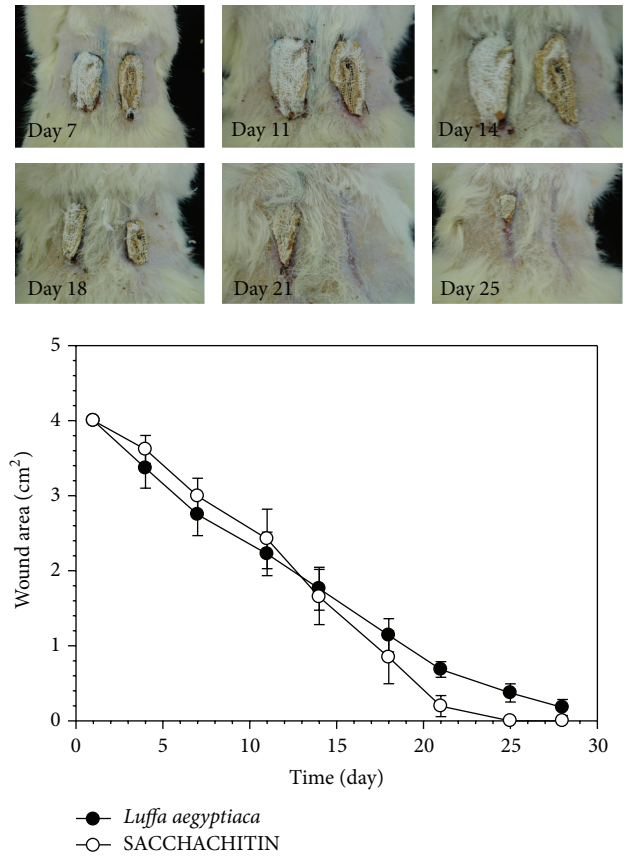

Figure 6: Top panel: example of photographic illustrations of the wound-healing process covered with either a *SACCHACHITIN* (right-hand side) or *LUFFACHITIN* membrane (left-hand side) on days 7, 11, 14, 18, 21, and 25. Bottom panel: comparison of the contraction curves of the wound areas after treatment with the *SACCHACHITIN* (○) and *LUFFACHITIN* membranes (●) ($n = 5$). $^*P < 0.05$.

of β-1,3-glucan on wound healing are elucidated in greater detail elsewhere [29–31]. The potential possibility of a 1,3-linkage for polysaccharides obtained from *L. aegyptiaca* is illustrated although the linkage of the glucose unit has not been confirmed. Since being another main component in the *LUFFACHITIN* membrane, the potential role of β-1,3-glucan in the promotion of wound healing and in the retardation of scar formation cannot be ignored. Biochemical evaluations of the wound-healing process treated with the *LUFFACHITIN* membrane are under progress.

Conflict of Interests

The authors declare that there is no conflict of interests regarding the publication of this paper.

Authors' Contribution

Ping-Lun Jiang and Mei-Yin Chien contributed equally to this work.

Acknowledgments

Both financial support from the Center of Excellence for Clinical Trials and Research in Neuroscience (DOH 100-TD-B-111-003) and partial support from the National Science Council (NSC-97-2320-B-038-005-MY3) are highly appreciated.

References

[1] C.-H. Su, C.-S. Sun, S.-W. Juan, C.-H. Hu, W.-T. Ke, and M.-T. Sheu, "Fungal mycelia as the source of chitin and polysaccharides and their applications as skin substitutes," *Biomaterials*, vol. 18, no. 17, pp. 1169–1174, 1997.

[2] C.-H. Su, S.-H. Liu, S.-Y. Yu et al., "Development of fungal mycelia as a skin substitute: characterization of keratinocyte proliferation and matrix metalloproteinase expression during improvement in the wound-healing process," *Journal of Biomedical Materials Research Part A*, vol. 72, no. 2, pp. 220–227, 2005.

[3] S. E. Gill and W. C. Parks, "Metalloproteinases and their inhibitors: regulators of wound healing," *International Journal*

of Biochemistry and Cell Biology, vol. 40, no. 6-7, pp. 1334–1347, 2008.

[4] R. K. Chittoria, "Role of growth factors in wound healing," *Journal of Society For Wound Care and Research*, vol. 5, no. 1, pp. 2–6, 2012.

[5] S.-C. Chang, M.-S. Lee, C.-H. Li et al., "Dietary fibre content and composition of vegetables in Taiwan area," *Asia Pacific Journal of Clinical Nutrition*, vol. 4, pp. 204–211, 1995.

[6] R. Pazzetto, S. B. Ferreira, E. J. Santos et al., "Preservation of Bacillus firmus strain 37 and optimization of cyclodextrin biosynthesis by cells immobilized on loofa sponge," *Molecules*, vol. 17, no. 8, pp. 9476–9488, 2012.

[7] S. A. Meleigy and M. A. Khalaf, "Biosynthesis of gibberellic acid from milk permeate in repeated batch operation by a mutant Fusarium moniliforme cells immobilized on loofa sponge," *Bioresource Technology*, vol. 100, no. 1, pp. 374–379, 2009.

[8] S. Kar, M. R. Swain, and R. C. Ray, "Statistical optimization of alpha-amylase production with immobilized cells of Streptomyces erumpens MTCC 7317 in *Luffa cylindrica* l. sponge discs," *Applied Biochemistry and Biotechnology*, vol. 152, no. 2, pp. 177–188, 2009.

[9] P. S. Saudagar, N. S. Shaligram, and R. S. Singhal, "Immobilization of Streptomyces clavuligerus on loofah sponge for the production of clavulanic acid," *Bioresource Technology*, vol. 99, no. 7, pp. 2250–2253, 2008.

[10] M. Phisalaphong, R. Budiraharjo, P. Bangrak, J. Mongkolkajit, and S. Limtong, "Alginate-loofa as carrier matrix for ethanol production," *Journal of Bioscience and Bioengineering*, vol. 104, no. 3, pp. 214–217, 2007.

[11] A. Hideno, J. C. Ogbonna, H. Aoyagi, and H. Tanaka, "Acetylation of loofa (*Luffa cylindrica*) sponge as immobilization carrier for bioprocesses involving cellulase," *Journal of Bioscience and Bioengineering*, vol. 103, no. 4, pp. 311–317, 2007.

[12] R. Ganguly, P. Dwivedi, and R. P. Singh, "Production of lactic acid with loofa sponge immobilized Rhizopus oryzae RBU2-10," *Bioresource Technology*, vol. 98, no. 6, pp. 1246–1251, 2007.

[13] M. Iqbal, A. Saeed, R. G. J. Edyvean, B. O'Sullivan, and P. Styring, "Production of fungal biomass immobilized loofa sponge (FBILS)-discs for the removal of heavy metal ions and chlorinated compounds from aqueous solution," *Biotechnology Letters*, vol. 27, no. 17, pp. 1319–1323, 2005.

[14] M. Iqbal and S. I. Zafar, "Vegetable sponge as a matrix to immobilize micro-organisms: a trial study for hyphal fungi, yeast and bacteria," *Letters in Applied Microbiology*, vol. 18, no. 4, pp. 214–217, 1994.

[15] T. Pekdemir, B. Keskinler, E. Yildiz, and G. Akay, "Process intensification in wastewater treatment: ferrous iron removal by a sustainable membrane bioreactor system," *Journal of Chemical Technology and Biotechnology*, vol. 78, no. 7, pp. 773–780, 2003.

[16] J.-P. Chen and T.-C. Lin, "Loofa sponge as a scaffold for culture of rat hepatocytes," *Biotechnology Progress*, vol. 21, no. 1, pp. 315–319, 2005.

[17] J.-P. Chen, S.-C. Yu, B. R.-S. Hsu, S.-H. Fu, and H.-S. Liu, "Loofa sponge as a scaffold for the culture of human hepatocyte cell line," *Biotechnology Progress*, vol. 19, no. 2, pp. 522–527, 2003.

[18] A. Altinişik, E. Gür, and Y. Seki, "A natural sorbent, *Luffa cylindrica* for the removal of a model basic dye," *Journal of Hazardous Materials*, vol. 179, no. 1–3, pp. 658–664, 2010.

[19] E. S. Z. El Ashtoukhy, "Loofa egyptiaca as a novel adsorbent for removal of direct blue dye from aqueous solution," *Journal of Environmental Management*, vol. 90, no. 8, pp. 2755–2761, 2009.

[20] H. Demir, A. Top, D. Balköse, and S. Ülkü, "Dye adsorption behavior of *Luffa cylindrica* fibers," *Journal of Hazardous Materials*, vol. 153, no. 1-2, pp. 389–394, 2008.

[21] G. Siqueira, J. Bras, N. Follain et al., "Thermal and mechanical properties of bio-nanocomposites reinforced by *Luffa cylindrica* cellulose nanocrystals," *Carbohydrate Polymers*, vol. 91, no. 2, pp. 711–717, 2013.

[22] C. A. Boynard, S. N. Monteiro, and J. R. M. D'Almeida, "Aspects of alkali treatment of sponge gourd (*Luffa cylindrica*) fibers on the flexural properties of polyester matrix composites," *Journal of Applied Polymer Science*, vol. 87, no. 12, pp. 1927–1932, 2003.

[23] G. Siqueira, J. Bras, and A. Dufresne, "*Luffa cylindrica* as a lignocellulosic source of fiber, microfibrillated cellulose, and cellulose nanocrystals," *BioResources*, vol. 5, no. 2, pp. 727–740, 2010.

[24] C. F. Chaplin, "Monosaccharides," in *Carbohydrate Analysis*, M. F. Chaplin and J. F. Kennedy, Eds., pp. 1–53, IRL Press, Oxford, UK, 1987.

[25] L. L. Balassa, "Use of chitin for promoting wound healing," U. S. Patent No. US3632754 (A). Lescarden LTD, Goshen, NY, USA, 1972.

[26] L. L. Balassa, "Chitin and chitin derivatives for promoting wound healing," U. S. Patent No. US3903268 (A). Lescarden LTD, Goshen, NY, USA, 1975.

[27] R. Singh and D. Singh, "Chitin membranes containing silver nanoparticles for wound dressing application," *International Wound Journal*, 2012.

[28] L. Y. C. Lip Yong Chung, R. J. Schmidt, P. F. Hamlyn, B. F. Sagar, A. M. Andrews, and T. D. Turner, "Biocompatibility of potential wound management products: fungal mycelia as a source of chitin/chitosan and their effect on the proliferation of human F1000 fibroblasts in culture," *Journal of Biomedical Materials Research*, vol. 28, no. 4, pp. 463–469, 1994.

[29] O. Karaaslan, Y. Kankaya, N. Sungur et al., "Case series of topical and orally administered beta-glucan for the treatment of diabetic wounds: clinical study," *Journal of Cutaneous Medicine and Surgery*, vol. 16, no. 3, pp. 180–186, 2012.

[30] T. Kiho, M. Sakushima, S. Wang, K. Nagai, and S. Ukai, "Polysaccharides in fungi. XXVI. Two branched (1 → 3)-β-D-glucans from hot water extract of Yuěr," *Chemical and Pharmaceutical Bulletin*, vol. 39, no. 3, pp. 798–800, 1991.

[31] K. Saito, M. Nishijima, and T. Miyazaki, "Further examination on the structure of an alkali-soluble glucan isolated from Omphalia lapidescens. Studies on fungal polysaccharide. XXXVI," *Chemical and Pharmaceutical Bulletin*, vol. 38, no. 6, pp. 1745–1747, 1990.

Hindawi Publishing Corporation
BioMed Research International
Volume 2014, Article ID 630757, 9 pages
http://dx.doi.org/10.1155/2014/630757

Research Article

Biological Safety of Fish (Tilapia) Collagen

Kohei Yamamoto, Kazunari Igawa, Kouji Sugimoto, Yuu Yoshizawa, Kajiro Yanagiguchi, Takeshi Ikeda, Shizuka Yamada, and Yoshihiko Hayashi

Department of Cariology, Nagasaki University Graduate School of Biomedical Sciences, Nagasaki 852-8588, Japan

Correspondence should be addressed to Yoshihiko Hayashi; hayashi@nagasaki-u.ac.jp

Received 26 December 2013; Accepted 26 February 2014; Published 7 April 2014

Academic Editor: Mitsuo Yamauchi

Marine collagen derived from fish scales, skin, and bone has been widely investigated for application as a scaffold and carrier due to its bioactive properties, including excellent biocompatibility, low antigenicity, and high biodegradability and cell growth potential. Fish type I collagen is an effective material as a biodegradable scaffold or spacer replicating the natural extracellular matrix, which serves to spatially organize cells, providing them with environmental signals and directing site-specific cellular regulation. This study was conducted to confirm the safety of fish (tilapia) atelocollagen for use in clinical application. We performed *in vitro* and *in vivo* biological studies of medical materials to investigate the safety of fish collagen. The extract of fish collagen gel was examined to clarify its sterility. All present sterility tests concerning bacteria and viruses (including endotoxin) yielded negative results, and all evaluations of cell toxicity, sensitization, chromosomal aberrations, intracutaneous reactions, acute systemic toxicity, pyrogenic reactions, and hemolysis were negative according to the criteria of the ISO and the Ministry of Health, Labour and Welfare of Japan. The present study demonstrated that atelocollagen prepared from tilapia is a promising biomaterial for use as a scaffold in regenerative medicine.

1. Introduction

Regenerative medicine consists of three components: cells, nutrients (growth factors, cytokines, and chemicals, etc.), and scaffold materials [1]. The combined application of these components is important. With respect to scaffold manufacturing, the use of bioactive natural organic materials originating from marine products is indispensable, as severe infections (zoonosis), including bovine spongiform encephalopathy, avian and swine influenza, and tooth-and-mouth disease in bovines, pigs, and buffalo, occur worldwide. Marine collagen derived from fish scales, skin, and bone has been widely investigated for its potential application as a scaffold material and carrier due to its bioactive properties, such as excellent biocompatibility, low antigenicity, and high biodegradability and cell growth potential [2, 3]. As fish collagen (FC) generally has a low degenerative temperature (T_d), it melts when placed in contact with the human body for clinical application, which renders this biomaterial difficult to handle *in vivo* at actual physical temperatures used in human medical applications. The low stability of FC is thought to be due to its low hydroxyproline content compared to that observed in bovine collagen [4]. Recently, our laboratory showed that the T_d of collagen extracted and purified from the skin of a tropical fish, tilapia, is 35-36°C (unpublished data). Therefore, tilapia collagen is believed to be a powerful candidate for use in making a clinical scaffold as an alternative to bovine collagen.

The aim of this study was to confirm the safety of FC for use in clinical application. We performed *in vitro* and *in vivo* biological examinations of medical materials to investigate the safety of FC. FC is used as a solution in order to promote stem cells suspension. Therefore, the extract of FC gel was examined to clarify its sterility. In addition, biological studies of low concentrations of FC solution were conducted in accordance with ISO standards.

2. Materials and Methods

2.1. Preparation of FC. Fish type I atelocollagen produced by solubilized tilapia skin was kindly supplied by Nippi Inc., Biomatrix Institute (Ibaragi, Japan). A total of 0.1% FC

dissolved in 1.5-fold concentrated PBS (−) (pH 7.4) was used for the following biological experiments.

2.2. Sterility Test

2.2.1. Aerobic and Anaerobic Bacteria Denial Tests. Two mL of 0.1% FC was added to a 90 mm culture dish. FC solution was gelled at 37°C for 30 minutes in an atmosphere of 5% CO_2 and air. Ten mL/dish of PBS (−) was added on FC gel and cultured at 37°C for three days in a CO_2 incubator (SCA-165DS, ASTEC Co., Ltd., Fukuoka, Japan). After three days of culture, PBS (−) was decanted into special culture vials containing medium for aerobic (BD BACTEC Plus Aerobic/F, BD and Company, Sparks, MD, USA) or anaerobic (BD BACTEC Plus+ Anaerobic/F, BD and Company) bacteria, respectively. The vials were cultured for five days and analyzed using a totally automatic blood culture testing apparatus (BACTEC 9240/9120, BD and Company, Franklin Lakes, NJ, USA).

2.2.2. Fungi Denial Test. A total of 0.4 mL of 0.1% FC was added to a 35 mm culture dish. FC solution was gelled at 37°C for 30 minutes in an atmosphere of 5% CO_2 and air. Two mL/dish of PBS (−) was added on FC gel and cultured at 37°C for three days in a CO_2 incubator. After five days of culture, PBS (−) was decanted into a special glass tube containing medium for fungi (Sabouraud 2 agar (SAB2-T), BioMerieux, Marcy l'Etoile, France). The tube was cultured for five days and analyzed using a totally automatic blood culture testing apparatus (BACTEC 9240/9120, BD and Company, Franklin Lakes, NJ, USA).

2.2.3. Endotoxin Denial Test. A total of 0.4 mL of 0.1% FC was added to a 35 mm culture dish. FC solution was gelled at 37°C for 30 minutes in an atmosphere of 5% CO_2 and air. Two mL/dish of PBS (−) was added on FC gel and cultured at 37°C for three days in a CO_2 incubator. After three days of culture, PBS (−) was mixed with limulus reagent (Wako Pure Chemical Industries Ltd., Osaka, Japan) and analyzed according to a turbidimetric time assay using a Wako Toxinometer (MT-5500, Wako Pure Chemical Industries Ltd.). A negative result was defined as a level below 1.0 pg/mL.

2.2.4. Mycoplasma and Virus Denial Test. Three mL of 0.1% FC was added to a 90 mm culture dish. FC solution was gelled at 37°C for 30 minutes in an atmosphere of 5% CO_2 and air. NOS-1 cells were seeded at a density of 1×10^5 cells on FC gel with 15 mL of α-MEM containing 10% fetal bovine serum and cultured at 37°C for five days in a CO_2 incubator. α-MEM decanted from the culture dish was assayed for the presence of mycoplasma, and NOS-1 cells retrieved from the surface of the FC gel by adding 2 mL of trypsin-EDTA to the culture dish and pipetting in α-MEM were analyzed for the presence of viruses using real-time PCR (Applied Biosystems 7900HT, Life Technologies Corp., Carlsbad, CA, USA).

2.3. Biological Evaluations of Fish Collagen

2.3.1. Cell Toxicity Test (ISO 10993-5:2009). In order to evaluate the cell toxicity of FC, V79 cells (a cell line consisting of fibroblasts derived from the lungs of male Chinese hamsters) were used to inhibit colony-formation according to the direct contact method. One mL of the cell suspension (40 cells/mL) was seeded in a 24-well culture plate and cultured for seven days. The following six groups were designed for comparison: (1) control (culture medium: MEM 10) group, (2) negative control material (plastic sheet) group, (3) positive control material (polyurethane containing 0.25% zinc (ZDBC)) group, (4) experimental (fish collagen gel (for gelation: 37°C, 30 minutes)) group, (5) control (DMSO: solvent for ZDBC) group, and (6) positive control (ZDBC) group. After seven days of culture, the culture medium was removed. The cells were fixed with 1 mL of 100% methanol for five minutes and were stained with 4% Giemsa stain solution (Merck KGaA, Darmstadt, Germany). The mean number of colonies ($n = 4$) was counted by the naked eye and was converted to a percentage of the total number of colonies (100%) in the control group. Cell toxicity was defined as a colony-formation ratio below 30% in the FC group.

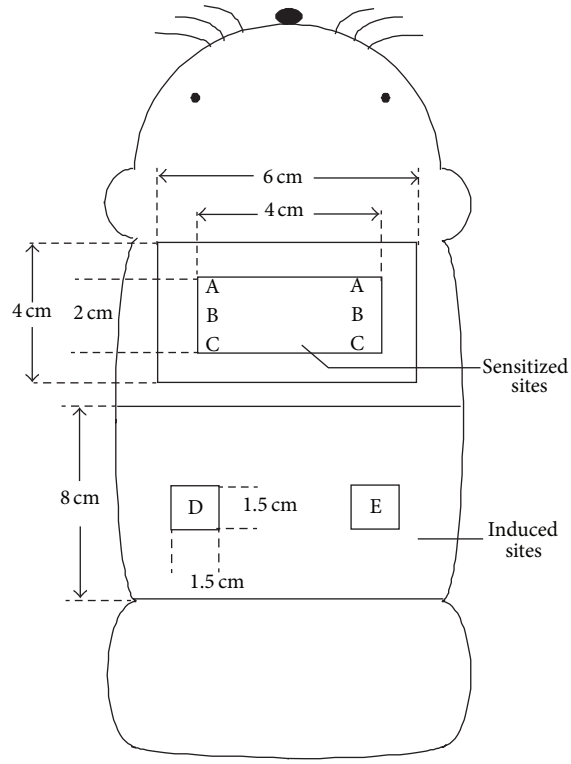

Figure 1: A schematic representation of sensitized (A, B, and C) and induced (D and E) sites in GPMT. A: water + FCA. B: FC. C: FC (two times concentrated) + FCA. D and E: close application sites.

2.3.2. Sensitization Test (ISO 10993-10:2010) (Figure 1). Sensitization to FC was investigated using a guinea pig maximization test (GPMT) [5]. Ten Scl:Hartley male guinea pigs (5 weeks of age) were used. A total of 0.1 mL/site of 0.1% FC with Freund's complete adjuvant (FCA) was injected intracutaneously into the back of the scapula in the experimental group. Seven days after intracutaneous sensitization, 10 w/w% sodium lauryl sulfate ointment as an inflammatory chemical

was openly applied to the same sensitized site, then removed after 24 hours. Subsequently, 0.2 mL/site of 0.1% FC was sensitized for 48 hours according to the close application method. Fourteen days after sensitization, 0.1 mL/site of either 0.1% FC or control sterile water was closely applied for 24 hours in the bilateral flank to induce inflammation. The applied site was observed 24 and 48 hours after the application of FC or water. In the negative control group, five guinea pigs were used, in which the injection water was injected intracutaneously and applied for sensitization in order to induce inflammation. In the positive control group, five guinea pigs were used, in which 0.1 w/w% 2,4-dinitrochlorobenzene was injected intracutaneously and applied for sensitization in order to induce inflammation. At 24 and 48 hours after the induction, the skin reaction (erythema and swelling) was observed by the naked eye and judged according to the criteria proposed by Magnusson and Kligman [5].

The Magnusson and Kligman criteria [5]:

0: no reaction,

1: discrete or porphyritic erythema,

2: moderately fused erythema,

3: extremely severe erythema and swelling.

2.3.3. Chromosomal Aberration Test (ISO 10993-3:2003). In order to evaluate the induction of chromosomal aberrations with FC application, CHL/IU cells (a cell line consisting of fibroblasts derived from the lungs of new-born female Chinese hamsters) were treated with a short-term method under the presence or absence of metabolic activation and a 24-hour continuous method under the absence of metabolic activation. PBS (−) was used as the negative control material, and mitomycin C (under the absence of metabolic activation) and cyclophosphamide monohydrate (under the presence of metabolic activation) were used as the positive controls. The volume in the experimental group was determined according to the "OECD 473, *in vitro* mammalian chromosome aberration test." The chromosomal structure and number of cells exhibiting aberration were examined at three observation doses of FC: 1.3, 2.5, and 5 μL/mL. The CHL/IU cells were seeded in 60 mm culture dishes at a density of 5×10^4 cells and were cultured in 10% bovine calf serum-MEM for 72 hours. The number of cells was counted using a hemocytometer under a phase-contrast microscope. Population doubling (PD) of cells was defined as

$$\mathrm{PD} = \frac{\left[\log\left(N/X_0\right)\right]}{\log 2}, \quad (1)$$

where X_0 is vital cell number (mean) at the start of the treatment and N is vital cell number (mean) after treatment (6 hours later).

The cell proliferation ratio (%) was converted to a percentage of the PD (100%) in the negative control. The inhibition of PD was defined as a cell proliferation ratio below 50%.

A 0.05 mL aliquot of 10 μg/mL colcemid (Life Technologies Corp., CA, USA) was added into the culture medium (final concentration: 0.1 μg/mL) two hours before the end of the culture period. The 5 mL of 0.075 mol/L KCL was added to the cell suspension for 30 minutes for hypotonic treatment at 37°C. After the cells were fixed with Carnoy's fixative (methanol : acetic acid = 3 : 1) for 30 minutes at 4°C, two drops of cell floating solution were dropped on the slide glass. The specimen was dried at room temperature and was stained with 3.0% Giemsa stain solution (pH 6.8, Merck KGaA) for 15 minutes.

Chromosomal Aberration Was Classified Based on the Following Criteria [6]

Structural aberrations:

chromatid breaks,
chromatid exchange,
chromosome breaks,
chromosome exchange,
others.

Numerical aberrations:

polyploidy,
endoreduplication.

The differences between the treatment and negative control groups were compared using Fisher's exact test (Bonferroni correction).

2.3.4. Intracutaneous Test (ISO 10993-10:2010). FC gel (for gelation: 37°C, 30 minutes) was extracted in physiological saline or sesame oil for 72 hours at 37°C. The extract was used to investigate intracutaneous irritability. A total of 0.2 mL/site of each extract was injected intracutaneously at five sites in the back in five Japanese white male rabbits. The sites of injection were observed at 24, 48, and 72 hours after treatment. In the control group, extract solvents (physiological saline and sesame oil) were injected using similar methods to those applied in the experimental group. The criteria for scoring were as follows.

(A) *Erythema and eschar:*

0: no erythema,

1: very slight erythema,

2: clear erythema,

3: moderate or severe erythema,

4: severe erythema (beet redness) to mild crust formation (deep wound).

(B) *Edema;*

0: no edema,

1: very slight edema,

2: slight edema (clear swelling),

3: moderate edema (approximately 1 mm in diameter),

4: severe edema (over 1 mm in diameter).

The score was defined as follows.

Total scores (A + B) at 24, 48, and 72 hours after treatment were divided by 15 (three (observation periods) by five (injected sites)).

The final score was obtained as follows.

The calculated score was divided by three (the number of animals). When the difference value (the mean score of the experimental group minus that of the control group) was below 1.0, the examined sample was judged to be negative.

2.3.5. Acute Systemic Toxicity Test (ISO 10993-11:2006). The extraction method applied to the FC gel was the same as that used in the intracutaneous test. The extract was used to investigate acute systemic toxicity. Each extract (50 mL/kg) was injected once into the caudal vein (physiological saline) or abdominal cavity (sesame oil) in five Crlj:CD1 male mice. In the control group (five mice), extract solvents (physiological saline and sesame oil) were injected using similar methods to those applied in the experimental group. The animals were observed at 4, 24, 48, and 72 hours after injection.

The Criteria Used to Assess Acute Systemic Toxicity.

Negative findings.

There were no differences in the biological response in the experimental group compared to the control animals during all observation periods.

Positive findings.

(1) More than two animals died after exposure to the experimental extract.

(2) More than two animals showed reactions associated with toxicity, such as convulsions and weakening, after exposure to the experimental extract.

(3) More than three animals showed a more than 10% weight loss after treatment with the experimental extract.

2.3.6. Pyrogenic Test (ISO 10993-11:2006). The extraction method applied to the FC gel was the same as that used in the intradermal test. Extract dissolved in physiological saline was used to investigate the presence of endotoxic and nonendotoxic pyrogens. The extract (10 mL/kg) was injected once into the auricular vein in three Japanese white male rabbits. The rectal temperature was measured six times at 30 minute intervals for three hours after injection. The increase in temperature was determined based on the difference between the highest temperature after injection and the control temperature. The sample was judged to be negative when the total increase in body temperature in three animals was below 1.3°C [7]. The sample was judged to be positive when the total increase in body temperature in three animals was over 2.5°C [7].

2.3.7. Hemolysis Test (ISO 10993-4:2002). The extraction method applied to the FC gel was the same as that used in the intracutaneous test. Extract dissolved in physiological saline was used to investigate hemolytic toxicity. Blood samples (0.1 mL) not containing fibrin were prepared from two Japanese white rabbits and added to the extract (5 mL). The mixture was incubated for one, two, and four hours at 37°C. The mixture was then spun using a centrifuge (EX-126, Tomy Seiko Co., Ltd., Tokyo, Japan) at 750 ×g for five minutes at 4°C. The supernatant was collected, and the absorbance (Ab) was read at 576 nm using an ultraviolet and visible spectrophotometer (UV-1600, Shimadzu Co., Kyoto, Japan). The hemolysis index (HI) (%) was defined as

$$\begin{aligned}\text{HI}\ (\%) = \Big(&\big(\text{Ab of experimental sample} \\ &- \text{Ab of negative control sample}\big) \\ &\times \big(\text{Ab of positive control sample} \\ &- \text{Ab of negative control sample}\big)^{-1}\Big) \times 100. \end{aligned} \quad (2)$$

The Criteria Used to Define Hemolysis [7]

HI ≤ 2: none.

2 < HI ≤ 10: slight.

10 < HI ≤ 20: moderate.

20 < HI ≤ 40: severe.

40 < HI: very severe.

2.3.8. Three-Dimensional (3D) Cell Culture (N = 3). Osteoblasts (NOS-1 cells [8]) derived from human osteosarcoma were seeded in a 65 mm culture dish at a density of 1×10^5 cells in α-MEM containing 10% fetal bovine serum and cultured in a humidified incubator at 37°C in an atmosphere of 5% CO_2 and air. The subconfluent monolayer was passaged via three-dimensional experiments conducted in a 4-well plate (1.9 cm^2 growth surface/well, NUNC, Thermo Fisher Scientific Inc., Roskilde, Denmark). First, the wells were precoated with a thin FC layer to prevent cell migration by adding 250 μL of 0.1% FC solution and incubating the mixture at 37°C for 30 minutes to enable gelation. Second, the same volume of FC solution was added to the gel bed. Third, NOS-1 cells were trypsinized (trypsin-EDTA, Gibco Lab) and resuspended with α-MEM. A total of 4.0×10^4 cells were mixed with FC solution and incubated at 37°C for 15 minutes to enable gelation. Finally, 500 μL of mineralization medium (supplemented with 10^{-7} M dexamethasone, 10 mM β-glycerophosphate, and 50 μg/mL of ascorbate 2-phosphate) or normal α-MEM was added to the FD gel. All samples were prepared in triplicate and cultured in a humidified incubator at 37°C in an atmosphere of 5% CO_2 and air. The medium was changed every three days. After 14 days of culture, the cells were washed with PBS (−), fixed with 100% methanol, and stained with 1% alizarin red S (Sigma-Aldrich Co., St. Louis, MO, USA).

3. Results

3.1. Sterility Test. Negative results (not detected) were obtained in all sterility tests for bacteria, mycoplasma,

Table 1: Results of colony-formation inhibition assay.

(a)

Test area	Colonies/well	Mean ± SD	Colony-formation ratio (%)
Control (MEM10 medium)	38, 43, 42, 40	40.8 ± 2.2	100
Negative control material			
Plastic sheet, toluene resisting	36, 40, 41, 41	39.5 ± 2.4	96.8
Positive control material B			
Polyurethane film containing 0.25% ZDBC	0, 0, 0, 0	0.0 ± 0.0	0.0
Test article			
Fish collagen	38, 40, 36, 39	38.3 ± 1.7	93.9

(b)

Test solution	Concentration (μg/mL)	Colonies/well	Mean ± SD	Colony-formation ratio (%)	IC_{50} (μg/mL)
Control (DMSO)	0	41, 37, 41, 44	40.8 ± 2.9	100	—
	1	37, 43, 37, 41	39.5 ± 3.0	96.8	
Positive control article	2	5, 11, 6, 6	7.0 ± 2.7	17.2	1.60
ZDBC	3	0, 0, 0, 0	0.0 ± 0.0	0.0	

ZDBC: Zinc dibutyldithiocarbamate.
DMSO: Dimethyl sulfoxide.

viruses, and endotoxin (below 1.0 pg/mL) in 0.1% FC solution ($n = 2$).

3.2. Biological Evaluations of Fish Collagen

3.2.1. Cell Toxicity Test (Table 1). The colony-formation ratio of cells seeded directly on FC gel was 93.9% and that observed in the negative and positive control groups was 96.8% and 0.0%, respectively. FC did not inhibit colony-formation, as the FC ratio was over 30%. The colony-forming ratio in the positive control group decreased dose-dependently, and the concentration at 50% inhibition of colony-formation (IC_{50}) was 1.60 μg/mL.

3.2.2. Sensitization Test. Neither an abnormal general condition nor changes in weight were observed in any animals during the experimental periods. Following sensitization with intracutaneous and topical application of 0.1% FC, no skin reactions were observed at the sites treated with 0.1% FC or control water to induce inflammation during the observation period in any of the 10 animals (Table 2). No skin reactions were noted at any of the sites in the five negative control animals. However, clear skin reactions (erythema and/or swelling) were detected during the observation period in all five positive control animals.

3.2.3. Chromosomal Aberration Test (Figures 2 and 3). No color changes in the medium, which occurred as a result of changes in pH, were observed after adding FC. The rate of cell proliferation calculated using population doubling did not decrease under either treatment condition (over 87%). The incidence of structural aberrations without metabolic activation after the application of 1.3, 2.5, and 5 μL/mL (short-term treatment) was 1.0, 0.0 and 0.0%, respectively (the negative control: 0.0%). The incidence with metabolic

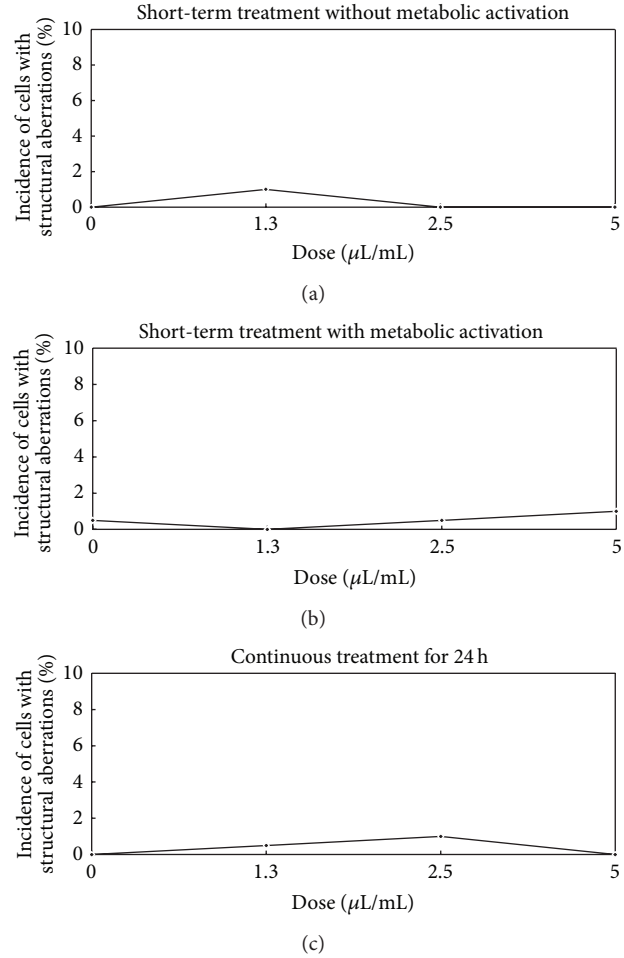

Figure 2: Dose-response curves (structural aberrations of chromosome) following short-term and continuous treatments.

Table 2: Individual score of the skin reaction on challenge sites.

Group	Animal no.	Treatment			Grading scale*	
		Induction		Challenge	24 hr**	48 hr**
		Intradermal injection	Topical application			
2	6	Fish collagen (0.1%)	Fish collagen (0.1%)	Fish collagen (0.1%)	0	0
				Water for injection	0	0
	7	Fish collagen (0.1%)	Fish collagen (0.1%)	Fish collagen (0.1%)	0	0
				Water for injection	0	0
	8	Fish collagen (0.1%)	Fish collagen (0.1%)	Fish collagen (0.1%)	0	0
				Water for injection	0	0
	9	Fish collagen (0.1%)	Fish collagen (0.1%)	Fish collagen (0.1%)	0	0
				Water for injection	0	0
	10	Fish collagen (0.1%)	Fish collagen (0.1%)	Fish collagen (0.1%)	0	0
				Water for injection	0	0

Notes: * Grading scale. Patch test reaction:
0: no reaction,
1: discrete or porphyritic erythema,
2: moderately fused erythema,
3: extremely severe erythema and swelling.
** Time (hours) after challenge.

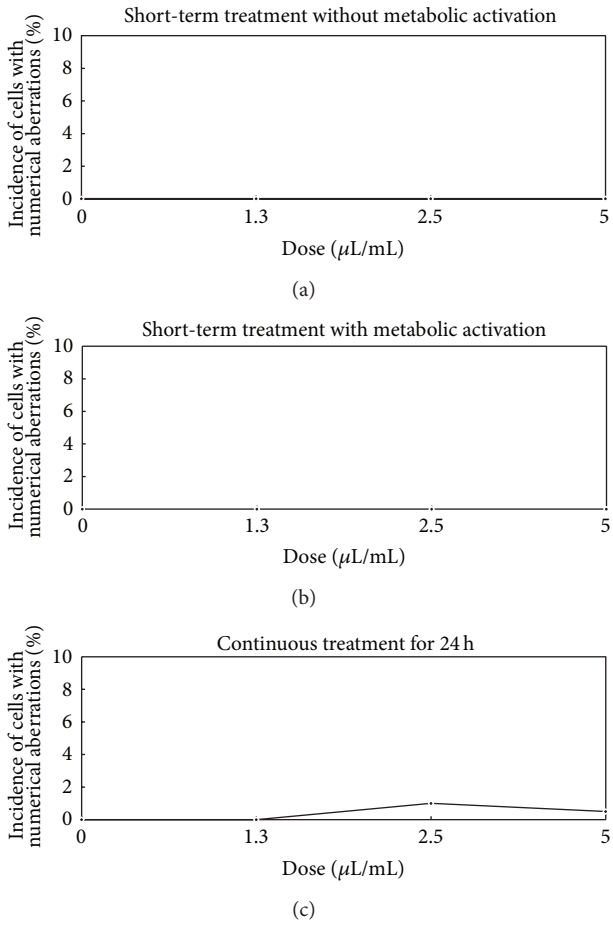

Figure 3: Dose-response curves (numerical aberrations of chromosome) following short-term and continuous treatments.

activation after the application of 1.3, 2.5, and 5 μL/mL (short-term treatment) was 0.0, 0.5, and 1.0%, respectively (the negative control: 0.5%). The incidence after the application of 1.3, 2.5, and 5 μL/mL (continuous treatment) was 0.5, 1.0, and 0.0%, respectively (the negative control: 0.0%). There were no significant differences in the chromosomal structures of cells exhibiting aberrations in the experimental group under either treatment condition compared to that observed in the negative control group ($P > 0.05$).

The incidence of numerical aberrations without metabolic activation after the application of 1.3, 2.5, and 5 μL/mL (short-term treatment) was 0.0% in all groups (the negative control: 0.0%). The incidence with metabolic activation after the application of 1.3, 2.5, and 5 μL/mL (short-term treatment) was 0.0% in all groups (the negative control: 0.0%). The incidence after the application of 1.3, 2.5, and 5 μL/mL (continuous treatment) was 0.0, 1.0, and 0.5%, respectively (the negative control: 0.0%). There were no significant differences in the number of cells exhibiting chromosomal aberrations in the experimental group under either treatment condition compared to that observed in the negative control group ($P > 0.05$).

3.2.4. Intracutaneous Test (Table 3). Neither death, an abnormal general condition, nor any change in weight was observed in any of the animals during the experimental period. No skin reactions (erythema or swelling) were noted after injection of the extracts in physiological saline (mean score: 0.00) or control solution (mean score: 0.00) during the observation period in the experimental or control animals. Skin reactions were observed after injection of the extracts in sesame oil as follows: score-1 erythema at all five sites in three animals and score-1 edema at one or two sites in two animals at 24, 48, and 72 hours after injection. The total score

Table 3: Irritation score (intracutaneous) in male rabbits.

Animal no.	Test and control articles*	Pre	Time (hour) after administration			Total score	Irritation** score $\sum(A+B)/15$	Total irritation score	Mean#	Difference of mean##
			24	48	72					
1	Physiological saline extract of Fish collagen	0	0	0	0	0	0.00	0.00	0.00	0.00
2		0	0	0	0	0	0.00			
3		0	0	0	0	0	0.00			
1	Physiological saline extract (control)	0	0	0	0	0	0.00	0.00	0.00	
2		0	0	0	0	0	0.00			
3		0	0	0	0	0	0.00			
1	Sesame oil extract of Fish collargen	0	6	6	6	18	1.20	3.60	1.20	−0.24
2		0	5	5	5	15	1.00			
3		0	7	7	7	21	1.40			
1	Sesame oil extract (control)	0	5	5	5	15	1.00	4.33	1.44	
2		0	8	8	7	23	1.53			
3		0	9	9	9	27	1.80			

Notes: *Each test and control article was administered to 5 sites per animal.
**Total score [erythema and eschar formation (A) and edema formation (B) of 24, 48, and 72 hours after administration of per animal]/15 [3 grading periods (24, 48, and 72 hours after administration) × 5 administered sites].
#Total irritation score/3 animals.
##Mean (each test article) − Mean (each control article).

Table 4: Body temperature in male rabbits.

Test article	Animal no.	Rectal temperature (°C)									Temperature rise (°C)	Total# (°C)	Pyrogenicity
		Before administration		Control temperature	After administration								
		1st	2nd		3rd	4th	5th	6th	7th	8th			
Physiological saline extract of fish collagen	1	38.8	38.7	38.75	38.9	39.1	39.2	39.2	39.2	39.2	0.45	1.15	−
	2	39.0	39.0	39.00	39.3	39.4	39.4	39.4	39.3	39.2	0.40		
	3	38.7	38.7	38.70	38.9	38.8	38.8	39.0	39.0	39.0	0.30		

Notes: #The total of the temperature rise.
−: Negative.

for erythema/eschar and edema was 3.60 (mean: 1.20) from 24 to 72 hours after injection. Skin reactions were observed after injection of the control sesame oil as follows: score-1 erythema at all five sites in three animals and score-1 edema at three or four sites in two animals at 24 and 48 hours after injection. Furthermore, skin reactions were also observed after injection of the control sesame oil as follows: score-1 erythema at all five sites in three animals and score-1 edema at two or four sites in two animals at 72 hours after injection. The total score for erythema/eschar and edema was 4.33 (mean: 1.44) from 24 to 72 hours after injection. The difference value (1.20 minus 1.44: −0.24) was below 1.0.

3.2.5. Acute Systemic Toxicity Test. No deaths, a normal general condition or normal changes in weight, and normal antopsy findings were observed in the experimental or control animals.

3.2.6. Pyrogenic Test (Table 4). No changes in weight or a normal general condition were observed in any of the animals throughout the experimental period. The total increase in temperature was 1.15°C at 30 minutes, 1 hour, 1 hour and 30 minutes, 2 hours, 2 hours and 30 minutes, and 3 hours after injection of FC extract in physiological saline. Therefore, FC was found to be a nonpyrogenic material.

3.2.7. Hemolytic Test. The mean HI in two animals injected with FC extract in physiological saline was 0.2% after one hour of incubation, 0.4% after two hours of incubation, and 1.0% after four hours of incubation. The HI was below 2% during all incubation periods. Therefore, FC was found to be a nonhemolytic material.

3.2.8. 3D Cell Culture. The NOS-1 cells grew while maintaining a globular shape in the FC gel (Figures 4 and 5). The cells proliferated inside the FC gel according to the number of seeded cells for 14 days in both media. The cells in the control medium grew rapidly compared to those cultured in the mineralization medium. Alizarin red S staining clearly demonstrated extracellular matrix mineralization among the cells cultured in the mineralization medium (Figure 6).

4. Discussion

The FC supplied by the manufacturer was prepared via extraction using pepsin in acetic acid and filtrated with a

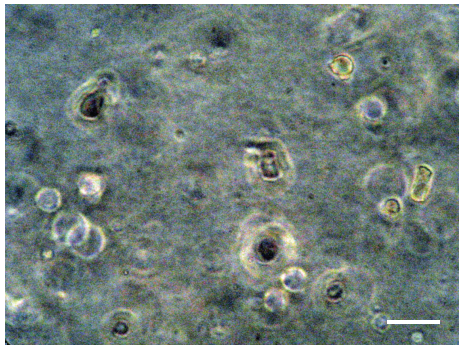

Figure 4: The NOS-1 cells maintained a globular shape in the FC gel cultured in the mineralization medium at seven days after seeding. Scale bar = 15 μm.

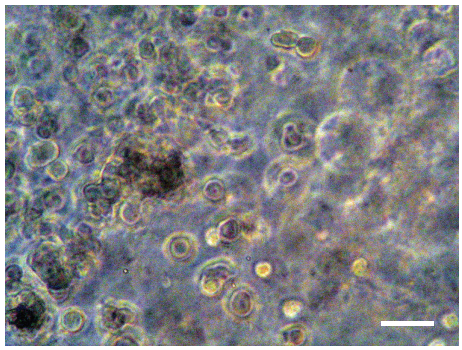

Figure 5: The NOS-1 cells exhibited a grape cluster, consisting of a stratified structure in the FC gel cultured in the mineralization medium at 14 days after seeding. Scale bar = 15 μm.

Figure 6: A representative photograph of the extracellular matrix mineralization in the FC gel (A). Note the lack of staining of the extracellular matrix in the control medium (B).

0.45 μm filter (personal communication). The FC used in this study can be stably supplied year round. The final concentration was prepared on a clean bench in our laboratory. All present sterility tests of bacteria and viruses (including endotoxin) were negative. Therefore, the process of FC preparation is considered acceptable for clinical application. With respect to conservation of FC, the preliminary study indicated that the FC was stable for over six months under frozen conditions at −20°C. The frozen FC was kept in a refrigerator for four to five hours before use.

The main reason for using collagen is its excellent biocompatibility, low antigenicity [9], and high direct cell adhesion properties and biodegradability compared to chitin/chitosan and synthetic polymers [10]. This is the first study to investigate the biological safety of FC in accordance with ISO standards. All tests for cell toxicity, sensitization, chromosomal aberrations, intracutaneous reactions, acute systemic toxicity, pyrogenic reactions, and hemolysis were negative according to the criteria of the ISO and the Ministry of Health, Labour and Welfare of Japan. These results are due to the long-term sterility of the material, the completion of gelation over 15 minutes at 37°C, and the proper and sufficient ateloconditions. The short-term gelation of FC solution is also suitable for extraction tests. Fish type I collagen is an effective material for a biodegradable scaffold or spacer replicating the natural extracellular matrix, which serves to spatially organize cells, providing them with environmental signals and directing site-specific cellular regulation [11, 12].

3D cultures are more physiologically relevant than conventional 2D cultures based on the seeding of cells on plastic dishes [13, 14]. As a result, 3D cultures enable the study of physiological processes that cannot be examined in 2D cultures, including differentiation [15] and morphogenesis [16, 17]. The 3D cell culture system used in this study clearly showed a high level of direct cell adhesion with FC gel as a scaffold with a greater degree of osteoblastic differentiation for mineralization, which indicates a high possibility for the clinical application of FC.

In conclusion, although further studies are required, particularly experiments using large animals, to evaluate the clinical suitability of FC, the atelocollagen prepared from tilapia is a strongly promising biomaterial for use as a scaffold in regenerative medicine.

Conflict of Interests

The authors declare that there is no conflict of interests regarding the publication of this paper.

Authors' Contribution

Kohei Yamamoto and Kazunari Igawa contributed equally to this work.

Acknowledgment

This work was supported in part by Geriatrics Research and Development Expenditure, Contract Grant Sponsor: Ministry of Health, Labour and Welfare of Japan and Contract Grant no. 23-10.

References

[1] Y. Hayashi, S. Yamada, T. Ikeda, Z. Koyama, and K. Yanagiguchi, "Chitosan and fish collagen as biomaterials for regenerative medicine," in *Marine Medical Food*, S.-K. Kim, Ed., vol. 65, chapter 6, pp. 107–120, Academic Press, London, UK, 2012.

[2] A. K. Dillow and A. M. Lowman, *Biomimetic Materials and Design: Biointerfacial Strategies, Tissue Engineering, and Targeted Drug Delivery*, Mercel Dekker, New York, NY, USA, 2002.

[3] S.-F. Yang, K.-F. Leong, Z.-H. Du, and C.-K. Chua, "The design of scaffolds for use in tissue engineering—part I. Traditional factors," *Tissue Engineering*, vol. 7, no. 6, pp. 679–689, 2001.

[4] A. D. Winter and A. P. Page, "Prolyl 4-hydroxylase is an essential procollagen-modifying enzyme required for exoskeleton formation and the maintenance of body shape in the nematode *Caenorhabditis elegans*," *Molecular and Cellular Biology*, vol. 20, no. 11, pp. 4084–4093, 2000.

[5] B. Magnusson and A. M. Kligman, "The identification of contact allergens by animal assay," *Journal of Investigative Dermatology*, vol. 52, no. 3, pp. 268–276, 1969.

[6] T. Sofuni, "Production mechanism, classification, and criteria of chromosomal aberrations," in *The Atlas of Chromosomal Aberrations Induced Compounds*, Environmental Mutagen Society of Japan and Mammalian Mutagenicity Study Group, Eds., pp. 16–35, Asakura Shoten, Tokyo, Japan, 1st edition, 1988.

[7] "Guideline for medical equipments," Ministry of Health, Labour and Welfare in Japan, Pharmaceutical and Food Safety Bureau, Notification 0301 no. 20, 2012.

[8] T. Hotta, T. Motoyama, and H. Watanabe, "Three human osteosarcoma cell lines exhibiting different phenotypic expressions," *Acta Pathologica Japonica*, vol. 42, no. 8, pp. 595–603, 1992.

[9] F. Pati, P. Datta, B. Adhikari, S. Dhara, K. Ghosh, and P. K. D. Mohapatra, "Collagen scaffolds derived from fresh water fish origin and their biocompatibility," *Journal of Biomedical Materials Research A*, vol. 100, no. 4, pp. 1068–1079, 2012.

[10] C. H. Lee, A. Singla, and Y. Lee, "Biomedical applications of collagen," *International Journal of Pharmaceutics*, vol. 221, no. 1-2, pp. 1–22, 2001.

[11] J.-H. Wang, C.-H. Hung, and T.-H. Young, "Proliferation and differentiation of neural stem cells on lysine-alanine sequential polymer substrates," *Biomaterials*, vol. 27, no. 18, pp. 3441–3450, 2006.

[12] Y. Hayashi, S. Yamada, and T. Ikeda, "Fish collagen and tissue repair," in *Marine Cosmeceuticals: Trends and Prospects*, S.-K. Kim, Ed., pp. 133–141, CRC Press, Boca Raton, Fla, USA, 2011.

[13] C. Frantz, K. M. Stewart, and V. M. Weaver, "The extracellular matrix at a glance," *Journal of Cell Science*, vol. 123, no. 24, pp. 4195–4200, 2010.

[14] C. M. Nelson and M. J. Bissell, "Of extracellular matrix, scaffolds, and signaling: tissue architecture regulates development, homeostasis, and cancer," *Annual Review of Cell and Developmental Biology*, vol. 22, pp. 287–309, 2006.

[15] J. Alcaraz, R. Xu, H. Mori et al., "Laminin and biomimetic extracellular elasticity enhance functional differentiation in mammary epithelia," *The EMBO Journal*, vol. 27, no. 21, pp. 2829–2838, 2008.

[16] H. Mori, A. T. Lo, J. L. Inman et al., "Transmembrane/cytoplasmic, rather than catalytic, domains of Mmp14 signal to MAPK activation and mammary branching morphogenesis via binding to integrin β1," *Development*, vol. 140, no. 2, pp. 343–352, 2013.

[17] C. M. Ghajar, X. Chen, J. W. Harris et al., "The effect of matrix density on the regulation of 3-D capillary morphogenesis," *Biophysical Journal*, vol. 94, no. 5, pp. 1930–1941, 2008.

Hindawi Publishing Corporation
BioMed Research International
Volume 2014, Article ID 745139, 8 pages
http://dx.doi.org/10.1155/2014/745139

Research Article

Induction of Reparative Dentin Formation on Exposed Dental Pulp by Dentin Phosphophoryn/Collagen Composite

Toshiyuki Koike, Mohammad Ali Akbor Polan, Masanobu Izumikawa, and Takashi Saito

Division of Clinical Cariology and Endodontology, Department of Oral Rehabilitation, School of Dentistry, Health Sciences University of Hokkaido, 1757 Tobetsu, Hokkaido 061-0293, Japan

Correspondence should be addressed to Takashi Saito; t-saito@hoku-iryo-u.ac.jp

Received 3 February 2014; Accepted 25 February 2014; Published 6 April 2014

Academic Editor: Yoshihiko Hayashi

The ultimate goal of vital pulp therapy is to regenerate rapidly dentin possessing an excellent quality using a biocompatible, bioactive agent. Dentin phosphophoryn (DPP), the most abundant noncollagenous polyanionic protein in dentin, cross-linked to atelocollagen fibrils was applied to direct pulp capping in rats. After 1, 2, and 3 weeks, the teeth applied were examined on the induction of reparative dentin formation and the response of pulp tissue, compared to calcium hydroxide-based agent conventionally used. The reparative dentin formation induced by DPP/collagen composite was more rapid than by calcium hydroxide. In the morphometrical analysis, the formation rate of reparative dentin by DPP/collagen composite was approximately the same as that by calcium hydroxide at 3 weeks. Nevertheless, the compactness of reparative dentin formed by DPP/collagen composite was much superior to what resulted from calcium hydroxide. Also, DPP/collagen composite showed high covering ability of exposed pulp. Moreover, DPP/collagen composite led only to slight pulp inflammation at the beginning whereas calcium hydroxide formed necrotic layer adjacent to the material and induced severe inflammation in pulp tissue at 1 week. The present study demonstrates a potential for DPP/collagen composite as a rapid biocompatible inducer for the formation of reparative dentin of excellent quality in rats.

1. Introduction

Direct pulp capping using calcium hydroxide-based agent has been a standard therapy for years. However, long-term studies have shown results to be variable and unpredictable [1–3]. Thus, clinical success rate of the therapy has not satisfied dentists. The agent does not provide close adaptation to dentin, does not promote consistent odontoblast differentiation, and has been shown to be cytotoxic in cell cultures, leading to the fact that the resultant reparative dentin formation can be characterized by tunnel defects [4–6]. Tunnel defects within reparative dentin may provide a pathway for the penetration of microorganisms to develop secondary infection of pulp tissue. Furthermore, low mechanical strength and pulpal resorption are potential disadvantage of the agent [5, 7]. Therefore, a biocompatible, bioactive agent that rapidly induces reparative dentin formation possessing a good quality is required to improve the clinical success rate of vital pulp therapy.

Dentin phosphophoryn (DPP), a member of small integrin-binding ligand N-linked glycoproteins (SIBLING) family, is the most abundant of the noncollagenous polyanionic proteins in dentin. DPP is dentin sialophosphoprotein (DSPP) gene product [8, 9]. It is predominantly expressed in odontoblasts and is known to be a marker of the differentiation of pulp cells into odontoblasts [10–12]. It contains the RGD motif at position of 26 from N-terminal and the repeating sequence of $(\text{asparatic acid-phosphoserine-phosphoserine})_n$ as its characteristic domains [13]. Aspartic acid and serine account for at least 75% of all amino acid sequences, and 85%–90% of the serine residues are phosphorylated. DPP is supported by *in vitro* mineralization data showing that DPP is an important initiator and modulator for the formation and growth of hydroxyapatite crystals due to many negatively charged regions [14–19]. In particular, DPP covalently cross-linked on collagen fibrils has high potential to nucleate hydroxyapatite according to the measure of interfacial energy [17–19].

Recently, DPP has been reported to induce the differentiation of human mesenchymal stem cells into osteoblasts as its RGD motif binds with $\alpha v\beta 3$ integrin on the cell surface followed by the activation of the MAP kinase and SMAD signaling pathway [20, 21]. Moreover, we demonstrated that DPP promotes not only differentiation or calcification but also cell migration by acting on integrin on the surface of pulp cells via its RGD motif *in vitro* [22]. However, the potential of DPP for dentin regeneration in animal model has not still been clear although there is much evidence on DPP *in vitro* ability.

The aim of this study was to investigate effects of DPP cross-linked to type I atelocollagen fibrils as a scaffold placed on experimentally created pulp exposures in first molar in rats on induction of reparative dentin formation and response of pulp tissue, compared to calcium hydroxide-based agent conventionally used.

2. Materials and Methods

2.1. Preparation of DPP Cross-Linked to Type I Atelocollagen Fibrils. The DPP was prepared from molar teeth extracted from 8-9-month-old porcine jaws following the method described by Butler [23]. The preparation was carried out at 4°C in solutions to which protease inhibitors (100 mM 6-aminohexanoic acid, 5 mM benzamidine-HCl, and 1 mM phenylmethylsulfonyl fluoride) were added. The DPP was extracted with calcium precipitation method and purified through the anion exchange chromatography step.

Type I atelocollagen fibrils, from which telopeptides known to be antigen had been removed, were used as a carrier of DPP in this study. The DPP was cross-linked to porcine-derived type I atelocollagen fibrils (collagen sponge, Nitta gelatin, Osaka, Japan) with divinylsulfone (Sigma Chemical, St. Louis, MO, USA) [24]. To remove unreacted divinylsulfone and DPP that was not covalently bound, the substrates were washed with 0.5 M NaCl, 0.05 M Tris-HCl, and pH 7.4, ten times and then washed with distilled water. The composite was analyzed for phosphate analysis [25] after alkaline hydrolysis to determine the amount of DPP cross-linked to type I atelocollagen fibrils.

2.2. Surgical Procedure. All animal procedures were in accordance with the guidelines of the Animal Care Committee of the Health Sciences University of Hokkaido. Eight-week-old male Wistar rats (Hokudo, Sapporo, Japan) were used in this study. Animals were anaesthetized with an intraperitoneal injection of pentobarbital (40 mg/kg). The vital pulp tissue was exposed by drilling the mesial buccal cusp of the maxilla first molar using a sterile, round steel bur (number 014, Dentsply, York, PA, USA). The exposed pulp tissue was treated with 10% sodium hypochlorite and 3% hydrogen peroxide. Then, bleeding was controlled with sterile cotton pellets. Subsequently, the exposed pulp tissue was covered with 0.5 μg of DPP covalently cross-linked to 29.5 μg of type I atelocollagen fibrils (DPP-Col), type I atelocollagen alone (Col), and multi-Cal (Ca) (Pulpdent, Watertown, MA, USA), one of calcium hydroxide-based agents which have been conventionally used for direct pulp capping. Twenty-one teeth were used in each group (DPP-Col, Col, and Ca) and were further divided into three groups on the basis of experimental period (1, 2, and 3 weeks). Following the pulp capping, each cavity was immediately sealed with glass-ionomer cement (Hy-bond Glasionomer CX, Shofu, Koto, Japan) and was filled with single step bonding system (Clearfil S-3 Bond, Kuraray, Tokyo, Japan) and composite resin (Unifil flow, GC, Tokyo, Japan).

2.3. Histological Examination. At 1, 2, and 3 weeks after surgery, the animals were killed by overinhalation of diethyl ether. Following death, all experimental teeth and the adjacent alveolar bone were removed and fixed with 10% neutral buffered formalin for 24 hours. Then, specimens were demineralized in 0.1 M EDTA, pH 7.4, at 4°C, embedded in paraffin, sectioned at 4 μm, and subsequently stained with hematoxylin and eosin. The sections were then analyzed in a light microscope (Eclipse E400, Nikon, Tokyo, Japan).

2.4. Morphometrical Analysis of Reparative Dentin Formed and Evaluation of Pulp Tissue. First, the formation rate of reparative dentin, that is, relative area of reparative dentin formed adjacent to the cavity to the area of pulp chamber of crown in each experimental tooth, was assessed in the longitudinal section covering the central part of the experimental wound. The areas in the sections were measured by means of Image J (Wayne Rasband, MD, USA) in three sections in separate seven teeth. Next, the compactness of reparative dentin formed in the sections was measured based on the area of defect in reparative dentin and the total area of reparative dentin. The formation rate and compactness of reparative dentin were calculated for formula as follows [26]:

$$\text{Formation rate (\%)} = \text{total area of tertiary dentin/coronal pulp chamber area} \times 100$$

$$\text{Compactness (\%)} = 1 - (\text{defects area} + \text{cells area})/\text{total area of tertiary dentin} \times 100.$$

Then, the covering degrees of exposed pulp tissue with reparative dentin formed were assessed in four scores; 4: completely covered, 3: almost covered (50% and over covering at the pulp exposure surface), 2: partially covered (49% and less covering at the pulp exposure surface), and 1: reparative dentin formation not observed. Moreover, the degrees of pulp inflammation induced by the materials were evaluated in four scores; 4: minimal inflammation (none or few scattered inflammatory cells present in the pulp at the exposure site, or same as normal dental pulp), 3: mild inflammation (some vasodilation of blood vessels, indicating mild hyperemia on the surface of the exposure site), 2: moderate inflammation (presence of weak vasodilation of blood vessels without infiltration of blood cells into the dental pulp, some inflammatory cells, such as polymorphonuclear leukocytes and neutrophils, observed), 1: severe inflammation (presence of strong vasodilation of blood vessels appearing as an abscess and significant inflammatory infiltration by polymorphonuclear leukocytes and neutrophils seen throughout the crown) [26].

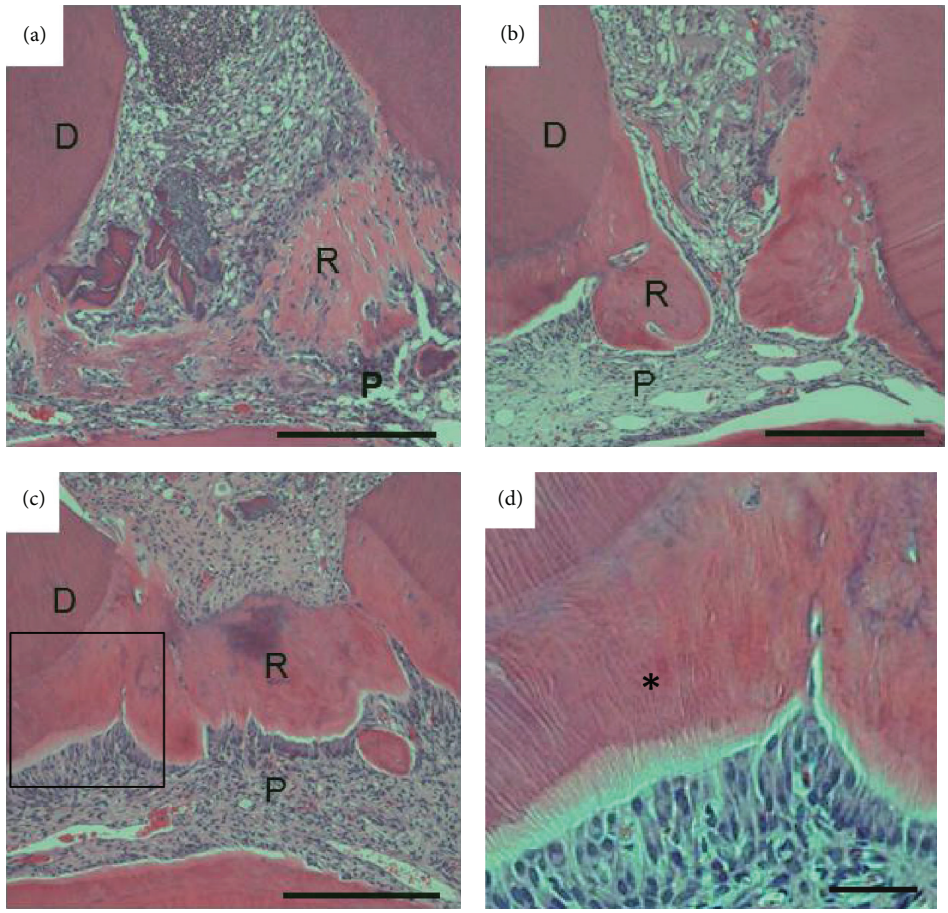

Figure 1: Micrographs showing upper first molars 1(a), 2(b), and 3 weeks ((c) and (d)) after treatment with DPP-Col. The compact reparative dentin was formed adjacent to the primary dentin at 2 weeks (b). The exposed pulp tissue was covered completely with reparative dentin at 3 weeks (c). Reparative dentin has dentinal tubules (asterisk) and regular arrangement of odontoblasts at 3 weeks ((d) higher magnification of the highlighted region in (c)). D: dentin, P: pulp tissue, and R: reparative dentin. Scale bar ((a), (b), and (c)) = 500 μm. Scale bar (d) = 100 μm.

2.5. Statistical Analysis. The results for the formation rate, the compactness of reparative dentin formed, and the degrees of pulp inflammation induced by the materials are expressed as means ± SD. They were analyzed by one-way analysis of variance with Tukey's multiple comparison test. Differences at $P < 0.05$ were considered statistically significant.

3. Results

The formation rate of reparative dentin by every group increased with time (Figures 1–3). In DPP-Col group, the formation rate of reparative dentin was significantly higher, compared with that by Col group throughout the experimental period (Figure 4(a)). It was also significantly higher than that by Ca group at 1 and 2 weeks. However, no significant difference was noted at 3 weeks between groups DPP-Col and Ca. In addition, the compactness of reparative dentin formed by DPP-Col group was significantly higher, compared with that formed by Ca group at 2 and 3 weeks (Figure 4(b)). In particular, it showed approximately 97% at 3 weeks. In DPP-Col group, reparative dentin possessing dentinal tubules was formed adjacent to the primary dentin at 3 weeks (Figures 1(c) and 1(d), asterisk). The exposed pulp tissue was covered completely with reparative dentin (Figures 1(c) and 4(c)) having regular arrangement of odontoblasts at 3 weeks (Figure 1(d)). The slight pulp inflammation was observed at 1 and 2 weeks, but no pulp inflammation was observed at 3 weeks (Figures 1 and 4(d)).

In Col group, reparative dentin formation was observed at 2 weeks, but reparative dentin did not cover exposed pulp tissue at even 3 weeks (Figures 2 and 4(c)). Moreover, the mild pulp inflammation was observed only at the early stage after operation (Figure 4(d)).

In Ca group, reparative dentin having considerable amount of gaps and tunnel defects was observed at 2 weeks (Figure 3(b), arrow). At 3 weeks, the reparative dentin covered exposed pulp tissue but still contained gaps and tunnel defects (Figure 4(c)). The arrangement of odontoblasts underneath reparative dentin formed by Ca group was not clear. The formation of necrotic layer adjacent to the material and severe inflammation in pulp tissue were observed at 1 week (Figure 3(a)). The mild pulp inflammation still remained at 3 weeks (Figures 3(c) and 4(d)).

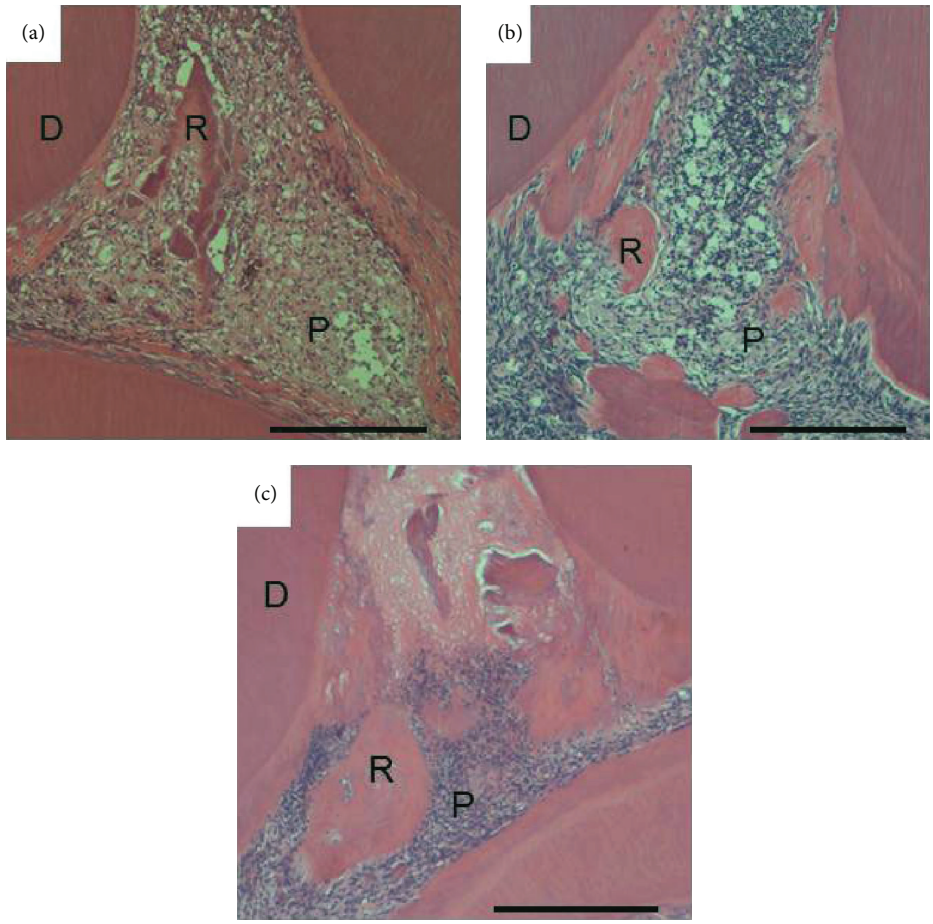

Figure 2: Micrographs showing upper first molars 1(a), 2(b), and 3 weeks (c) after treatment with Col. Reparative dentin is observed at 2 weeks but does not cover exposed pulp tissue even at 3 weeks. D: dentin, P: pulp tissue, and R: reparative dentin. Scale bar = 500 μm.

4. Discussion

It has been reported in clinical studies that the success rate of direct pulp capping with calcium hydroxide that has been used conventionally is approximately 60% even though it has been considered the standard therapy [27]. The clinical failures of direct pulp capping have led to the search for new therapeutic agents. The potential of bioactive agents such as dentin extracellular matrix molecules, for example, BMP-2, BMP-4, and BMP-7 (osteogenic protein-1: OP-1), dentin matrix protein-1 (DMP-1), matrix extracellular phosphoglycoprotein (MEPE), bone sialoprotein (BSP), and so forth, enamel matrix derivative, or stem cells is currently under study [11, 28–34]. Recently, mineral trioxide aggregate (MTA) was found to be an excellent pulp-capping agent because of its high biocompatibility [35]. However, dentin bridge formation by MTA was shown to be slower compared to calcium hydroxide [36]. In the clinical case, exposed pulp should be closed by the complete dentin bridge in a short period. The dentin extracellular matrix molecules are promising materials because of being involved in dentinogenesis during the development of teeth [37]. Therefore, they can bring out the potential of stem cells or progenitor cells located within the pulp, to the maximum, to proliferate, differentiate into odontoblast-like cells, and consequently produce the extracellular matrix, which will ultimately undergo mineralization.

In the present study, we confirmed DPP's high ability for dentin regeneration in animal model. After direct pulp capping with DPP cross-linked to type I collagen, biocompatible scaffold, the formation of reparative dentin was more rapid at the beginning than with calcium hydroxide. The rapid induction of reparative dentin reduces the chance of secondary infection of the pulp. No significant difference was found in the formation rate of reparative dentin between DPP cross-linked to collagen and calcium hydroxide at 3 weeks after operation. However, the compactness of reparative dentin formed by DPP cross-linked to collagen was significantly higher compared with that formed by calcium hydroxide at 2 and 3 weeks. In particular, the porous reparative dentin having tunnel defect was formed by calcium hydroxide. It has been reported that 89% of dentin bridges formed by calcium hydroxide contained tunnel defects [5]. The tunnel defects fail to provide a hermetic seal to the underlying pulp against recurring infection due to microleakage. This reparative dentin has a bone-like structure that does not possess odontoblast layer underneath it and consequently does

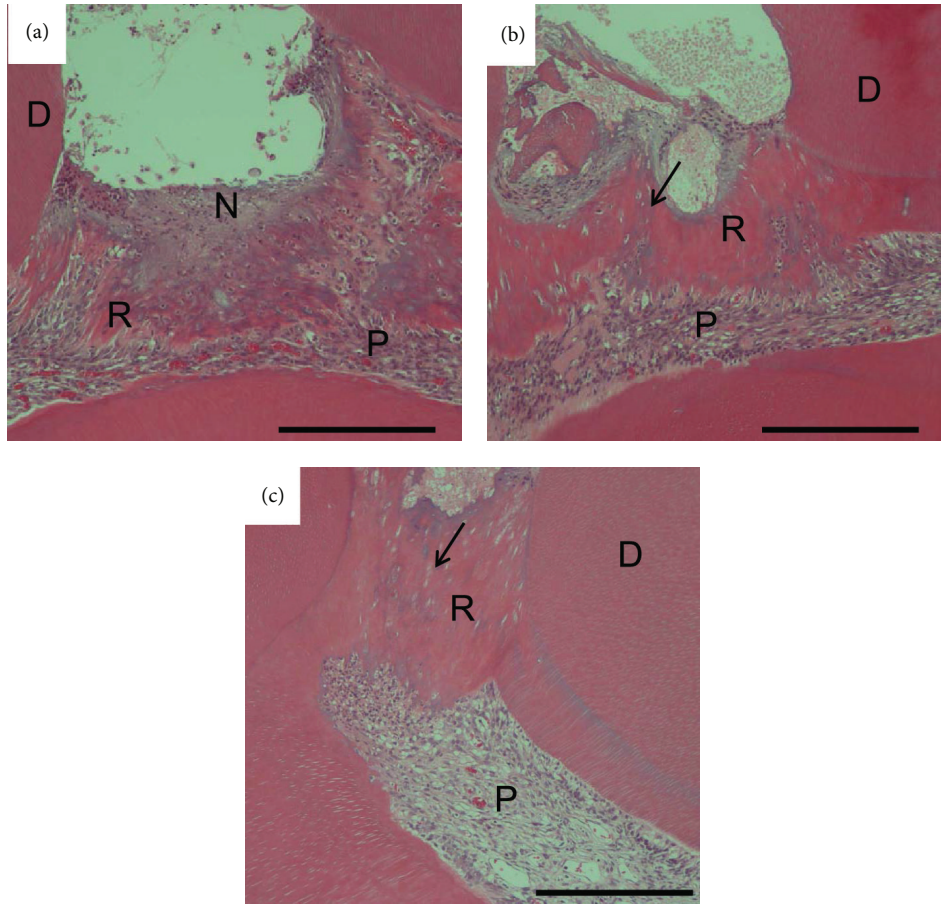

Figure 3: Micrographs showing upper first molars 1(a), 2(b), and 3 weeks (c) after treatment with Ca. Reparative dentin having gaps and tunnel defects was observed at 2 weeks (arrow). This dentin still contained gaps and tunnel defects at 3 weeks. A necrotic superficial layer (N) formed beneath the material. D: dentin, P: pulp tissue, and R: reparative dentin. Scale bar = 500 μm.

not contain dentinal tubules. In contrast, DPP immobilized to type I collagen induced the compact reparative dentin having regular arrangement of odontoblasts and dentinal tubules. This accounts for the quality difference of reparative dentin formed between DPP immobilized to type I collagen and calcium hydroxide. Thus, it was suggested that DPP induced differentiation from undifferentiated pulp cells into odontoblasts on type I collagen fibrils, suitable scaffolds for the cell differentiation, after the activation of the MAP kinase and SMAD signaling pathway [20, 21].

DPP immobilized to type I collagen caused only slight pulp inflammation at the early stage after operation due to the biocompatibility of collagen. The pulp exposure and implantation onto the pulp of biomaterials induce inflammation. Many studies report that the healing sequence includes an initial inflammation process [38–40]. In inflammatory phenomena, pulp cells express class II antigens [41]. They are implicated in the immune reaction. Immune cells such as dendritic cells and macrophages are crucial in the control of cell proliferation and apoptosis [42]. They contribute in the exposed pulp to resolve inflammatory process [43]. Then, the reparative process follows after inflammation. Therefore, inflammatory reaction may be another prerequisite for the repair process of dentin/pulp complex. On the other hand, calcium hydroxide formed necrosis layer underneath the agent due to its high alkalinity and also caused pulp inflammation. It has been reported that 41% of them were associated with recurring pulp inflammation or necrosis [5]. Thus, calcium hydroxide cannot be considered as a biocompatible agent although it is often used as a convenient low-cost material for vital pulp therapy.

In the present study, divinylsulfone was used for covalent cross-linking of DPP to type I collagen fibrils. It has been reported as a cross-linker of biomaterials *in vitro* and *in vivo* [44, 45]. It is contained in the osteoarthritis knee pain relief treatment agent for clinical use [46]. Thus, DPP/collagen composite can be considered as a safe material. For clinical application of DPP/collagen, however, unreacted divinylsulfone should be removed from the composite completely after cross-linking procedure, due to its toxicity [47].

This is the first time that DPP/collagen composite showing stimulation of reparative dentin formation was reported. Our observation might help develop a reliable and safe vital pulp therapy. However, it is necessary to develop artificial materials such as recombinant protein and synthetic peptide of DPP for clinical trial for avoiding possible immune

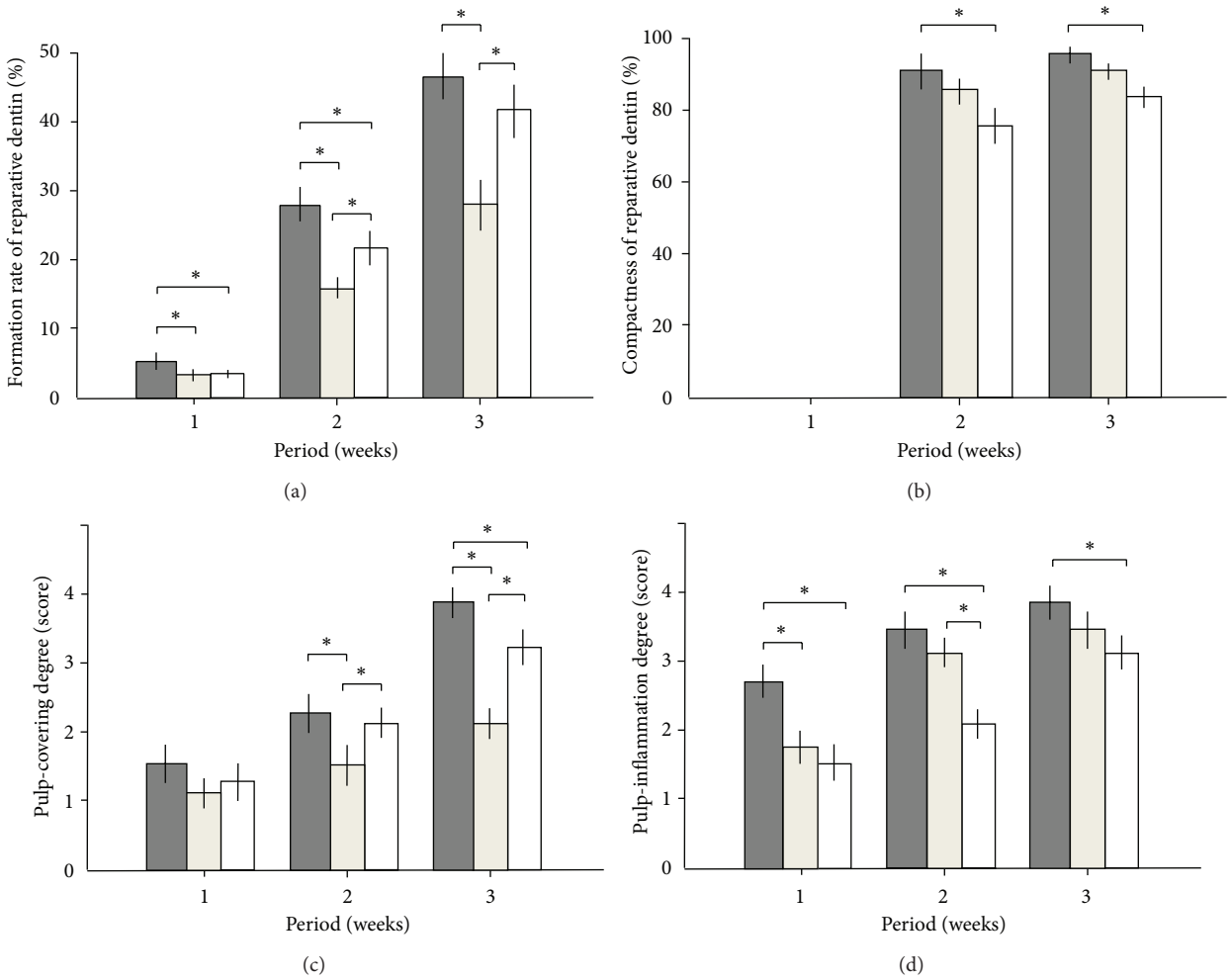

Figure 4: Evaluation of the reparative dentin and dental pulp tissue. (a) Formation rate of the reparative dentin (%), (b) compactness of the reparative dentin (%), (c) degree of coverage by the reparative dentin (score), and (d) inflammation degree of the dental pulp tissue (score). Gray columns: DPP-Col, beige columns: Col, and white columns: Ca. Twenty-one teeth were used in each group (DPP-Col, Col, and Ca) and were further divided into three groups on the basis of experimental period (1, 2, and 3 weeks). $^{*}P < 0.05$.

reaction and contamination of unidentified factors. Also, more investigations in long-term experiments will reveal more characteristics of DPP/collagen composite for dentin regeneration, and the further refinement of the collagen scaffold is necessary in order to utilize maximally the potential of DPP to stimulate the formation of reparative dentin as a hard tissue barrier. Moreover, it is crucial to understand the mechanisms underlining the process of pulp repair as well as dentin regeneration.

5. Conclusion

The present study demonstrates a potential for DPP/collagen composite as a rapid biocompatible inducer for the formation of reparative dentin of excellent quality in rats. Therefore, it is a promising biocompatible pulp capping material for the future.

Disclosure

The authors declare that this paper is original, has not been published before, and is not currently being considered for publication elsewhere. They confirmed that the paper has been approved by all named authors. They further confirm that the order of authors listed in the paper has been approved by all of them.

Conflict of Interests

The authors declare that there is no conflict of interests regarding the publication of this paper.

Acknowledgment

This work was supported by a Grant-in-Aid for Scientific Research from the Japanese Society for the Promotion of Science (Grant nos. 20390484 and 23390436).

References

[1] P. Hørsted, B. Søndergaard, A. Thylstrup, K. El Attar, and O. Fejerskov, "A retrospective study of direct pulp capping with calcium hydroxide compounds," *Endodontics & Dental Traumatology*, vol. 1, no. 1, pp. 29–34, 1985.

[2] L. J. Baume and J. Holz, "Long term clinical assessment of direct pulp capping," *International Dental Journal*, vol. 31, no. 4, pp. 251–260, 1981.

[3] C. R. Barthel, B. Rosenkranz, A. Leuenberg, and J. Roulet, "Pulp capping of carious exposures: treatment outcome after 5 and 10 years: a retrospective study," *Journal of Endodontics*, vol. 26, no. 9, pp. 525–528, 2000.

[4] U. Schröder, "Effects of calcium hydroxide-containing pulp-capping agents on pulp cell migration, proliferation, and differentiation," *Journal of Dental Research*, vol. 64, pp. 541–548, 1985.

[5] C. F. Cox, R. K. Sübay, E. Ostro, S. Suzuki, and S. H. Suzuki, "Tunnel defects in dentin bridges: their formation following direct pulp capping," *Operative Dentistry*, vol. 21, no. 1, pp. 4–11, 1996.

[6] W. E. Andelin, S. Shabahang, K. Wright, and M. Torabinejad, "Identification of hard tissue after experimental pulp capping using dentin sialoprotein (DSP) as a marker," *Journal of Endodontics*, vol. 29, no. 10, pp. 646–650, 2003.

[7] M. Hwas and J. L. Sandrik, "Acid and water solubility and strength of calcium hydroxide bases," *The Journal of the American Dental Association*, vol. 108, no. 1, pp. 46–48, 1984.

[8] H. H. Ritchie and L. Wang, "The presence of multiple rat DSP-PP transcripts," *Biochimica et Biophysica Acta-Gene Structure and Expression*, vol. 1493, no. 1-2, pp. 27–32, 2000.

[9] K. Gu, S. Chang, H. H. Ritchie, B. H. Clarkson, and R. B. Rutherford, "Molecular cloning of a human dentin sialophosphoprotein gene," *European Journal of Oral Sciences*, vol. 108, no. 1, pp. 35–42, 2000.

[10] X. Wei, J. Ling, L. Wu, L. Liu, and Y. Xiao, "Expression of mineralization markers in dental pulp cells," *Journal of Endodontics*, vol. 33, no. 6, pp. 703–708, 2007.

[11] T. Saito, M. Ogawa, Y. Hata, and K. Bessho, "Acceleration effect of human recombinant bone morphogenetic protein-2 on differentiation of human pulp cells into odontoblasts," *Journal of Endodontics*, vol. 30, no. 4, pp. 205–208, 2004.

[12] W. E. Andelin, S. Shabahang, K. Wright, and M. Torabinejad, "Identification of hard tissue after experimental pulp capping using dentin sialoprotein (DSP) as a marker," *Journal of Endodontics*, vol. 29, no. 10, pp. 646–650, 2003.

[13] A. George, L. Bannon, B. Sabsay et al., "The carboxyl-terminal domain of phosphophoryn contains unique extended triplet amino acid repeat sequences forming ordered carboxyl-phosphate interaction ridges that may be essential in the biomineralization process," *Journal of Biological Chemistry*, vol. 271, no. 51, pp. 32869–32873, 1996.

[14] A. L. Boskey, M. Maresca, S. Doty, B. Sabsay, and A. Veis, "Concentration-dependent effects of dentin phosphophoryn in the regulation of in vitro hydroxyapatite formation and growth," *Bone and Mineral*, vol. 11, no. 1, pp. 55–65, 1990.

[15] A. George and J. Hao, "Role of phosphophoryn in dentin mineralization," *Cells Tissues Organs*, vol. 181, no. 3-4, pp. 232–240, 2006.

[16] G. He, A. Ramachandran, T. Dahl et al., "Phosphorylation of phosphophoryn is crucial for its function as a mediator of biomineralization," *Journal of Biological Chemistry*, vol. 280, no. 39, pp. 33109–33114, 2005.

[17] T. Saito, A. L. Arsenault, M. Yamauchi, Y. Kuboki, and M. A. Crenshaw, "Mineral induction by immobilized phosphoproteins," *Bone*, vol. 21, no. 4, pp. 305–311, 1997.

[18] T. Saito, M. Yamauchi, and M. A. Crenshaw, "Apatite induction by insoluble dentin collagen," *Journal of Bone and Mineral Research*, vol. 13, no. 2, pp. 265–270, 1998.

[19] T. Saito, M. Yamauchi, Y. Abiko, K. Matsuda, and M. A. Crenshaw, "In vitro apatite induction by phosphophoryn immobilized on modified collagen fibrils," *Journal of Bone and Mineral Research*, vol. 15, no. 8, pp. 1615–1619, 2000.

[20] J. Jadlowiec, H. Koch, X. Zhang, P. G. Campbell, M. Seyedain, and C. Sfeir, "Phosphophoryn regulates the gene expression and differentiation of NIH3T3, MC3T3-E1, and human mesenchymal stem cells via the integrin/MAPK signaling pathway," *Journal of Biological Chemistry*, vol. 279, no. 51, pp. 53323–53330, 2004.

[21] J. A. Jadlowiec, X. Zhang, J. Li, P. G. Campbell, and C. Sfeir, "Extracellular matrix-mediated signaling by dentin phosphophoryn involves activation of the Smad pathway independent of bone morphogenetic protein," *Journal of Biological Chemistry*, vol. 281, no. 9, pp. 5341–5347, 2006.

[22] Y. Yasuda, M. Izumikawa, K. Okamoto, T. Tsukuba, and T. Saito, "Dentin phosphophoryn promotes cellular migration of human dental pulp cells," *Journal of Endodontics*, vol. 34, no. 5, pp. 575–578, 2008.

[23] W. A. Butler, "Dentin-specific proteins," *Methods in Enzymology*, vol. 145, pp. 290–303, 1987.

[24] A. Lihme, C. Schafer-Nielsen, and K. P. Larsen, "Divinylsulphone-activated agarose. Formation of stable and non-leaking affinity matrices by immobilization of immunoglobulins and other proteins," *Journal of Chromatography-Biomedical Applications*, vol. 376, pp. 299–305, 1986.

[25] A. A. Baykov, O. A. Evtushenko, and S. M. Avaeva, "A malachite green procedure for orthophosphate determination and its use in alkaline phosphatase-based enzyme immunoassay," *Analytical Biochemistry*, vol. 171, no. 2, pp. 266–270, 1988.

[26] K. Hayashi, K. Handa, T. Koike, and T. Saito, "The possibility of genistein as a direct pulp capping agent," *Dental Materials Journal*, vol. 32, no. 6, pp. 976–985, 2013.

[27] I. Mejare, "Endodontics in primary teeth," in *Textbook of Endodontology*, G. Bergenholtz, P. Horsted-Bindslev, and C. Reit, Eds., pp. 102–119, 2003.

[28] M. Nakashima, "Induction of dentin formation on canine amputated pulp by recombinant human bone morphogenetic proteins (BMP)-2 and -4," *Journal of Dental Research*, vol. 73, no. 9, pp. 1515–1522, 1994.

[29] R. B. Rutherford, L. Spångberg, M. Tucker, D. Rueger, and M. Charette, "The time-course of the induction of reparative dentine formation in monkeys by recombinant human osteogenic protein-1," *Archives of Oral Biology*, vol. 39, no. 10, pp. 833–838, 1994.

[30] M. Goldberg, N. Six, F. Decup et al., "Application of bioactive molecules in pulp-capping situations," *Advances in Dental Research*, vol. 15, pp. 91–95, 2001.

[31] F. Decup, N. Six, B. Palmier et al., "Bone sialoprotein-induced reparative dentinogenesis in the pulp of rat's molar," *Clinical oral investigations*, vol. 4, no. 2, pp. 110–119, 2000.

[32] A. Gericke, C. Qin, Y. Sun et al., "Different forms of DMP1 play distinct roles in mineralization," *Journal of Dental Research*, vol. 89, no. 4, pp. 355–359, 2010.

[33] N. Six, D. Septier, C. Chaussain-Miller, R. Blacher, P. DenBesten, and M. Goldberg, "Dentonin, a MEPE fragment initiates pulp-healing response to injury," *Journal of Dental Research*, vol. 86, no. 8, pp. 780–785, 2007.

[34] Y. Nakamura, L. Hammarström, E. Lundberg et al., "Enamel matrix derivative promotes reparative processes in the dental pulp," *Advances in Dental Research*, vol. 15, pp. 105–107, 2001.

[35] T. Okiji and K. Yoshiba, "Reparative dentinogenesis induced by mineral trioxide aggregate: a review from the biological and physicochemical points of view," *International Journal of Dentistry*, vol. 2009, Article ID 464280, 12 pages, 2009.

[36] M. L. R. Accorinte, A. D. Loguercio, A. Reis et al., "Response of human dental pulp capped with MTA and calcium hydroxide powder," *Operative Dentistry*, vol. 33, no. 5, pp. 488–495, 2008.

[37] P. Bornstein and E. H. Sage, "Matricellular proteins: extracellular modulators of cell function," *Current Opinion in Cell Biology*, vol. 14, no. 5, pp. 608–616, 2002.

[38] M. Goldberg, J. Farges, S. Lacerda-Pinheiro et al., "Inflammatory and immunological aspects of dental pulp repair," *Pharmacological Research*, vol. 58, no. 2, pp. 137–147, 2008.

[39] S. A. Eming, T. Krieg, and J. M. Davidson, "Inflammation in wound repair: molecular and cellular mechanisms," *Journal of Investigative Dermatology*, vol. 127, no. 3, pp. 514–525, 2007.

[40] M. Goldberg and A. Smith, "Cells and extracellular matrices of dentin and pulp. A biological basis for repair and tissue engineering," *Critical Reviews in Oral Biology & Medicine*, vol. 15, no. 1, pp. 13–27, 2004.

[41] M. Jontell, G. Bergenholtz, A. Scheynius, and W. Ambrose, "Dendritic cells and macrophages expressing class II antigens in the normal rat incisor pulp," *Journal of Dental Research*, vol. 67, no. 10, pp. 1263–1266, 1988.

[42] S. Nishikawa and F. Sasaki, "Apoptosis of dental pulp cells and their elimination by macrophages and MHC class II-expressing dendritic cells," *Journal of Histochemistry and Cytochemistry*, vol. 47, no. 3, pp. 303–311, 1999.

[43] M. Jontell, T. Okiji, U. Dahlgren, and G. Bergenholtz, "Immune defense mechanisms of the dental pulp," *Critical Reviews in Oral Biology and Medicine*, vol. 9, no. 2, pp. 179–200, 1998.

[44] K. Tanaka, T. Goto, T. Miyazaki, Y. Morita, S. Kobayashi, and T. Takahashi, "Apatite-coated hyaluronan for bone regeneration," *Journal of Dental Research*, vol. 90, no. 7, pp. 906–911, 2011.

[45] Y. A. Petrenko, R. V. Ivanov, A. Y. Petrenko, and V. I. Lozinsky, "Coupling of gelatin to inner surfaces of pore walls in spongy alginate-based scaffolds facilitates the adhesion, growth and differentiation of human bone marrow mesenchymal stromal cells," *Journal of Materials Science: Materials in Medicine*, vol. 22, no. 6, pp. 1529–1540, 2011.

[46] X. Chevalier, J. Jerosch, P. Goupille et al., "Single, intra-articular treatment with 6 ml hylan G-F 20 in patients with symptomatic primary osteoarthritis of the knee: a randomised, multicentre, double-blind, placebo controlled trial," *Annals of the Rheumatic Diseases*, vol. 69, no. 1, pp. 113–119, 2010.

[47] G. Marcì, G. Mele, L. Palmisano, P. Pulito, and A. Sannino, "Environmentally sustainable production of cellulose-based superabsorbent hydrogels," *Green Chemistry*, vol. 8, no. 5, pp. 439–444, 2006.

Hindawi Publishing Corporation
BioMed Research International
Volume 2014, Article ID 702821, 7 pages
http://dx.doi.org/10.1155/2014/702821

Research Article

Characterization of Genipin-Modified Dentin Collagen

Hiroko Nagaoka,[1] Hideaki Nagaoka,[2] Ricardo Walter,[3] Lee W. Boushell,[1] Patricia A. Miguez,[4] Andrew Burton,[2] André V. Ritter,[1] and Mitsuo Yamauchi[2]

[1] *Department of Operative Dentistry, School of Dentistry, University of North Carolina at Chapel Hill, Chapel Hill, NC 27599, USA*
[2] *NC Oral Health Institute, School of Dentistry, University of North Carolina at Chapel Hill, Chapel Hill, NC 27599, USA*
[3] *Department of Preventive and Restorative Sciences, School of Dental Medicine, University of Pennsylvania, Philadelphia, PA 19104, USA*
[4] *Department of Periodontics, School of Dental Medicine, University of Pennsylvania, Philadelphia, PA 19104, USA*

Correspondence should be addressed to Mitsuo Yamauchi; yamauchm@dentistry.unc.edu

Received 24 January 2014; Accepted 16 February 2014; Published 25 March 2014

Academic Editor: Yoshihiko Hayashi

Application of biomodification techniques to dentin can improve its biochemical and biomechanical properties. Several collagen cross-linking agents have been reported to strengthen the mechanical properties of dentin. However, the characteristics of collagen that has undergone agent-induced biomodification are not well understood. The objective of this study was to analyze the effects of a natural cross-linking agent, genipin (GE), on dentin discoloration, collagen stability, and changes in amino acid composition and lysyl oxidase mediated natural collagen cross-links. Dentin collagen obtained from extracted bovine teeth was treated with three different concentrations of GE (0.01%, 0.1%, and 0.5%) for several treatment times (0–24 h). Changes in biochemical properties of NaB^3H_4-reduced collagen were characterized by amino acid and cross-link analyses. The treatment of dentin collagen with GE resulted in a concentration- and time-dependent pigmentation and stability against bacterial collagenase. The lysyl oxidase-mediated trivalent mature cross-link, pyridinoline, showed no difference among all groups while the major divalent immature cross-link, dehydro-dihydroxylysinonorleucine/its ketoamine in collagen treated with 0.5% GE for 24 h, significantly decreased compared to control ($P < 0.05$). The newly formed GE-induced cross-links most likely involve lysine and hydroxylysine residues of collagen in a concentration-dependent manner. Some of these cross-links appear to be reducible and stabilized with NaB^3H_4.

1. Introduction

Fibrillar type I collagen is the major organic component in dentin matrix and functions as a stable template to spatially regulate mineral deposition and growth [1–3]. One of the functionally important characteristics of collagen is its unique posttranslational modifications. Covalent intermolecular cross-linking is the final posttranslational modification and is crucial for the stability, tensile strength, and viscoelasticity of collagen matrix [4–8].

Lysyl oxidase (LOX-) mediated collagen cross-linking has been extensively studied [5, 9–12]. The chemical structure and the quantity of these cross-links are primarily determined by the extent of hydroxylation of specific lysine (Lys) residues in the collagen molecule and the extent of oxidative deamination of the Lys and hydroxylysine (Hyl) residues in the telopeptide domains of the molecule. Lysyl hydroxylases and LOX/LOX-like proteins catalyze the reactions for these modifications, respectively. The glycosylation pattern of specific helical Hyl residues that are involved in cross-linking may modulate the maturation of collagen cross-links [13]. The cross-linking pattern can also be determined by the maturation/turnover rate of tissues [14–18], the details of molecular packing structure [18–20], and the physical force exerted on the tissue [21].

Collagen cross-links can also be induced nonenzymatically by treatment with chemicals and natural plant/fruit extracts [22]. Such cross-linking has been shown to facilitate preservation of substrate shape in scaffolds [23], improve physiological function of tissues [24–27], and increase the

mechanical properties of collagen [22, 28–30]. For instance, the synthetic cross-linking agent glutaraldehyde (GA) has been widely used as a fixative agent. It is well documented that GA treatment improves the stability of various collagen-based tissues [26, 31–33]. However, the direct application of GA to biological tissues has limitation due to its cytotoxicity [24, 34].

Genipin (GE), a traditional Chinese herbal medicine extracted from fruit of *Gardenia jasminoides,* has been found to be an effective collagen cross-linking agent [35]. GE has relatively mild *in vitro* cytotoxicity, and GE-treated collagen has increased toughness when compared to GA-treated collagen [24, 36].

While several studies on the effects of GE on dentin have been published [30, 37, 38], experimental conditions for GE treatment are not well defined and the nature of GE-induced cross-linking remains elusive. A better understanding of GE-induced collagen modification in dentin may provide insights into the development of novel biomodification technology which is useful in dentistry. As the first step towards this goal, we characterized the effects of various GE treatment regimens on dentin discoloration, collagen stability, amino acid composition, and LOX-mediated collagen cross-links.

2. Materials and Methods

2.1. Sample Collection, Demineralization, and GE Treatment. Extracted intact bovine incisors (≤1 year old animals) were used in this study. Enamel, cementum, and pulp were removed using high-speed diamond burs with water/air-cooling. Dentin was pulverized under liquid N_2 by a Spex Freezer Mill (SPEX CertiPrep, Inc., Metuchen, NJ, USA) and extensively washed with cold distilled water and lyophilized. The resultant dentin powder was demineralized with 0.5 M ethylenediaminetetraacetic acid (EDTA, pH 7.4) at 4°C for 14 days. The EDTA solution was changed twice each week during the demineralization period. The demineralized dentin matrix protein (~90% collagen) was extensively washed with cold distilled water and lyophilized. 2 mg aliquots of the collagen were randomly allocated to the following four treatment groups based on GE concentration (n = 21/group).

Group 1 (control): specimens were treated with phosphate buffered saline (PBS).

Group 2 (0.01% GE): specimens were treated with 0.01% GE in PBS.

Group 3 (0.1% GE): specimens were treated with 0.1% GE in PBS.

Group 4 (0.5% GE): specimens were treated with 0.5% GE in PBS.

Previously, ~0.5% of GE treatment has been shown to improve dentin mechanical properties [30, 38] but lower concentrations have not been investigated in this context.

2.2. Discoloration and Stability of GE-Modified Dentin Collagen. 2 mg aliquots of demineralized dentin collagen were treated with 1 mL of PBS or GE (Wako Pure Chemical Industries, Ltd., Osaka, Japan) according to groups 1–4 and incubated for 30 min, 1 h, 4 h, 8 h, 12 h, and 24 h at 37°C with agitation (n = 3/time point, n = 18/group). After treatment, the samples were extensively washed with distilled water, lyophilized, and observed for their discoloration.

Collagen stability was assessed in the same samples by enzymatic degradation assay as reported [30]. Samples were suspended in 1 mL of 50 mM ammonium bicarbonate and digested with 5% w/w bacterial collagenase derived from *Clostridium histolyticum* (Worthington Biochemical Corp., Lakewood, NJ, USA, 1,075 U/mg) for 24 h at 37°C. After digestion, the samples were centrifuged for 15 min at 15,000 g, and the residues (undigested collagen) were washedwith distilled water by repeated centrifugation and lyophilized. The residues were hydrolyzed with 300 μL of 6 N HCl (Pierce, Rockford, IL, USA) *in vacuo* after flushing with N_2 gas for 22 h at 105°C. The hydrolysates were dried, reconstituted in 300 μL of distilled water, filtered, and subjected to hydroxyproline (Hyp) analysis using a high-performance liquid chromatography (HPLC) system (Prostar 240/310, Varian, Walnut Creek, CA, USA) fitted with a cation exchange column (AA911; Transgenomic, Inc., San Jose, CA, USA) [39]. The primary outcome measure for this analysis was the Hyp recovered in the undigested residue in nM, which is expressed as means ± standard deviation (SD).

2.3. Amino Acid and Collagen Cross-Link Analyses. 2 mg aliquots of demineralized dentin collagen were treated with PBS or GE according to groups 1–4 and incubated for 24 h at 37°C (n = 3/group). After treatment, the samples were extensively washed with distilled water, lyophilized, reduced with standardized NaB^3H_4 to stabilize and label reducible cross-links, and hydrolyzed. An aliquot of each hydrolysate was subjected to amino acid analysis as described [39]. The relative amount of each amino acid was calculated as residues per 1,000 total amino acids. The hydrolysates with known amounts of Hyp were then analyzed for cross-links [39]. The major reducible immature cross-links, dehydrodihydroxylysinonorleucine (deH-DHLNL)/its ketoamine and dehydrohydroxylysinonorleucine/its ketoamine (deH-HLNL), were analyzed as their reduced forms, that is, dihydroxylysinonorleucine (DHLNL) and hydroxylysinonorleucine (HLNL), respectively. The nonreducible mature cross-links, pyridinoline (Pyr) and deoxy-Pyr (d-Pyr), were also analyzed simultaneously as described [39]. For their chemical structures, see [5]. The major cross-links in dentin collagen, DHLNL and Pyr, were quantified as moles/mole of collagen based on the value of 300 residues of Hyp per collagen molecule. All analyses were done in triplicate in independent experiments.

2.4. Statistical Analysis. The statistical analyses were performed using two-way ANOVA and Fisher's PLSD (Stat View software, SAS Institute Inc., Cary, NC,USA). A p value of less than 0.05 was considered statistically significant.

3. Results

3.1. Discoloration and Stability of GE-Modified Dentin Collagen. The demineralized dentin collagen treated with GE exhibited distinct features. Dentin collagen in the control group presented a white color while a concentration- and time-dependent dark blue pigmentation was observed in the GE-treated groups (Figure 1). Hyp analysis showed that dentin collagen in all 18 control groups was almost completely digested. However, when treated with GE, the digestibility markedly decreased in a concentration- and time-dependent manner (Figure 2). The Hyp contents in the insoluble residues (nM ± SD, treatment time in parenthesis) in the samples treated with 0.5% GE were 81.9 ± 4.9 nM* (30 min), 166.4 ± 3.8 nM* (1 h), 926.6 ± 37.6 nM** (4 h), 1,243.5 ± 50.6 nM** (8 h), 1,259.1 ± 48.3 nM** (12 h), and 1,259.3 ± 61.4 nM** (24 h). Twenty-four-hour treatment with PBS (control), 0.01% GE, and 0.1% GE resulted in the recovery of 2.0 ± 1.7 nM^{b}, 166.0 ± 19.3 nM^{*,b,‡}, and 1,054.3 ± 47.3 nM^{**,a} Hyp in the insoluble residues, respectively ($^{*}P < 0.001$, $^{**}P < 0.0001$ which are different from the value of control. $^{‡}P < 0.0001$ which is different from the value of 0.1% GE. $^{a}P < 0.001$, $^{b}P < 0.0001$ which are different from the value of 0.5% GE) (see Figure 2).

3.2. Amino Acid Analysis. Amino acid compositions in all groups at all-time points were essentially identical to one another (data not shown) with the exception of Lys and Hyl. The amounts of Lys and Hyl in all groups treated for 24 h are shown in Table 1. Lys and Hyl in the GE-treated groups were significantly decreased in a concentration-dependent manner when compared to the control. No significant changes were observed for other amino acids.

3.3. Collagen Cross-Link Analysis. Typical chromatographic profiles of reducible and nonreducible collagen cross-links are shown in Figures 3(a) and 3(b), respectively. Two major cross-links, DHLNL (reducible) and Pyr (nonreducible), were identified in all groups. In all of these samples, HLNL and d-Pyr were less than 1/10 of DHLNL and Pyr, respectively, and thus they were not calculated. In addition, two unknown (unk), $NaB^{3}H_{4}$-reducible peaks were identified in the GE-treated groups (peaks at 22 min: unk 1, and peaks at 64 min: unk 2, resp.) (Figure 3(a)). The results of the quantitative cross-link analyses of DHLNL, Pyr, unk 1, and unk 2 comparing PBS- and GE-treated groups are summarized in Table 2.

The amounts of DHLNL in 0.01% and 0.1% GE for 24 h were not significantly different from those of control, but DHLNL in 0.5% GE for 24 h (1.13 ± 0.07 M) was significantly decreased when compared to that of control (1.36 ± 0.17 M) ($P < 0.05$) (Figure 3(a) and Table 2). The amount of Pyr in all three GE groups treated for 24 h showed no significant differences when compared with control (Figure 3(b) and Table 2).

The amounts of newly GE-induced reducible cross-links/compounds, unk 1 and unk 2, in GE groups treated for 24 h were significantly increased in a concentration-dependent manner (Figure 3(a) and Table 2).

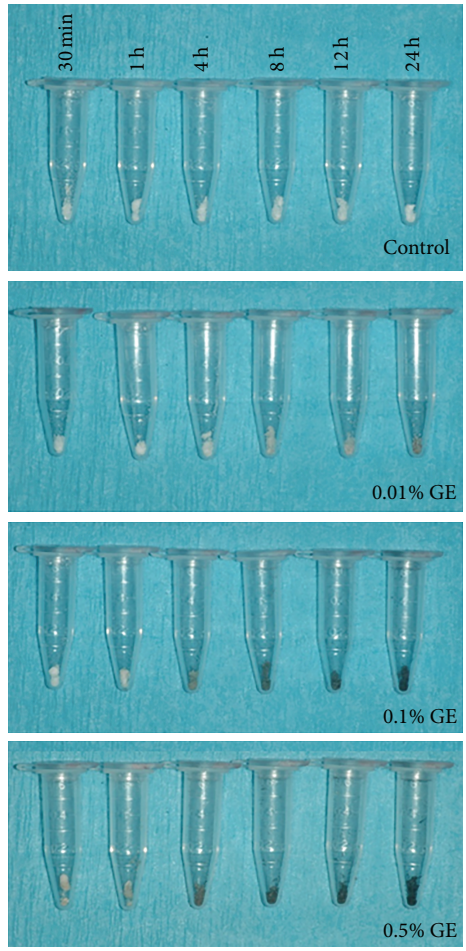

Figure 1: Discoloration of GE-modified dentin collagen. Photographs of the representative discoloration of dentin collagen treated with PBS (control) and three different concentrations (0.01%, 0.1%, and 0.5%) of genipin (GE) for six treatment durations (30 min, 1 h, 4 h, 8 h, 12 h, and 24 h).

Table 1: The amounts of lysine and hydroxylysine in a 24-hour treatment duration of PBS (control) and three concentrations of genipin (0.01%, 0.1%, and 0.5%) groups.

	Control	0.01% GE	0.1% GE	0.5% GE
Lys	26.2 (3.5)	18.8 (0.8)^{a}	9.8 (2.3)^{c,e}	2.3 (1.6)^{c,f,h}
Hyl	12.8 (0.8)	7.5 (1.8)^{b}	4.3 (0.3)^{c,d}	1.6 (0.4)^{c,e,g}

All values are shown as relative amounts in 1,000 total residues (means and standard deviations). GE: genipin; Lys: lysine; Hyl: hydroxylysine; $n = 3$; $^{a}P < 0.05$ which is different from the value of control; $^{b}P < 0.005$ which is different from the value of control; $^{c}P < 0.001$ which is different from the value of control; $^{d}P < 0.05$ which is different from the value of 0.01% GE; $^{e}P < 0.005$ which is different from the value of 0.01% GE; $^{f}P < 0.001$ which is different from the value of 0.01% GE; $^{g}P < 0.05$ which is different from the value of 0.1% GE; $^{h}P < 0.01$ which is different from the value of 0.1% GE.

Table 2: The contents of enzymatic and GE-induced cross-links in a 24-hour treatment duration of PBS (control) and three concentrations of genipin (0.01%, 0.1%, and 0.5%) groups.

	Control	0.01% GE	0.1% GE	0.5% GE
DHLNL	1.36 (0.17)	1.35 (0.23)	1.23 (0.19)	1.13 (0.07)[a]
Pyr	0.190 (0.085)	0.188 (0.014)	0.187 (0.084)	0.186 (0.083)
unk 1 (22 min)	3169 (793)	26991 (4007)	110483 (6525)[a,f]	142893 (25133)[c,e]
unk 2 (64 min)	1787 (90)	29160 (8418)	136342 (21531)[b,d]	253668 (45338)[b,e]

All values in DHLNL and Pyr are expressed in moles/mole collagen (means and standard deviations). All values in unk 1 and 2 are expressed in disintegrations per minute (DPM) (means and standard deviations). DHLNL: dihydroxylysinonorleucine; Pyr: pyridinoline; unk: unknown; GE: genipin; $n = 3$; [a]$P < 0.05$ which is different from the value of control; [b]$P < 0.01$ which is different from the value of control; [c]$P < 0.001$ which is different from the value of control; [d]$P < 0.05$ which is different from the value of 0.01% GE; [e]$P < 0.005$ which is different from the value of 0.01% GE; [f]$P < 0.001$ which is different from the value of 0.01% GE.

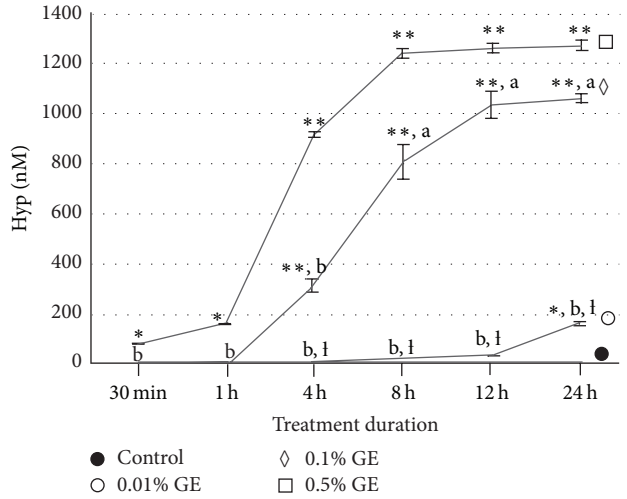

Figure 2: Collagen stability of GE-modified dentin collagen. 2 mg aliquots of demineralized dentin treated with PBS (control) and three concentrations of genipin (GE) (0.01%, 0.1%, and 0.5%) for six treatment durations (30 min, 1 h, 4 h, 8 h, 12 h, and 24 h) were subjected to collagenase digestion and hydroxyproline (Hyp) analysis. The mean amounts of undigested collagen with bacterial collagenase are shown as Hyp content (nM) in the insoluble residues. ($n = 3$). $^{*}P < 0.001$, $^{**}P < 0.0001$ which are different from the value of control. $^{ł}P < 0.0001$ which is different from the value of 0.1% GE. [a]$P < 0.001$, [b]$P < 0.0001$ which are different from the value of 0.5% GE.

4. Discussion

The present study was undertaken to evaluate the effects of GE treatments under various conditions on dentin collagen using biochemical approaches such as Hyp analysis, amino acid analysis, and quantitative cross-link analysis. GE-treatment of collagen resulted in blue pigmentation as previously reported [24, 30, 40]. The blue discoloration of demineralized dentin collagen by GE increases in a concentration- and time-dependent manner. The blue pigmentation is possibly formed through a series of oxygen radical-involved polymerization and dehydrogenation of several intermediary pigments [41, 42] utilizing the ε-amino group of Lys and Hyl. These compounds are likely associated with intra- and intermolecular cross-linking of collagen as the intensity of the color corresponded well with the collagen stability against enzymatic digestion. Collagen stability was evaluated by digestibility with bacterial collagenase which hydrolyzes the peptide bond on the amino-terminal side of Gly in -X-Gly-Pro [43]. Based on the mean values of Hyp in 2 mg demineralized dentin matrix in this study, the rate of collagen digestion was 93.6%, 86.9%, 27.2%, 2.3%, 1.1%, and 1.1% in 0.5% GE for 30 min, 1 h, 4 h, 8 h, 12 h, and 24 h, respectively. Treatment with PBS, 0.01% GE, and 0.1% GE for 24 h resulted in 99.8%, 87.0%, and 17.2% collagen digestion, respectively. Thus, the rate of collagen digestion with GE treatment clearly decreased in a concentration- and time-dependent manner (Figure 2). Almost no collagen was digested when collagen was treated with 0.5% GE for 12 h and 24 h. We hypothesize that GE-induced cross-linking hinders the enzyme accessibility to collagen and/or generates a large cross-linked collagen complex so that collagenase cleavage no longer solubilizes the complex. Further studies are warranted to test this hypothesis.

Results of the amino acid analysis demonstrated that Lys and Hyl residues were the only amino acids that decreased significantly with GE treatment in a concentration-dependent manner. When the values of Lys and Hyl were calculated on residues per 1,000 amino acids basis, the mean number of Lys in GE groups for 24 h decreased from 26.2 (±3.5) in the control group to 2.3 (±1.6) in the 0.5% GE group. In the case of Hyl, it decreased from 12.8 (±0.8) in the control group to 1.6 (±0.4) in the 0.5% GE group (note: some of the Lys residues are derived from noncollagenous proteins). These data indicate that approximately 90% of both Lys and Hyl residues were utilized for GE-induced cross-links when treated with 0.5% GE treatment for 24 h. Since some of the Hyl residues in dentin type I collagen are glycosylated [44], the data also indicate that the post-translational modifications of Lys, that is, 5-hydroxylation, and subsequent O-glycosylation do not significantly hinder the formation of such cross-linking. Under the conditions used, no other amino acids including arginine (Arg) were significantly changed by GE treatment. Sung et al. reported that Arg in addition to Lys and Hyl was used in the reaction

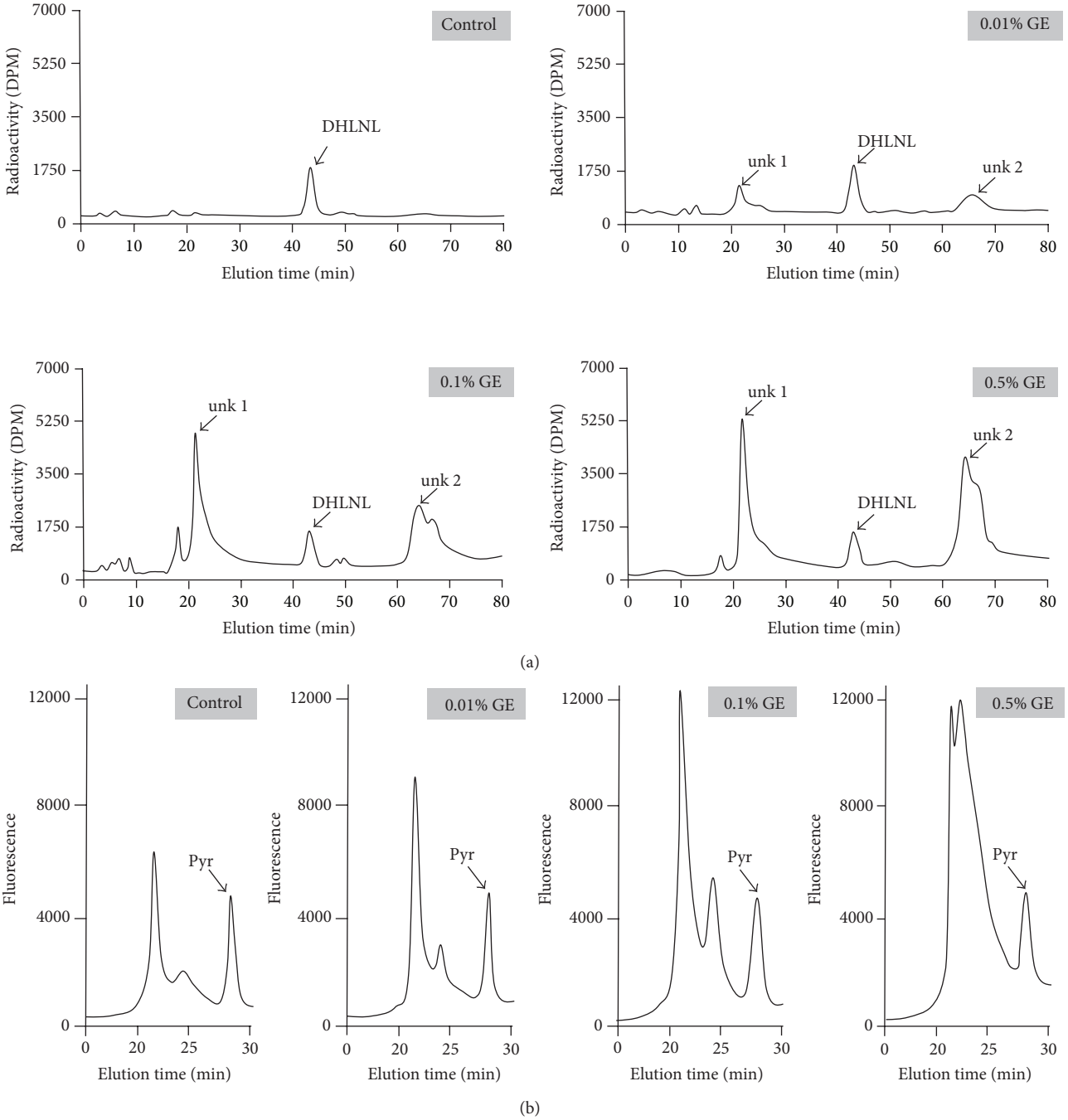

Figure 3: Representative chromatographs of (a) reducible and (b) nonreducible collagen cross-links in 24 h treatment duration of PBS (control) and three concentrations of genipin (GE) (0.01%, 0.1%, and 0.5%) groups.

with GE in porcine pericardia [24]. Possibly, under the treatment conditions and tissues used in the current study, the GE reaction favors the ε-amino groups on Lys and Hyl.

Cross-link analysis revealed at least two unidentified, reducible compounds in the GE-treated groups. These major radioactive peaks eluted at 22 and 64 min were observed in our HPLC system, and they increased in a concentration-dependent manner. Thus, these two newly formed reducible compounds are likely associated with GE-induced cross-links involving Lys and Hyl residues of collagen. Two cross-linking mechanisms between GE and biopolymers (such as collagen) containing primary amine groups were proposed by Butler et al. [45], one via the nucleophilic attack of the GE C3 atom from a primary amine group forming an intermediate aldehyde leading to the formation of heterocyclic compound linking GE and the biopolymer and the other via nucleophilic

substitution of the ester group in GE forming a secondary amide link to the biopolymer. However, a number of intermediates [41, 42] and further condensations/polymerization [46] are likely to occur. Some of these cross-linking compounds could be reduced with $NaBH_4$ and stabilized. Further studies are warranted to identify the structures of these cross-links by isolating and characterizing these compounds and collagen-derived cross-linked peptides by, for instance, biochemical and mass spectrometric approaches [13]. There was a slight but significant decrease of DHLNL in 0.5% GE group treated for 24 h when compared to that of control. The cause of this decrease is not clear but it could be due to the GE-induced modification of the unstable aldimine bond of deH-DHLNL which was present prior to its rearrangement to a stable ketoamine. The decrease in DHLNL, however, needs to be confirmed by increasing the number of analyses. The maturational product of deH-DHLNL/its ketoamine, Pyr, showed no significant changes in all groups in this study due likely to the stability of this cross-link.

Further characterization of GE-induced cross-links in dentin collagen and their long-term stability, dentin mechanical properties, and restorative procedures is warranted. A natural compound-based dentin treatment for tooth or restoration reinforcement may help develop a reliable and safer therapy with applications in dentistry.

5. Conclusions

Under the conditions of this study, the treatment of bovine dentin collagen with GE results in a concentration- and time-dependent increase in discoloration and collagen stability against bacterial collagenase. The GE-induced, reducible cross-links/compounds involving Lys and Hyl residues increase in a concentration-dependent manner. GE treatment may modify some of the immature divalent cross-links.

Disclosure

The authors declare that this paper is original, has not been published before, and is not currently being considered for publication elsewhere. They confirm that the paper has been read and approved by all named authors and there are no other persons who satisfied the criteria for authorship that are not listed. The authors further confirm that the order of authors listed in the paper has been approved by all of them.

Conflict of Interests

The authors declare that there is no conflict of interests regarding the publication of this paper.

Acknowledgment

The research is partly funded by NIH (DE020909 and AR060978).

References

[1] Y. Kuboki and G. L. Mechanic, "Comparative molecular distribution of cross-links in bone and dentin collagen. Structure-function relationships," *Calcified Tissue International*, vol. 34, no. 3, pp. 306–308, 1982.

[2] W. G. Stetler-Stevenson and A. Veis, "Type I collagen shows a specific binding affinity for bovine dentin phosphophoryn," *Calcified Tissue International*, vol. 38, no. 3, pp. 135–141, 1986.

[3] F. H. Silver and W. J. Landis, "Deposition of apatite in mineralizing vertebrate extracellular matrices: a model of possible nucleation sites on type I collagen," *Connective Tissue Research*, vol. 52, no. 3, pp. 242–254, 2011.

[4] M. Nimni and R. Harkness, "Molecular structures and functions of collagen," in *Collagen Biochemistry*, M. Nimni, Ed., pp. 1–77, CRC Press, Boca Raton, Fla, USA, 1988.

[5] M. Yamauchi and G. L. Mechanic, "Cross-linking of collagen," in *Collagen*, M. NImni and B. Olsen, Eds., pp. 157–172, CRC Press, Boca Raton, Fla, USA, 1988.

[6] H. M. Kagan, "Intra- and extracellular enzymes of collagen biosynthesis as biological and chemical targets in the control of fibrosis," *Acta Tropica*, vol. 77, no. 1, pp. 147–152, 2000.

[7] M. Yamauchi, "Collagen biochemistry: an overview," in *Bone Morphogenetic Protein and Collagen*, G. Phillips, Ed., pp. 93–148, World Scientific Publishing, River Edge, NJ, USA, 2002.

[8] P. A. Miguez, P. N. R. Pereira, P. Atsawasuwan, and M. Yamauchi, "Collagen cross-linking and ultimate tensile strength in dentin," *Journal of Dental Research*, vol. 83, no. 10, pp. 807–810, 2004.

[9] A. J. Bailey, "Molecular mechanisms of ageing in connective tissues," *Mechanisms of Ageing and Development*, vol. 122, no. 7, pp. 735–755, 2001.

[10] D. R. Eyre, M. A. Paz, and P. M. Gallop, "Cross-linking in collagen and elastin," *Annual Review of Biochemistry*, vol. 53, pp. 717–748, 1983.

[11] M. Tanzer, "Cross-linking," in *Biochemistry of Collagen*, G. Ramachandran and A. Reddi, Eds., pp. 137–162, Plenum Press, New York, NY, USA, 1976.

[12] M. Yamauchi, "Collagen, The major matrix molecule in mineralized tissues," in *Calcium and Phosphorus in Health and Disease*, J. J. B. Anderson and S. C. Garner, Eds., pp. 127–145, CRC Press, Boca Raton, Fla, USA, 1996.

[13] M. Sricholpech, I. Perdivara, M. Yokoyama et al., "Lysyl hydroxylase 3-mediated glucosylation in type I collagen: molecular loci and biological significance," *Journal of Biological Chemistry*, vol. 287, pp. 22998–23009, 2012.

[14] A. J. Bailey and M. S. Shimokomaki, "Age related changes in the reducible cross-links of collagen," *FEBS Letters*, vol. 16, no. 2, pp. 86–88, 1971.

[15] T. Moriguchi and D. Fujimoto, "Age-related changes in the content of the collagen crosslink, pyridinoline," *Journal of Biochemistry*, vol. 84, no. 4, pp. 933–935, 1978.

[16] D. R. Eyre, I. R. Dickson, and K. Van Ness, "Collagen cross-linking in human bone and articular cartilage. Age-related changes in the content of mature hydroxypyridinium residues," *Biochemical Journal*, vol. 252, no. 2, pp. 495–500, 1988.

[17] M. Yamauchi, D. T. Woodley, and G. L. Mechanic, "Aging and cross-linking of skin collagen," *Biochemical and Biophysical Research Communications*, vol. 152, no. 2, pp. 898–903, 1988.

[18] M. Yamauchi, E. P. Katz, and G. L. Mechanic, "Intermolecular cross-linking and stereospecific molecular packing in type I

collagen fibrils of the periodontal ligament," *Biochemistry*, vol. 25, no. 17, pp. 4907–4913, 1986.

[19] G. L. Mechanic, E. P. Katz, M. Henmi, C. Noyes, and M. Yamauchi, "Locus of a histidine-based, stable trifunctional, helix to helix collagen cross-link: stereospecific collagen structure of type I skin fibrils," *Biochemistry*, vol. 26, no. 12, pp. 3500–3509, 1987.

[20] E. P. Katz and C. W. David, "Unique side-chain conformation encoding for chirality and azimuthal orientation in the molecular packing of skin collagen," *Journal of Molecular Biology*, vol. 228, no. 3, pp. 963–969, 1992.

[21] K. Otsubo, E. P. Katz, G. L. Mechanic, and M. Yamauchi, "Cross-linking connectivity in bone collagen fibrils: the COOH-terminal locus of free aldehyde," *Biochemistry*, vol. 31, no. 2, pp. 396–402, 1992.

[22] H. W. Sung, Y. Chang, C. T. Chiu, C. N. Chen, and H. C. Liang, "Crosslinking characteristics and mechanical properties of a bovine pericardium fixed with a naturally occurring crosslinking agent," *Journal of Biomedical Materials Research*, vol. 47, pp. 116–126, 1999.

[23] H. W. Sung, I. L. Liang, C. N. Chen, R. N. Huang, and H. F. Liang, "Stability of a biological tissue fixed with a naturally occurring crosslinking agent (genipin)," *Journal of Biomedical Materials Research*, vol. 55, pp. 538–546, 2001.

[24] H. W. Sung, R. N. Huang, L. L. Huang, C. C. Tsai, and C. T. Chiu, "Feasibility study of a natural crosslinking reagent for biological tissue fixation," *Journal of Biomedical Materials Research*, vol. 42, pp. 560–567, 1998.

[25] H.-W. Sung, Y. Chang, C.-T. Chiu, C.-N. Chen, and H.-C. Liang, "Mechanical properties of a porcine aortic valve fixed with a naturally occurring crosslinking agent," *Biomaterials*, vol. 20, no. 19, pp. 1759–1772, 1999.

[26] Y. Chang, C.-C. Tsai, H.-C. Liang, and H.-W. Sung, "In vivo evaluation of cellular and acellular bovine pericardia fixed with a naturally occurring crosslinking agent (genipin)," *Biomaterials*, vol. 23, no. 12, pp. 2447–2457, 2002.

[27] H.-C. Liang, Y. Chang, C.-K. Hsu, M.-H. Lee, and H.-W. Sung, "Effects of crosslinking degree of an acellular biological tissue on its tissue regeneration pattern," *Biomaterials*, vol. 25, no. 17, pp. 3541–3552, 2004.

[28] L. L. Huang, H. W. Sung, C. C. Tsai, and D. M. Huang, "Biocompatibility study of a biological tissue fixed with a naturally occurring crosslinking reagent," *Journal of Biomedical Materials Research*, vol. 42, pp. 568–576, 1998.

[29] B. Han, J. Jaurequi, B. W. Tang, and M. E. Nimni, "Proanthocyanidin: a natural crosslinking reagent for stabilizing collagen matrices," *Journal of Biomedical Materials Research A*, vol. 65, no. 1, pp. 118–124, 2003.

[30] R. Walter, P. A. Miguez, R. R. Arnold, P. N. R. Pereira, W. R. Duarte, and M. Yamauchi, "Effects of natural cross-linkers on the stability of dentin collagen and the inhibition of root caries in vitro," *Caries Research*, vol. 42, no. 4, pp. 263–268, 2008.

[31] A. K. B. Bedran-Russo, D. H. Pashley, K. Agee, J. L. Drummond, and K. J. Miescke, "Changes in stiffness of demineralized dentin following application of collagen crosslinkers," *Journal of Biomedical Materials Research B*, vol. 86, no. 2, pp. 330–334, 2008.

[32] M. C. V. B. Braile, N. C. Carnevalli, G. Goissis, V. A. Ramirez, and D. M. Braile, "In vitro properties and performance of glutaraldehyde-crosslinked bovine pericardial bioprostheses treated with glutamic acid," *Artificial Organs*, vol. 35, no. 5, pp. 497–501, 2011.

[33] A. K. B. Bedran-Russo, C. S. Castellan, M. S. Shinohara, L. Hassan, and A. Antunes, "Characterization of biomodified dentin matrices for potential preventive and reparative therapies," *Acta Biomaterialia*, vol. 7, no. 4, pp. 1735–1741, 2011.

[34] H.-W. Sung, R.-N. Huang, L. L. H. Huang, and C.-C. Tsai, "In vitro evaluation of cytotoxicity of a naturally occurring cross-linking reagent for biological tissue fixation," *Journal of Biomaterials Science, Polymer Edition*, vol. 10, no. 1, pp. 63–78, 1999.

[35] Y. Chang, C.-C. Tsai, H.-C. Liang, and H.-W. Sung, "Reconstruction of the right ventricular outflow tract with a bovine jugular vein graft fixed with a naturally occurring crosslinking agent (genipin) in a canine model," *Journal of Thoracic and Cardiovascular Surgery*, vol. 122, no. 6, pp. 1208–1218, 2001.

[36] C. C. Tsai, R. N. Huang, H. W. Sung, and H. C. Liang, "In vitro evaluation of the genotoxicity of a naturally occurring crosslinking agent (genipin) for biologic tissue fixation," *Journal of Biomedical Materials Research*, vol. 52, pp. 58–65, 2000.

[37] A. K. B. Bedran-Russo, P. N. R. Pereira, W. R. Duarte, J. L. Drummond, and M. Yamaychi, "Application of crosslinkers to dentin collagen enhances the ultimate tensile strength," *Journal of Biomedical Materials Research B*, vol. 80, no. 1, pp. 268–272, 2007.

[38] A. Al-Ammar, J. L. Drummond, and A. K. Bedran-Russo, "The use of collagen cross-linking agents to enhance dentin bond strength," *Journal of Biomedical Materials Research B*, vol. 91, no. 1, pp. 419–424, 2009.

[39] M. Yamauchi and M. Shiiba, "Lysine hydroxylation and cross-linking of collagen," *Methods in Molecular Biology*, vol. 446, pp. 95–108, 2008.

[40] S.-W. Lee, J.-M. Lim, S.-H. Bhoo, Y.-S. Paik, and T.-R. Hahn, "Colorimetric determination of amino acids using genipin from Gardenia jasminoides," *Analytica Chimica Acta*, vol. 480, no. 2, pp. 267–274, 2003.

[41] R. Touyama, Y. Takeda, K. Inoue et al., "Studies on the blue pigments produced from genipin and methylamine. I. Structures of the brownish-red pigments, intermediates leading to the blue pigments," *Chemical and Pharmaceutical Bulletin*, vol. 42, no. 3, pp. 668–673, 1994.

[42] R. Touyama, K. Inoue, Y. Takeda et al., "Studies on the blue pigments produced from genipin and methylamine. II. On the formation mechanisms of brownish-red intermediates leading to the blue pigment formation," *Chemical and Pharmaceutical Bulletin*, vol. 42, no. 8, pp. 1571–1578, 1994.

[43] K. Watanabe, "Collagenolytic proteases from bacteria," *Applied Microbiology and Biotechnology*, vol. 63, no. 5, pp. 520–526, 2004.

[44] M. Wohllebe and D. J. Carmichael, "Biochemical characterization of guanidinium chloride-soluble dentine collagen from lathyritic-rat incisors," *Biochemical Journal*, vol. 181, no. 3, pp. 667–676, 1979.

[45] M. F. Butler, Y.-F. Ng, and P. D. A. Pudney, "Mechanism and kinetics of the crosslinking reaction between biopolymers containing primary amine groups and genipin," *Journal of Polymer Science A*, vol. 41, no. 24, pp. 3941–3953, 2003.

[46] F.-L. Mi, S.-S. Shyu, and C.-K. Peng, "Characterization of ring-opening polymerization of genipin and pH-dependent cross-linking reactions between chitosan and genipin," *Journal of Polymer Science A*, vol. 43, no. 10, pp. 1985–2000, 2005.

Hindawi Publishing Corporation
BioMed Research International
Volume 2014, Article ID 789591, 9 pages
http://dx.doi.org/10.1155/2014/789591

Research Article

A Proteomic View to Characterize the Effect of Chitosan Nanoparticle to Hepatic Cells: Is Chitosan Nanoparticle an Enhancer of PI3K/AKT1/mTOR Pathway?

Ming-Hui Yang,[1,2,3] Shyng-Shiou Yuan,[2,3,4,5] Ying-Fong Huang,[6,7] Po-Chiao Lin,[8,9] Chi-Yu Lu,[9,10] Tze-Wen Chung,[11] and Yu-Chang Tyan[2,6,9,12]

[1] *Instrument Technology Research Center, National Applied Research Laboratories, Hsinchu 300, Taiwan*
[2] *Translational Research Center, Kaohsiung Medical University Chung-Ho Memorial Hospital, Kaohsiung 807, Taiwan*
[3] *Department of Medical Research, Kaohsiung Medical University Chung-Ho Memorial Hospital, Kaohsiung 807, Taiwan*
[4] *Department of Obstetrics and Gynecology, Kaohsiung Medical University Chung-Ho Memorial Hospital, Kaohsiung 807, Taiwan*
[5] *School of Medicine, College of Medicine, Kaohsiung Medical University, Kaohsiung 807, Taiwan*
[6] *Department of Medical Imaging and Radiological Sciences, Kaohsiung Medical University, Kaohsiung 807, Taiwan*
[7] *Department of Nuclear Medicine, Kaohsiung Medical University Chung-Ho Memorial Hospital, Kaohsiung 807, Taiwan*
[8] *Department of Chemistry, National Sun Yat-sen University, Kaohsiung 804, Taiwan*
[9] *National Sun Yat-sen University-Kaohsiung Medical University Joint Research Center, Kaohsiung 807, Taiwan*
[10] *Department of Biochemistry, College of Medicine, Kaohsiung Medical University, Kaohsiung 807, Taiwan*
[11] *Department of Biomedical Engineering, National Yang-Ming University, Taipei 112, Taiwan*
[12] *Center of Biomedical Engineering and System Biology, Kaohsiung Medical University, Kaohsiung 807, Taiwan*

Correspondence should be addressed to Tze-Wen Chung; twchung@ms.ym.edu.tw and Yu-Chang Tyan; yctyan@kmu.edu.tw

Received 27 November 2013; Accepted 10 February 2014; Published 16 March 2014

Academic Editor: Yoshihiko Hayashi

Chitosan nanoparticle, a biocompatible material, was used as a potential drug delivery system widely. Our current investigation studies were the bioeffects of the chitosan nanoparticle uptake by liver cells. In this experiment, the characterizations of chitosan nanoparticles were measured by transmission electron microscopy and particle size analyzer. The average size of the chitosan nanoparticle was 224.6 ± 11.2 nm, and the average zeta potential was +14.08 ± 0.7 mV. Moreover, using proteomic approaches to analyze the differential protein expression patterns resulted from the chitosan nanoparticle uptaken by HepG2 and CCL-13 cells identified several proteins involved in the PI3K/AKT1/mTOR pathway. Our experimental results have demonstrated that the chitosan nanoparticle may involve in the liver cancer cell metastasis and proliferation.

1. Introduction

Biomaterials play important roles in regenerative medicine, tissue engineering, and drug delivery [1]. Nanomedicine is the application of nanotechnology in medicine, which enabled the development of nanoparticle therapeutic carriers. These drug carriers are targeted to tumor cell surfaces through the enhanced permeability and retention effect; thus, they are very suitable for the chemotherapeutics delivery in cancer treatment. Nanomaterials have increased surface to volume ratio compared with their bulk materials, and this may confer interesting properties, such as increased mechanical strength. Their distinct physicochemical characteristics, obtained by changing the size and shape, are very different from their natural materials and thus granting new possibilities [2]. Different nanomaterials have various effects on cells. For example, the uptake of silver nanoparticles caused cell proliferation inhibition in mouse leukaemic monocyte macrophage cells [3] and human keratinocytes [4]. In addition, low concentration of gold nanoparticles

resulted reduced cell proliferation in rat pheochromocytoma cells and human umbilical vein endothelial cells [5]. On the other hand, single-wall carbon nanotubes (SWCNTs) were investigated for biomedical applications and showed no negative effect for cell proliferation [6].

Chitosan, a biocompatible and biodegradable polymer, is a modified natural carbohydrate polymer prepared by the partial N-deacetylation of chitin (primary unit: 2-deoxy-2-(acetylamino) glucose). Chitosan and chitin, next to cellulose, are the second most plentiful nature and nontoxic, biodegradable cationic polymers. It is a natural biopolymer derived from crustacean shells such as krill, shrimps, lobsters, and crabs [1]. As such, chitosan is an abundant natural polymer available from a renewable resource. Chitosan, a mucopolysaccharide having structural characteristics similar to glycosamines, is a linear $\beta(1 \rightarrow 4)$-D-glucosamine and acetyl-$\beta(1 \rightarrow 4)$-D-glucosamine, which can be obtained by alkaline N-deacetylation derivative of chitin [7]. Thus, chitosan is usually not a homopolymer of D-glucosamine but a copolymer containing less than 40% N-acetyl-D-glucosamine residues. Chitosan has both reactive amino and hydroxyl groups, which can be used to chemically alter these properties under mild reaction conditions. Therefore, there are many interesting chitosan derivatives, especially for biomedical applications [1, 8, 9]. Chitosan has been proposed for the development of membranes and fibers of hemodialysis and blood oxygenators, skin substitute, wound dressing and suture materials intended for immobilization of enzymes and cells to bind with bile and fatty acids and as a vehicle for drug and gene delivery [10–14]. It has been widely used in several fields of developing treatments as diverse as lung surfactant additives, wound healing, and tissue engineering. Although chitosan is suitable for medical applications, for those applications that involve blood contact such as hemodialysis membranes, chitosan promotes surface induced thrombosis and embolization [10, 12]. It is indicated in the literature that chitosan has the capacity to activate both complement and blood coagulation system [15, 16]. Chitosan is also a bioactive carbohydrate polymer and potentially useful in tissue engineering and for gene and drug delivery [17, 18]. However, none is without disadvantages. For example, chitosan may prevent the absorption of needed vitamins and minerals. It may also be dangerous to those who are allergic to shellfish.

Chitosan nanoparticle prepared by ionotropic gelation technique was first reported by Calvo et al. [19]. It can be formed with sodium tripolyphosphate. The chitosan nanoparticles have gained more attention as drug delivery carriers because of better stability, low toxicity, simple and mild preparation method, and providing versatile routes of administration [20]. Chitosan nanoparticles accumulation typically occurs around the defect area in cells and tissues by hydrophobic interactions. In addition, several physiochemical characteristics of chitosan nanoparticles, such as abilities to cross biological barriers, to protect macromolecules from degradation and to deliver a compound at a target site, were examined as favorable [21].

The development of nanoparticulate drug carriers has followed several routes depending on the final application. Although a wide variety of systems have been designed with their own advantages and limitations, the common goal is to rationalize drug delivery to enhance the bioavailability of the drugs towards targeted diseased cells, promoting the required response while minimizing side effects. Therefore, to use chitosan derivatives for biomedical applications, a test for evaluating biocompatibility must be performed.

In this study, we investigated various methods to analyze and characterize the parameters that influence the uptake of cells on chitosan nanoparticle. The CCL-13 and HepG2 cells were served as cell models for the uptake of chitosan nanoparticles. For instance, using colorimetric techniques such as LDH or BrdU assay is a convenient method and typically applied to many biomaterial researches. Characterizations of chitosan nanoparticles were observed by TEM, particle sizer, and zeta potential. To evaluate early responses of CCL-13 and HepG2 cells to chitosan nanoparticles, a mass spectrometry-based profiling system was adopted for assessing characteristic proteins that were expressed due to the interactions of CCL-13 and HepG2 cells with chitosan nanoparticles. Through the investigation, various proteins that influence the early responses of CCL-13 and HepG2 cells on chitosan nanoparticle were found, and, as we know, some of them have not been reported in the study of cell-nanoparticle interactions.

2. Materials and Methods

2.1. Chitosan Nanoparticle Preparation. Chitosan nanoparticles were prepared according to Calvo et al. [19]. Briefly, water-soluble chitosan was dissolved in aqueous solution. Nanoparticles were formed spontaneously upon addition of 2 mL of the sodium tripolyphosphate (TPP in sodium citrate, 238503, Sigma-Aldrich) aqueous solution (10%) to 100 mL of the chitosan acidic solution (448869, Sigma-Aldrich, low molecular weight, 75–85% deacetylation, 1 mg/mL, w/v) under magnetic stirring at room temperature. The pH of chitosan solution varied between 3.0 and 5.0. PEG (10 mg/mL, 1 mL) was dissolved in the chitosan solution after the addition of the TPP solution. Nanoparticles were isolated by ultracentrifugation (25,000 g, 15 min) and then resuspended in water by manual shaking.

2.2. Characterization of Chitosan Nanoparticles. The morphological examination of the chitosan nanoparticles was performed by transmission electron microscopy at an accelerating voltage of 100 kV (TEM, JEM 1200CX II, JEOL). The sample was stained with 2% (w/v) phosphotungstic acid and placed on copper grids for viewing by TEM.

The particle size and size distributions of the chitosan nanoparticles were performed by particle size analyzer (90 plus particle sizer, Brookhaven Instruments Corp., USA). For the particle size analysis, each sample was diluted to the appropriate concentrating with filtered distilled water. Each analysis lasted 2 min and was performed at 25°C with an angle detection of 90°.

Measurement of the zeta potential of nanoparticles was performed by Zeta plus 90 particle sizer (Brookhaven Instruments Corp., USA) with a 5 mW He-Ne laser (λ = 663 nm). The zeta potential values were calculated from the mean electrophoretic mobility values using Smoluchowski's equation.

2.3. Cell Culture. HepG2 (liver tumor cell) and CCL-13 (liver normal cell) cells were maintained at 37°C and 5% CO_2 in RPMI 1640 medium (Gibco, USA) supplemented with 10% fetal bovine serum (FBS, Hyclone Laboratories, Logan, UT), 1% penicillin/streptomycin (Gibco, Grand Island, NY, USA), and 44 mM $NaHCO_3$ (Sigma, USA). After three days, the cells were washed with serum-free RPMI 1640 medium and incubated with the serum-free medium containing chitosan nanoparticles at concentrations of 1 to 5 μg/mL for 12 h.

2.4. BrdU and LDH Assay. CCL-13 and HepG2 cells were seeded in a sterile 96-well tissue culture plate at 2×10^5 cells/mL in 100 μL/well of appropriate cell culture media with chitosan nanoparticles. The cell proliferation was determined by bromodeoxyuridine assay (BrdU Cell Proliferation Assay, Millipore, USA). The cytotoxicity of chitosan nanoparticles was evaluated *in vitro* using the lactate dehydrogenase assay (LDH Cytotoxicity Assay, ScienCell Research Laboratories, USA). These assays were performed according to the manufacturers' instructions. The absorbance values were measured by an ELISA reader (Multiskan EX, Thermo scientific, Vantaa, Finland, reference wavelength: 450 nm).

2.5. Cell Morphology. For cell morphologies of HepG2 and CCL-13 before and after incubation with chitosan nanoparticles, the cell live images were observed with a microscope equipped with fluorescence light source (FLoid cell fluorescence imaging Station, Invitrogen), and the cell micrographs were taken with a CCD camera.

2.6. Protein Sample Preparation. After incubation with chitosan nanoparticles, the HepG2 and CCL-13 cells were lysed by cell lysis buffer (3500-1, Epitomics, Inc, USA), and cell lysates were centrifuged at 1500 ×g for 10 min at 4°C. The supernatants were flitted by 0.8 μm filter and the protein concentrations were adjusted to 1 mg/mL by 25 mM ammonium bicarbonate.

Cell lysates samples (100 μL) were transferred into the 1.5 mL Eppendorf tubes and incubated at 37°C for 3 h after mixing with 25 μL of 1 M dithiothreitol (DTT, USB Corporation, 15397). Then cell lysates samples were reduced and alkylated in the dark at room temperature for 30 min after addition of 25 μL of 1 M iodoacetamide (IAA, Amersham Biosciences, RPN6302V) in 25 mM ammonium bicarbonate. Approximately 10 μL of 0.1 μg/μL modified trypsin digestion buffer (Trypsin Gold, Mass Spectrometry Grade, V5280, Promega, WI, USA) in 25 mM ammonium bicarbonate was added to the cell lysates samples, and the cell lysates samples were incubated at 37°C for at least 12 h in a water bath. Two microliter of formic acid was added to each sample before mass spectrometric analysis for protein identification.

2.7. Proteomic Analysis. The complex peptide mixtures were separated by RP-nano-UPLC-ESI-MS/MS. The protein tryptic digests were fractionated using a flow rate of 400 nL/min with a nano-UPLC system (nanoACQUITY UPLC, Waters, Milford, MA) coupled to an ion trap mass spectrometer (LTQ Orbitrap Discovery Hybrid FTMS, Thermo, San Jose, CA) equipped with an electrospray ionization source. For RP-nano-UPLC-ESI-MS/MS, a sample (2 μL) of the desired peptide digest was loaded into the reverse phase column (Symmetry C18, 5 μm, 180 μm × 20 mm) by an autosampler. The RP separation was performed using a linear acetonitrile gradient from 99% buffer A (100% D.I. water/0.1% formic acid) to 85% buffer B (100% acetonitrile/0.1% formic acid) in 100 min using the micropump. The separation is performed on a C18 microcapillary column (BEH C18, 1.7 μm, 75 μm × 100 mm) using the nanoseparation system. As peptides eluted from the microcapillary column, they were electrosprayed into the ESI MS/MS with the application of a distal 2.1 kV spraying voltage with heated capillary temperature of 200°C. Each cycle of one full scan mass spectrum (m/z 400–2000) was followed by four data dependent tandem mass spectra with the collision energy set at 35%.

2.8. Database Search. For protein identification, Mascot software (Version 2.2.1, Matrix Science, London, UK) was used to search the Swiss-Prot human protein sequence database. Positive protein identifications were defined when Mowse scores greater than 100 were considered significant ($P < 0.05$). Proteins were annotated by similar searches using UniProtKB/Swiss-Prot databases. The protein-protein interaction pathways were performed by String 9.1 Web software.

2.9. Statistical Analysis. All calculations used the SigmaStat statistical software (Jandel Science Corp., San Rafael, CA). All statistical significances were evaluated at 95% of confidence level or better. Data are presented as mean ± standard error.

3. Results and Discussions

3.1. Size, Zeta Potential, and Morphology of Chitosan Nanoparticles. As determined by particle size and zeta potential analyzers, the average size of the chitosan nanoparticle was 224.6 ± 11.2 nm, and the average zeta potential was +14.08 ± 0.7 mV in phosphate-buffered saline. The size and surface morphology of chitosan nanoparticles was shown in Figure 1. The TEM image displays the clear spherical morphology of the chitosan nanoparticles having a mean diameter of chitosan nanoparticles about 236.3 nm as shown. Zeta potential is the surface charge of nanoparticles and can influence the nanoparticle stability in suspension through the electrostatic repulsion between nanoparticles. In this study, the surface charge of chitosan nanoparticles was positive, according to the protonation of NH_2 functional groups of glucosamine units to NH_3^+ ion.

3.2. In Vivo Chitosan Nanoparticle Uptake. In vitro uptake of chitosan nanoparticles was evaluated by fluorescence microscopy. CCL-13 and HepG2 cells were incubated with

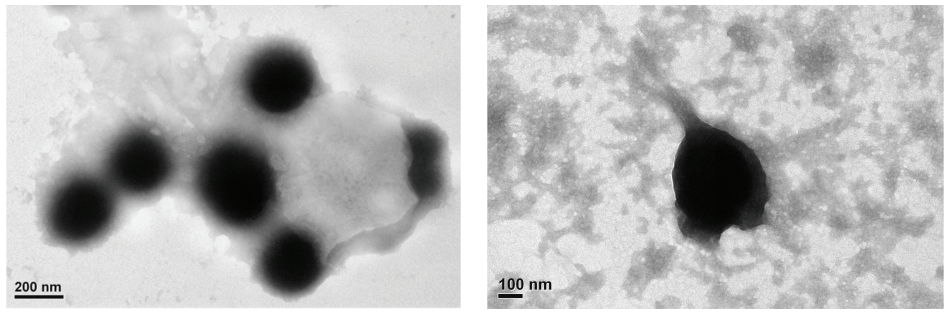

(a) (b)

Figure 1: The morphological examination of the chitosan nanoparticles was performed by transmission electron microscopy at an accelerating voltage of 100 kV. The mean of diameter is around 236.3 nm.

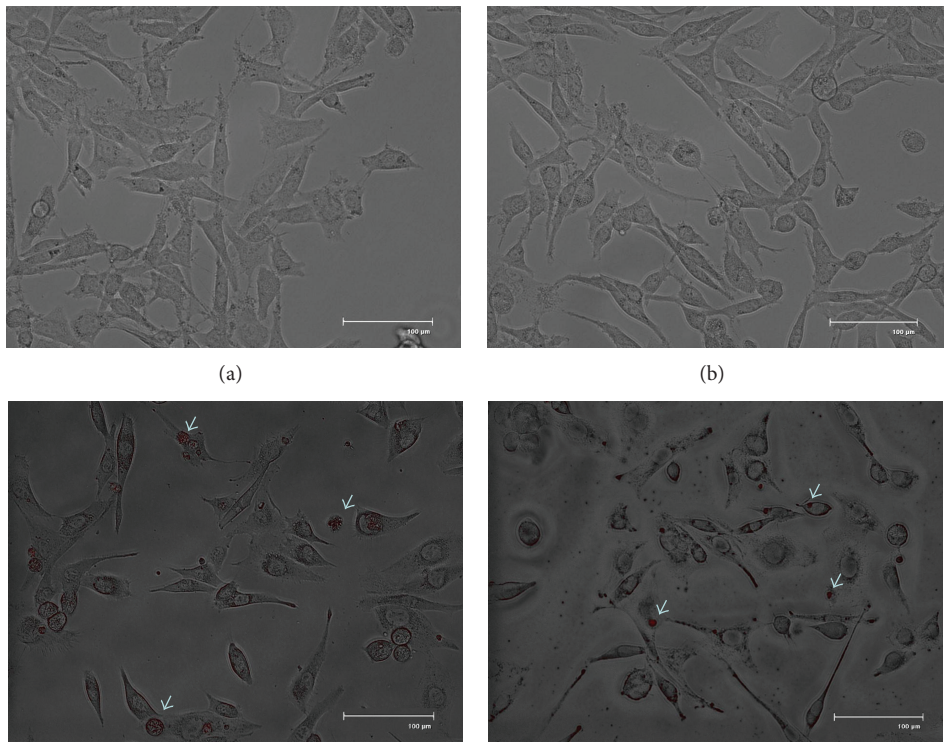

(a) (b)

(c) (d)

Figure 2: The live fluorescent images of chitosan nanoparticles (red) taken by CCL-13 cells (a, c) and HepG2 cells (b, d). (a) and (b): cells without chitosan nanoparticles; (c) and (d): cells with chitosan nanoparticles at a concentration of 5 μg/mL for 12 h at 37°C; the red fluorescence was localized near by the cell nuclei. Those images represented merged images of DIC and red fluorescence. (600x, scale bar: 100 μm).

the growth medium containing chitosan nanoparticles at a concentration of 5 μg/mL for 12 h at 37°C, respectively. As expected, no red fluorescence signals were detected in sections of the cells without chitosan nanoparticles (Figure 2(a): CCL-13 and Figure 2(b): HepG2, 600x, scale bar: 100 μm). Cell micrographs from chitosan nanoparticles treated CCL-13 and HepG2 cells reveled red fluorescence localized near by the cell nuclei (Figure 2(c): CCL-13 and Figure 2(d): HepG2, 600x, scale bar: 100 μm). In some HepG2 cells, the fluorescence was also localized in the cytoplasm.

3.3. Cytotoxicity of Chitosan Nanoparticle. To examine the cytotoxicity, HepG2 and CCL-13 cells were incubated with chitosan nanoparticles for 12 h. LDH and BrdU assays are quantitative colorimetric assays for mammalian cell survival and cell proliferation.

The cell death is assayed by the quantification of a stable cytoplasmic enzyme activity, LDH, which was released into the cell culture supernatant upon cell death and damage of the cytoplasmic membrane. BrdU is integrated into newly synthesized DNA strands of actively proliferating cells. Following partial denaturation of double stranded DNA, BrdU is detected immunochemically allowing the assessment of the number of cells which are synthesizing DNA. As shown in Figure 3, the LDH concentrations were decreased and observed between the groups treated with different concentration of chitosan nanoparticle and control

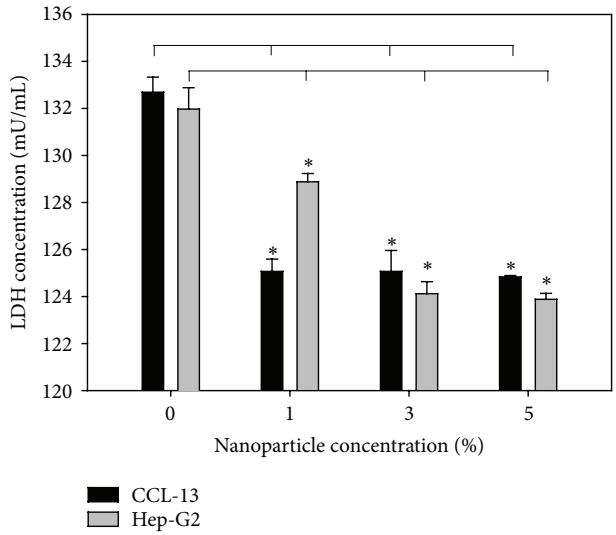

Figure 3: LDH test of chitosan nanoparticle (CSNP) effects on Chang and HepG2 cells ($N = 6$, mean ± standard error, t-test, $P < 0.05$).

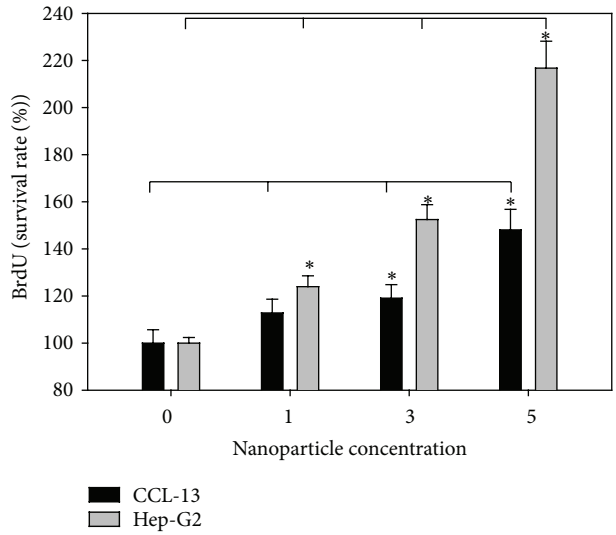

Figure 4: Proliferation (BrdU) test of chitosan nanoparticle (CSNP) effects on Chang and HepG2 cells ($N = 6$, mean ± standard error, t-test, $P < 0.05$).

($P < 0.05$, $N = 6$). Compared with the control, the BrdU was upregulated in the groups treated with chitosan nanoparticle with significantly increase (Figure 4, $P < 0.05$, $N = 6$). Those results indicate that the chitosan nanoparticle was no significant cytotoxicity observed; in addition, the chitosan nanoparticle improved the cell growth and proliferation. In previous studies, it was indicated that the metal or metal oxide nanoparticles were with high cell toxicity [22–24]. Unlike metal or metal oxide nanoparticles, the chitosan nanoparticle was nontoxic. The cell growth and survival rate were increased with the higher concentration of chitosan nanoparticles. As shown in Figures 3 and 4, the chitosan nanoparticle was enhanced cell growth in a dose dependent manner.

3.4. Proteomic Analysis of Cell Response to Chitosan Nanoparticle. To investigate the effect of chitosan nanoparticle on liver normal and tumor cells, a proteomic approach, such as RP-nano-UPLC-ESI-MS/MS analysis, was utilized to analyze cell lysates. The traditional methods use individual antibodies to evaluate the cell response to nanoparticles, but the proteomic approach can be used to analyze an enormous number of proteins simultaneously. In this study, HepG2 and CCL-13 cells were incubated with chitosan nanoparticles. After 12 h, the HepG2 and CCL-13 cells were lysed, and the cell lysates were digested by trypsin; generating tryptic peptides was subsequently analyzed by RP-nano-HPLC-ESI-MS/MS, respectively. The RP-nano-HPLC-ESI-MS/MS approach is perhaps the most representative method in proteome researches. The fragmentation spectra obtained by the RP-nano-HPLC-ESI-MS/MS analysis in gradient detection mode were compared with a nonredundant protein database using Mascot software. All Mascot results were visually confirmed. In addition, the criterion requires a readily observable series of at least four y ions for an identified peptide [25]. When a protein

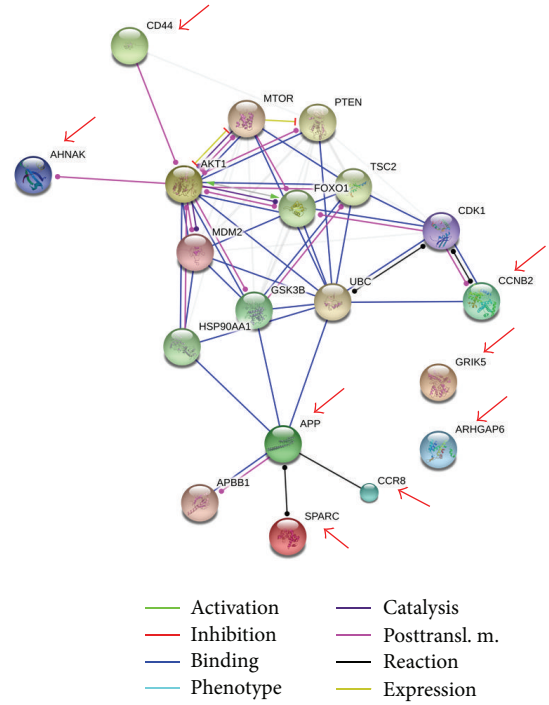

Figure 5: The protein-protein interaction pathways were performed. Proteins identified in this study were marked by arrows. The CD44 and APP can turn on the PI3K/AKT/mTOR pathway, which is responsible for the proliferation and is required for survival of the majority of cells.

was identified by three or more unique peptides, no visual assessment of spectra was conducted and the protein was considered to be present in the sample.

In this study, more than one hundred proteins were identified and most of these were identified at the minimal confidence level, which was only one unique peptide sequence matched. Experimental results reported a

Table 1: The eight unique proteins identified by the higher confidence level (at least three unique peptide sequences matched) with significant difference between CCL-13 and HepG2 cells incubation with chitosan nanoparticles in this study.

Cell	Swiss-Prot Number	Protein Name	Subcellular location	MW (Da)	Score	Queries	pI	Molecular function	Sequence coverage	Peptide
CCL-13	Q16478	Glutamate receptor, ionotropic kainate 5 (GRIK5)	Cell membrane	109195	82	9	8.54	extracellular-glutamate-gated ion channel activity kainate selective glutamate receptor activity	28%	K.VSTIIIDANASISHLILRK.A + Deamidated (NQ); 2 Phospho (ST) R.LQYLRFASVSLYPSNEDVSLAVSRILK.S + 2 Deamidated (NQ) K.VGPEETPRLQYLR.F R.LNCNLTQIGGLLDTK.G + 2 Deamidated (NQ); Phospho (ST) R.LNCNLTQIGGLLDTK.G + 3 Deamidated (NQ); Phospho (ST) R.RLNCNLTQIGGLLDTK.G + 2 Deamidated (NQ); Phospho (ST) K.VSTIIIDANASISHLILRK.A + Deamidated (NQ); 2 Phospho (ST) M.PAELLLLLIVAFASPSCQVLSSLR.M + Deamidated (NQ) -.MPAELLLLLIVAFASPSCQVLSSLRMAAILDDQTVCGR.G + Carbamidomethyl (C); Deamidated (NQ); Oxidation (M); 2 Phospho (ST) R.EQQVTQK.K K.DPGMTGSSGDIFESSSLR.A + 4 Phospho (ST) -.MSAQSLLHSVFSCSSPASSSAASAK.G + Deamidated (NQ); Oxidation (M); 3 Phospho (ST) R.EQQVTQKKLSSANSLPAGEQDSPR.L + 2 Phospho (ST)
	O43182	Rho GTPase-activating protein 6 (ARHGAP6)	Cytoplasm	105882	72	13	7.11	Rho GTPase activator activity SH3/SH2 adaptor activity phospholipase activator activity	29%	K.DASDFVASLLPFGNK.R + Deamidated (NQ); Phospho (ST) R.LRSVPIQSLSELERAR.L + Deamidated (NQ) R.LRSVPIQSLSELERAR.L + Phospho (ST) K.MTSLNLATIFGPNLLHKQK.S + Deamidated (NQ); Oxidation (M) K.DPGMTGSSGDIFESSSLR.A + 4 Phospho (ST) R.TQAAAPATEGR.A + Deamidated (NQ); Phospho (ST) R.TQAAAPATEGR.A + Deamidated (NQ); Phospho (ST) K.DPGMTGSSGDIFESSSLR.A + 4 Phospho (ST) R.HSSTDSNKASSGDISPYDNNSPVLSER.S + Deamidated (NQ); 6 Phospho (ST)

Table 1: Continued.

Cell	Swiss-Prot Number	Protein Name	Subcellular location	MW (Da)	Score	Queries	pI	Molecular function	Sequence coverage	Peptide
HepG2	P05067	Amyloid beta A4 protein (APP)	Membrane	86888	49	4	4.73	DNA binding heparin binding peptidase activator activity serine-type endopeptidase inhibitor activity transition metal ion binding	19%	R.LNMHMNVQNGK.W + Deamidated (NQ); 2 Oxidation (M) K.WDSDPSGTKTCIDTK.E + 5 Phospho (ST) K.GAIIGLMVGGVVIATVIVITLVMLKK.K + Oxidation (M); Phospho (ST) R.ALEVPTDGNAGLLAEPQIAMFCGR.L + 2 Deamidated (NQ); Oxidation (M); Phospho (ST) R.ESCEKSSSCQQHSSR.S + Carbamidomethyl (C); Deamidated (NQ); 3 Phospho (ST) R.ESCEKSSSCQQHSSR.S + Carbamidomethyl (C); 2 Deamidated (NQ); 5 Phospho (ST) R.ESCEKSSSCQQHSSR.S + Carbamidomethyl (C); 2 Deamidated (NQ); 5 Phospho (ST) R.ESCEKSSSCQQHSSR.S + Carbamidomethyl (C); 2 Deamidated (NQ); 5 Phospho (ST)
	P51685	C-C chemokine receptor type 8 (CCR8)	Cell membrane	40817	47	4	8.66	C-C chemokine receptor activity chemokine receptor activity coreceptor activity	12%	
	P16070	CD44 antigen (CD44)	Membrane	81487	60	3	5.13	collagen binding hyaluronic acid binding hyaluronoglucosaminidase activity	4%	R.YGFIEGHVVIPR.I K.ALSIGFETCRYG FIEGHVVIPR.I K.EQWFGNRWHEGYR.Q
	O95067	G2/mitotic-specific cyclin-B2 (CCNB2)		45253	58	3	9.21		16%	R.KKLQLVGITALLLASK.Y K.VPVQPTKTTNVNKQLKPTASVKPVQMEK.L + Deamidated (NQ); Oxidation (M); Phospho (ST) K.AQNTKVPVQPTKTTNVNK.Q + 3 Deamidated (NQ); 2 Phospho (ST)
	Q09666	Neuroblast differentiation-associated protein (AHNAK)	Nucleus	628699	39	7	5.8		12%	K.GPKFKIPEMHLK.A K.FKMPSMNIQTHK.I + Deamidated (NQ); Oxidation (M); Phospho (ST) K.MDAEVPDVNIEGPDAKLK.G + Deamidated (NQ) K.KSRLSSSSSNDSGNK.V + 2 Deamidated (NQ); 6 Phospho (ST) K.MKLPQFGISTPGSDLHVNAK.G K.VHAPGLNLSGVGGKMQVGGDGVK.V + Deamidated (NQ); Oxidation (M); Phospho (ST)
	P09486	Osteonectin/SPARC protein (SPARC)	Secreted	34610	89	3	4.73	calcium ion binding collagen binding extracellular matrix binding	4%	R.AGAISASGPELQGAGHSKLQVTMPGIKVGGSGVNVNAK.G + 2 Deamidated (NQ); Oxidation (M); 4 Phospho (ST) R.LEAGDHPVELLAR.D K.HGKVCELDENNTPMCVCQDPTSCPAPIGEFEK.V + 3 Carbamidomethyl (C) R.APLIPMEHCTTR.F

total of eight protein identifications with higher confidence levels (at least three unique peptide sequences matched) and exhibited significant differences between the chitosan nanoparticle treated and nontreated cells. Those cell lysate proteins were involved in cell growth, differentiation, division, cycle regulation (6 in HepG2 cells and 2 in CCL-13 cells).

A summary of the protein identifications achieved is shown in Table 1. For the eight protein identifications, six proteins were positively identified as Amyloid beta A4 protein (APP, P05067), C-C chemokine receptor type 8 (CCR8, P51685), CD44 antigen (CD44, P16070), G2/mitotic-specific cyclin-B2 (CCNB2, O95067), Neuroblast differentiation-associated protein (AHNAK, Q09666), and Osteonectin/SPARC protein (SPARC, P09486) in HepG2 cell lysate. Two proteins, Glutamate receptor ionotropic, kainate 5 (GRIK5, Q16478), and Rho GTPase-activating protein 6 (ARHGAP6, O43182) were found in the CCL-13 cell lysate. The protein-protein interaction pathways were performed by String 9.1 Web software. Eight proteins identified in this study were marked by red arrows (Figure 5).

GRIK5 and ARHGAP6 were not detected in the HepG-2 cells but in CCL-13 cells. GRIK5 gene belongs to the kainate family of glutamate receptor in the cerebellum and the suprachiasmatic nuclei (SCN) of the hypothalamus, which is composed of four subunits and function as ligand-activated ion channels [26]. It is the predominant excitatory neurotransmitter receptor in the brain of mammalian and is involved in the neurophysiologic processes, such as the transmission of light information from the retina to the hypothalamus.

ARHGAP6 is a regulatory protein which can bind to activated G proteins and stimulate their GTPase activity. Regulation of G proteins is important because these proteins are involved in a variety of important cellular processes. It may result in transduction of signaling from the G protein-coupled receptor for a variety of signaling processes like hormonal signaling and involve in processes like cellular trafficking and cell cycling [27]. In this study, GRIK5 and ARHGAP6 were identified in the CCL-13 cells after chitosan nanoparticle treatment. However, the analyses of protein functions and protein-protein interaction pathways did not show the serious effect in CCL-13 cells.

In this study, the main finding of chitosan nanoparticle treated cells is the chitosan nanoparticles enhancing the PI3K/AKT1/mTOR pathway in Hep-G2 cells which may result in tumor metastasis. There were six proteins identified in HepG-2 cell lysate samples, which may relate to metastasis and cell proliferation. Using the protein-protein interaction pathway analysis, those six proteins were related to the PI3K/AKT1/mTOR pathway (Figure 5). The CD44 can turn on the PI3K/AKT1/mTOR pathway, which is responsible for the proliferation and is required for survival of the majority of cells. The PI3K/AKT1/mTOR pathway can also be turned on by GSK3B when GSK3B is bound with APP and SPARC.

The mammalian target of rapamycin pathway (mTOR pathway, also known as FRAP, RAFT1, and RAP1 pathway) has been identified as a key kinase acting downstream of the activation of phosphoinositide-3-kinase (PI3K) [28]. The PI3K/AKT1/mTOR pathway is responsible for the proliferation and is required for survival of the majority of cancer cells. The hypothesis of the mTOR pathway is acting as a master switch of cellular catabolism and anabolism, thereby determining whether cells grow and proliferate of tumor cells [29, 30]. Activation of PI3K/AKT1/mTOR signaling through mutation of pathway components as well as through activation of upstream signaling molecules occurs in a majority of cancer cells contributing to deregulation of proliferation, resistance to apoptosis, and changes in metabolism characteristic of transforming cells [31].

4. Conclusion

As previous reports have indicated that the chitosan nanoparticle was nontoxic for cell lines and appropriate as a drug carrier in micro capsule. In this study, the experimental results showed that it is a dose dependent manner to enhance cell growth. However, according to the proteomics analysis, chitosan nanoparticle induced the liver cancer cell to secret several proteins which may active or enhance PI3K/AKT1/mTOR pathway. The PI3K/AKT1/mTOR pathway was related to the cancer call metastasis and proliferation. Although there are no direct evidences to prove the relevance between chitosan nanoparticle and PI3K/AKT1/mTOR pathway in our study, it is still worth to be considered, especially as an anticancer drug delivery system.

Conflict of Interests

The authors declare that there is no conflict of interests regarding the publication of this paper.

Authors' Contribution

Ming-Hui Yang and Shyng-Shiou Yuan contributed equally to this work as first authors.

Acknowledgments

The authors thank the Center of Excellence for Environmental Medicine, Kaohsiung Medical University for the assistance in protein identification. This work was supported by research Grant nos. NSC-102-3114-Y-492-076-023, NSC-101-2221-E-010-013-MY2, NSC-100-2320-B-037-007-MY3, and NSC-099-2811-E-224-002 from the National Science Council, MOHW103-TD-B-111-05 from Ministry of Health and Welfare, and NSYSUKMU 102-P006 from NSYSU-KMU Joint Research Project, Taiwan.

References

[1] Q. Li, E. T. Dunn, E. W. Grandmaison, and M. F. A. Goosen, "Applications and properties of chitosan," *Journal of Bioactive and Compatible Polymers*, vol. 7, no. 4, pp. 370–397, 1992.

[2] L. Shang and G. U. Nienhaus, "Small fluorescent nanoparticles at the nano—bio interface," *Materials Today*, vol. 16, no. 3, pp. 58–66, 2013.

[3] P. Orlowski, M. Krzyzowska, R. Zdanowski et al., "Assessment of in vitro cellular responses of monocytes and keratinocytes to tannic acid modified silver nanoparticles," *Toxicology in Vitro*, vol. 27, no. 6, pp. 1798–1808, 2013.

[4] C. Zanette, M. Pelin, M. Crosera et al., "Silver nanoparticles exert a long-lasting antiproliferative effect on human keratinocyte HaCaT cell line," *Toxicology in Vitro*, vol. 25, no. 5, pp. 1053–1060, 2011.

[5] S. J. Soenen, B. Manshian, J. M. Montenegro et al., "Cytotoxic effects of gold nanoparticles: a multiparametric study," *ACS Nano*, vol. 6, no. 7, pp. 5767–5783, 2012.

[6] B. D. Holt, K. N. Dahl, and M. F. Islam, "Cells take up and recover from protein-stabilized single-wall carbon nanotubes with two distinct rates," *ACS Nano*, vol. 6, no. 4, pp. 3481–3490, 2012.

[7] S. Hirano and Y. Noishiki, "The blood compatibility of chitosan and N-acylchitosans," *Journal of Biomedical Materials Research*, vol. 19, no. 4, pp. 413–417, 1985.

[8] K. Y. Lee and D. J. Mooney, "Alginate: properties and biomedical applications," *Progress in Polymer Science*, vol. 37, no. 1, pp. 106–126, 2012.

[9] M. R. Kasaai, J. Arul, and G. Charlet, "Fragmentation of chitosan by acids," *The Scientific World Journal*, vol. 2013, Article ID 508540, 11 pages, 2013.

[10] K. S. V. Krishna Rao, B. Vijaya Kumar Naidu, M. C. S. Subha, M. Sairam, and T. M. Aminabhavi, "Novel chitosan-based pH-sensitive interpenetrating network microgels for the controlled release of cefadroxil," *Carbohydrate Polymers*, vol. 66, no. 3, pp. 333–344, 2006.

[11] M. Rani, A. Agarwal, and Y. Negi, "Characterization and biodegradation studies for interpenetrating polymeric network (IPN) of chitosan-amino acid beads," *Journal of Biomaterials and Nanobiotechnology*, vol. 2, no. 1, pp. 71–84, 2011.

[12] M. E. I. Badawy and E. I. Rabea, "A biopolymer chitosan and its derivatives as promising antimicrobial agents against plant pathogens and their applications in crop protection," *International Journal of Carbohydrate Chemistry*, vol. 2011, Article ID 460381, 29 pages, 2011.

[13] J.-I. Murata, Y. Ohya, and T. Ouchi, "Possibility of application of quaternary chitosan having pendant galactose residues as gene delivery tool," *Carbohydrate Polymers*, vol. 29, no. 1, pp. 69–74, 1996.

[14] P. Kandra, M. M. Challa, and H. K. Jyothi, "Efficient use of shrimp waste: present and future trends," *Applied Microbiology and Biotechnology*, vol. 93, no. 1, pp. 17–29, 2012.

[15] S. Minami, H. Suzuki, Y. Okamoto, T. Fujinaga, and Y. Shigemasa, "Chitin and chitosan activate complement via the alternative pathway," *Carbohydrate Polymers*, vol. 36, no. 2-3, pp. 151–155, 1998.

[16] J. Zhang, W. Xia, P. Liu et al., "Chitosan modification and pharmaceutical/biomedical applications," *Marine Drugs*, vol. 8, no. 7, pp. 1962–1987, 2010.

[17] F. Talaei, M. Azhdarzadeh, H. Hashemi Nasel et al., "Core shell methyl methacrylate chitosan nanoparticles: in vitro mucoadhesion and complement activation," *DARU, Journal of Pharmaceutical Sciences*, vol. 19, no. 4, pp. 257–265, 2011.

[18] J. Venkatesan and S.-K. Kim, "Chitosan composites for bone tissue engineering: an overview," *Marine Drugs*, vol. 8, no. 8, pp. 2252–2266, 2010.

[19] P. Calvo, C. Remuñan-López, J. L. Vila-Jato, and M. J. Alonso, "Chitosan and chitosan/ethylene oxide-propylene oxide block copolymer nanoparticles as novel carriers for proteins and vaccines," *Pharmaceutical Research*, vol. 14, no. 10, pp. 1431–1436, 1997.

[20] I. M. Van der Lubben, J. C. Verhoef, G. Borchard, and H. E. Junginger, "Chitosan for mucosal vaccination," *Advanced Drug Delivery Reviews*, vol. 52, no. 2, pp. 139–144, 2001.

[21] T. López-León, E. L. S. Carvalho, B. Seijo, J. L. Ortega-Vinuesa, and D. Bastos-González, "Physicochemical characterization of chitosan nanoparticles: electrokinetic and stability behavior," *Journal of Colloid and Interface Science*, vol. 283, no. 2, pp. 344–351, 2005.

[22] Y. Guichard, J. Schmit, C. Darne et al., "Cytotoxicity and genotoxicity of nanosized and microsized titanium dioxide and iron oxide particles in Syrian hamster embryo cells," *The Annals of Occupational Hygiene*, vol. 56, no. 5, pp. 631–644, 2012.

[23] J. C. K. Lai, M. B. Lai, S. Jandhyam et al., "Exposure to titanium dioxide and other metallic oxide nanoparticles induces cytotoxicity on human neural cells and fibroblasts," *International Journal of Nanomedicine*, vol. 3, no. 4, pp. 533–545, 2008.

[24] R. Liu, R. Rallo, S. George et al., "Classification NanoSAR development for cytotoxicity of metal oxide nanoparticles," *Small*, vol. 7, no. 8, pp. 1118–1126, 2011.

[25] J. D. Jaffe, H. C. Berg, and G. M. Church, "Proteogenomic mapping as a complementary method to perform genome annotation," *Proteomics*, vol. 4, no. 1, pp. 59–77, 2004.

[26] P. E. Schauwecker, "Differences in ionotropic glutamate receptor subunit expression are not responsible for strain-dependent susceptibility to excitotoxin-induced injury," *Molecular Brain Research*, vol. 112, no. 1-2, pp. 70–81, 2003.

[27] A. J. Kimple, M. Soundararajan, S. Q. Hutsell et al., "Structural determinants of G-protein α subunit selectivity by regulator of G-protein signaling 2 (RGS2)," *Journal of Biological Chemistry*, vol. 284, no. 29, pp. 19402–19411, 2009.

[28] S. Faivre, G. Kroemer, and E. Raymond, "Current development of mTOR inhibitors as anticancer agents," *Nature Reviews Drug Discovery*, vol. 5, no. 8, pp. 671–688, 2006.

[29] N. Khan, F. Afaq, F. H. Khusro, V. Mustafa Adhami, Y. Suh, and H. Mukhtar, "Dual inhibition of phosphatidylinositol 3-kinase/Akt and mammalian target of rapamycin signaling in human nonsmall cell lung cancer cells by a dietary flavonoid fisetin," *International Journal of Cancer*, vol. 130, no. 7, pp. 1695–1705, 2012.

[30] K. E. O'Reilly, F. Rojo, Q.-B. She et al., "mTOR inhibition induces upstream receptor tyrosine kinase signaling and activates Akt," *Cancer Research*, vol. 66, no. 3, pp. 1500–1508, 2006.

[31] H.-Y. Zhou and S.-L. Huang, "Current development of the second generation of mTOR inhibitors as anticancer agents," *Chinese Journal of Cancer*, vol. 31, no. 1, pp. 8–18, 2012.

Hindawi Publishing Corporation
BioMed Research International
Volume 2014, Article ID 654913, 13 pages
http://dx.doi.org/10.1155/2014/654913

Review Article

Chitooligosaccharide and Its Derivatives: Preparation and Biological Applications

Gaurav Lodhi,[1,2] Yon-Suk Kim,[1,2] Jin-Woo Hwang,[1,2] Se-Kwon Kim,[3] You-Jin Jeon,[4] Jae-Young Je,[5] Chang-Bum Ahn,[6] Sang-Ho Moon,[7] Byong-Tae Jeon,[7] and Pyo-Jam Park[1,2,7]

[1] *Department of Biotechnology, Konkuk University, Chungju 380-701, Republic of Korea*
[2] *Department of Applied Life Science, Konkuk University, Chungju 380-701, Republic of Korea*
[3] *Specialized Graduate School of Convergence Science and Technology, Department of Marine Bioconvergence Science, Busan 608-737, Republic of Korea*
[4] *School of Marine Biomedical Sciences, Jeju National University, Jeju 690-756, Republic of Korea*
[5] *Department of Marine Bio-Food Sciences, Chonnam National University, Yeosu 550-749, Republic of Korea*
[6] *Division of Food and Nutrition, Chonnam National University, Gwangju 550-757, Republic of Korea*
[7] *Nokyong Research Center, Konkuk University, Chungju 380-701, Republic of Korea*

Correspondence should be addressed to Pyo-Jam Park; parkpj@kku.ac.kr

Received 3 January 2014; Accepted 22 January 2014; Published 3 March 2014

Academic Editor: Yoshihiko Hayashi

Chitin is a natural polysaccharide of major importance. This biopolymer is synthesized by an enormous number of living organisms; considering the amount of chitin produced annually in the world, it is the most abundant polymer after cellulose. The most important derivative of chitin is chitosan, obtained by partial deacetylation of chitin under alkaline conditions or by enzymatic hydrolysis. Chitin and chitosan are known to have important functional activities but poor solubility makes them difficult to use in food and biomedicinal applications. Chitooligosaccharides (COS) are the degraded products of chitosan or chitin prepared by enzymatic or chemical hydrolysis of chitosan. The greater solubility and low viscosity of COS have attracted the interest of many researchers to utilize COS and their derivatives for various biomedical applications. In light of the recent interest in the biomedical applications of chitin, chitosan, and their derivatives, this review focuses on the preparation and biological activities of chitin, chitosan, COS, and their derivatives.

1. Introduction

Synthetic polymers are gradually being replaced by biodegradable materials especially those derived from replenishable, natural resources [1]. Natural biopolymers have several advantages, such as availability from replenishable agricultural or marine food resources, biocompatibility, and biodegradability, thereby leading to ecological safety and the possibility of preparing a variety of chemically or enzymatically modified derivatives for specific end uses. Polysaccharides, as a class of natural macromolecules, have the tendency to be extremely bioactive and are generally derived from agricultural feedstock or crustacean shell wastes [2].

Chitosan is a natural nontoxic biopolymer produced by the deacetylation of chitin, a major component of the shells of crustaceans such as crab, shrimp, and crawfish; chitooligosaccharides (COS) are the degraded products of chitosan or chitin prepared by enzymatic or chemical hydrolysis of chitosan.

Chitosan and its derivatives have shown various functional properties that have made them possible to be used in many fields including food [3], cosmetics [4], biomedicine [5], agriculture [6], environmental protection [7], and wastewater management [8]. Furthermore, biodegradable, nontoxic, and nonallergenic nature of chitosan especially encourages its potential use as a bioactive material [9]. Even though chitosan is known to have important functional activities,

poor solubility makes them difficult to use in food and biomedicinal applications. Unlike chitosan, its hydrolyzed products and COS are readily soluble in water due to their shorter chain lengths and free amino groups in D-glucosamine units [10]. The low viscosity and greater solubility of COS at neutral pH have attracted the interest of many researchers to utilize chitosan in its oligosaccharide form. Especially, research on COS in food and nutrition fields has emphasized their ability to improve food quality and human health progression.

In light of the recent interest in the biomedical applications of chitin, chitosan, and its derivatives, this review focuses on the preparation and biological activities of chitin, chitosan, COS, and their derivatives.

2. Chitin

Chitin (Figure 1), a mucopolysaccharide and the supporting material of crustaceans and insects, is the second most abundant polymer after cellulose found in nature; it is produced by many living organisms and is present usually in a complex with other polysaccharides and proteins. Chitin was found as a major component in arthropods (insects, crustaceans, arachnids, and myriapods), nematodes, algae, and fungi [11–14].

Its immunogenicity is exceptionally low in spite of the presence of nitrogen. It is highly insoluble material resembling cellulose with its solubility and low chemical reactivity. It may be regarded as cellulose with hydroxyl at position C-2 replaced by an acetamido group. Like cellulose, it functions naturally as a structural polysaccharide. It is white, hard inelastic nitrogenous polysaccharide [15, 16].

Chitin is a linear polysaccharide composed of (1 → 4) linked 2-acetamido-2-deoxy-β-d-glucopyranosyl units and occurs naturally in three polymorphic forms with different orientations of the microfibrils, known as α-, β-, and γ-chitin [1, 17]. The α-form has antiparallel chains and is a common and the most stable polymorphic form of chitin in nature, which is prevalent in crustaceans and in insect chitinous cuticles [18–20]. The β-form of chitin is rare; it occurs in pens of mollusks and is characterized by a loose-packing parallel chains fashion with weak intermolecular interactions and higher solubility and swelling than α-form; β-chitin was prepared from the pens of the squid *Ommastrephes bartrami* [21, 22], *Loligo* species, and cuttlefish (*Sepia officinalis*) [18, 23–25]. The γ-form is characterized by a mixture of antiparallel and parallel chains and was found in the cocoons of insects [26].

Besides its application as a starting material for the synthesis of chitosan and chitooligosaccharides, chitin itself has been a center of many therapeutic applications and is thought to be a promising biomaterial for tissue engineering and stem cell technologies [27].

Bae et al. [28] demonstrated that oral administration of chitin (α and β forms) is beneficial in preventing food allergies; the oral administration of chitin was accomplished by milling it to particle size less than 20 μm and mixing it with feed. Their results showed that α-form reduced serum levels of peanut-specific IgE and both the forms decreased the levels of interleukins (IL), IL-5 and IL-10, and increased the levels of IL-12. Dietary supplementation of chitin has shown to exert positive immunomodulatory effects [29, 30]; antibacterial activity of chitin, prepared from shrimp shell waste, was reported by Benhabiles et al. [31].

3. Chitosan

Chitosan [poly-(β-1/4)-2-amino-2-deoxy-D-glucopyranose] is a natural nontoxic biopolymer produced by the deacetylation of chitin. Chitosan (Figure 1) has three types of reactive functional groups, an amino group as well as both primary and secondary hydroxyl groups at the C-2, C-3, and C-6 positions, respectively. Chemical modifications of these groups have provided numerous useful materials in different fields of application. Currently, chitosan has received considerable attention for its commercial applications in the biomedical, food, and chemical industries [9, 32–36].

Chitosan solubility, biodegradability, reactivity, and adsorption of many substrates depend on the amount of protonated amino groups in the polymeric chain and thereby on the proportion of acetylated and nonacetylated glucosamine units. The amino groups (pKa from 6.2 to 7.0) are completely protonated in acids with pKa smaller than 6.2 making chitosan soluble. Chitosan is insoluble in water, organic solvents, and aqueous bases and it is soluble after stirring in acids such as acetic, nitric, hydrochloric, perchloric, and phosphoric [37–39].

Applications of chitin are limited compared to chitosan because chitin is chemically inert and is insoluble in both water and acid, while chitosan is relatively reactive and can be produced in various forms. Chitosan is normally insoluble in neutral or basic pH conditions while being soluble in acidic pH. The solubility of chitosan depends upon the distribution of free amino and N-acetyl groups. In dilute acids (pH < 6), the free amino groups are protonated and the molecule becomes soluble [40].

Due to its unique biological characteristics, including biodegradability and nontoxicity, many applications have been found either alone or blended with other natural polymers (starch, gelatin, and alginates) in the food, pharmaceutical, textile, agriculture, water treatment, and cosmetics industries [41–46].

Chitosan lacks irritant or allergic effects and is biocompatible with both healthy and infected human skin [47]. When chitosan was administered orally in mice, the LD_{50} was found to be in excess of 16 g/kg, which is higher than that of sucrose [48]. The intriguing properties of chitosan have been known previously and the polymer has been used in the fields of agriculture, industry, and medicine. In agriculture, chitosan has been described as a plant antivirus, an additive in liquid multicomponent fertilizers [49], and it has also been investigated as a metal-recovering agent in agriculture and industry [50]. Chitosan has been noted for its application as a film-forming agent in cosmetics [51], a dye binder for textiles, a strengthening additive in paper [52], and a hypolipidic material in diets [53]. It has been used extensively as a biomaterial [54], owing to its immunostimulatory activities [55], anticoagulant properties [56], antibacterial

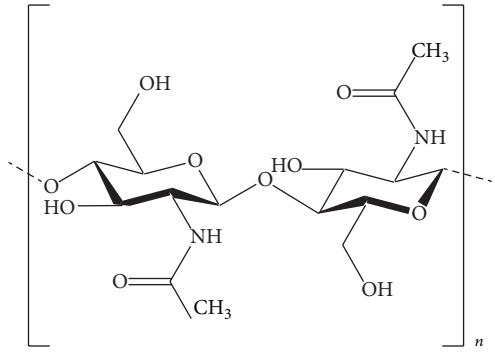

Chitin

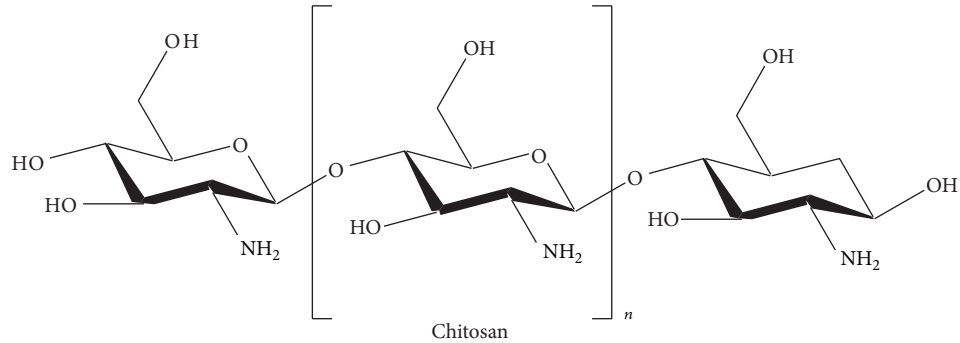

Chitosan

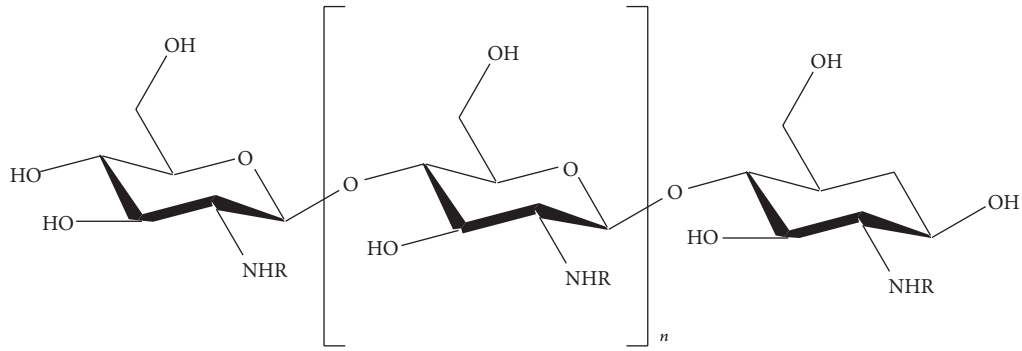

R = H or Ac, n = 0 to 8

Chitooligosaccharide

Figure 1

and antifungal action [57], and its action as a promoter of wound healing in the field of surgery [58].

Chitosan and its derivatives possess some special properties for use in regenerative medicine. Several studies have examined the host tissue response to chitosan based implants. In general, these materials are nontoxic and biodegradable with living tissues and evoke a minimal foreign body reaction with little or no fibrous encapsulation [59].

Antimicrobial activity of chitosan has been demonstrated against many bacteria, filamentous fungi, and yeasts [60–63]. Chitosan has wide spectrum of activity and high killing rate against Gram-positive and Gram-negative bacteria but lower toxicity toward mammalian cells [64, 65].

Owing to the presence of hydroxyl, amine, and acetylated amine groups, chitosan, low molecular weight chitosan, and COS interact readily with various cell receptors that trigger a

cascade of interconnected reactions in living organisms resulting in anti-inflammatory [66], anticancerogenic [67], antidiabetic [68], antimicrobial [69], anti-HIV-1 [70], antioxidant [71], antiangiogenic [72], neuroprotective [73], and immunostimulative [74] effects.

4. Chitooligosaccharides

Chitosans with degrees of polymerization (DPs) <20 and an average molecular weight less than 3900 Da are called chitosan oligomers, chitooligomers, or chitooligosaccharides [75]. COS (Figure 1) are generated by depolymerization of chitin or chitosan using acid hydrolysis, hydrolysis by physical methods and enzymatic degradation [76].

Hydrolysis of chitosan can progress by use of acid as hydrochloric acid, acid with electrolytes, nitrous acid, phosphoric acid, hydrofluoric acid, or oxidative reductive methods with hydrogen peroxide or persulfate. Other acids as lactic acid [77], trichloroacetic acid [78], formic acid [79], and acetic acid have also been studied for their degradative effect on chitin or chitosan. However, due to the complexity of controlling the progress of the reaction, these treatments also result in the formation of secondary compounds that are difficult to remove [75]. With hydrolysis by physical methods such as irradiation with low-frequency ultrasound (20 kHz), partial depolymerization is obtained, reducing the average MW from 2000 kDa down to 450 kDa or from 300 kDa to 50 kDa, but the reduction of molecular weight is limited [75].

Enzymatic methods for the hydrolysis of chitosan involve the use chitosanases and other nonspecific enzymes; this method is performed in gentle conditions and the MW distribution of the product can be controlled [80, 81]. Pantaleone et al. [82] reported the hydrolytic susceptibility of chitosan to a wide range of enzymes, including glycanases, proteases, and lipases derived from bacterial, fungal, mammalian, and plant sources.

Recently, COS have been the subject of increased attention in terms of their pharmaceutical and medicinal applications, due to their nontoxic and high solubility properties as well as their positive physiological effects.

Recent advances have insight into the health benefits of COS, possessing several beneficial biological effects including lowering blood cholesterol, lowering high blood pressure, protective effects against infections, controlling arthritis, improvement of calcium uptake, and enhancing antitumor properties.

The radical scavenging effects of COS were reported by Mendis et al. [83]. They reported that COS successively participated in scavenging intracellular radicals and also suppressed NF-κB activation.

The antitumor activity of COS was first reported in early 1970s [84]. This activity was suggested mainly due to its cationic property exerted by amino groups, and later it was accepted that the molecular weight also plays a major role for the antitumor activity [85]. Some researchers found that antitumor effects of COS were due to increased activity of natural killer lymphocytes as observed in sarcoma 180-bearing mice [86]. There have also been studies showing the apoptotic effect of COS on human hepatocellular carcinoma cells by the upregulation of Bax (Bcl-2-associated X protein) [87]. Pangestuti et al. [88] suggested that COS with molecular weight <1 kDa exhibit potent anti-inflammatory activity and also that treatment with COS results in attenuation of proinflammatory mediators in LPS (lipopolysaccharides) stimulated BV2 microglia by MAPK (mitogen activated protein kinases) signaling pathway. Administration of COS has been found to be effective against cyclophosphamide induced immunosuppression in mice [89]. The study of Mei et al. [89] also suggested that COS may also be effective in enhancing systemic immune responses and in modulating the functions of immunocompetent cells.

Wei et al. [90] showed that a high concentration of COS significantly proliferated the mice marrow cells and induced CD34+ cells into megakaryocyte progenitor cells. However, in their study, COS could not enhance the proliferation of CD19+ and CD4+ and promote CD34+ cells to differentiate into lymphoid progenitor cells suggesting that COS can promote hematopoietic stem/progenitor cells hyperplasia in mice.

Senevirathne et al. [91] studies on the effect of COS on tert-butyl hydroperoxide (t-BHP) induced damage in Chang liver cells showed that COS protected Chang liver cells against oxidative damage induced by t-BHP via inhibiting production of ROS and lipid peroxidation and the elevation of the levels of antioxidant enzymes.

The inhibitory effects of COS on degranulation and cytokine generation in rat basophilic leukemia RBL-2H3 cells were investigated by Vo et al. [92]. Their results indicated that COS contribute to attenuation of allergic reactions. Their study suggested that COS (MW: 1 to 3 kDa) possess the highest inhibitory effects on degranulation and cytokine generation of mast cells. They also suggested that COS with different molecular weight ranges might lead to variable absorption, which corresponds to the different inhibitory effects in mast cells.

Efficacy of COS in the management of diabetes in alloxan induced mice was evaluated by Katiyar et al. [93]. Their study suggested that COS have significant effect of antidiabetic activity, hypolipidemic activity, and antioxidative properties in alloxan induced diabetic mice.

5. Chitooligosaccharide Derivatives

5.1. Amino Derived COS. COS, hydrolytic products of chitosan, have amino groups or acetamide groups at C-2 position depending on their degree of acetylation. Partly based on these functional groups, they have exhibited a number of biological activities.

Ngo et al. [94] synthesized aminoethyl COS (AE-COS, Figure 2) by grafting aminoethyl functionality to improve its angiotensin I converting enzyme inhibitor potential. ACE plays an important physiological role in regulating blood pressure by converting an inactive form of decapeptide, angiotensin I, to a potent vasoconstrictor, octapeptide,

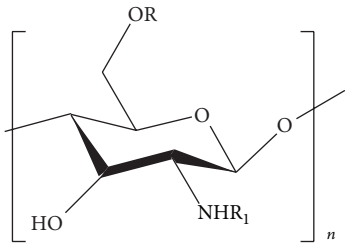

Figure 2: Aminoethyl chitooligosaccharide.

angiotensin II, and by inactivating catalytic function of bradykinin, which has depressor action. Therefore, inhibition of ACE is considered to be an important therapeutic approach for controlling hypertension [95].

Ngo et al. [94] replaced the hydroxyl group at C-6 position by aminoethyl group because the C-6 hydroxyl groups had the highest reactivity for aminoethylation, while the structure of COS was maintained; the AE-COS thus formed was completely soluble in water. In their study, AE-COS with molecular mass ranging between 800.79 and 4765 Da was prepared from COS with molecular weight 800–3000 Da by grafting aminoethyl groups at C-6 position of pyranose ring and its effects on ACE inhibition were investigated. Their study showed that AE-COS exhibited an 89.3% ACE inhibition at 2.5 mg/mL and its IC50 value was 0.8017 mg/mL.

Ngo et al. [96] investigated the inhibitory effects of AE-COS on oxidative stress in mouse macrophages (RAW 264.7 cells). They prepared AE-COS by adding 2-chlorethylamino hydrochloride to COS while stirring at 40°C. NaOH was added to the reaction mixture dropwise and continuously stirred for 48 h. The solution was then filtered and the reaction mixture was acidified with 0.1 N HCl and dialyzed against water for 2 days. The product was freeze-dried to give AE-COS (Figure 3). The results of Ngo et al. [96] indicated that in HL-60 cells, AE-COS exhibited a greater inhibitory effect (a 20% increase) on myeloperoxidase activity as compared to COS at 100 μg/mL. They also reported that AE-COS can prevent oxidative stress to membrane protein of live cells and exhibits inhibitory effect against DNA oxidation in live cells. Ngo et al. [96] investigated the direct scavenging effects of AE-COS and COS in live cell system. For that, RAW 264.7 cells were labeled with fluorescence probe DCFH-DA (dichlorodihydrofluorescein diacetate), which is the specific probe for reactive oxygen species (ROS) that was used. Their study confirmed that AE-COS has antioxidant activity in dose- and time-dependent manner and has potent direct free radicals scavenging ability in a cellular environment.

The antioxidant and anti-inflammatory activities of AE-COS in murine microglial cells (BV-2) were investigated by Ngo et al. [97]. Neuroinflammation or inflammation of the brain is closely involved in pathogenesis of several neurodegenerative diseases, such as Parkinson's disease, Alzheimer's disease, human immunodeficiency virus-associated dementia, and multiple sclerosis. It was found that the treatment

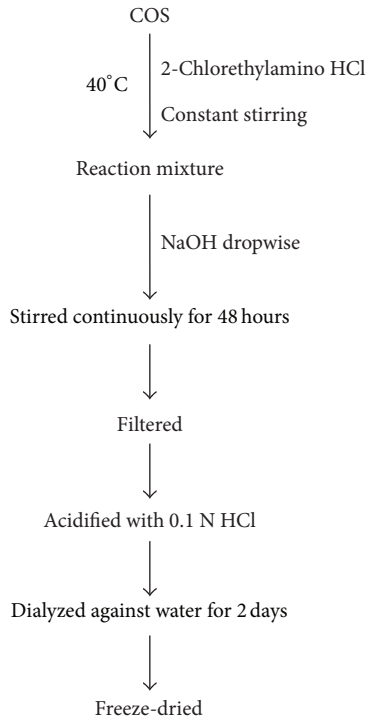

Figure 3: Synthesis of AE-COS.

of AE-COS in BV-2 cells at 100 μg/mL inhibited ROS, DNA, protein, and lipid oxidation. AE-COS was also studied for its inhibitory activity against lipopolysaccharide induced inflammatory responses in BV-2 cells. It was found that AE-COS reduced the level of nitric oxide (NO) and prostaglandin E2 production by diminishing the expression of inducible NO synthase and cyclooxygenase-2 without significant cytotoxicity. They also observed that in LPS treated BV-2 cells, AE-COS lowered the levels of TNF-α and IL-1β in a dose-dependent manner.

Karagozlu et al. [98] synthesized water-soluble amino derivatized COS derivatives, aminoethyl COS (AE-COS), dimethyl aminoethyl COS (DMAE-COS), and diethyl aminoethyl COS (DEAE-COS) and evaluated their apoptotic activity on human stomach adenocarcinoma (AGS cells). Their study showed that exposure of AGS cells to the aminoethylated COS derivatives resulted in the inhibition of cell proliferation in a dose-dependent manner; at 50 and 500 μg/mL, AE-COS inhibited the cell proliferation by 22% and 84%, DMAE-COS by 45% and 85%, and DEAE-COS by 68% and 86%. Karagozlu et al. [98] also suggested that COS and amino derivatized COS derivatives induced apoptosis in AGS cancer cells by mitochondrial pathways, via the upregulation of Bax expression and activation caspases.

Antiproliferative effects of amino derivatized COS on AGS human gastric cancer cells were investigated by Karagozlu et al. [99]. They were able to deduce that exposure of AGS cells to increasing concentrations of amino derivatized COS resulted in a dose- and time-dependent decrease in cell viability relative to control cells and that amino derivatized COS

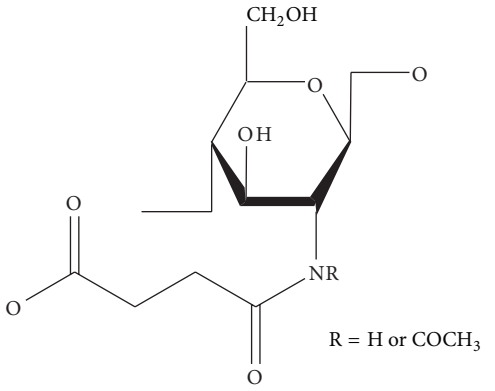

Figure 4: Carboxylated chitooligosaccharide.

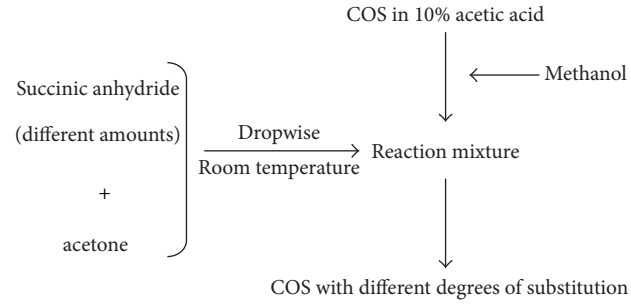

Figure 5: Synthesis of CCOS.

induce cell death in AGS cells through a typical apoptotic pathway. Karagozlu et al. [99] reported that AE-COS induced apoptosis via induction of p53 and p21 and inhibition of Bcl-2 and Bax and DEAE-COS induced apoptosis via induction of p53 and p21, activation of Bax, and inhibition of Bcl-2.

5.2. Carboxylated COS. The functional properties of COS derivatives are mainly dependent upon their functional groups and molecular weight. Low molecular weight COS derivatives not only are easily solubilized in aqueous media, but also are preferred to be used for numerous applications. Rajapakse et al. [100] synthesized carboxylated chitooligosaccharides (CCOS; Figure 4) by introducing carboxyl group ($COCH_2CH_2COO-$) to the amino position of pyranose unit. They accomplished this by adding methanol to a solution of COS in 10% acetic acid followed by addition of different amounts of succinic anhydride dissolved in acetone dropwise at room temperature for 1 h, to obtain CCOS with different substitution degrees (Figure 5). Rajapakse et al. [100] evaluated the effect of these synthesized CCOS on MMP-9 (matrix metalloproteinases-9) expression in human fibrosarcoma cells.

MMPs are a structurally related class of zinc-binding proteases (metzincin) which selectively cleave polypeptide bonds in extracellular matrix (ECM) and remodel structural proteins. However, in several disease states pathological tissue degradation and remodeling take place due to over expression and imbalanced activation of MMPs. In cancer, MMP-9 (gelatinase B, 92 kDa) is thought to play a major role in tumor growth, angiogenesis, and metastasis [101]. Rajapakse et al. [100] reported in their study that CCOS exerted a dose- dependent inhibitory effect on MMP-9 in human fibrosarcoma cell line (HT1080); they observed that reduction in MMP-9 expression was due to downregulation of MMP-9 transcription that was mediated via inhibition of AP-1 (activator protein-1) and this inhibition of MMP-9 expression led to inhibition of tumor invasiveness.

Effect of CCOS on ACE inhibition was assessed by Huang et al. [102]. They observed that attachment of carboxyl group to COS was beneficial for ACE inhibition because it enhanced the binding ability of COS to the obligatory active site of the enzyme.

Rajapakse et al. [103] tested the cellular antioxidant effects of CCOS, by assessing the oxidation inhibition potential on cellular biomolecules such as lipids, proteins, and direct scavenging of reactive oxygen species (ROS). Their results indicated that CCOS inhibited membrane lipid peroxidation in a dose-dependent manner and at low concentrations; it also showed a significantly higher inhibition of cellular lipid peroxidation as compared to COS. The study of Rajapakse et al. [103] also demonstrated that CCOS inhibited membrane protein oxidation and myeloperoxidase and their free radical scavenging studies using 2′,7′-dichlorofluorescein diacetate (DCFH-DA) on RAW264.7 cells showed that oxidation protection effects exerted by CCOS are due to direct scavenging of cellular radicals.

5.3. Gallyl COS. Phenolic compounds are some of the most widespread molecules among plant secondary metabolites [104]. These phenolics are rich in some foods and medicinal plants and considered as natural antioxidants [105]. Among them, gallic acid is particularly abundant in processed beverages such as red wine and green tea [106]. It has been reported that gallic acid possesses a wide range of biological activities, including antioxidant, anti-inflammatory, antimicrobial, and anticancer activities [107].

Ngo et al. [108] synthesized gallic acid conjugated COS (G-COS; Figure 6) to evaluate its inhibitory effects on intracellular free radical generation. G-COS was synthesized by mixing two solutions, solution A which was prepared by dissolving COS in distilled water (DW) and methanol and the pH of this solution was adjusted to 6.8 with triethylamine and solution B which was prepared by dissolving gallic acid in methanol and mixing it with DCC-(dicyclohexylcarbodiimide-) methanol mixture. Solution B was gradually added to solution A with constant stirring for 5 hours; the mixture was filtered and kept overnight at 2°C and diethyl ether was added; the precipitate formed was filtered, dissolved in DW, and dialyzed (dialysis membranes molecular weight cutoff below 1 kDa) against DW; the solution was then freeze- dried to obtain G-COS (Figure 7).

Ngo et al. [108] findings suggest that G-COS is a potent scavenger of free radicals and is able to inhibit and prevent oxidative damage to DNA, proteins, and lipids in SW1353 cells; it increased the levels of intracellular antioxidant enzymes (superoxide dismutase (SOD) and glutathione (GSH)) and suppressed the NF-κB activation and expression

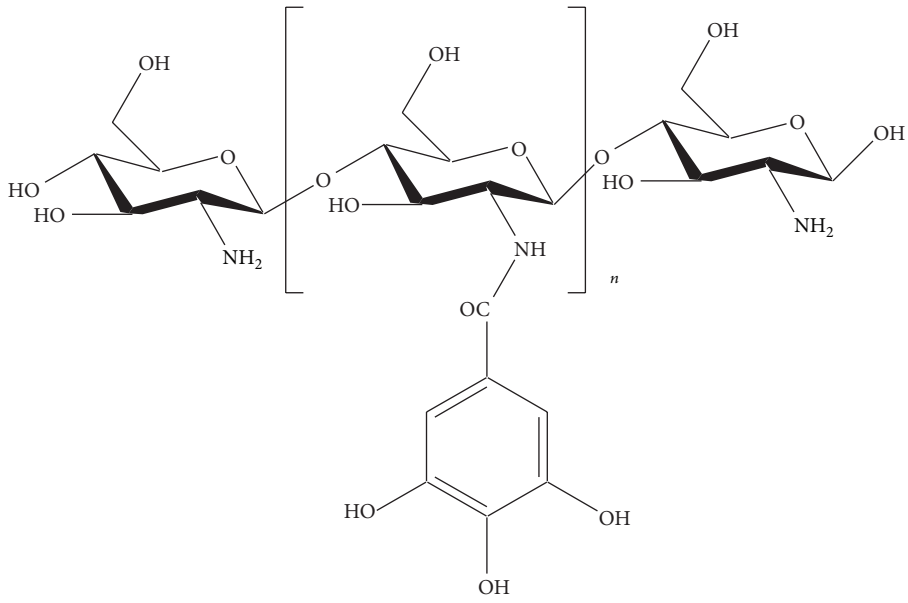

Figure 6: Gallyl chitooligosaccharide.

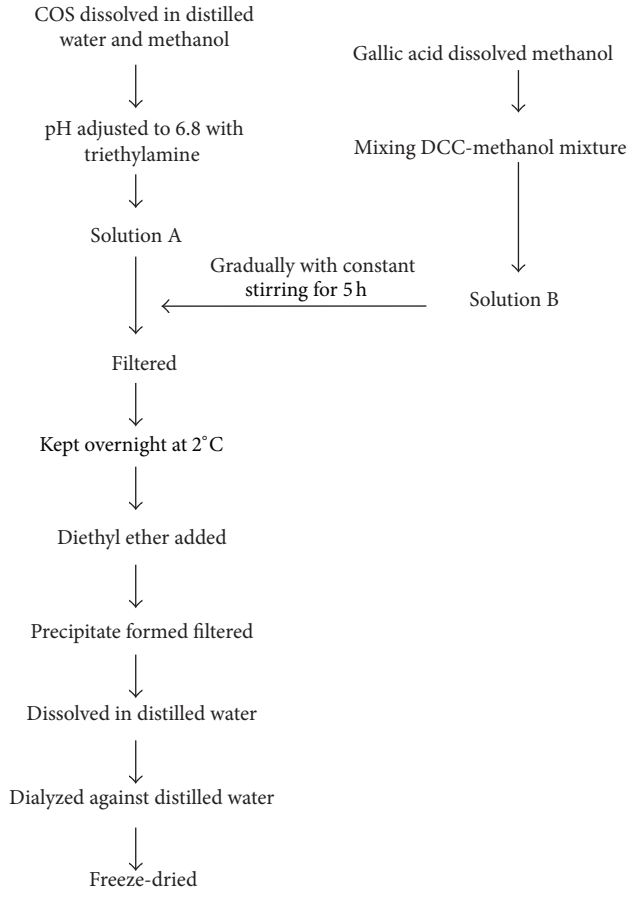

Figure 7: Synthesis of Gallyl COS.

in H_2O_2 induced SW1353 cells, thereby reducing and preventing the oxidative damage to cellular biomolecules in living cells by both indirect and direct ways.

Ngo et al. [109] evaluated the antioxidant effect of gallate chitooligosaccharides in mouse macrophage RAW264.7 cells. They reported that G-COS was able to scavenge cellular radicals in RAW264.7 cells and was able to inhibit oxidative damage to lipids, proteins, and DNA; they also deduced that G-COS could decrease the activation and expression of NF-κB and increase the level of intracellular antioxidant enzymes (SOD and GSH) in oxidative stress induced RAW264.7 cells.

Allergy is considered as a disorder of the immune system in which an exaggerated response occurs when a person is exposed to normally harmless environmental substances, such as animal dander, house dust mites, foods, pollen, insects, and chemical agents [110, 111]. The effect of G-COS on antigen induced allergic reactions in RBL-2H3 mast cells was studied by Vo et al. [112]; they observed the effect of G-COS on the degranulation of mast cells by measuring the amount of histamine released and found that G-COS inhibited the release of histamine in a dose- dependent manner. They concluded that diminished histamine production on treatment with G-COS may be due to the decreased in expression of HDC (L-histidine decarboxylase). The study of Vo et al. [112] also showed that G-COS suppressed intracellular Ca^{2+} elevation and IL-4 and TNF-α in antigen stimulated RBL-2H3 mast cells. The suppression in cytokines IL-4 and TNF-α might be due to regulation of the MAPKs and NF-κB activation [113]. The overall conclusion of Vo et al. [112] was that the inhibitory effects of G-COS on antigen induced allergic reactions in RBL-2H3 mast cells were shown due to suppression of FcεRI expression which might cause the inhibition of intracellular signaling activation and subsequent inhibition of intracellular Ca^{2+} elevation, cytokine generation, and histamine release and production. FcεRI has been well known to play a central role in the induction and maintenance of allergic reactions [114].

5.4. Sulfated COS. Glucose sensing is a very important function of pancreatic beta cells and serves in maintaining an appropriate blood glucose level. Impairment of glucose sensing by beta cells results in an alteration in the glucose concentration dependence of insulin secretion in pancreatic beta cells, which may lead to type 2 diabetes [113, 115]. Ishihara et al. [116] characterized the properties of transport, phosphorylation, and utilization of glucose in MIN6 cells and demonstrated that these characteristics are very similar to those in normal pancreatic islets and beta cells.

Protective effect of different substituted sulfated COS (COS-S; Figure 8) on MIN6 cells was evaluated by Lu et al. [117]. They synthesized COS-S with different degrees of substitution by using two kinds of sulfating reagent, chlorosulfonic acid and anhydrous formamide in different ratios (1 : 8 and 1 : 12) [117]. Chitosan was suspended in anhydrous formamide by stirring for 30 min, and the sulfating reagents were added drop by drop. The mixture was maintained at 50°C for 3 h with continuous stirring. At the end of the reaction, the mixture was cooled, neutralized with NaOH, and treated by adding ethanol. The precipitate was dissolved in DW, dialyzed exhaustively against DW, and then lyophilized (Figure 9) [117]. The study of Lu et al. [117] showed that COS-S with different degrees of substitution protected MIN6 from H_2O_2 induced apoptosis; their study suggested that COS-S prevented apoptosis probably by downregulating H_2O_2 induced Bax mRNA expression, Caspase-3 mRNA expression, and NF-κB/p65 activation and upregulating Bcl-2 mRNA expression.

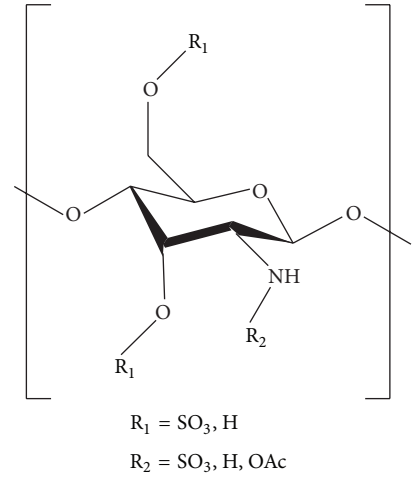

Figure 8: Sulfated chitooligosaccharide.

Lu et al. [118] evaluated the protective effects of COS-S against hydrogen peroxide-induced damage in MIN6 cells. They tested the effect of COS-S on cell viability, morphology, insulin contents, malondialdehyde (MDA) inhibition, lactate dehydrogenase (LDH) release, and levels of antioxidant enzymes including catalase (CAT), SOD, and glutathione peroxidase (GPx) under oxidative damage by H_2O_2. The study of Lu et al. [118] demonstrated that COS-S exhibited antioxidant effect and enhanced the cell viability; it attenuated the production of ROS, MDA, and LDH. Lu et al. [118] suggested that the protective effects of COS-S can be partly attributed to increase of antioxidant enzyme activities and reduction of intracellular ROS, along with the capacity of suppressing MIN6 cell apoptosis.

The antioxidant effect of COS-S on H_2O_2 induced oxidative damage in Chang cells was reported by Lee et al. [119]. COS-S was prepared by deacetylating chitin using sodium hydroxide to get chitosan; the chitosan was then hydrolyzed to COS by using lactic acid and UF membrane reactor system. The chitosan and COS were lyophilized and dispersed in DW and anhydrous sodium carbonate, trimethylamine sulfur trioxide was added to it, and the mixture was heated at 65°C until a viscous solution or gel was formed. The mixture was cooled and dialyzed exhaustively against DW and freeze-dried to get sulfated chitosan and COS-S. Lee et al. [119] tested these synthesized sulfated chitosan and COS-S for their protective effects against H_2O_2 induced oxidative damage in Chang cells and concluded that sulfated chitosan and COS-S possess potent protective effect on liver and DNA against oxidative stress.

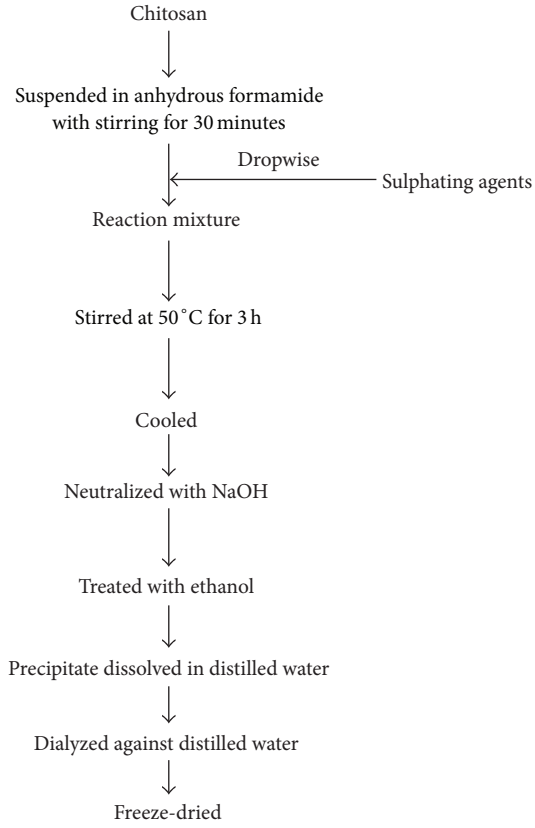

Figure 9: Synthesis of sulfated chitooligosaccharides.

The inhibitory effects of COS-S with different molecular weights on angiotensin I-converting enzyme were reported by Qian et al. [120]. Their study concluded that molecular weights of COS and COS derivatives are important factors of ACE inhibition and medium molecular weight COS-S and low molecular weight COS-S inhibited ACE by specifically binding to the active site of ACE and by competing with its natural substrate.

The effect of COS-S as inhibitor of prolyl endopeptidase (PEP) was reported by Je et al. [121]. PEP is a proline-specific endopeptidase with a serine-type mechanism and hydrolyzes peptide bonds at the carboxyl terminus of prolyl residues; it has been reported to be involved in neurodegenerative disorders. Je et al. [121] synthesized COS with high, medium, and low molecular weight and with different degrees of deacetylation (90, 75 and 50%) which were then converted into their corresponding sulphates. Je et al. [121] reported that medium molecular weight, 50% deacetylated COS-S showed the maximum inhibitory action on PEP.

The anti-HIV-1 activity of low molecular weight COS-S was reported by Artan et al. [122]. They reported that COS-S with molecular weight range between 3 and 5 kDa was most effective in inhibiting HIV-1 replication. At nontoxic concentrations, COS-S exhibited remarkable inhibitory activities on HIV-1 induced syncytia formation, lytic effect, and p24 antigen production. In contrast, unsulfated chitooligosaccharides showed no activity against HIV-1. Furthermore, Artan et al. [122] concluded that COS-S blocked viral entry and virus-cell fusion probably by disrupting the binding of HIV-1 gp120 to CD4 cell surface receptor.

Karadeniz et al. [123] reported the antiadipogenic effect of COS-S in 3T3-L1 adipocytes. Their study suggested that COS-S inhibited the mRNA expressions and protein levels of key adipogenic markers such as peroxisome proliferator activated receptor (PPAR)-γ and CCAAT enhancer binding protein (C/EBP)-α, thereby highlighting its efficacy in the management of obesity.

Ryu et al. [124] reported the effects of COS-S with different molecular weights on the degradation of articular cartilage through unregulated collagenase expression. Their study suggested that COS-S with molecular weight between 3 and 5 kDa effectively inhibited the expressions of collagenases 1 and 3 and thereby prevented TNF-α induced degradation of collagen in human chondrosarcoma cells (SW-1353). They concluded that COS-S prevented collagen degradation by inhibiting collagenases 1 and 3 via suppressing TNF-α induced NF-κB signaling.

5.5. Phenolic Acid Conjugated COS. Phenolic acids, especially hydroxycinnamic acids such as p-coumaric, caffeic, ferulic, and sinapinic acid, and benzoic acids derivatives such as p-hydroxybenzoic, protocatechuic, vanillic, and syringic acids are natural plant hydrophilic antioxidants [125].

Eom et al. [126] synthesized various derivatives of COS conjugating them with protocatechuic, 4-hydroxybenzoic, vanillic, syringic, p-coumaric, caffeic, ferulic, and sinapinic acids and tested their antioxidant activity. Their studies showed that among all the PA-c-COSs synthesized, protocatechuic acid conjugated COSs, and caffeic acid conjugated COS showed the strongest antioxidant activities.

Conflict of Interests

The authors declare that there is no conflict of interests regarding the publication of this paper.

Acknowledgment

This work was carried out with the support of the "Cooperative Research Program for Agriculture Science and Technology Development (Project no. PJ907038)," Rural Development Administration, Republic of Korea.

References

[1] R. N. Tharanathan, "Biodegradable films and composite coatings: past, present and future," *Trends in Food Science and Technology*, vol. 14, no. 3, pp. 71–78, 2003.

[2] H. P. Ramesh and R. N. Tharanathan, "Carbohydrates: the renewable raw materials of high biotechnological value," *Critical Reviews in Biotechnology*, vol. 23, no. 2, pp. 149–173, 2003.

[3] F. Shahidi, J. K. V. Arachchi, and Y.-J. Jeon, "Food applications of chitin and chitosans," *Trends in Food Science and Technology*, vol. 10, no. 2, pp. 37–51, 1999.

[4] M. N. V. Ravi Kumar, "A review of chitin and chitosan applications," *Reactive and Functional Polymers*, vol. 46, no. 1, pp. 1–27, 2000.

[5] O. Felt, P. Buri, and R. Gurny, "Chitosan: a unique polysaccharide for drug delivery," *Drug Development and Industrial Pharmacy*, vol. 24, no. 11, pp. 979–993, 1998.

[6] A. Yamada, N. Shibbuya, O. Komada et al., "Induction of phytoalexin formation in suspension-cultured rice cells by N-acetylchitooligosaccharides," *Bioscience, Biotechnology and Biochemistry*, vol. 57, no. 3, pp. 405–409, 1993.

[7] C. Peniche-Covas, L. W. Alvarez, and W. Arguelles-Monal, "Adsorption of mercuric ions by chitosan," *Journal of Applied Polymer Science*, vol. 46, no. 7, pp. 1147–1150, 1992.

[8] C. Jeuniaux, "Chitosan as a tool for the purification of waters," in *Chitin in Nature and Technology*, pp. 551–570, Plenum Press, New York, NY, USA, 1986.

[9] K. Kurita, "Chemistry and application of chitin and chitosan," *Polymer Degradation and Stability*, vol. 59, no. 1–3, pp. 117–120, 1998.

[10] Y.-J. Jeon, F. Shahidi, and S.-K. Kim, "Preparation of chitin and chitosan oligomers and their applications in physiological functional foods," *Food Reviews International*, vol. 16, no. 2, pp. 159–176, 2000.

[11] K. M. Rudall and W. Kenchington, "The chitin system," *Biological Reviews of the Cambridge Philosophical Society*, vol. 48, no. 4, pp. 597–636, 1973.

[12] R. A. A. Muzzarelli, *Chitin*, Pergamon Press, New York, NY, USA, 1977.

[13] J. H. Willis, "Cuticular proteins in insects and crustaceans," *American Zoologist*, vol. 39, no. 3, pp. 600–609, 1999.

[14] J. Synowiecki and N. A. Al-Khateeb, "Production, properties, and some new applications of chitin and its derivatives," *Critical Reviews in Food Science and Nutrition*, vol. 43, no. 2, pp. 145–171, 2003.

[15] R. A. A. Muzzarelli, *Natural Chelating Polymers*, Pergamon Press, New York, NY, USA, 1973.

[16] J. P. Zikakis, *Chitin, Chitosan and Related Enzymes*, Academic Press, Orlando, Fla, USA, 1984.

[17] K. M. Rudall, "The chitin/protein complexes of insect cuticles," *Advances in Insect Physiology*, vol. 1, pp. 257–313, 1963.

[18] B. Focher, A. Naggi, G. Torri, A. Cosani, and M. Terbojevich, "Structural differences between chitin polymorphs and their precipitates from solutions-evidence from CP-MAS ^{13}C-NMR, FT-IR and FT-Raman spectroscopy," *Carbohydrate Polymers*, vol. 17, no. 2, pp. 97–102, 1992.

[19] H. Merzendorfer and L. Zimoch, "Chitin metabolism in insects: structure, function and regulation of chitin synthases and chitinases," *Journal of Experimental Biology*, vol. 206, no. 24, pp. 4393–4412, 2003.

[20] T. Kameda, M. Miyazawa, H. Ono, and M. Yoshida, "Hydrogen bonding structure and stability of α-chitin studied by ^{13}C solid-state NMR," *Macromolecular Bioscience*, vol. 5, no. 2, pp. 103–106, 2005.

[21] K. Kurita, K. Tomita, T. Tada, S. Ishii, S.-I. Nishimura, and K. Shimoda, "Squid chitin as a potential alternative chitin source. Deacetylation behavior and characteristic properties," *Journal of Polymer Science A*, vol. 31, no. 2, pp. 485–491, 1993.

[22] S. S. Kim, S. H. Kim, and Y. M. Lee, "Preparation, characterization, and properties of β-chitin and N-acetylated β-chitin," *Journal of Polymer Science B*, vol. 34, no. 14, pp. 2367–2374, 1996.

[23] A. Chandumpai, N. Singhpibulporn, D. Faroongsarng, and P. Sornprasit, "Preparation and physico-chemical characterization of chitin and chitosan from the pens of the squid species, Loligo lessoniana and Loligo formosana," *Carbohydrate Polymers*, vol. 58, no. 4, pp. 467–474, 2004.

[24] K. van de Velde and P. Kiekens, "Structure analysis and degree of substitution of chitin, chitosan and dibutyrylchitin by FT-IR spectroscopy and solid state13C NMR," *Carbohydrate Polymers*, vol. 58, no. 4, pp. 409–416, 2004.

[25] M. Rhazi, J. Desbrières, A. Tolaimate, A. Alagui, and P. Vottero, "Investigation of different natural sources of chitin: Influence of the source and deacetylation process on the physicochemical characteristics of chitosan," *Polymer International*, vol. 49, no. 4, pp. 337–344, 2000.

[26] W. Kenchington, *The Insect Integument*, Elsevier Science, Amsterdam, The Netherlands, 1976.

[27] A. C. A. Wan and B. C. U. Tai, "CHITIN—a promising biomaterial for tissue engineering and stem cell technologies," *Biotechnology Advances*, vol. 31, no. 8, pp. 1776–1785, 2013.

[28] M. J. Bae, H. S. Shin, En-Kyoung Kim et al., "Oral administration of chitin and chitosan prevents peanut-induced anaphylaxis in a murine food allergy model," *International Journal of Biological Macromolecules*, vol. 61, pp. 164–168, 2013.

[29] R. Harikrishnan, J.-S. Kim, C. Balasundaram, and M.-S. Heo, "Dietary supplementation with chitin and chitosan on haematology and innate immune response in Epinephelus bruneus against Philasterides dicentrarchi," *Experimental Parasitology*, vol. 131, no. 1, pp. 116–124, 2012.

[30] R. Harikrishnan, J.-S. Kim, C. Balasundaram, and M.-S. Heo, "Immunomodulatory effects of chitin and chitosan enriched diets in Epinephelus bruneus against Vibrio alginolyticus infection," *Aquaculture*, vol. 326-329, pp. 46–52, 2012.

[31] M. S. Benhabiles, R. Salah, H. Lounici, N. Drouiche, M. F. A. Goosen, and N. Mameri, "Antibacterial activity of chitin, chitosan and its oligomers prepared from shrimp shell waste," *Food Hydrocolloids*, vol. 29, no. 1, pp. 48–56, 2012.

[32] D. Knorr, "Use of chitinous polymers in food: a challenge for food research and development," *Food Technology*, vol. 38, no. 1, pp. 85–97, 1984.

[33] E. Furusaki, Y. Ueno, N. Sakairi, N. Nishi, and S. Tokura, "Facile preparation and inclusion ability of a chitosan derivative bearing carboxymethyl-β-cyclodextrin," *Carbohydrate Polymers*, vol. 29, no. 1, pp. 29–34, 1996.

[34] K. Kurita, "Chemical modifications of chitin and chitosan," in *Chitin in Nature and Technology*, pp. 287–293, Plenum Press, New York, NY, USA, 1986.

[35] R. R. A. Muzzarelli, *Chitin Enzymology*, European Chitin Society, Ancona, Italy, 1996.

[36] A. Razdan and D. Pettersson, "Effect of chitin and chitosan on nutrient digestibility and plasma lipid concentrations in broiler chickens," *British Journal of Nutrition*, vol. 72, no. 2, pp. 277–288, 1994.

[37] M. W. Anthonsen and O. Smidsrød, "Hydrogen ion titration of chitosans with varying degrees of N-acetylation by monitoring induced ^{1}H-NMR chemical shifts," *Carbohydrate Polymers*, vol. 26, no. 4, pp. 303–305, 1995.

[38] M. Rinaudo, "Chitin and chitosan: properties and applications," *Progress in Polymer Science*, vol. 31, no. 7, pp. 603–632, 2006.

[39] N. Sankararamakrishnan and R. Sanghi, "Preparation and characterization of a novel xanthated chitosan," *Carbohydrate Polymers*, vol. 66, no. 2, pp. 160–167, 2006.

[40] S. V. Madihally and H. W. T. Matthew, "Porous chitosan scaffolds for tissue engineering," *Biomaterials*, vol. 20, no. 12, pp. 1133–1142, 1999.

[41] I. S. Arvanitoyannis, A. Nakayama, and S.-I. Aiba, "Chitosan and gelatin based edible films: state diagrams, mechanical and permeation properties," *Carbohydrate Polymers*, vol. 37, no. 4, pp. 371–382, 1998.

[42] I. S. Arvanitoyannis, "Totally and partially biodegradable polymer blends based on natural and synthetic macromolecules: preparation, physical properties, and potential as food packaging materials," *Journal of Macromolecular Science C*, vol. 39, no. 2, pp. 205–271, 1999.

[43] T. Haque, H. Chen, W. Ouyang et al., "Superior cell delivery features of poly(ethylene glycol) incorporated alginate, chitosan, and poly-L-lysine microcapsules," *Molecular Pharmaceutics*, vol. 2, no. 1, pp. 29–36, 2005.

[44] H.-J. Kim, F. Chen, X. Wang, and N. C. Rajapakse, "Effect of chitosan on the biological properties of sweet basil (*Ocimum basilicum L.*)," *Journal of Agricultural and Food Chemistry*, vol. 53, no. 9, pp. 3696–3701, 2005.

[45] G. A. F. Roberts, *Chitin Chemistry*, MacMillan Press, London, UK, 1992.

[46] K. Yamada, Y. Akiba, T. Shibuya, A. Kashiwada, K. Matsuda, and M. Hirata, "Water purification through bioconversion of phenol compounds by tyrosinase and chemical adsorption by chitosan beads," *Biotechnology Progress*, vol. 21, no. 3, pp. 823–829, 2005.

[47] W. Malette, H. Quigley, and E. Adickes, *Chitin in Nature and Technology*, Plenum Press, 1986.

[48] K. Arai, T. Kinumaki, and T. Fujita, *Bulletin of Tokai Regional Fisheries Research Laboratory*, 1968.

[49] H. Struszczyk, H. Pospieszny, and S. Kotlinski, "Some new application of chitosan," in *Chitin and Chitosan*, G. Skjoak-Brok, T. Anthonsen, and P. Sandford, Eds., pp. 733–742, Elseiver Science, London, UK, 1989.

[50] E. Onsoyen and O. Skaugrud, "Metal recovery using chitosan," *Journal of Chemical Technology and Biotechnology*, vol. 49, no. 4, pp. 395–404, 1990.

[51] G. Lang and T. Clausen, "The use of chit os an in cosmetics," in *Chitin and Chitosan*, G. Skjoak-Brok, T. Anthonsen, and P. Sandford, Eds., pp. 139–147, Elseiver Science, London, UK, 1989.

[52] N. A. Ashford, D. B. Hattis, and A. E. Murray, *MIT Sea Grant Program*, Massachusetts Institute of Technology, 1977.

[53] Y. Fukada, K. Kimura, and Y. Ayaki, "Effect of chitosan feeding on intestinal bile acid metabolism in rats," *Lipids*, vol. 26, no. 5, pp. 395–399, 1991.

[54] Y. Shigemasa and S. Minami, *Biotechnology & Genetic Engineering Reviews*, Intercept, 1995.

[55] K. Nishimura, S.-I. Nishimura, and H. Seo, "Effect of multiporous microspheres derived from chitin and partially deacetylated chitin on the activation of mouse peritoneal macrophages," *Vaccine*, vol. 5, no. 2, pp. 136–140, 1987.

[56] J. Dutkiewicz and M. Kucharska, *Advances in Chitin and Chitosan*, Elsevier Science, 1992.

[57] H. Seo, K. Mitsuhashi, and H. Tanibe, *Advances in Chitin and Chitosan*, Elsevier Science, 1992.

[58] R. Muzzarelli, G. Biagini, A. Pugnaloni et al., "Reconstruction of parodontal tissue with chitosan," *Biomaterials*, vol. 10, no. 9, pp. 598–603, 1989.

[59] C. Shi, Y. Zhu, X. Ran et al., "Therapeutic potential of chitosan and its derivatives in regenerative medicine," *Journal of Surgical Research*, vol. 133, no. 2, pp. 185–192, 2006.

[60] S. Hirano and N. Nagao, "Effects of chitosan, pectic acid, lysozyme, andchitinase on the growth of several phytopathogens," *Agricultural and Biological Chemistry*, vol. 53, no. 11, pp. 3065–3066, 1989.

[61] D. F. Kendra and L. A. Hadwiger, "Characterization of the smallest chitosan oligomer that is maximally antifungal to *Fusarium solani* and elicits pisatin formation in *Pisum sativum*," *Experimental Mycology*, vol. 8, no. 3, pp. 276–281, 1984.

[62] Y. Uchida, M. Izume, and A. Ohtakara, *Chitin and Chitosan*, Elsevier, London, UK, 1989.

[63] K. Ueno, T. Yamaguchi, N. Sakairi et al., *Advances in Chitin Science*, Jacques Andre, Lyon, France, 1997.

[64] T. J. Franklin and G. A. Snow, *Biochemistry of Antimicrobial Action*, Chapman and Hall, London, UK, 3rd edition, 1981.

[65] K. Takemono, J. Sunamoto, and M. Askasi, *Polymers and Medical Care*, Mita, Tokyo, 1989.

[66] J. C. Fernandes, H. Spindola, V. De Sousa et al., "Anti-inflammatory activity of chitooligosaccharides in vivo," *Marine Drugs*, vol. 8, no. 6, pp. 1763–1768, 2010.

[67] R. Huang, E. Mendis, N. Rajapakse, and S.-K. Kim, "Strong electronic charge as an important factor for anticancer activity of chitooligosaccharides (COS)," *Life Sciences*, vol. 78, no. 20, pp. 2399–2408, 2006.

[68] C. Ju, W. Yue, Z. Yang et al., "Antidiabetic effect and mechanism of chitooligosaccharides," *Biological and Pharmaceutical Bulletin*, vol. 33, no. 9, pp. 1511–1516, 2010.

[69] E. J. Jung, D. K. Youn, S. H. Lee, H. K. No, J. G. Ha, and W. Prinyawiwatkul, "Antibacterial activity of chitosans with different degrees of deacetylation and viscosities," *International Journal of Food Science and Technology*, vol. 45, no. 4, pp. 676–682, 2010.

[70] M. Artan, F. Karadeniz, M. Z. Karagozlu, M.-M. Kim, and S.-K. Kim, "Anti-HIV-1 activity of low molecular weight sulfated chitooligosaccharides," *Carbohydrate Research*, vol. 345, no. 5, pp. 656–662, 2010.

[71] D.-N. Ngo, S.-H. Lee, M.-M. Kim, and S.-K. Kim, "Production of chitin oligosaccharides with different molecular weights and their antioxidant effect in RAW 264.7 cells," *Journal of Functional Foods*, vol. 1, no. 2, pp. 188–198, 2009.

[72] H. Quan, F. Zhu, X. Han, Z. Xu, Y. Zhao, and Z. Miao, "Mechanism of anti-angiogenic activities of chitooligosaccharides may be through inhibiting heparanase activity," *Medical Hypotheses*, vol. 73, no. 2, pp. 205–206, 2009.

[73] Y. Gong, L. Gong, X. Gu, and F. Ding, "Chitooligosaccharides promote peripheral nerve regeneration in a rabbit common peroneal nerve crush injury model," *Microsurgery*, vol. 29, no. 8, pp. 650–656, 2009.

[74] J.-S. Moon, H.-K. Kim, H. C. Koo et al., "The antibacterial and immunostimulative effect of chitosan-oligosaccharides against infection by *Staphylococcus aureus* isolated from bovine mastitis," *Applied Microbiology and Biotechnology*, vol. 75, no. 5, pp. 989–998, 2007.

[75] V. K. Mourya, N. N. Inamdar, and Y. M. Choudhari, "Chitooligosaccharides: synthesis, characterization and applications," *Polymer Science A*, vol. 53, no. 7, pp. 583–612, 2011.

[76] B. B. Aam, E. B. Heggset, A. L. Norberg, M. Sørlie, K. M. Vårum, and V. G. H. Eijsink, "Production of chitooligosaccharides and their potential applications in medicine," *Marine Drugs*, vol. 8, no. 5, pp. 1482–1517, 2010.

[77] A. V. Il'ina and V. P. Varlamov, "Hydrolysis of chitosan in lactic acid," *Applied Biochemistry and Microbiology*, vol. 40, no. 3, pp. 300–303, 2004.

[78] T. Ando and S. Kataoka, "Acylation of chtin in trichloroacetic acid based solvent," *Kobunshi Ronbunshu*, vol. 37, no. 1, pp. 1–7, 1980.

[79] R. Yamaguchi, Y. Arai, and T. Itoh, "A microfibril formation from depolymerized chitosan by N-acetylation," *Agricultural and Biological Chemistry*, vol. 46, no. 9, pp. 2379–2381, 1982.

[80] Y.-J. Jeon, P.-J. Park, and S.-K. Kim, "Antimicrobial effect of chitooligosaccharides produced by bioreactor," *Carbohydrate Polymers*, vol. 44, no. 1, pp. 71–76, 2001.

[81] C. Qin, B. Zhou, L. Zeng et al., "The physicochemical properties and antitumor activity of cellulase-treated chitosan," *Food Chemistry*, vol. 84, no. 1, pp. 107–115, 2004.

[82] D. Pantaleone, M. Yalpani, and M. Scollar, "Unusual susceptibility of chitosan to enzymic hydrolysis," *Carbohydrate Research*, vol. 237, pp. 325–332, 1992.

[83] E. Mendis, M.-M. Kim, N. Rajapakse, and S.-K. Kim, "An in vitro cellular analysis of the radical scavenging efficacy of chitooligosaccharides," *Life Sciences*, vol. 80, no. 23, pp. 2118–2127, 2007.

[84] R. A. A. Muzzarelli, *Chitin*, Oxford Pergamon Press, London, UK, 1977.

[85] C. Qin, Y. Du, L. Xiao, Z. Li, and X. Gao, "Enzymic preparation of water-soluble chitosan and their antitumor activity," *International Journal of Biological Macromolecules*, vol. 31, no. 1–3, pp. 111–117, 2002.

[86] Y. Maeda and Y. Kimura, "Antitumor effects of various low-molecular-weight chitosans are due to increased natural killer activity of intestinal intraepithelial lymphocytes in sarcoma 180-bearing mice," *Journal of Nutrition*, vol. 134, no. 4, pp. 945–950, 2004.

[87] Q. Xu, J. Dou, P. Wei et al., "Chitooligosaccharides induce apoptosis of human hepatocellular carcinoma cells via up-regulation of Bax," *Carbohydrate Polymers*, vol. 71, no. 4, pp. 509–514, 2008.

[88] R. Pangestuti, S.-S. Bak, and S.-K. Kim, "Attenuation of pro-inflammatory mediators in LPS-stimulated BV2 microglia by chitooligosaccharides via the MAPK signaling pathway," *International Journal of Biological Macromolecules*, vol. 49, no. 4, pp. 599–606, 2011.

[89] Y. X. Mei, H. X. Chen, J. Zhang et al., "Protective effect of chitooligosaccharides against cyclophosphamide-induced immunosuppression in mice," *International Journal of Biological Macromolecules*, vol. 62, pp. 330–335, 2013.

[90] X. Wei, W. Chen, F. Mao et al., "Effect of chitooligosaccharides on mice hematopoietic stem/progenitor cells," *International Journal of Biological Macromolecules*, vol. 54, pp. 71–75, 2013.

[91] M. Senevirathne, C.-B. Ahn, and J.-Y. Je, "Hepatoprotective effect of chitooligosaccharides against tert-butylhydroperoxide-induced damage in Chang liver cells," *Carbohydrate Polymers*, vol. 83, no. 2, pp. 995–1000, 2011.

[92] T.-S. Vo, C.-S. Kong, and S.-K. Kim, "Inhibitory effects of chitooligosaccharides on degranulation and cytokine generation in rat basophilic leukemia RBL-2H3 cells," *Carbohydrate Polymers*, vol. 84, no. 1, pp. 649–655, 2011.

[93] D. Katiyar, B. Singh, A. M. Lall, and C. Haldar, "Efficacy of chitooligosaccharides for the management of diabetes in alloxan induced mice: A correlative study with antihyperlipidemic and antioxidative activity," *European Journal of Pharmaceutical Sciences*, vol. 44, no. 4, pp. 534–543, 2011.

[94] D.-N. Ngo, Z.-J. Qian, J.-Y. Je, M.-M. Kim, and S.-K. Kim, "Aminoethyl chitooligosaccharides inhibit the activity of angiotensin converting enzyme," *Process Biochemistry*, vol. 43, no. 1, pp. 119–123, 2008.

[95] P.-J. Park, J.-Y. Je, and S.-K. Kim, "Angiotensin I converting enzyme (ACE) inhibitory activity of hetero-chitooligosaccharides prepared from partially different deacetylated chitosans," *Journal of Agricultural and Food Chemistry*, vol. 51, no. 17, pp. 4930–4934, 2003.

[96] D.-N. Ngo, M.-M. Kim, and S.-K. Kim, "Protective effects of aminoethyl-chitooligosaccharides against oxidative stress in mouse macrophage RAW 264.7 cells," *International Journal of Biological Macromolecules*, vol. 50, no. 3, pp. 624–631, 2012.

[97] D.-H. Ngo, D.-N. Ngo, T.-S. Vo, B. Ryu, Q. Van Ta, and S.-K. Kim, "Protective effects of aminoethyl-chitooligosaccharides against oxidative stress and inflammation in murine microglial BV-2 cells," *Carbohydrate Polymers*, vol. 88, no. 2, pp. 743–747, 2012.

[98] M. Z. Karagozlu, F. Karadeniz, C.-S. Kong, and S.-K. Kim, "Aminoethylated chitooligomers and their apoptotic activity on AGS human cancer cells," *Carbohydrate Polymers*, vol. 87, no. 2, pp. 1383–1389, 2012.

[99] M. Z. Karagozlu, J.-A. Kim, F. Karadeniz, C.-S. Kong, and S.-K. Kim, "Anti-proliferative effect of aminoderivatized chitooligosaccharides on AGS human gastric cancer cells," *Process Biochemistry*, vol. 45, no. 9, pp. 1523–1528, 2010.

[100] N. Rajapakse, M.-M. Kim, E. Mendis, R. Huang, and S.-K. Kim, "Carboxylated chitooligosaccharides (CCOS) inhibit MMP-9

expression in human fibrosarcoma cells via down-regulation of AP-1," *Biochimica et Biophysica Acta*, vol. 1760, no. 12, pp. 1780–1788, 2006.

[101] Y. Jiang and R. J. Muschel, "Regulation of matrix metalloproteinase-9 (MMP-9) by translational efficiency in murine prostate carcinoma cells," *Cancer Research*, vol. 62, no. 6, pp. 1910–1914, 2002.

[102] R. Huang, E. Mendis, and S.-K. Kim, "Improvement of ACE inhibitory activity of chitooligosaccharides (COS) by carboxyl modification," *Bioorganic and Medicinal Chemistry*, vol. 13, no. 11, pp. 3649–3655, 2005.

[103] N. Rajapakse, M.-M. Kim, E. Mendis, and S.-K. Kim, "Inhibition of free radical-mediated oxidation of cellular biomolecules by carboxylated chitooligosaccharides," *Bioorganic and Medicinal Chemistry*, vol. 15, no. 2, pp. 997–1003, 2007.

[104] J. H. J. R. Makoi and P. A. Ndakidemi, "Biological, ecological and agronomic significance of plant phenolic compounds in rhizosphere of the symbiotic legumes," *African Journal of Biotechnology*, vol. 6, no. 12, pp. 1358–1368, 2007.

[105] T. Li, X. Zhang, and X. Zhao, "Powerful protective effects of gallic acid and tea polyphenols on human hepatocytes injury induced by hydrogen peroxide or carbon tetrachloride in vitro," *Journal of Medicinal Plant Research*, vol. 4, no. 3, pp. 247–254, 2010.

[106] H. N. Graham, "Green tea composition, consumption, and polyphenol chemistry," *Preventive Medicine*, vol. 21, no. 3, pp. 334–350, 1992.

[107] S.-H. Kim, C.-D. Jun, K. Suk et al., "Gallic acid inhibits histamine release and pro-inflammatory cytokine production in mast cells," *Toxicological Sciences*, vol. 91, no. 1, pp. 123–131, 2006.

[108] D.-H. Ngo, Z.-J. Qian, D.-N. Ngo, T.-S. Vo, I. Wijesekara, and S.-K. Kim, "Gallyl chitooligosaccharides inhibit intracellular free radical-mediated oxidation," *Food Chemistry*, vol. 128, no. 4, pp. 974–981, 2011.

[109] D.-H. Ngo, Z.-J. Qian, T.-S. Vo, B. Ryu, D.-N. Ngo, and S.-K. Kim, "Antioxidant activity of gallate-chitooligosaccharides in mouse macrophage RAW264.7 cells," *Carbohydrate Polymers*, vol. 84, no. 4, pp. 1282–1288, 2011.

[110] S. H. Arshad, "Does exposure to indoor allergens contribute to the development of asthma and allergy?" *Current Allergy and Asthma Reports*, vol. 10, no. 1, pp. 49–55, 2010.

[111] E. Milián and A. M. Díaz, "Allergy to house dust mites and asthma," *Puerto Rico health sciences journal*, vol. 23, no. 1, pp. 47–57, 2004.

[112] T. S. Vo, D. H. Ngo, and S. K. Kim, "Gallic acid-grafted chitooligosaccharides suppress antigen-induced allergic reactions in RBL-2H3 mast cells," *European Journal of Pharmaceutical Sciences*, vol. 47, no. 2, pp. 527–533, 2012.

[113] N. Vionnet, M. Stoffel, J. Takeda et al., "Nonsense mutation in the glucokinase gene causes early-onset non-insulin-dependent diabetes mellitus," *Nature*, vol. 356, no. 6371, pp. 721–722, 1992.

[114] D. Von Bubnoff, N. Novak, S. Kraft, and T. Bieber, "The central role of FcεRi in allergy," *Clinical and Experimental Dermatology*, vol. 28, no. 2, pp. 184–187, 2003.

[115] H. Katagiri, T. Asano, H. Ishihra et al., "Nonsense mutation of glucokinase gene in late-onset non-insulin-dependent diabetes mellitus," *Lancet*, vol. 340, no. 8831, pp. 1316–1317, 1992.

[116] H. Ishihara, T. Asano, K. Tsukuda et al., "Pancreatic beta cell line MIN6 exhibits characteristics of glucose metabolism and glucose-stimulated insulin secretion similar to those of normal islets," *Diabetologia*, vol. 36, no. 11, pp. 1139–1145, 1993.

[117] X. Lu, H. Guo, L. Sun et al., "Protective effects of sulfated chitooligosaccharides with different degrees of substitution in MIN6 cells," *International Journal of Biological Macromolecules*, vol. 52, pp. 92–98, 2013.

[118] X. Lu, H. Guo, and Y. Zhang, "Protective effects of sulfated chitooligosaccharides against hydrogen peroxide-induced damage in MIN6 cells," *International Journal of Biological Macromolecules*, vol. 50, no. 1, pp. 50–58, 2012.

[119] S. J. Lee, E. K. Kim, J. W. Hwang et al., "Antioxidative effects of sulfated chitooligosaccharides on oxidative injury," *Journal of Chitin and Chitosan Science*, vol. 14, no. 4, pp. 192–196, 2009.

[120] Z. J. Qian, T. K. Eom, B. Ryu et al., "Angiotensin I-converting enzyme inhibitory activity of sulfated chitooligosaccharides with different molecular weights," *Journal of Chitin and Chitosan Science*, vol. 15, no. 2, pp. 75–79, 2010.

[121] J.-Y. Je, E.-K. Kim, C.-B. Ahn et al., "Sulfated chitooligosaccharides as prolyl endopeptidase inhibitor," *International Journal of Biological Macromolecules*, vol. 41, no. 5, pp. 529–533, 2007.

[122] M. Artan, F. Karadeniz, M. Z. Karagozlu, M.-M. Kim, and S.-K. Kim, "Anti-HIV-1 activity of low molecular weight sulfated chitooligosaccharides," *Carbohydrate Research*, vol. 345, no. 5, pp. 656–662, 2010.

[123] F. Karadeniz, M. Z. Karagozlu, S.-Y. Pyun, and S.-K. Kim, "Sulfation of chitosan oligomers enhances their anti-adipogenic effect in 3T3-L1 adipocytes," *Carbohydrate Polymers*, vol. 86, no. 2, pp. 666–671, 2011.

[124] B. Ryu, S. W. A. Himaya, R. J. Napitupulu, T.-K. Eom, and S.-K. Kim, "Sulfated chitooligosaccharide II (SCOS II) suppress collagen degradation in TNF-induced chondrosarcoma cells via NF-κB pathway," *Carbohydrate Research*, vol. 350, pp. 55–61, 2012.

[125] M.-C. Figueroa-Espinoza and P. Villeneuve, "Phenolic enzymatic lipophilization," *Journal of Agricultural and Food Chemistry*, vol. 53, no. 8, pp. 2779–2787, 2005.

[126] T. K. Eom, M. Senevirathne, and S. K. Kim, "Synthesis of phenolic acid conjugated chitooligosaccharides and evaluation of their antioxidant activity," *Environmental Toxicology and Pharmacology*, vol. 34, no. 2, pp. 519–527, 2012.

Hindawi Publishing Corporation
BioMed Research International
Volume 2014, Article ID 485867, 4 pages
http://dx.doi.org/10.1155/2014/485867

Research Article

D-Glucosamine Promotes Transfection Efficiency during Electroporation

Kazunari Igawa,[1] Naoko Ohara,[2] Atsushi Kawakubo,[1] Kouji Sugimoto,[1] Kajiro Yanagiguchi,[1] Takeshi Ikeda,[1] Shizuka Yamada,[1] and Yoshihiko Hayashi[1]

[1] *Department of Cariology, Nagasaki University School of Biomedical Sciences, Nagasaki 852-8588, Japan*
[2] *Department of Conservative Dentistry, Okayama University Graduate School of Medicine, Dentistry and Pharmaceutical Sciences, Okayama 700-8558, Japan*

Correspondence should be addressed to Yoshihiko Hayashi; hayashi@nagasaki-u.ac.jp

Received 26 November 2013; Accepted 6 January 2014; Published 11 February 2014

Academic Editor: Hideo Kusaoke

D-Glucosamine is a useful medicament in various fields of medicine and dentistry. With respect to stability of the cell membrane, it has been reported that bradykinin-induced nociceptive responses are significantly suppressed by the direct application of D-glucosamine. Electroporation is usually used to effectively introduce foreign genes into tissue culture cells. Buffers for electroporation with or without D-glucosamine are used in experiments of transfection vectors. This is the first study to indirectly observe the stability and protection of the osteoblast membrane against both electric stress and gene uptake (the proton sponge hypothesis: osmotic rupture during endosomes prior to fusion with lysosomes) in electroporation with D-glucosamine application. The transfection efficiency was evaluated as the fluorescence intensity of the transfected green fluorescent protein (GFP) in the cultured cells (osteoblasts; NOS-1 cells). The transfection efficiency increased over 30% in the electroporation samples treated with D-glucosamine-supplemented buffer after one day. The membrane absorption of D-glucosamine is the primary mechanism of membrane stress induced by electric stress. This new function of D-glucosamine is useful and meaningful for developing more effective transformation procedures.

1. Introduction

D-Glucosamine is a useful medicament in various fields of medicine and dentistry [1, 2]. For example, it is an attractive candidate for adjunctive therapy in patients with arthritis due to both its chondroprotective actions and anti-inflammatory and wound healing effects achieved via the suppression of the neutrophil function and chemokine production [3]. D-Glucosamine also has a significant antipain effect in patients with osteoarthritis. Therefore, D-glucosamine is widely used in an attempt to suppress the pain associated with the disability of osteoarthritis [4]. Recently, our group reported that bradykinin-induced nociceptive responses were significantly suppressed by the direct application of D-glucosamine [5], suggesting that D-glucosamine has a direct effect in relieving pain by ensuring membrane stability. Furthermore, we previously reported that D-glucosamine hydrochloride promoted the lysosomal escape of quantum dots inside cells (unpublished data).

The aim of this study was to confirm the maintenance of cell membrane stability via the direct effects of D-glucosamine. We used the electroporation technique for gene transfection as an experimental model to investigate both membrane protection (stability) and gene protection. A buffer solution with or without D-glucosamine was used in electroporation of the transfection vector. The transfection efficiency was quantitatively evaluated as the fluorescence intensity of transfected green fluorescent protein (GFP) in the cultured cells.

2. Materials and Methods

2.1. Preparation of Cultured Cells. Osteoblasts (NOS-1 cells [6]) derived from human osteosarcoma were used and

Figure 1: Wire type of electrode for electroporation.

cultured in α-MEM containing 10% FBS together with antibiotics. One day before electroporation, the NOS-1 cells were prepared to loose confluence in a 60 mm culture dish. After passage, the NOS-1 cells were seeded in a 35 mm glass-bottomed culture dish (number P35Gcol-1.5-14-C, MatTek Corp., MA, USA) at a density of 5×10^5 cells (each group: three dishes), and α-MEM containing 10% FBS without antibiotics was used for culture in a humidified incubator at 37°C in an atmosphere of 5% CO_2 and air.

2.2. Preparation of Chitosan Solution and Buffer. D-Glucosamine hydrochloride (molecular weight: approximately 215) was kindly supplied by Koyo Chemical Co., Ltd (Osaka, Japan). A 1% (W/V) stock solution was prepared by dissolving powder in 0.1% (V/V) acetic acid. The completely dissolved solution was neutralized to a pH value of 7.4, then sterilized with a 0.2 μm filter. Electroporation buffer with or without 0.005% (W/V) D-glucosamine in α-MEM without either FBS or antibiotics was prepared for electroporation.

2.3. Procedures for Electroporation. Electroporation was performed using a wire type electrode (Figure 1) that was set vertical to the surface of the culture dish. One day after passage, the cells attached on the culture dish were treated using a commercial electroporator (CUY21B, Tokiwa Science Limited Company, Fukuoka, Japan), connected to the electrode. The pIRES2-EGFP vector (Clontech, Takara Bio Company, Shiga, Japan) was used as an expression plasmid during transfection. A total of 10 μg/mL of the vector was prepared by dissolving the vector in the buffer. The treatment conditions consisted of five pulses of 120 V (effective voltage: 40–70 V, effective current: 40–4.4 A), each on: 5 ms and off: 95 ms, in 1 mL of electrode buffer with or without 0.005% (W/V) D-glucosamine.

2.4. Fluorescence Microscopy. The cells were cultured with α-MEM without either FBS or antibiotics for one day after electroporation and viewed using a confocal laser microscope (TCS SL, Leica Microsystems GmbH, Wetzlar, Germany) at a magnification of ×630.

2.5. Statistical Analysis. The number of GFP-positive cells was counted and converted to a percentage of the original cell number (100%) in three areas selected at random from the examined group supplemented with or without D-glucosamine. The statistical significance ($P < 0.05$) of differences between the two groups was assessed using paired Student's t-test. All values are expressed as the mean ± SD.

3. Results

No necrotic cells were observed after electroporation treatment. The percentage of GFP-positive cells was 86.4 ± 4.3% (Figures 2(a) and 2(b)) following electroporation with 0.005% D-glucosamine-containing buffer and 48.7 ± 2.9% (Figures 3(a) and 3(b)) following that without D-glucosamine-containing buffer. The transfection efficiency increased approximately 38%. The percentage between the two groups was significantly different ($P < 0.01$).

4. Discussion

This is the first study to observe the stability and protection of the osteoblast membrane against electric stress and genes against lysosomal attack during electroporation with D-glucosamine application. This function of D-glucosamine is relevant for cell biology and biological applications, such as gene therapy.

D-Glucosamine is used as an effective medicament in various fields of medicine and dentistry. For example, it is an attractive candidate for adjunctive therapy in patients with arthritis [7]. D-Glucosamine also has a significant antipain effect in patients with osteoarthritis, a disease with low expectations on the value of treatment [8, 9]. The membrane absorption of D-glucosamine is the primary mechanism of quantum dot (QD) transport into cells (unpublished data). A dramatic increase in the cellular uptake of QDs via attachment with the cell membrane is induced by a positive charge and biocompatibility of conjugated D-glucosamine. This phenomenon was confirmed in control experiments, which clearly indicated that nonconjugated QDs have difficulty entering cells. Another interesting finding is the escape of QDs from lysosomes inside cells, which was confirmed with the observation of merged fluorescence of both QDs and lysosomes. The significant increase in transfection efficiency observed in the present study using D-glucosamine was likely produced by the same mechanism as that underlying the observation of stability and protection of intracellularly distributed QDs following D-glucosamine application. This proton sponge hypothesis, while not definitively proven, has been invoked to explain the relatively high transfection efficiency of other proton-sponge-type materials, such as lipopolyamines [10, 11], PAMAM dendrimers [12], and various imidazole-containing polymers [13–15]. The original hypothesis proposed that PEI buffering

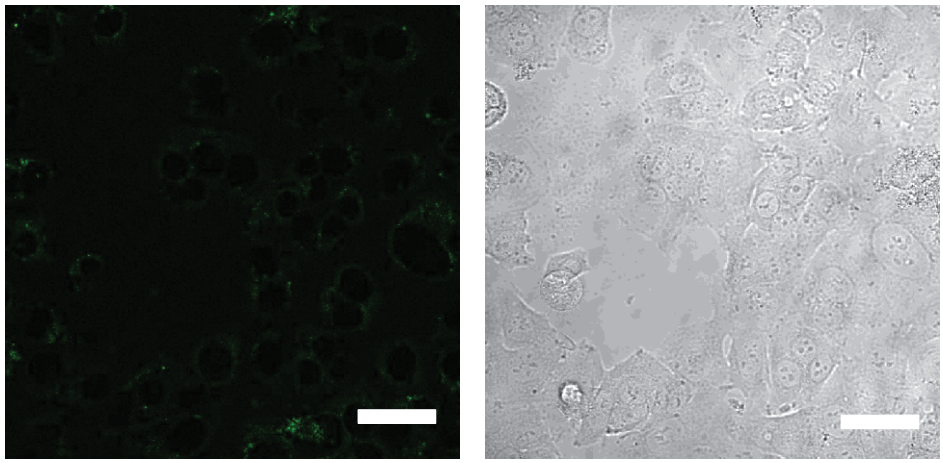

(a) (b)

Figure 2: (a) GFP-positive cells after electroporation with 0.005% D-glucosamine-containing buffer. (b) Phase contrast image of area A. Scale bar = 20 μm.

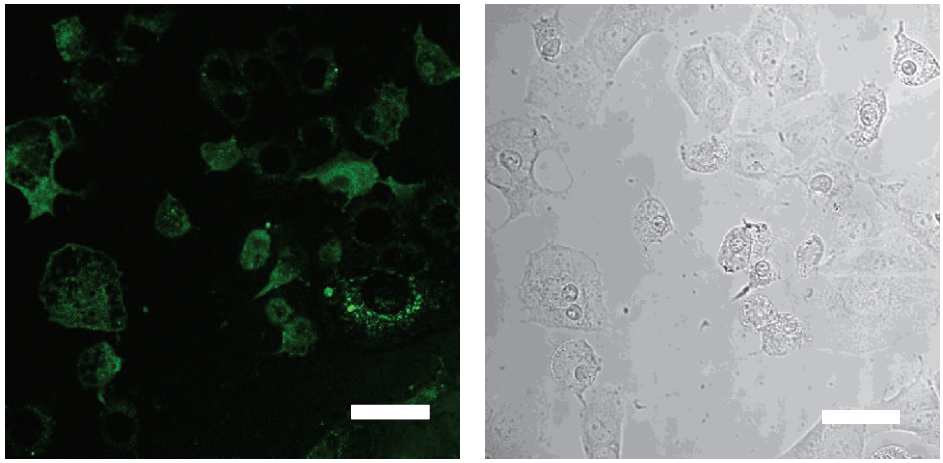

(a) (b)

Figure 3: (a) GFP-positive cells after electroporation without 0.005% D-glucosamine-containing buffer. (b) Phase contrast image of area A. Scale bar = 20 μm.

in lysosomes induced osmotic rupture and subsequent escape [16]. Although the proton sponge hypothesis based on their findings of a lack of lysosomal involvement is challenged in polyethylenimine- (PEI-) mediated gene transfer, a version of this hypothesis, whereby PEI buffering induces osmotic rupture in endosomes prior to fusion with lysosomes [10, 17], is consistent with the findings of Godbey et al. [18]. Although the pH value of D-glucosamine hydrochloride is acidic (3.5–4.5), the present D-glucosamine solution was used after neutralization. The concentration of endosomal chloride ions originated from D-glucosamine hydrochloride leads to osmotic rupture in endosomes [10, 16], which involves the escape of plasmid vectors from endosomes and lysosomes. The newly proven polycationic function of D-glucosamine through the adsorption to cell membrane and accumulation into cytoplasm (the proton sponge hypothesis: escape from the degradative lysosomal trafficking pathway) is useful and meaningful for both cell biology and clinical applications.

5. Conclusion

This is the first study to investigate the stability and protection of the osteoblast membrane against electric stress and genes against lysosomal attack during electroporation with D-glucosamine application. The newly proven polycationic function of D-glucosamine (the proton sponge hypothesis: escape from the degradative lysosomal trafficking pathway) is useful and meaningful for both cell biology and clinical applications.

Conflict of Interests

The authors declare that they have no conflict of interests.

Authors' Contribution

Kazunari Igawa and Naoko Ohara contributed equally to this work.

Acknowledgment

This work was supported by a Grant-in-Aid for Challenging Exploratory Research from the Japan Society, contract grant sponsor: Ministry of Education, Science, Sports and Culture of Japan, Contract Grant no. 16390547.

References

[1] Y. Shigemasa and S. Minami, "Applications of chitin and chitosan for biomaterials," *Biotechnology and Genetic Engineering Reviews*, vol. 13, pp. 413–420, 1996.

[2] R. A. A. Muzzarelli, M. Mattioli-Belmonte, A. Pugnaloni, and G. Biagini, "Biochemistry, histology and clinical uses of chitins and chitosans in wound healing," in *Chitin and Chitinases*, P. Jolles and R. A. A. Muzzarelli, Eds., pp. 285–293, Birkhäuser, Basel, Switzerland, 1999.

[3] J. Hua, K. Sakamoto, and I. Nagaoka, "Inhibitory actions of glucosamine, a therapeutic agent for osteoarthritis, on the functions of neutrophils," *Journal of Leukocyte Biology*, vol. 71, no. 4, pp. 632–640, 2002.

[4] G. Crolle and E. D'Este, "Glucosamine sulphate for the management of arthrosis: a controlled clinical investigation," *Current Medical Research and Opinion*, vol. 7, no. 2, pp. 104–109, 1980.

[5] K. Kaida, H. Yamashita, K. Toda, and Y. Hayashi, "Effects of glucosamine on tooth pulpal nociceptive responses in the rat," *Journal of Dental Sciences*, vol. 8, pp. 68–73, 2013.

[6] T. Hotta, T. Motoyama, and H. Watanabe, "Three human osteosarcoma cell lines exhibiting different phenotypic expressions," *Acta Pathologica Japonica*, vol. 42, no. 8, pp. 595–603, 1992.

[7] J. Hua, K. Sakamoto, and I. Nagaoka, "Inhibitory actions of glucosamine, a therapeutic agent for osteoarthritis, on the functions of neutrophils," *Journal of Leukocyte Biology*, vol. 71, no. 4, pp. 632–640, 2002.

[8] L. S. Lohmander and E. M. Roos, "Clinical update: treating osteoarthritis," *The Lancet*, vol. 370, no. 9605, pp. 2082–2084, 2007.

[9] J. S. Borer, H. Pouleur, E. Abadie et al., "Cardiovascular safety of drugs not intended for cardiovascular use: need for a new conceptual basis for assessment and approval," *European Heart Journal*, vol. 28, no. 15, pp. 1904–1909, 2007.

[10] J.-P. Behr, "The proton sponge: a trick to enter cells the viruses did not exploit," *Chimia*, vol. 51, no. 1-2, pp. 34–36, 1997.

[11] J.-S. Remy, C. Sirlin, P. Vierling, and J.-P. Behr, "Gene transfer with a series of lipophilic DNA-binding molecules," *Bioconjugate Chemistry*, vol. 5, no. 6, pp. 647–654, 1994.

[12] M. X. Tang and F. C. Szoka, "The influence of polymer structure on the interactions of cationic polymers with DNA and morphology of the resulting complexes," *Gene Therapy*, vol. 4, no. 8, pp. 823–832, 1997.

[13] D. W. Pack, D. Putnam, and R. Langer, "Design of imidazole-containing endosomolytic biopolymers for gene delivery," *Biotechnology and Bioengineering*, vol. 67, pp. 217–223, 2000.

[14] P. Midoux and M. Monsigny, "Efficient gene transfer by histidylated polylysine/pDNA complexes," *Bioconjugate Chemistry*, vol. 10, no. 3, pp. 406–411, 1999.

[15] D. Putnam, C. A. Gentry, D. W. Pack, and R. Langer, "Polymer-based gene delivery with low cytotoxicity by a unique balance of side-chain termini," *Proceedings of the National Academy of Sciences of the United States of America*, vol. 98, no. 3, pp. 1200–1205, 2001.

[16] O. Boussif, F. LezoualC'H, M. A. Zanta et al., "A versatile vector for gene and oligonucleotide transfer into cells in culture and in vivo: polyethylenimine," *Proceedings of the National Academy of Sciences of the United States of America*, vol. 92, no. 16, pp. 7297–7301, 1995.

[17] A. Akinc, M. Thomas, A. M. Klibanov, and R. Langer, "Exploring polyethylenimine-mediated DNA transfection and the proton sponge hypothesis," *Journal of Gene Medicine*, vol. 7, no. 5, pp. 657–663, 2005.

[18] W. T. Godbey, M. A. Barry, P. Saggau, K. K. Wu, and A. G. Mikos, "Poly(ethylenimine)-mediated transfection: a new paradigm for gene delivery," *Journal of Biomedical Materials Research*, vol. 51, pp. 321–328, 2000.